

**A MOLECULAR DYNAMICS STUDY OF THE MICROSCOPIC
PROPERTIES OF SIMPLE DENSE FLUIDS**

Thesis by

Paul Lee Fehder

In Partial Fulfillment of the Requirements

**For the Degree of
Doctor of Philosophy**

California Institute of Technology

Pasadena, California

1970

(Submitted November 26, 1969)

To my family

ACKNOWLEDGMENTS

I wish to express my sincere appreciation to those individuals and organizations who have contributed so much to this research, and to my personal happiness and well-being during my tenure at CalTech--

Professor G. W. Robinson, my research advisor, for his interest, encouragement, and support over the four years during which this research was being pursued. Were it not for his generosity and personal flexibility, such a project could not even have been initiated.

Dr. R. P. Futrelle, who has been most instrumental in introducing me to the mysteries of modern classical statistical mechanics. His helpful suggestions and enlightening hints have been a significant contribution to my research efforts.

Dr. C. A. Emeis, a most worthy colleague. His ability to enter into an unfamiliar field of research, and within the short span of a year to make several important contributions to that research effort, is indeed commendable.

Professor C. J. Pings, whose expressions of interest and encouragement seemed always to come at just the right time to assuage my occasional sense of frustration. Professor Pings and Dr. S. C. Smelser are most responsible for rekindling my interest in the radial distribution functions computed from the simulation data.

Mrs. Adria D. Larson, whose cheerful willingness to undertake tasks "above and beyond the call of duty" has served to expedite my efforts in many small and often not-so-small ways.

Professor F. B. Thompson, who has done a great deal to broaden my thinking with respect to the scientific application of automatic data processing.

Frank Rouser, Kiku Matsumoto, Joe Daly, Dallas Oller, and other members of the Booth Computing Center staff; their assistance has been invaluable in finding solutions to a number of rather knotty programming problems.

The C. I. T. Chemistry Department provided the "seed money" to support the initial phases of this research; the bulk of the project was supported by grants from the National Science Foundation. Personal financial support was provided by the Chemistry Department, NSF, E. I. du Pont de Nemours and Company, and through summer grants by the Shell Company Foundation and American Cyanamid. I would especially like to thank du Pont for its generosity during the 1967-68 academic year; the (relative) munificence of the du Pont Award for Postgraduate Teaching permitted me to discover many of the finer aspects of life in Southern California. I would also like to thank my parents, Mr. and Mrs. Lee G. Fehder, for their frequent "grants-in-aid" during times of financial stress.

And finally, I would like to express my appreciation to the International Business Machines Corporation for providing me with the incentive to complete my research, and this dissertation, as quickly as possible.

ABSTRACT

The microscopic properties of a two-dimensional model dense fluid of Lennard-Jones disks have been studied using the so-called "molecular dynamics" method. Analyses of the computer-generated simulation data in terms of "conventional" thermodynamic and distribution functions verify the physical validity of the model and the simulation technique.

The radial distribution functions $g(r)$ computed from the simulation data exhibit several subsidiary features rather similar to those appearing in some of the $g(r)$ functions obtained by X-ray and thermal neutron diffraction measurements on real simple liquids. In the case of the model fluid, these "anomalous" features are thought to reflect the existence of two or more alternative configurations for local ordering.

Graphical display techniques have been used extensively to provide some intuitive insight into the various microscopic phenomena occurring in the model. For example, "snapshots" of the instantaneous system configurations for different times show that the "excess" area allotted to the fluid is collected into relatively large, irregular, and surprisingly persistent "holes". Plots of the particle trajectories over intervals of 2.0 to 6.0×10^{-12} sec indicate that the mechanism for diffusion in the dense model fluid is "cooperative" in nature, and that extensive diffusive migration is generally restricted to groups of particles in the vicinity of a hole.

A quantitative analysis of diffusion in the model fluid shows that the cooperative mechanism is not inconsistent with the statistical

predictions of existing theories of singlet, or self-diffusion in liquids. The relative diffusion of proximate particles is, however, found to be retarded by short-range dynamic correlations associated with the cooperative mechanism--a result of some importance from the standpoint of bimolecular reaction kinetics in solution.

A new, semi-empirical treatment for relative diffusion in liquids is developed, and is shown to reproduce the relative diffusion phenomena observed in the model fluid quite accurately. When incorporated into the standard Smoluchowski theory of diffusion-controlled reaction kinetics, the more exact treatment of relative diffusion is found to lower the predicted rate of reaction appreciably.

Finally, an entirely new approach to an understanding of the liquid state is suggested. Our experience in dealing with the simulation data--and especially, graphical displays of the simulation data--has led us to conclude that many of the more frustrating scientific problems involving the liquid state would be simplified considerably, were it possible to describe the microscopic structures characteristic of liquids in a concise and precise manner. To this end, we propose that the development of a formal language of partially-ordered structures be investigated.

TABLE OF CONTENTS

Page

I. INTRODUCTION

A. Some General Comments Regarding the Liquid State	2
B. A Brief Outline of Theories of the Liquid State	4
Formal Theories	7
Superposition Approximation	8
PY Equation	10
"Scaled-Particle" Method	11
Model Theories	12
Cell Theory	14
Hole Theory	15
Cell-Cluster Theory	16
Tunnel Theory	17
Significant Structure Theory	19
C. A Review of Molecular Dynamics Studies at Other Laboratories	22
D. An Informal Description of the Approach Taken in This Research.	25
REFERENCES.	28

II. TECHNICAL DESCRIPTION OF METHODS AND
PROCEDURES

A. The Basic Molecular Dynamics Algorithm	32
---	----

	Page
B. Equipment	35
C. Implementation of the Algorithm	35
D. Auxilliary Procedures	44
III. CONVENTIONAL ANALYSES OF THE SIMULATION DATA	
A. Introductory Comments	50
B. Paper No. 1: Molecular Dynamics Studies of the Microscopic Properties of Dense Fluids	52
C. Notes and Addenda to Paper No. 1.	94
D. Paper No. 2: "Anomalies" in the Radial Distribution Functions for Simple Liquids	97
E. Notes and Addenda to Paper No. 2.	124
IV. DIFFUSION, RELATIVE DIFFUSION, AND CHEMICAL REACTION KINETICS IN DENSE FLUIDS	
A. Introductory Comments	127
B. Paper No. 3: The Microscopic Mechanism for Self-Diffusion and Relative Diffusion in Simple Liquids	129
C. Paper No. 4: The Microscopic Mechanism for Diffusion, and the Rates of Diffusion-Controlled Reactions in Simple Liquid Solvents	179
V. FORMAL LANGUAGE FOR THE DESCRIPTION OF LIQUID STRUCTURES--A PROPOSAL	
A. Explanatory Comments	209
B. Statement of the Problem	209

	Page
C. A Formal Language of Partially-Ordered Structures	211
D. The Radial Distribution Function $g(r)$	214
E. Geometrical Neighbors.	216
F. Discussion	219
VI. PROPOSITIONS	
Proposition 1: Elucidation of the Role of SO_2 in Atmospheric Aerosol Formation	224
Proposition 2: A Spectroscopic Search for an HgCO Complex	237
Proposition 3: Improvements on the Photochemical Space Intermittency Method for Measuring the Diffusion Coefficients of Free Halogen Atoms in Solution	246
Proposition 4: A Molecular Dynamics Study of Cavity Formation Works in a Simple Liquid.	263
Proposition 5: An Examination of Solute Diffusion as a Function of the Relative Sizes and Masses of the Solute and Solvent Molecules	277

SECTION I
INTRODUCTION

A. Some General Comments Regarding the Liquid State

The foundations for our physical understanding of the vapor state were established during the eighteenth and early nineteenth centuries.¹ And somewhat more recently, x-ray and now thermal neutron diffraction measurements have provided extremely detailed information regarding the microscopic structures of a large number of crystalline solids. But the liquid state, occupying as it does a kind of "middle ground" between solids and gases, is undoubtedly more complex and less well understood than either.

The solid state is stable at low temperatures and/or high pressures, is characterized by high cohesion and rigidity, and at the molecular levels exhibits a high degree of (crystalline) order and structure. Gases are stable at low pressures and high temperatures, are characterized by low cohesion, a complete lack of rigidity and low resistance to flow, and to a good approximation are entirely devoid of structure or order at the molecular level. The liquid state is stable over an intermediate range of temperatures and pressures, and is characterized by a high cohesion, a lack of rigidity, and a comparatively low resistance to flow.

The microscopic structures characteristic of the liquid state remain something of a mystery. The lack of rigidity and low resistance to flow suggest a disordered structure rather like that of the vapor state; indeed the liquid and vapor states become indistinguishable at high temperatures. But as a rule, fusion is accompanied by only a

relatively small increase in volume (of the order of 12% for the solid inert gases), and thus the spatial arrangement of the atoms or molecules in a liquid must--at least in the region of the melting point--bear some similarity to the crystalline structure of the corresponding solid. This proposition is also supported by the well-known experimental fact that the latent heat of fusion is always much smaller than the latent heat of vaporization; the cohesive forces between the molecules of a substance must not therefore change appreciably with melting. And finally, we note that the specific heat of condensed bodies is only slightly affected by fusion, indicating that thermal motion in the solid and liquid near the melting point must be fundamentally rather similar.

The ambiguity implied by the macroscopic physical properties of the liquid state is at least partially resolved by the results of x-ray diffraction and thermal neutron scattering measurements.² These measurements, in addition to some spectroscopic data,³ indicate that the liquid state is characterized by a microscopic structure that is essentially neither vapor-like nor solid-like.⁴ Rather, liquids are "partially ordered" at the molecular level; that is, the spatial arrangement of neighbors around an individual molecule in a liquid is similar to the arrangement of molecules in the crystalline lattice of the corresponding solid--but the lattice "defined" by the arrangement of neighbors around one molecule may be inconsistent with a regular extension of the lattice similarly defined by the neighbors of another molecule only a few diameters distant. An operationally useful, intuitive understanding of this concept of "partial ordering" is, unfortunately, rather difficult to achieve. And perhaps even more

important, the statistical-geometric⁵ techniques necessary to establish a quantitative measure of the "degree" of order in a partially-ordered structure have not as yet been devised. For a more detailed discussion of this latter point, see the discussion in section V.

Of all the physical sciences, classical chemistry is perhaps most dependent upon an intuitive understanding of the physical phenomena it purports to investigate. Organic chemists tend to think of molecules as real physical entities comprised of real atoms arranged in a reasonably well-defined spatial configuration--and of chemical reaction mechanisms in terms of the re-arrangement of these configurations during the encounter between two molecules in a reaction medium. This reaction medium is most frequently some liquid solvent; yet, because of the dearth of "practical" information regarding the microscopic processes characteristic of the liquid state, even very "intuitive" descriptions of a chemical reaction mechanism will frequently fail to consider possible dynamic interactions between the activated complex and molecules of the surrounding solvent. It is true, of course, that the so-called "solvent cage effect" is occasionally called upon to explicate the mechanism for, e. g., a complicated molecular rearrangement. But even this very simple model for solvent-solute interactions is not well defined, and it appears that different chemists envision the physical processes underlying the "effect" in different ways. Again, the Smoluchowski treatment of diffusion-controlled reaction kinetics in solution (see section IV. C, page 179) would seem to view the solvent as a "barrier" to encounter between reactive solute molecules, while

the "collision" theory of chemical reaction kinetics invokes a "solvent cage" model to explain the observed rates of reactions requiring a (supposedly) high activation energy or a specific steric orientation for the reactant molecules.

Other chemico-physical phenomena are also interpreted in terms of "operational" models for the liquid state. For example, nuclear spin-lattice relaxation in solution by nuclear-spin-internal-rotation coupling requires a dynamic interaction between the NMR-active solute molecule and the molecules in the surrounding solvent environment. The absorption spectra of atomic mercury dissolved in a variety of (apparently) inert liquids is thought³ to reflect the different types of local solvent environment in which a ground-state solute mercury atom might find itself. But the physical models for these interactions and solvent environments must be viewed with some skepticism until a more definitive model is fashioned for the liquid state itself. And, as we shall see in the next section, present efforts to construct a good theory of liquids do not seem to aspire to the development of such a model.

B. A Brief Outline of Theories of the Liquid State

During the last four decades, a great deal of research effort has been directed toward the development and articulation of a number of different theories of the liquid state. The literature reporting work in this area is so extensive that even a superficial summary of the results achieved by the various theories is well beyond the scope of this dissertation. Instead, our purpose here is to provide a brief

outline of the approach taken in the development of a representative sampling of these theoretical treatments; this outline will then serve as a background against which we may contrast the direction and results of our own research.

For the sake of discussion, the various theories of the liquid state may conveniently be divided into two groups. The "formal" theories of the sort pioneered by Kirkwood and Mayer offer the aesthetic pleasure of initial rigor. But approximations have always been necessary at some point in the development of these theories to make the mathematics tractable, and while most of the approximations are almost assuredly valid from a purely mathematical point of view, the physical implications of a given approximation are often not immediately obvious.

The theories falling into the second group--the "model" theories --are each based on some operational model for the microscopic structure and dynamics of the liquid state. In selecting a given model for study, the theoretician supposes that: (i) the mathematics deriving from the model will be tractable without further approximation, and (ii) the model is a reasonable representation of the real liquid. Some simplifying approximations are usually made during the mathematical development of a "model" theory. But these approximations are fundamentally different from those necessary to the development of the "formal" theories; they are usually more straightforward, have few if any physical implications (since most of the physical reasoning has been applied in devising the model itself), and can generally be tested, if necessary, by a more conscientious mathematical treatment of the model.

The "model" approach to liquid theory offers the advantage that, within the limits of any simplifying approximations, the theoretical formulations developed from a given model are at least a valid statistical-mechanical treatment of that model. If a "model" theory is capable of reproducing the thermodynamic or equation-of-state data for a real liquid, then it is generally assumed that the model is a reasonably accurate representation of reality. In fact, however, the thermodynamic functions do not serve as a critical test for the validity of a theoretical model; the statistical averaging implicit in any of the thermodynamic quantities is so extensive that even a patently "naive" model may experience some success in obtaining agreement with experimental data. The transport properties might conceivably serve as a medium for more severe tests of the various theoretical treatments. Unfortunately, most of the models that have been examined are static in nature and do not lend themselves to the calculation of transport-related quantities.

Formal Theories

The "formal" approach to a theory of the liquid state is based on attempts to devise an a priori method whereby the radial distribution function $g(r)$ for a liquid can be calculated. If the molecules of a liquid interact with pair-wise additive, central forces (possibly a rather gross assumption), knowledge of the radial distribution function permits us to calculate the equation-of-state and total energy. If $\varphi(r_{12})$ is the interaction potential between pairs of molecules in the liquid, the virial theorem leads to an equation-of-state of the form:

$$PV = Nk_B T - \frac{N^2}{6V} \int_0^\infty r g(r) \frac{\partial \varphi(r)}{\partial r} 4\pi r^2 dr .$$

The total internal energy is similarly related to $g(r)$:

$$E = \frac{3}{2} Nk_B T + \frac{N^2}{2V} \int_0^\infty g(r) \varphi(r) 4\pi r^2 dr .$$

From the equation-of-state and total energy, all the thermodynamic properties of the system can be calculated.

Kirkwood,⁶ Born and Green,⁷ Yvon,⁸ and Bogoliubov⁹ have developed a number of essentially equivalent integral equations for the molecular-pair distribution function $n^{(2)}(\underline{r}_1, \underline{r}_2)$, defined as the probability of finding an arbitrary pair of molecules in the configuration $(\underline{r}_1, \underline{r}_2)$. That is, $n^{(2)}(\underline{r}_1, \underline{r}_2)$ is the probability of simultaneously finding a molecule in the volume element $d^3 \underline{r}_1$ around \underline{r}_1 and a second molecule in the volume element $d^3 \underline{r}_2$ around \underline{r}_2 . Higher-order correlation functions $n^{(3)}(\underline{r}_1, \underline{r}_2, \underline{r}_3)$, $n^{(4)}(\underline{r}_1, \underline{r}_2, \underline{r}_3, \underline{r}_4)$, etc., are similarly defined.

For an isotropic fluid, $n^{(2)}(\underline{r}_1, \underline{r}_2)$ is dependent only upon the scalar distance $r_{12} = |\underline{r}_{12}| = |\underline{r}_1 - \underline{r}_2|$, and is directly related to the radial distribution function:

$$n^{(2)}(r) = \frac{N}{V} \frac{(N-1)}{V} g(r) \cong \frac{N^2}{V} g(r) .$$

By a rather tedious statistical-mechanical derivation, it can be shown that the change in $n^{(2)}(\underline{r}_1, \underline{r}_2)$ effected by moving particle 1 while holding particle 2 fixed is given by:

$$\frac{\partial n^{(2)}(\underline{r}_1, \underline{r}_2)}{\partial \underline{r}_1} = - \frac{n^{(2)}(\underline{r}_1, \underline{r}_2)}{k_B T} \frac{\partial \varphi(r_{12})}{\partial \underline{r}_1} - \frac{1}{k_B T} \int \frac{\partial \varphi(r_{13})}{\partial \underline{r}_1} n^{(3)}(\underline{r}_1, \underline{r}_2, \underline{r}_3) d\underline{r}_3 ,$$

and similarly, that $\partial n^{(3)}(\underline{r}_1, \underline{r}_2, \underline{r}_3)/\partial \underline{r}_1$ is given by a formula involving the next higher correlation function $n^{(4)}(\underline{r}_1, \underline{r}_2, \underline{r}_3, \underline{r}_4)$. Thus to calculate $n^{(2)}$ --and thence $g(r)$ --we need $n^{(3)}$; to obtain $n^{(3)}$ we need $n^{(4)}$, etc.

To break this chain of linked equations, Kirkwood proposed the so-called "superposition approximation":

$$n^{(3)}(\underline{r}_1, \underline{r}_2, \underline{r}_3) = \frac{[n^{(2)}(r_{12}) \cdot n^{(2)}(r_{23}) \cdot n^{(2)}(r_{31})]}{\rho_0}$$

where $\rho_0 = N/V$ is the number density of the system. Born and Green,⁷ and Yvon⁸ have shown that the equation obtained by substituting the superposition approximation for $n^{(3)}$ into the equation above for $\partial n^{(2)}(\underline{r}_1, \underline{r}_2)/\partial \underline{r}_1$ can be integrated over \underline{r}_1 to obtain:

$$k_B T \ln \frac{n^{(2)}(r_{12})}{\rho_0^2} = -\varphi(r_{12}) + 2\pi\rho_0 \int_0^\infty \int_{\underline{r}-\underline{r}_{13}}^{\underline{r}+\underline{r}_{13}} \frac{\partial \varphi(r_{13})}{\partial \underline{r}_{13}} \frac{n^{(2)}(r_{13})}{\rho_0^2} \times \left(\frac{n^{(2)}(r_{23})}{\rho_0^2} - 1 \right) \left[\frac{r_{13}^2 - (r_{23} - r_{12})^2}{2r_{23}} \right] r_{23} dr_{23} dr_{13}$$

where $\varphi(-r) = \varphi(r)$ and $n^{(2)}(-r) = n^{(2)}(r)$, by definition. Kirkwood and Bogoliubov obtained slightly different equations using different mathematical approaches.

Within the limits of accuracy for the superposition approximation, the BGY equation above and the similar equations obtained by Kirkwood and Bogoliubov each constitute a rigorous (though perhaps not intuitively enlightening) theory of the liquid state. In fact, the BBGYK equations are found to reproduce the broad features of the radial distribution functions obtained by x-ray diffraction measurements² on real liquids at moderate densities. For higher densities the superposition approximation begins to fail; in particular, the theoretical distribution functions begin to diverge from the experimental functions just in the regions where $\varphi(r)$ and $\partial\varphi(r)/\partial r$ make the largest contributions to the integrands in the formulas for the total energy and equation-of-state.

Perkus and Yevick¹⁰ obtained a very different integral equation for $g(r)$ by applying the "method of collective variables."¹¹ With this method, disorder in the microscopic structure of a liquid is represented by the superposition of a large number of acoustic waves. The Hamiltonian for the system is then transformed so that, to a good approximation, the configuration integral--and thence the partition function--can be calculated.

Consider first a one-dimensional system of N particles constrained to move on a line of length L . An instantaneous configuration of this system would usually be described in terms of the coordinates $x_1, x_2, x_3, \dots, x_N$ of the particles. In the method of collective variables however, each "collective" coordinate depends on all the x_i 's and has the general form

$$q_n = \sum_{i=1}^N \sin(2\pi x_i / \lambda_n)$$

where $\lambda_n = 2L/n$ and n is an integer. N of these collective coordinates, $q_1 \dots q_N$, are required to describe the one-dimensional system.

For real three-dimensional liquids, $3N$ collective coordinates are used and the system is assumed to be confined to a cube with edge dimension L . The reformulation of the Hamiltonian requires a number of complex mathematical procedures; some of these procedures are still open to question. Suffice it to say that, using the transformed Hamiltonian, the partition function and thence all the thermodynamic properties of the liquid can be calculated.

The Percus-Yevick treatment leads to the integral equation:

$$g(r)e^{\varphi(r)/k_B T} = 1 + \rho_0 \int g(s) \left[1 - e^{\varphi(s)/k_B T} \right] \left[g(|s-r|) - 1 \right] ds$$

for the radial distribution function. Broyles¹² has obtained numerical solutions to this equation for fluids of Lennard-Jones particles at a number of different temperatures and densities. The resulting radial distribution functions compare favorably with those calculated using the Monte-Carlo and "molecular dynamics" simulation techniques--to a radius of about $r = 1.5 \sigma$. For larger r the agreement is not quite so satisfactory, although the results are still much better than those obtained using any of the BBGYK equations. The PY equation appears to fail at low densities.

The "scaled particle" method developed by Reiss and co-workers¹³ represents potentially yet another "formal" approach to a theory of the liquid state. The method is based on the idea that, as the volume of a void or "hole" in a liquid is increased, the number of

molecules that will fit into that void changes discontinuously. The probability of finding a spherical hole of a given radius in the liquid is then calculated in terms of the reversible work necessary to create such a hole.

As originally formulated, the scaled particle method is directly applicable only to the treatment of dense fluids of rigid spherical particles. For such fluids the equation-of-state is a function only of $G(\sigma)$, the average density of particles in contact with a given particle in the fluid, and not the form of the radial distribution function for all $r > \sigma$. The equation-of-state

$$\frac{PV}{Nk_B T} = \frac{1+x+x^2}{(1-x)^3}, \quad \text{where } x = \frac{N\pi\sigma^3}{6V}$$

obtained by the scaled particle method is however in remarkably good agreement with the results obtained by simulation calculations on systems of "hard" spheres,¹⁴ and has even experienced some success in predicting the thermodynamic properties of several real liquids.¹⁵

Model Theories

The "model" approach to a theory of the liquid state involves an attempt to obtain a mathematically tractable formulation for the canonical partition function $Z_N(V, T)$ of a liquid by calculating instead the partition function for a model representing the microscopic structure and dynamics of that liquid. The partition function for a thermodynamic system is related to the Helmholtz free energy:

$$A(N, V, T) = -k_B T \ln Z_N(V, T) \quad ,$$

and if the free energy is known as a function of temperature and density, all the other thermodynamic properties can be calculated. In particular, the equation-of-state is obtained from the relation $P = -(\partial A / \partial V)_T$.

The partition function for a classical system of N identical particles is given by the $6N$ -dimensional integral

$$Z_N = \frac{1}{N! h^{3N}} \int \dots \int \exp\{-\beta U(\underline{r}_1, \dots, \underline{r}_N, \underline{\rho}_1, \dots, \underline{\rho}_N)\} \\ d\underline{r}_1 \dots d\underline{r}_N, d\underline{\rho}_1 \dots d\underline{\rho}_N$$

where h is Planck's constant, $\beta = (k_B T)^{-1}$, \underline{r}_i and $\underline{\rho}_i$ are the position and momentum of particle i , respectively, and $U(\underline{r}_1, \dots, \underline{r}_N, \underline{\rho}_1, \dots, \underline{\rho}_N)$ is the total energy of the system in configuration $(\underline{r}_1 \dots \underline{\rho}_N)$. The momenta may be integrated immediately to give:

$$Z_N = \left(\frac{2\pi m}{\beta h^2} \right)^{\frac{3}{2}N} Q_N(V, T)$$

where m is the particle mass and Q_N the configurational partition function

$$Q_N = \frac{1}{N!} \int_V \dots \int_V \exp\{-\beta \Phi(\underline{r}_1, \dots, \underline{r}_N)\} d\underline{r}_1, \dots, d\underline{r}_N \quad .$$

$\Phi(\underline{r}_1 \dots \underline{r}_N)$ is the total potential energy of the spatial configuration $(\underline{r}_1 \dots \underline{r}_N)$. The various models are therefore chosen to make the calculation of Q_N practicable.

The simplest theories are based on a "cell" model for the liquid state. The volume occupied by a system of N particles is divided into a lattice of N identical cells; one particle is confined to each cell, and thus the configurational partition function for these models factorizes into a product of N one-particle partition functions:

$$Q_N = \exp(-\beta\Phi_0) v_f^N$$

where Φ_0 is the lattice energy when all particles lie at the centers of their respective cells, and the "free volume" v_f is given by:

$$v_f = \int_{\text{cell}} \exp\{-\beta[\psi(\underline{r}) - \psi(o)]\} d\underline{r} \quad .$$

The quantity $\psi(\underline{r})$ is the "cell potential"; i. e., the potential energy of a particle positioned at \underline{r} relative to the center of its cell.

The various cell theories differ primarily in the manner in which $\psi(\underline{r})$ is calculated. In the most elementary treatment--the Lennard-Jones-Devonshire (LJD) theory-- $\psi(\underline{r})$ is calculated under the assumption that all the neighbors to the particle of interest are "localized" at the centers of their respective cells. More sophisticated treatments permit the neighbors to move about in their cells in response to the motion of the central particle; the results obtained by these treatments do not, however, differ appreciably from those obtained with the simple LJD theory.

It is obvious that the cell theories are, in reality, theories of the solid and not the liquid state. Although the cell theories do predict the existence of a first-order phase transition, it can be argued that

this transition is from a solid to an "expanded solid" configuration, and not from the liquid to the vapor states. The much-heralded fact that the simple LJD theory provides a reasonably accurate prediction for the critical temperature of liquid argon-- $T_{C, LJD}^* = 1.30$; the experimental value is $T_C^* = 1.259$ (reduced units)--can hardly be more than fortuitous, since the predicted critical density is about 80% higher than that observed experimentally.

From a thermodynamic point of view, the cell theories, in all versions, exhibit two main defects: (i) the predicted values for the pressure at liquid-like densities are too low; alternatively, the predicted volumes for the liquid are too small, and (ii) the predicted values for the entropy of the liquid are much too low. These defects are the result of two fundamentally unrealistic assumptions made in the cell model. The first assumption is that the coordination number of each particle remains constant for all densities; this implies that the size of the cells grows proportional to the volume allotted to the system. The second unrealistic assumption is that each particle moves about in its cell independent of the positions of the particles in neighboring cells. Thus the cell theories are essentially independent-particle theories.

To relax the first assumption, Eyring¹⁶ introduced a "hole" theory for the liquid state. In this theory, the volume occupied by a system of N particles is divided into a virtual lattice of $(N+n)$ identical cells. With each particle assigned to a single cell, this leaves n cells unoccupied, or n "holes". The number of holes is assumed to vary with the density of the system.

Actually, a number of different hole theories exist, depending upon the method by which the ratio $n:N$ is determined and the manner in which the holes are assumed to be distributed throughout the virtual lattice. Even a superficial summary of the various treatments is impossible here; it is found however that all of the existing versions of the hole theory predict $n:N$ ratios that are too small and, like the simple cell theories, liquid densities that are too large. The introduction of holes into the cell model does not increase the predicted values for the entropy significantly.

The independent-particle aspect of the simple cell theories is relaxed in the "cell-cluster" theory of de Boer.¹⁷ In this treatment, the volume occupied by an N -particle system is again divided into N identical cells. But the walls separating some ℓ adjacent cells in the center of the virtual lattice are removed, thus permitting the ℓ particles contained therein to move about in one "super-cell". The $(N-\ell)$ remaining particles are assumed to be "localized" at the centers of their respective cells.

The potential field within the cell-cluster is determined by two factors: (i) the mutual interactions between the ℓ particles comprising the cluster, and (ii) interactions with the $(N-\ell)$ surrounding neighbors. The partition function is accordingly written as a series of terms: the first term gives the contribution of one-cell clusters (from the simple cell theories), the second term gives the contribution from cell-clusters of two cells (introducing the effects of two-particle correlations), etc. The successive terms increase in complexity very rapidly with increasing ℓ ; indeed, in the nine years between 1953--when the de Boer

treatment was proposed--and 1962, only the first and second terms in the series for Lennard-Jones particles were completed.¹⁸ The results obtained with this two-term treatment indicate that the cell-cluster theory, when fully developed, may provide much more realistic estimates of the entropy of the liquid state. But like the simple cell theories, the cell-cluster treatment may tend to underestimate the volume of the liquid. A cell-cluster theory including holes has been worked-out by Dahler and Cohen,¹⁹ but numerical results for any realistic pair potential are exceedingly difficult to obtain.

The simple cell, hole, and cell-cluster models for the liquid state are all basically rather similar, and for this reason the theories stemming from these models exhibit similar deficiencies. The "tunnel" theory developed by Barker²⁰ overcomes some of these deficiencies by permitting the particles comprising the liquid greater freedom of movement (thus allowing for more microscopic disorder in the model), yet retains much of the computational simplicity of the more elementary cell treatments.

The idea behind the tunnel theory is that, within the framework of classical statistical mechanics, the configurational partition function for a one-dimensional fluid can be solved exactly. The "tunnel" model is accordingly one in which the particles of a liquid are packed into a large number of parallel lines. The particles in one line are distributed along that line completely independent of the distributions of particles along any of the adjacent lines; thus the relative positions of particles on different lines are completely disordered. If the lines are packed tightly together, the motion of a particle along the axis of

the "tunnel" formed by particles on the adjacent lines will be almost independent of its motion perpendicular to the axis. The configurational partition function can then be factored into two terms: a one-dimensional partition function for motion along the tunnels, and a two-dimensional function describing motion across the tunnels.

Let us assume that the volume V occupied by an N -particle system is divided into K close-packed hexagonal cylinders, each ℓ long and containing $M = N/K$ particles. The configurational partition function then has the form:

$$Q_N(V, T) = \left[\frac{N!}{(M!)^K} \right] Q_M^{(1)}(\ell, T) \left(\frac{1}{N!} \right) Q_N^{(2)}(A, T)$$

where $Q_M^{(1)}$ is the one-dimensional partition function

$$Q_M^{(1)}(\ell, T) = \int_0^\ell \dots \int_0^\ell \exp\{-\beta\Phi^{(1)}(z_1, \dots, z_M)\} dz_1 \dots dz_M$$

$$\Phi^{(1)} = \sum_{i \neq j}^M \varphi(|z_i - z_j|)$$

and $Q_N^{(2)}$ is the partition function describing motion in the plane perpendicular to the tunnel axis. $Q_N^{(2)}$ is usually obtained by a two-dimensional version of the simple LJD cell theory (see, for example, the Appendix to Paper No. 1, Section III. B, page 85), in which case it is of the form:

$$Q_N^{(2)}(A, T) = \exp(-\beta\Phi_0) a_f^N$$

where the "free area" a_f is given by:

$$a_f = \int_{\text{cell}} \exp\{-\beta[\psi(\underline{r}) - \psi(o)]\} d\underline{r} .$$

As described above in the discussion of the simple cell theories, the "cell potential" $\psi(\underline{r})$ may be calculated under a variety of different assumptions, leading to "tunnel" treatments of varying degrees of mathematical complexity.

Using the Lennard-Jones pair potential, the tunnel theory is found to reproduce the equation-of-state for liquid argon over a range of moderate, liquid-like densities. Thus the theory is ^{truly}~~truly~~ one of the liquid--and not the solid--state. Although the entropy values predicted by the theory are somewhat lower than those measured experimentally, the results for the entropy are superior to those obtained by any of the cell-like theories. The theory does not provide a good prediction for the critical properties of a liquid, apparently because the "tunnel" model breaks down at low densities.

The "significant structure" theory introduced by Eyring²¹ represents a radical departure from the other theories discussed above. According to the significant structure model, the "excess" volume acquired by a liquid through thermal expansion is distributed throughout the structure of the liquid in the form of particle-size holes or "vacancies." Unlike the holes in the cell-like "hole" model (also ~~on~~ ^{an} Eyring contribution), the vacancies in the significant structure model are "fluidized"--i. e., free to move about in the liquid. Thus the vacancies impart something of a gas-like character to the particles immediately surrounding them at any instant (since any particle on the

edge of a vacancy may potentially "jump" into the void--permitting the vacancy to jump into its place); the particles not adjacent to a vacancy are assumed to librate in a solid-like environment.

The partition function for the significant structure model is written as the weighted product of two factors:

$$Z_N(V, T) = (z_s)^{N(V_s/V)} (z_g)^{N(V-V_s)/V_s}$$

where z_s and z_g are the partition functions for solid-like and gas-like degrees of freedom, respectively, and V_s is the volume of the corresponding solid (perhaps a poorly-defined quantity). The partition function for an Einstein oscillator is used for z_s ; z_g is approximated by the nonlocalized ideal gas partition function. The exponents $N(V_s/V)$ and $N(V-V_s)/V_s$ weigh the contributions of these two factors in terms of the amount of "excess" volume--and hence, the ratio of particles to vacancies--in the system. In fact, however, the final form of the partition function is not quite so simple:

$$Z_N = \left\{ \frac{e^{E_s/RT}}{(1 - e^{-\theta/T})^3} \left[1 + n \left(\frac{V-V_s}{V_s} \right) \exp \left(- \frac{a E_s V_s}{(V-V_s) RT} \right) \right] \right\}^{N \frac{V_s}{V}} \\ \times \left\{ \left(\frac{2\pi m}{h^2 \beta} \right)^{\frac{3}{2}} \frac{eV}{N} \right\}^{N \left(\frac{V-V_s}{V_s} \right)}$$

where E_s is the energy of sublimation and θ the Einstein characteristic temperature for the corresponding solid, and n and a are adjustable parameters.

The significant structure theory has achieved a measure of success in treating a wide variety of liquids, including the liquified inert gases, organic and inorganic liquids, and even molten metals and fused salts. And because the significant structure model is dynamic in nature, the theory can also be extended to include a treatment of such macroscopic quantities as the transport properties, surface tension, and dielectric constant.²² The parameterization employed in the mathematical development of the theory has however led to criticism in some circles. For example, in the formula for the partition function \underline{n} and \underline{a} are explicitly designated as "adjustable" parameters; but E_s , θ , and V_s can also be "adjusted" within not too well-defined limits, should the need arise. It has been said that, "With a formula including mixed non-linear and exponential terms, and containing five disposable parameters, one should be able to 'fit' any conceivable function."²³

In summary, one might opine that the existing theories of the liquid state actually provide very little insight into the structures and dynamic processes characteristic of liquids at the molecular level. The mathematical complexity of the "formal" theories almost precludes the possibility that they will eventually lead to any intuitive understanding of the microscopic properties of liquids. On the other hand, most of the "model" theories have been based on manifestly simplistic models for the liquid state, and thus contribute little to our understanding of the "chemical" processes occurring in liquids.

C. A Review of Molecular Dynamics Studies at Other Laboratories

The so-called "molecular dynamics" technique refers, generically, to a number of different algorithms that permit a digital computer to simulate a model for a real physical system. In essence, the computer performs a numerical time-integration of the classical equations of motion for the perhaps several hundred particles comprising the model. The time-dependent position and velocity data generated by the calculations can then be analyzed: (i) to determine if the model is indeed a valid prototype for the real system, and (ii) to obtain a detailed description of the microscopic structures and processes occurring in the model (and hence the real system, if accurately represented). Furthermore, the simulation data can provide for a stringent test of any theoretical treatments of the real system; even if the model is only an approximate replica of the real system, the theories can usually be re-worked to treat the model exactly, since the system parameters (e. g., inter-particle interaction potentials, etc.) for the model must be well-defined in the dynamics programming.

Some of the earliest (<1959) work with the molecular dynamics technique was done by B. J. Alder and T. E. Wainwright at the Lawrence Radiation Laboratory. An algorithm was devised for simulating dense fluids of "hard" particles,²⁴ and used in an extensive study of the thermodynamic properties of hard-sphere liquids.²⁵ A phase transition observed in the hard-sphere system was investigated in detail with dense fluids of hard disks.²⁶

In recent years, Alder has turned his attention toward the

theoretical implications of his hard-sphere simulation data. The breakdown of the superposition approximation for hard-sphere fluids was examined,²⁷ and "free-path" distributions calculated from the simulation data were used to refute the "jump" model for diffusion suggested by significant structure theory.²⁸ It is rumored that Alder has now begun to investigate "cooperative" mechanisms for diffusion in his hard-sphere model, but no written reports of this work have come into this author's possession.

In 1964, A. Rahman reported some preliminary results from molecular dynamics calculations simulating liquid argon.²⁹ A Lennard-Jones pair potential was used, and the thermodynamic properties and self-diffusion coefficient computed from the simulation data were found to be in surprisingly good agreement with experimental values. As a staff member of the Argonne National Laboratory, Rahman has directed much of his effort toward calculation of the van Hove, and other correlation functions of specific interest in thermal neutron scattering experiments. He has however--following Alder's lead--examined the validity of the superposition approximation and PY equation when applied to the radial distribution functions computed from his argon simulation data.³⁰ And more recently, he has reported the results of a rather novel investigation of the short-time mechanism for self-diffusion in a dense fluid of particles interacting with the Buckingham pair potential.³¹ (See also, Paper No. 3, Section IV. B, page 129.)

Encouraged by the exceptional quality of Rahman's initial results, L. Verlet has extended the simulation calculations for a Lennard-Jones

fluid (argon model) to a wide range of temperatures and densities.³² The equation-of-state, high-frequency elastic moduli, and isotopic separation factors computed from the simulation data are in very good agreement with the experimental values for liquid argon. An empirical method was devised for determining the melting point of the model system, and the fusion temperature vs. density curve obtained in this manner was found to reproduce the experimental curve for solid argon quite accurately. The critical constants obtained for the model fluid were not, however, in good agreement with the argon values.

Much of Verlet's work seems to have been influenced by his contact with J. L. Lebowitz and J. K. Perkus during his tenure at Yeshiva University.³³ For example, the equation-of-state data reported in his first paper are "corrected" to account for the "tail" of the truncated Lennard-Jones potential actually used in the simulation calculations. Again, in his second paper³⁴--dealing with the equilibrium correlation functions obtained by analysis of the simulation data--the radial distribution functions are similarly corrected for the truncated pair potential, and a method based on the PY equation used to extrapolate $g(r)$ outward and the direct correlation function $c(r)$ inward.

Verlet's research has been hindered somewhat during the last two years, first by his return to Paris from Yeshiva (New York City), and then by a ^{an} ~~near-fatal~~ automobile accident. He is however said to be presently engaged in an investigation of various (transport-related?) time-correlation functions computed from his argon simulation data.

D. An Informal Description of the Approach Taken in This Research

In the remainder of this dissertation we describe a molecular dynamics study of two-dimensional model dense fluids of Lennard-Jones disks. The primary goal of this investigation was to obtain a better intuitive understanding of the "chemically" important microscopic processes characteristic of the liquid state. In particular, we were interested in the local structures that might be exhibited by the model, and the manner in which these structures would evolve with time and with the relative diffusion of individual pairs of fluid particles.

A two-, rather than three-dimensional model was studied for several reasons. From a purely economic standpoint, the dynamics calculations could be expected to proceed more rapidly for a two- than a three-dimensional model--thus permitting us to examine more thermodynamic states of the system or, alternatively, to observe the kinetic evolution of the system (in a given state) over a longer time interval. But perhaps more important was the ease with which graphical or pictorial displays of the two-dimensional simulation data could be generated.

It would be difficult to overemphasize the importance of graphical display techniques to the type of investigation we originally envisioned. It was noted in subsection [B] above that the ^{clearth}~~dirt~~ of really definitive experimental information regarding the microscopic properties of dense fluids has been a serious handicap in the development of a ^{truly}~~truly~~ serviceable theory of the liquid state. But such information as does exist suggests that the liquid state is quite complex, both structurally and dynamically, at the molecular level. Thus there was--and

still remains--good reason to believe that the old saw: "A picture is worth a thousand words!" would be especially applicable to a study aimed at achieving a better intuitive understanding of liquids.

From an operational standpoint, the study involved a number of interrelated activities:

- (i) Preparation of the computer programming and generation of simulation data.
- (ii) Verification of the physical validity of the simulation data. That is, calculation of well-established distribution and correlation functions (e. g., speed and velocity distributions, $g(r)$, etc.) from the simulation data to show that they behave in a physically acceptable manner.
- (iii) Examination of graphical displays of the simulation data to gain insight into the microscopic processes occurring in the model system.
- (iv) Formulation of new space- and time-correlation functions describing specific processes observed in the graphical displays. Analysis of the simulation data in terms of these new correlation functions to obtain a quantitative measure of our intuitive insight into the microscopic phenomena occurring in the model.
- (v) Application of our findings, where possible, to existing theoretical treatments of various liquid state phenomena.

Some technical details of the computer programming techniques used in this study are described in Section II. The rather "conventional" analyses of the simulation data reported in Paper No. 1 (reproduced in subsection III. B) tend to support the physical validity of the model system.

Examination of graphical displays of the simulation data suggested that diffusion in the high-density model fluid proceeds by a mechanism that is primarily "cooperative" in nature. This observation was verified by the calculation of several new time-correlation functions discussed in Paper No. 3 (subsection IV. B). In Paper No. 4 (subsection IV. C), the results of our investigation of diffusion and relative diffusion in the model fluid are applied to the standard Smoluchowski treatment for diffusion-controlled reaction rates in solution.

REFERENCES FOR SECTION I

1. For a brief history of the development of the kinetic theory of gases, see: R. D. Present, Kinetic Theory of Gases (McGraw-Hill, New York, 1958), Ch. 1.
2. P. A. Egelstaff, Brit. J. Appl. Phys. 16, 1219 (1965).
3. G. W. Robinson, Mol. Phys. 3, 301 (1960).
4. "Our data shows that liquids are very liquid-like."--P. A. Egelstaff, during presentation at the 1967 Gordon Research Conference on the Chemistry and Physics of Liquids.
5. J. D. Bernal is perhaps most responsible for ^{arguing}~~arguing~~ the case for a "statistical-geometric" approach to liquid structure. See, for example: Nature 183, 141 (1959); 185, 68 (1960).
6. J. G. Kirkwood, J. Chem. Phys. 3, 300 (1935).
7. M. Born and H. S. Green, Proc. Roy. Soc. A188, 10 (1946).
8. J. Yvon, Actualities Scientifiques at Industrielles (Hermann et Cie, Paris, 1935).
9. N. H. Bogoliubov, in Studies in Statistical Mechanics, J. de Boer and G. E. Uhlenbeck, eds. (North-Holland Publishing Co., Amsterdam, 1962), Vol. I, Part A.
10. J. K. Perkus and G. J. Yevick, Phys. Rev. 110, 1 (1958).
11. The "method of collective variables" was originally proposed by D. Pines and D. Bohm, Phys. Rev. 85, 338 (1951).
12. A. A. Broyles, J. Chem. Phys. 34, 359, 1068 (1961); ibid., 35, 493 (1961).

13. H. Reiss, H. L. Frisch, and J. L. Lebowitz, J. Chem. Phys. 31, 369 (1959); H. Reiss, H. L. Frisch, E. Helfand, and J. L. Lebowitz, ibid. 32, 119 (1960); E. Helfand, H. Reiss, H. L. Frisch, and J. L. Lebowitz, ibid. 33, 1379 (1960); E. Helfand, H. L. Frisch, and J. L. Lebowitz, ibid. 34, 1037 (1961).
14. W. W. Wood and J. D. Jacobson, J. Chem. Phys. 27, 1207 (1957).
15. F. H. Stillinger, Jr., J. Chem. Phys. 35, 1581 (1961); H. Reiss and S. W. Mayer, ibid. 34, 2001 (1961); S. W. Mayer, ibid. 35, 1513 (1961); 38, 1803 (1963); S. J. Yosim and B. B. Owens, ibid. 39, 2222 (1963).
16. H. Eyring, J. Chem. Phys. 4, 283 (1936).
17. J. de Boer, Physica 20, 655 (1954).
18. M. Weissmann and R. M. Mazo, J. Chem. Phys. 37, 2930 (1962).
19. J. S. Dahler and E. G. D. Cohen, Physica 26, 81 (1960).
20. J. A. Barker, Aust. J. Chem. 13, 187 (1960); Proc. Roy. Soc. A259, 442 (1961).
21. H. Eyring, T. Ree, and N. Hirai, Proc. Nat. Acad. Sci. (US), 44, 683 (1958); H. Eyring and T. Ree, ibid. 47, 526 (1961); H. Eyring and R. P. Marchi, J. Chem. Ed. 40, 562 (1963).
22. A rather complete review of the significant structure theory of liquids is given in the new book: H. Eyring and M. S. Jhon, Significant Liquid Structures (John Wiley and Sons, New York, 1969).
23. (Quote not for attribution.)
24. B. J. Alder and T. E. Wainwright, J. Chem. Phys. 31, 459 (1959).

25. B. J. Alder and T. E. Wainwright, J. Chem. Phys. 33, 1439 (1960).
26. B. J. Alder and T. E. Wainwright, Phys. Rev. 127, 359 (1962).
27. B. J. Alder, Phys. Rev. Let. 12, 317 (1964).
28. B. J. Alder and T. Einwohner, J. Chem. Phys. 43, 3399 (1965).
29. A. Rahman, Phys. Rev. 136, A405 (1964).
30. A. Rahman, Phys. Rev. Let. 12, 575 (1964).
31. A. Rahman, J. Chem. Phys. 45, 2585 (1966).
32. L. Verlet, Phys. Rev. 159, 98 (1967).
33. J. L. Lebowitz, J. K. Perkus, and L. Verlet, Phys. Rev. 153, 250 (1967).
34. L. Verlet, Phys. Rev. 165, 201 (1968).

SECTION II

TECHNICAL DESCRIPTION OF METHODS
AND PROCEDURES

A. The Basic Molecular Dynamics Algorithm

The "molecular dynamics" algorithm described here permits a digital computer to simulate the microscopic dynamics of a model dense fluid by performing a simultaneous step-wise numerical time-integration of the Newtonian equations of motion of the fluid particles. The algorithm is of the predictor-corrector type, and can be used for either two- or three-dimensional models. Although the formulations given below are for a fluid of particles interacting with the Lennard-Jones pair potential

$$\varphi_{\text{LJ}}(r) = 4\epsilon \left\{ (\sigma/r)^{12} - (\sigma/r)^6 \right\} ,$$

the algorithm can easily be modified for use with other smooth potentials such as the Morse, Buckingham, Buckingham-Corner, etc.¹ For pair potentials having discontinuous first derivatives (e.g., Sutherland, "hard" sphere or disk, square-well, etc.) other algorithms, such as the one devised by Alder and Wainwright,² are more suitable.

¹A number of pair-potentials are described and discussed in: J. O. Hirschfelder, C. F. Curtiss, and R. B. Byrd, Molecular Theory of Gases and Liquids, John Wiley and Sons, Inc., New York (1954), p. 31 ff.

²B. J. Alder and T. E. Wainwright, J. Chem. Phys. 31, 459 (1959).

Let x_i and v_i be components of the position and velocity of particle i in a system of N identical particles. Then:

$$dx_i/dt = v_i \quad (2.1)$$

$$\frac{dv_i}{dt} = a_i = 24 \left(\frac{\epsilon}{m} \right) \sum_{j \neq i}^N \frac{x_i - x_j}{r_{ij}^2} \left\{ 2 \left(\frac{\sigma}{r_{ij}} \right)^{12} - \left(\frac{\sigma}{r_{ij}} \right)^6 \right\} \quad (2.2)$$

It is convenient to "reduce" the dynamical variables entering into the calculations to units involving σ and ϵ , the distance and energy parameters in the pair potential, and m , the particle mass. Taking σ as the unit of distance and $(\epsilon/m)^{1/2}$ as the unit of velocity, and using the dimensionless variables χ , ν , ρ , α , and τ in place of x , v , r , a , and t , respectively, eqns. (1) and (2) reduce to:

$$d\chi_i/d\tau = \nu_i \quad (2.3)$$

$$\frac{d\nu_i}{d\tau} = \alpha_i = 24 \sum_{j \neq i}^N \frac{\chi_i - \chi_j}{\rho_{ij}^2} \left\{ \frac{2}{\rho_{ij}^{12}} - \frac{1}{\rho_{ij}^6} \right\} \quad (2.4)$$

The reduced time increment ($\Delta\tau$) corresponding to the increment (Δt) employed in the dynamics integration is then given by

$$(\Delta\tau) = (\Delta t) (\epsilon/m)^{1/2} \sigma^{-1}, \quad (2.5)$$

and "logical" time (i. e., time as defined for the model system by the dynamics integration) becomes quantized in units of the interval ($\Delta\tau$).

If we are given the positions $\chi_i(n-1)$ of the particles at time $\tau(n-1)$, and the positions $\chi_i(n)$, velocities $\nu_i(n)$, and accelerations

$\alpha_i(n)$ of the particles at time $\tau(n)$, we can predict the positions of the particles at time $\tau(n+1)$:

$$\chi_i^0(n+1) = \chi_i(n-1) + 2(\Delta\tau) \nu_i(n) \quad . \quad (2.6)$$

From these predicted positions we can calculate predicted accelerations at time $\tau(n+1)$:

$$\alpha_i^0(n+1) = 24 \sum_{j \neq i}^N \frac{\chi_i^0(n+1) - \chi_j^0(n+1)}{\rho_{ij}^0(n+1)^2} \left\{ \frac{2}{\rho_{ij}^0(n+1)^{12}} - \frac{1}{\rho_{ij}^0(n+1)^6} \right\}, \quad (2.7)$$

and thence new velocities and positions:

$$\nu_i(n+1) = \nu_i(n) + \frac{1}{2} (\Delta\tau) \{ \alpha_i(n) + \alpha_i^0(n+1) \} \quad (2.8)$$

$$\chi_i(n+1) = \chi_i(n) + \frac{1}{2} (\Delta\tau) \{ \nu_i(n) + \nu_i(n+1) \} \quad . \quad (2.9)$$

The positions obtained by eqn. (9) may then be inserted into eqn. (7) in place of the predicted positions, and the steps corresponding to eqns. (7), (8), and (9) repeated (iterated) until the position values $\chi_i(n+1)$ obtained from two successive iterations differ by less than some prescribed value. In practice, it is found³ that a single iteration yields sufficient accuracy for our purposes if argon parameters⁴ are used for σ , ϵ , and m , and a time increment corresponding to $(\Delta t) = 10^{-14}$ sec is chosen.

³See: A. Rahman, Phys. Rev. 136, A405 (1964).

⁴The parameter values $\sigma = 3.405 \text{ \AA}$, $(\epsilon/k_B) = 119.8^\circ \text{ K}$, $m = 6.6321 \times 10^{-23} \text{ gr.}$, where k_B is the Boltzmann constant, were used in the calculations described here.

B. Equipment

The basic dynamics calculations and subsequent analyses of the simulation data were performed using the C. I. T. -IBM 7040/7094 Shared-file computer system.⁵ The California Computer Corporation (CalComp) Model 763 incremental X-Y plotter incorporated into the 7040/7094 system was used to plot functional data obtained by analyses of the simulation data; direct graphical displays of the simulation data (vide infra) were generated using a Stromberg-Carlson Model 4020 CRT plotter operated by the North American/Rockwell Corporation.⁶ The 16 mm film processing necessary to produce motion pictures from the simulation data was done by Consolidated Film Industries, 959 Seward Street, Hollywood, California. The author is especially indebted to Mr. Wm. Funke of the CFI Title and Optical Division for his patience and understanding while dealing with a novice film producer.

C. Implementation of the Algorithm

The procedures employed in generating the simulation data are described in general terms in Paper No. 1, reproduced in section III. B of this dissertation. Our purpose here is to provide detailed information regarding some of the programming techniques used in implementing the "molecular dynamics" algorithm. This information is perhaps of little interest from a purely scientific standpoint, but is included

⁵This computer system was replaced by an IBM System/360 Model 75 computer in December, 1968.

⁶Access to this plotter was provided as a service by the Booth Computing Center.

for the sake of completeness and as a possible guide to others wishing to implement the algorithm for calculations on different fluid models.

Except for FORTRAN-encoded auxiliary sub-programs for input-output operations, the bulk of the dynamics programming was written in the MAP assembly language for the IBM 7094 computer. However, since FORTRAN is a more widely recognized computer programming language, the MAP-encoded programs will be described here in terms of their FORTRAN analogues.

At the beginning of each step or "cycle"⁷ in the dynamics integration, the algorithm requires the component positions of the particles from the two preceding cycles and the component velocities and accelerations at the end of the immediately preceding cycle. Since the dynamics program was found to require about 8 seconds of 7094 time to complete a single cycle (or about 400 cycles per hour), it was not practical to calculate a complete set of equilibrium simulation data for a given temperature-density state of the model fluid during a single execution of the program. Instead, the necessary position-velocity-acceleration data from the last two cycles completed during a given execution of the program were recorded in a reserved region of the IBM 1301 disk file incorporated into the 7040/7094 computer system. This "restart data" could then be retrieved from the disk at the beginning of a subsequent execution of the program and used immediately to

⁷We will use the term "cycle" hereafter to avoid confusion with the computational steps necessary to advance the dynamics integration a single time increment.

continue the calculations for the same temperature-density state, or modified appropriately to start the calculations for a new state.

The dynamics programming was written to handle systems of up to $N = 500$ particles, although the full capacity was not used in any of the calculations reported in this dissertation. In the programming, the system is confined to a square, two-dimensional "space-box" with an edge dimension integral in units of 0.5σ (vide infra). Periodic boundary conditions are employed, so that opposite edges of the space-box are logically adjacent and the density of the system remains constant during the course of a given calculation. The space in which the fluid particles move is therefore topologically equivalent to the surface of a torus.

Because of complications introduced by the periodic boundary conditions, and for reasons of economy, the Lennard-Jones pair potential is truncated at $r_c = 2.5 \sigma$; i.e., the actual pair-potential used in the calculations is, in reduced units:

$$\begin{aligned} \varphi^*(\rho_{ij}) &= 4 \{ \rho_{ij}^{-12} - \rho_{ij}^{-6} \} & \text{for } \rho_{ij} \leq 2.5 \\ &= 0 & \text{for } \rho_{ij} > 2.5 \end{aligned}$$

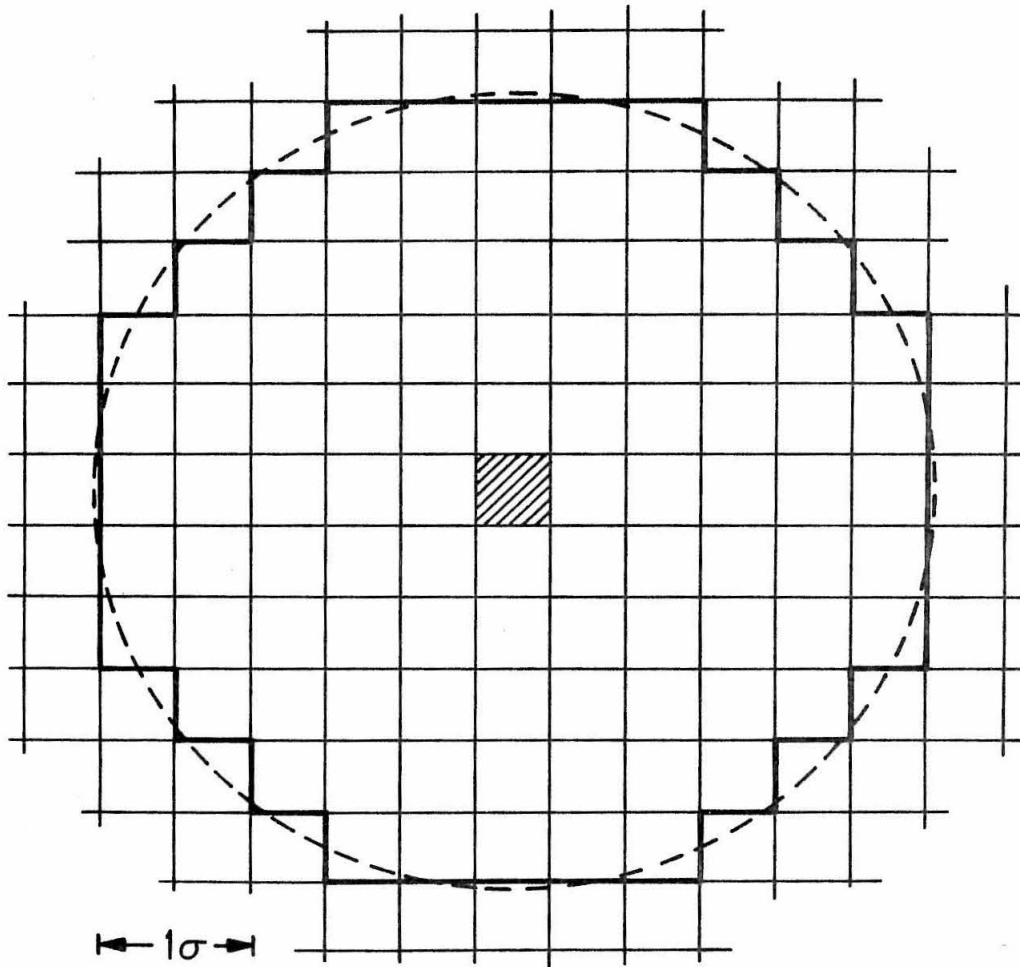
The summation indicated by eqn. (7) can then be limited to the n_i "effective" neighbors lying within 2.5σ of a given particle i .

In order to avoid having to calculate the distances between all pairs of particles in the system (a procedure complicated by the periodic boundary conditions), a "neighbor search" technique was devised so that the "effective" neighbors for any given particle could

be determined in a more or less straightforward manner. The space-box is divided into a grid of square sub-boxes of dimension 0.5σ (hence the requirement that the edge dimension of the space-box be integral in units of 0.5σ). Each sub-box is identified by the pair of indices LX and LY, where sub-box [LX, LY] covers the $0.25 \sigma^2$ region of the space-box centered at $x = (LX - \frac{1}{2}) 0.5 \sigma$, $y = (LY - \frac{1}{2}) 0.5 \sigma$. A "location matrix" LMTX is established such that LMTX (LX, LY) contains the number of the particle lying in sub-box [LX, LY]. If a sub-box is empty, the corresponding location in LMTX is set to zero; because of the repulsive r^{-12} "core" of the pair potential, the probability that two particles will occupy the same sub-box is negligibly small.

To identify the particles that are "effective" neighbors to some particle i, the locations in LMTX corresponding to the pattern of sub-boxes shown in the diagram on the next page are examined and a list of the non-zero entries compiled. The pattern is centered on the sub-box occupied by particle i, and special care must be taken with the LMTX indexing during the "search" to account for the periodic boundary conditions.

In later versions of the dynamics programming an alternative method for neighbor identification was employed. It is assumed that no two particles further than 3.5σ apart can diffuse to within 2.5σ of each other during an interval of 5×10^{-13} sec. The neighbor-search pattern was therefore extended to a radius of 3.5σ , and lists of the neighbors within 3.5σ of each particle compiled only every 50 cycles.



Neighbor-search pattern for identifying the "effective" neighbors to some particle \underline{i} in the system. The lighter lines show a portion of the grid of 0.5σ sub-boxes superimposed on the space-box; particle \underline{i} lies in the crosshatched sub-box at the center. All particles lying in the pattern of sub-boxes enclosed by the heavy lines are assumed to be "effective" neighbors to particle \underline{i} . The dashed circle is drawn with radius $(2.5 + \frac{1}{4} \sqrt{2}) \sigma$.

Between searches, the "effective" neighbors to any given particle i are determined by examining the particles cited in its "extended" neighbor list (taking account of the periodic boundary conditions, of course). If at any time one of the neighbors is found to be more than 3.5σ from i , its number is deleted from the list; thus the number of active entries in the "extended" neighbor list for each particle decreases steadily between searches.

This second technique for neighbor identification offers the advantage that the system is searched for the neighbors to each particle only periodically; a great deal of additional storage space is however required by the programming to store the neighbor lists between searches. Because of hardware (principally core storage) limitations intrinsic to the IBM 7074 computer, the dynamics calculations were found to proceed at about the same speed when either the first or second neighbor identification techniques were employed. But if a computer providing more core storage is used--and especially if a three-dimensional model system is being simulated--the second technique would appear to offer a more efficient means of keeping account of the "effective" neighbors to each particle.

In addition to that required by the "neighbor search" operations, the dynamics programming uses the following indexed storage:

```
DIMENSION PX(500), PY(500), X(500), Y(500),
          VX(500), VY(500), AX(500), AY(500),
          TEMPX(500), TEMPY(500),
          AXN(500), AYN(500)
```

Let us assume that the program has just completed the cycle for time $\tau(n)$. Then $PX(I)$ and $PY(I)$ contain the x and y coordinates of particle I for time $\tau(n-1)$, $X(I)$ and $Y(I)$ the coordinates for time $\tau(n)$, and $VX(I)$, $VY(I)$ the velocity and $AX(I)$, $AY(I)$ the acceleration components for time $\tau(n)$. The calculation for cycle (n+1) proceeds as follows:

1. The predicted x and y coordinates of the particles at time $\tau(n+1)$ are computed according to eqn. (6). For each particle I:

$$PX(I) = PX(I) + 2(\Delta\tau) * VX(I)$$

$$PY(I) = PY(I) + 2(\Delta\tau) * VY(I)$$

2. The predicted accelerations for time $\tau(n+1)$ are computed according to eqn. (7). For each particle I, set $TEMPX(I) = TEMPY(I) = 0$ and determine the list of "effective" neighbors to be included in the summation. Then for each neighbor J to particle I, calculate the distances

$$DX = PX(I) - PX(J)$$

$$DY = PY(I) - PY(J)$$

taking into account the periodic boundary conditions.

Calculate the powers of $\rho_{ij}^0(n+1)$:

$$R2 = DX ** 2 + DY ** 2$$

$$R6 = R2 ** 3$$

$$R12 = R6 ** 2$$

and the force factor:

$$F = (24.0/R2) * ((2.0/R12) - (1.0/R6)) .$$

Then sum the contributions of neighbor J into the component accelerations of particle I:

$$\text{TEMPX}(I) = \text{TEMPX}(I) + \text{DX} * F$$

$$\text{TEMPY}(I) = \text{TEMPY}(I) + \text{DY} * F$$

3. The velocities for time $\tau(n+1)$ are calculated according to eqn. (8). For each particle I:

$$\text{TEMPX}(I) = \text{VX}(I) + \frac{1}{2}(\Delta\tau) * (\text{TEMPX}(I) + \text{AX}(I))$$

$$\text{TEMPY}(I) = \text{VY}(I) + \frac{1}{2}(\Delta\tau) * (\text{TEMPY}(I) + \text{AY}(I))$$

4. The data ^{are} ~~is~~ rearranged, and positions for time $\tau(n+1)$ calculated according to eqn. (9). For each particle I:

$$\text{PX}(I) = \text{X}(I)$$

$$\text{PY}(I) = \text{Y}(I)$$

$$\text{X}(I) = \text{PX}(I) + \frac{1}{2}(\Delta\tau) * (\text{TEMPX}(I) + \text{VX}(I))$$

$$\text{Y}(I) = \text{PY}(I) + \frac{1}{2}(\Delta\tau) * (\text{TEMPY}(I) + \text{VY}(I))$$

and the velocity component values in $\text{VX}(I)$ and $\text{VY}(I)$ are exchanged with those in $\text{TEMPX}(I)$ and $\text{TEMPY}(I)$, respectively.

Note: At this point, PX and PY contain the particle coordinates for time $\tau(n)$, TEMPX and TEMPY the velocity components for time $\tau(n)$, X and Y the new particle coordinates for time $\tau(n+1)$, and VX and VY the new velocity components for time $\tau(n+1)$.

5. The component acceleration values for time $\tau(n)$ are saved

$$\text{AXN}(I) = \text{AX}(I)$$

$$\text{AYN}(I) = \text{AY}(I)$$

and new accelerations for time $\tau(n+1)$ are computed using the same procedure as outlined under step 2 above--except that DX and DY are calculated from the coordinate values in the X and Y vectors, and the acceleration components are summed into AX(I) and AY(I) instead of TEMPX(I) and TEMPY(I).

6. "Corrected" velocities and positions for time $\tau(n+1)$ are computed according to eqns. (8) and (9), respectively. For each particle I:

$$VX(I) = TEMPX(I) + \frac{1}{2}(\Delta\tau) * (AX(I) + AXN(I))$$

$$VY(I) = TEMPY(I) + \frac{1}{2}(\Delta\tau) * (AY(I) + AYN(I))$$

$$X(I) = PX(I) + \frac{1}{2}(\Delta\tau) * (VX(I) + TEMPX(I))$$

$$Y(I) = PY(I) + \frac{1}{2}(\Delta\tau) * (VY(I) + TEMPY(I))$$

7. "Corrected" accelerations are computed on the basis of the "corrected" position values using the same procedure as outlined under step 2--except that DX and DY are calculated from the coordinate values in the X and Y vectors, and the acceleration components are summed into AX(I) and AY(I) instead of TEMPX(I) and TEMPY(I).

Steps 6 and 7 may be repeated (iterated) as many times as desired.

The calculation then returns to step 1 for time $\tau(n+2)$.

After each cycle in the dynamics integration, the positions and velocities of the particles are recorded on magnetic tape in a $(4N+4)$ -word logical record. The first four "tag" words in the record contain identifying information, while the remaining four blocks of N words each are written from the X, Y, VX, and VY vectors, respectively.

The first "tag" word contains N in the decrement field and the "integer box dimension" (in units of 0.5σ) in the address field;⁸ the second "tag" word contains the "true" space-box edge dimension (in units of σ) in floating-point format. Each cycle in the dynamics integration is assigned a "cycle number" (corresponding to the time-counter n used above) that is incremented after each step; this number is recorded in the third "tag" word. And finally, the data generated during a given execution of the dynamics program ^{are} is assigned a six character alphanumeric data label. This label is recorded, in BCD format, in the fourth "tag" word.

D. Auxilliary Procedures

The calculations for the model fluid were started with a system of 364 particles symmetrically arranged in four 91-particle hexagonal "crystals" in a space-box with edge dimension 25.0σ . The particles in each crystal were placed in a perfect two-dimensional hexagonal closest-packed configuration with a lattice spacing of $2^{1/6} \sigma$; the crystals were centered in each of the four quadrants of the space-box. To obtain a randomized thermal motion in the fluid, a value of 0.33389 was randomly assigned, either positive or negative, to the x and y velocity components of each of the particles. Center-of-mass motion was then eliminated by, for example, summing the x -velocity components, dividing the sum by 364, and subtracting the resulting "error component" from the x -velocity of each of the particles.

⁸The terminology here is specific to the storage configuration of the IBM 7094 computer.

As shown by Fig. 1 in Paper No. 1 (page 58), the component velocities were found to achieve an equilibrium Gaussian distribution very quickly after the start of the dynamics calculations. The hexagonal closest-packed configuration with lattice spacing $2^{1/6} \sigma$ (the potential minimum distance for the Lennard-Jones pair potential) was used so that the temperature of the fluid after equilibration could be predicted on the basis of the initial value assigned to the velocities. The symmetric disposition of particles within the space-box was required to prevent center-of-mass motion from being introduced through potential interactions between the particles. But because the system was found to achieve an equilibrium spatial configuration only rather slowly, the particles were initially arranged in a number of quick-melting "crystals" rather than a space-filling lattice.

Following the format developed in subsection C above, let us assume that the assigned particle coordinates for $\tau(0)$ are stored in the X and Y vectors and the assigned velocity components in the VX and VY vectors. Component accelerations for $\tau(0)$ can be computed from the assigned positions using the procedure described under step 2 in the outline flow diagram, except that DX and DY are calculated from the coordinate values in the X and Y vectors and the acceleration contributions are summed into AX(I) and AY(I) instead of TEMPX and TEMPY. Then for the first cycle in the dynamics calculation, the predicted positions for time $\tau(1)$ are computed according to the formula:

$$\chi_i^0(1) = \chi_i(0) + \nu_i(0) (\Delta\tau) + \frac{1}{2} \alpha_i(0) (\Delta\tau)^2$$

or, for each particle I:

$$PX(I) = X(I) + VX(I) * (\Delta\tau) + 0.5 * AX(I) * (\Delta\tau) ** 2$$

$$PY(I) = Y(I) + VY(I) * (\Delta\tau) + 0.5 * AY(I) * (\Delta\tau) ** 2 \quad .$$

From this point, the calculations proceed as indicated by step 2 in the outline flow diagram.

In practice, it is necessary to start a dynamics calculation with the system in an entirely artificial configuration only once. Subsequent calculations for different temperature-density states can then be started from the appropriately modified "restart data" generated by some previous execution of the dynamics program.

An isochoric change in the temperature of the model fluid can be effected by either of two procedures: (1) the component velocities of all the particles in the system may be multiplied by some constant factor near unity (e.g., 1.0005 for "warming," or 0.9995 for "cooling") after each cycle in a special dynamics calculation, or (2) the velocity component values in, for example, a set of "restart data" from a previous calculation may be multiplied by the factor required to change the temperature of the system to the desired new value at once. Both procedures entail certain advantages and disadvantages. Because of the statistical temperature fluctuations intrinsic to an isolated system of relatively so few particles, it is possible with neither procedure to predict accurately what the final equilibrium temperature of the new state will be. But since the system has been found to remain near equilibrium during even a relatively rapid change in temperature

(e. g., 20° K in 10^{-12} seconds), the first procedure provides a more practical means of achieving a specific temperature if the "special" dynamics calculation is continued until the temperature of the fluid reaches the desired new value. The second procedure is definitely more economical than the first, but may force the system into a metastable non-equilibrium state if the initial temperature-density state lies in or near a phase-transition region. Although the system ideally has no net center-of-mass velocity in either the x or y directions, small fluctuations may combine with computer round-off errors to produce a net component along either or both axes in the velocity data for any given step in the dynamics integration (even though the time-average center-of-mass velocity may vanish). Either temperature-modification procedure may serve to amplify these small errors, but the problem is particularly serious with the second procedure since it works with only a single set of velocity values.

As a result of the programming constraint that the space-box edge dimension be integral in units of 0.5σ (a constraint that may be relaxed if other "neighbor-searching" techniques are employed), the density of the model system can only be changed "instantaneously"--i. e., between two cycles in the dynamics integration. For reduced densities below about 0.6, the system can be expanded or contracted by changing the space-box edge dimension and then multiplying the particle coordinates by the factor:

$$\left(\frac{\text{new edge dimension}}{\text{old edge dimension}} \right) .$$

This procedure is equivalent to changing the size of the particles relative to the available area of the space-box, and has been found to work well if the initial and final densities do not differ greatly. Some difficulty was encountered however in obtaining a rapid re-equilibration of the system after an expansion to very low densities (see Paper No. 1, section III. B, page 57), and compressions from initial densities above about 0.5 are frequently accompanied by an undesirably large increase in temperature. No technique for accurately predicting the change in temperature that will accompany a given expansion or contraction of the system has been found.

From initial densities above about 0.6, further increases in density are best effected by inserting additional particles into the system. If the new particles are placed in "holes" in the system microstructure and located at a distance of $2^{1/6} \sigma$ from the centers of two neighboring particles, a significant increase in the system density can be obtained with little change in temperature. This procedure has, for example, been used to raise the density of the system from 0.6319 to 0.7014 to 0.7708 by successive additions of 40 particles each to a system initially containing 364 particles and confined to a space-box with edge dimension 24.0σ .

SECTION III

CONVENTIONAL ANALYSES OF THE SIMULATION DATA

A. Introductory Comments

In this section we reproduce two papers dealing with the results obtained by some rather conventional analyses of the simulation data. The first paper [since published in J. Chem. Phys. 50, 2617 (1969)] contains a brief description of the computational techniques employed in generating and analyzing the simulation data and reports equilibrium thermodynamic data for eighteen temperature-density states of the model fluid. Some qualitative observations regarding the microscopic structures and mechanisms for diffusion noted in graphical displays of the simulation data are discussed at length, and a Lennard-Jones-Devonshire (theoretical) treatment of the model fluid is developed in an appendix. A number of the qualitative observations have since found support in quantitative measurements made on the simulation data, and are discussed in greater detail in the two papers reproduced in Section IV of this dissertation.

The second paper [to be published in the Journal of Chemical Physics] reports the appearance of some interesting subsidiary structure in the radial distribution functions for the model fluid. Similar structure have been observed in the distribution functions obtained by experimental x-ray or neutron diffraction measurements on real liquids, but has generally been attributed to experimental errors or to practical limitations on the experimental technique. Since the distribution functions computed directly from the simulation data are not subject to

these errors and limitations, our results may shed some light on the controversy regarding the nature and authenticity of the subsidiary features appearing in the experimental data.

Notes and addenda amplifying various statements made in the two papers are proffered in subsections following each of the manuscripts. These comments are for the most part parenthetical in nature, and were omitted from the manuscripts for publication in an attempt to achieve some semblance of conciseness. Each comment is keyed to the text of the preceding manuscript by a superscript lower-case Roman character enclosed in parentheses.

B. Paper No. 1

Molecular Dynamics Studies of the
Microscopic Properties of Dense Fluids*

Paul L. Fehder

Arthur Amos Noyes Laboratory of Chemical Physics,[†]

California Institute of Technology, Pasadena, California 91109

Abstract. Molecular dynamics calculations have been performed on a two-dimensional system of Lennard-Jones disks. Equilibrium thermodynamics data for eighteen temperature-density states of the system are presented and compared with values obtained from a simple Lennard-Jones-Devonshire treatment. Three types of graphical displays of the data have been examined: "snapshots" of the system configuration at some instant of time, motion pictures of the system dynamics created from sequences of snapshots, and plots of the trajectories of particle centers over various time intervals. The snapshots reveal the presence of the relatively large vacancies in the spatial distribution of particles in the system, and the trajectory plots and motion pictures show that these vacancies may persist in the same region for times in excess of 10^{-12} sec. The trajectory plots also indicate that cooperative motion is very important in the self-diffusion process. The nature of the vacancies and the diffusive motion suggest a more than passive role of the attractive interparticle potential in determining the micro-structure and micro-kinetics of the liquid state.

*This work was supported in part by a grant from the National Science Foundation, No. GP-7258.

[†]Contribution No. 3758.

I. INTRODUCTION

Beginning with the first papers by Alder and Wainwright,¹ an increasing amount of information concerning computer calculations on various models for dense fluids has been published. While early work in this area dealt almost exclusively with systems of hard disks and spheres,²⁻⁴ the increased sophistication of modern computer hardware has made possible the treatment of models involving more complex, and physically more realistic inter-particle interaction potentials. The more recent papers by Rahman^{5, 6} and Verlet,⁷ for example, report the results of calculations on models in which Lennard-Jones and Buckingham potentials were employed.

To date, much of the published work in this area has been concerned with the calculation of thermodynamic quantities and certain familiar correlation functions. The results of these calculations are important in that they provide for a comparison between the models and real fluids. But perhaps more significantly, such data may also serve as the basis for a critical evaluation of the various existing theoretical treatments of the liquid state, since the inter-particle interactions and other system parameters are well-defined for the computer models. (a)

Future work on this type of calculation is expected to branch-out in many new directions. Rahman,⁶ for example, has recently examined the short-time mechanism of self-diffusion in dense fluids in terms of instantaneous fluctuations in local

particle distributions. Molecular dynamics calculations may also provide a source of detailed information regarding the characteristic microscopic properties of liquids important to chemical processes. For example, the true nature of the microscopic local structures and dynamics associated with reactant diffusion and encounter, and with the so-called "solvent cage effect" might be elucidated. Non-equilibrium processes such as photodissociation and recombination of molecular solutes in liquid solvents could also be modeled.^(b)

In a "chemical" approach to the analysis of molecular dynamics data, graphical displays of the micro-processes in the model systems should be of great intuitive value. Even a "pictorial" interpretation of the characteristic local behavior of liquids, as might be exhibited by a solvent about a reaction site, could prove a valuable adjunct to the understanding of the detailed mechanisms of more complex molecular rearrangement reactions. It is furthermore likely that the extraction of quantitative information of a chemical nature from the computer data will require the definition of new correlation functions encompassing the spatial distributions and relative motions of comparatively large numbers of particles. Graphical displays, taken in conjunction with the established intuition about chemical reaction kinetics, may well provide valuable insight toward the formulation of such functions.

In preparation for such an investigation of the chemical aspects of dense fluid dynamics, a series of calculations on a

two-dimensional model system of 364 Lennard-Jones disk-particles has been performed. In this paper we briefly review the computational techniques employed, comment on the general behavior of the system, present some thermodynamic data for the states of the system examined thus far, and exhibit some of the graphical display techniques to be used in future investigations. In particular, discussion of the microscopic configurations and motions associated with diffusion processes in the model system will be emphasized.

II. THE DYNAMICS CALCULATIONS

A. The Algorithm

The algorithm for the dynamics calculations was taken, with minor modification, from the Appendix of Ref. 5. As described there, all dynamical variables entering into the calculations are reduced in units involving m , the particle mass, and σ and ϵ , the distance and energy parameters in the Lennard-Jones pair potential. Distances are expressed in units of σ , velocities in units of $(\frac{\epsilon}{m})^{\frac{1}{2}}$, and the reduced time increment $\Delta\tau$ corresponding to time increment Δt is given by:

$$\Delta\tau = (\Delta t)(\frac{\epsilon}{m})^{\frac{1}{2}}(\frac{1}{\sigma}).$$

The pair potential is truncated at a "cut-off" radius $r_c = 2.50 \sigma$, beyond which it is set equal to zero. A time increment equivalent to 10^{-14} sec was used in the dynamics integration.

The system is confined to a square "space-box"; periodic boundary conditions are employed in the computational algorithm

so that opposite edges of the box are logically contiguous and the system density remains constant during the course of a calculation. The space in which the particles move is therefore topologically equivalent to the surface of a torus, with the result that the time-average angular momentum of the system about any point in the space remains uniformly zero. Alternatively, the space-box may be regarded as a single cell in an infinite square lattice of identical cells, a conceptualization preferable when considering diffusion and related transport processes.^(c)

B. Fluctuations

Lebowitz, Perkus, and Verlet⁸ have recently examined the theoretical significance of fluctuations of thermodynamic quantities in the microcanonical ensemble with particular application to molecular dynamics calculations. The computational model is isochoric and adiabatic, and hence isoenergetic. In practice, however, numerical round-off errors may introduce variations in the total system energy on the order of $\pm 1\%$ during the course of a calculation spanning 10^{-11} sec, or instantaneous errors in the kinetic or potential energies of approximately 0.3% of the average statistical fluctuations in these quantities.

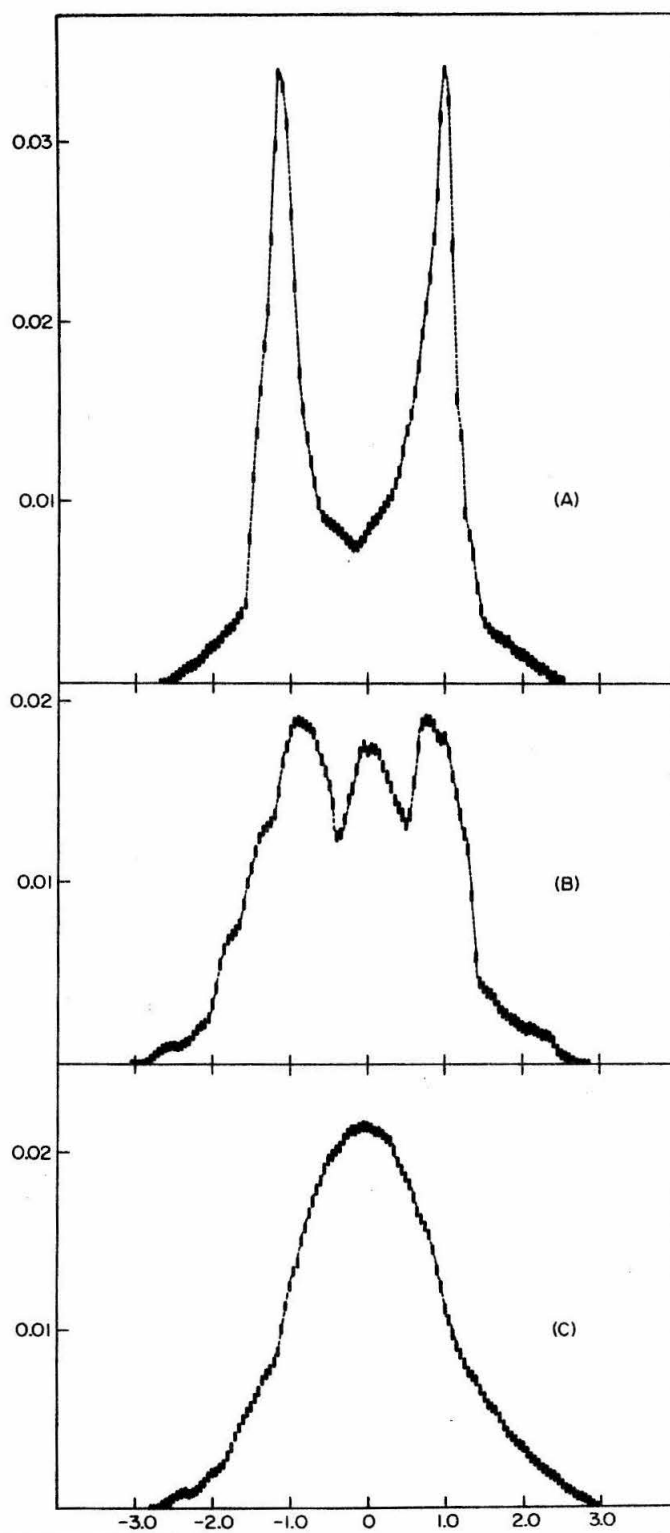
C. Initial Conditions

It is necessary to start the dynamics calculations with the system in an entirely artificial configuration only once. Subsequent

calculations for different thermodynamic states may be started by modifying the conditions existing at the end of some prior calculation. Density alterations are achieved by effectively changing the size of the particles relative to the area of the space-box. Since the particle size parameter σ is also employed as the unit of distance in the calculations, this must be done by changing the numerical value of the space-box edge dimension and scaling the particle coordinates by the factor: new edge dimension \div old edge dimension. Programming constraints dictate that density alterations be done "instantaneously"--that is, between steps in the dynamics integration.

Changes in the system temperature at constant density may be effected by multiplying the component velocities of all particles by some factor near unity. This may be done either "instantaneously", or after each successive step in a dynamics calculation. Experience has shown that the system remains near equilibrium during even a relatively rapid temperature alteration (e.g. 20°K in 10^{-12} sec) if the latter technique is employed and if a phase transition region is not approached. Re-equilibration after an "instantaneous" temperature alteration is also generally quite rapid, as may be illustrated by the plots in Fig. 1. In contrast, an "instantaneous" change in density may displace the system far from equilibrium, and re-equilibration may proceed slowly. This is particularly evident at lower densities, where the equilibration processes appear to be complicated by a clustering phenomenon discussed in Sec. IV.

FIG. 1. Velocity distributions showing rapid equilibration of kinetic energy in the system at density $\rho^* = 0.63$, nominal average temperature $T^* = 1.05$. Initial distribution obtained by randomly assigning, positive or negative, a value of 1.0263 to the x and y velocity components of each particle. Plots show distribution after (A) 1.5×10^{-13} , (B) 3.0×10^{-13} , and (C) 2.0×10^{-12} sec.



III. THERMODYNAMIC QUANTITIES

A. Reduced Variables

Thermodynamic quantities computed directly from the reduced dynamical variables are similarly obtained in reduced units. ^(d)

Temperatures are obtained in units of $T_{\epsilon} = (\epsilon/k_B)$, where k_B is the Boltzmann constant, pressures in units of (ϵ/σ^2) , and energies in units of ϵ per particle. Except for dynamical variables, an asterisk (*) will be used to denote quantities in reduced units.

The reduced area A^* and density ρ^* of a system are related by:

$$A^* = \frac{A}{N\sigma^2} = \frac{1}{\rho^*} \quad , \quad (1)$$

where N is the number of particles in the system and A is the true area. A second density measure, the relative density ρ_R , may also conveniently be employed. The relative density is the ratio of the actual system density to that of closest packing, and is given by:

$$\rho_R = \frac{N}{A} \cdot \frac{\sqrt{3}}{2} \delta_{\min}^2 \quad , \quad (2)$$

where $\delta_{\min} = 1.1132 \sigma$ is the lattice parameter found computationally to give the lowest energy for a two-dimensional hexagonal closest-packed array of disks interacting with the truncated Lennard-Jones potential.

B. Temperature and Pressure

If γ_i is the velocity of the i^{th} particle in units of $(\epsilon/m)^{\frac{1}{2}}$, the two-dimensional temperature of the system is given by:

$$T^* = \frac{1}{2N} \sum_{i=1}^N \gamma_i^2. \quad (3)$$

In the reduced units, the temperature and kinetic energy K^* are equivalent. The potential energy V^* follows directly from the reduced pair potential

$$\begin{aligned} \varphi^*(\rho_{ij}) &= 4 \{ \rho_{ij}^{-12} - \rho_{ij}^{-6} \} \\ V^* &= \frac{2}{N} \sum_{i=1}^N \sum_{j \neq i}^{n_i} \{ \rho_{ij}^{-12} - \rho_{ij}^{-6} \}, \end{aligned} \quad (4)$$

where φ^* is in units of ϵ ,
where ρ_{ij} is the distance between particles i and j in units of σ ,
and the sum over j includes only the n_i particles for which $\rho_{ij} < 2.50$.

The pressure is computed in accordance with the virial formula

$$\frac{PA}{Nk_B T} = 1 - \left(\frac{1}{4k_B T} \right) \left\langle r_{ij} \cdot \frac{\partial \varphi(r)}{\partial r} \right\rangle_{r_{ij}}, \quad (5)$$

where P is in units of force per unit length, and $\left. \frac{\partial \varphi(r)}{\partial r} \right|_{r_{ij}}$ is the force acting on particle i due to particle j . If $\varphi(r)$ is the truncated Lennard-Jones pair potential, Eq. (5) takes the computational form:

$$P^* = \frac{K^*}{A^*} + \frac{6}{A^*} \sum_{i=1}^N \left[\left(\frac{1}{n_i} \right) \sum_{j \neq i}^{n_i} \left\{ \frac{2}{\rho_{ij}^{12}} - \frac{1}{\rho_{ij}^6} \right\} \right]. \quad (6)$$

C. Results

The equilibrium values of these thermodynamic functions for eighteen temperature-density states of the system are listed in Table I. In Fig. 2, the data are plotted in the form of four pressure vs temperature isochores. If argon parameters, $T_c = 119.8^\circ\text{K}$, $\sigma = 3.405 \text{ \AA}$, are assumed, the unit of pressure is $14.264 \text{ dynes} \cdot \text{cm}^{-1}$, which is roughly equivalent to 4 atm if the model system is considered to be a σ -thick slice of a three-dimensional fluid.

In Table II, the pressures of the states listed in Table I are compared with those predicted by the two-dimensional Lennard-Jones-Devonshire theory. In all instances the L-J-D values are somewhat larger than those obtained directly from the dynamics data although, as might be expected from the solid-like nature of the L-J-D model, the differences are relatively smaller for the higher-density states.

D. Relation to Critical Point

The reduced temperature and density of the triple and critical points of real liquid argon are, respectively, $T_{tp}^* = 0.699$, $\rho_{tp}^* = 0.8387$, $T_c^* = 1.259$, and $\rho_c^* = 0.3164$.⁹ Evidence indicates however, that the critical point for the two-dimensional model system lies at a much lower temperature. For example, the (pseudo) critical temperature for an argon monolayer adsorbed on graphite is approximately $T_{2c}^* = 0.57$.¹⁰ The curvature of the isochores in Fig. 2 for $T^* < 0.9$ is consistent with a critical temperature on the

TABLE I. Thermodynamic state data from molecular dynamics calculations.

	ρ_R	ρ^*	$T^* = K^*$	P^*	V^*	U^*
1.	0.6781	0.6319	1.436	2.110	-1.544	-0.109
2.	0.6781	0.6319	1.067	1.328	-1.669	-0.603
3.	0.6781	0.6319	0.927	0.990	-1.750	-0.823
4.	0.6781	0.6319	0.896	0.888	-1.716	-0.820
5.	0.6508	0.6064	1.645	2.280	-1.434	+0.211
6.	0.6250	0.5824	1.558	1.849	-1.437	+0.122
7.	0.6250	0.5824	1.175	1.212	-1.503	-0.327
8.	0.6250	0.5824	1.015	0.923	-1.561	-0.546
9.	0.6250	0.5824	0.845	0.594	-1.580	-0.735
10.	0.6250	0.5824	$\left\{ \begin{array}{l} 0.792 \\ 0.763 \end{array} \right\}$	$\left\{ \begin{array}{l} 0.434 \\ 0.510 \end{array} \right\}$	$\left\{ \begin{array}{l} -1.716 \\ -1.688 \end{array} \right\}$	-0.925
11.	0.5358	0.4993	1.441	1.145	-1.231	+0.211
12.	0.5358	0.4993	1.099	0.759	-1.292	-0.193
13.	0.5358	0.4993	0.880	0.474	-1.406	-0.526
14.	0.5358	0.4993	0.838	0.411	-1.361	-0.523
15.	0.4645	0.4328	1.339	0.800	-1.090	+0.249
16.	0.4645	0.4328	1.145	0.625	-1.162	-0.017
17.	0.4645	0.4328	0.850	0.326	-1.216	-0.366
18.	0.4645	0.4328	0.815	0.285	-1.179	-0.365

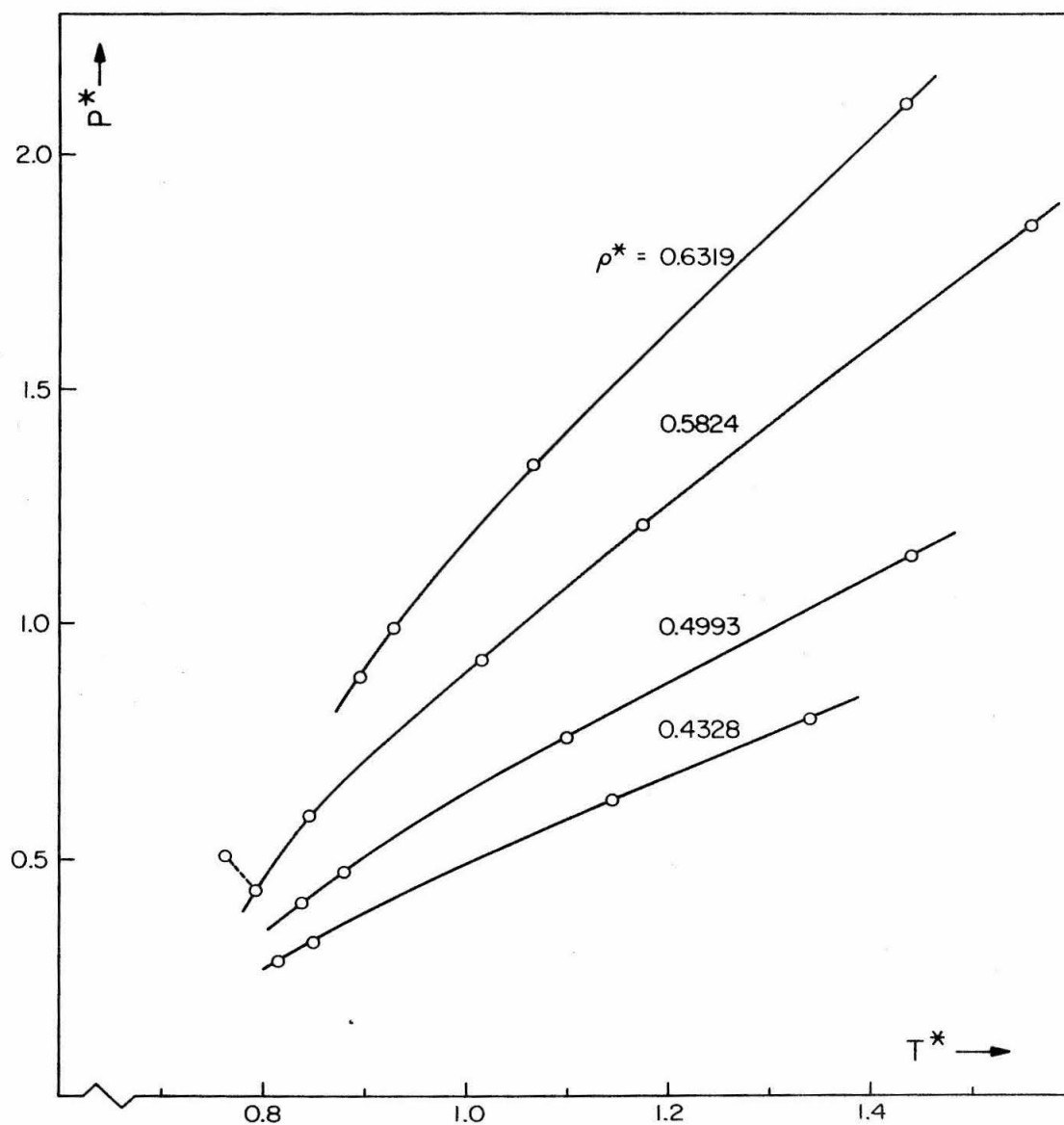


FIG. 2. Equilibrium thermodynamic data plotted as reduced pressure-temperature isochores. Off-isochore point may be related to a phase transition (see text).

TABLE II. Comparison of Molecular Dynamics and
Lennard-Jones-Devonshire Theory State Data

	A^*	ρ^*	T^*	P_{LJD}^*	\bar{P}_{MD}^*	$P_{LJD}^* - \bar{P}_{MD}^*$
1.	1.5824	0.6319	1.436	2.272	2.110	0.162
2.	1.5824	0.6319	1.067	1.397	1.328	0.069
3.	1.5824	0.6319	0.927	1.052	0.990	0.062
4.	1.5824	0.6319	0.896	0.975	0.888	0.087
5.	1.6490	0.6064	1.645	2.514	2.280	0.234
6.	1.7170	0.5824	1.558	2.143	1.849	0.294
7.	1.7170	0.5824	1.175	1.411	1.212	0.199
8.	1.7170	0.5824	1.015	1.096	0.923	0.173
9.	1.7170	0.5824	0.845	0.757	0.594	0.163
10.	1.7170	0.5824	0.792	0.650	0.434	0.216
			0.763	0.591	0.510	0.082
11.	2.0027	0.4993	1.441	1.403	1.145	0.258
12.	2.0027	0.4993	1.099	0.936	0.759	0.177
13.	2.0027	0.4993	0.880	0.635	0.474	0.161
14.	2.0027	0.4993	0.838	0.577	0.411	0.166
15.	2.3104	0.4328	1.339	0.957	0.800	0.157
16.	2.3104	0.4328	1.145	0.757	0.625	0.132
17.	2.3104	0.4328	0.850	0.450	0.326	0.124
18.	2.3104	0.4328	0.815	0.414	0.285	0.129

order of 0.7 for our two-dimensional system. A two-dimensional Lennard-Jones-Devonshire calculation (see Appendix) predicts a critical state $T_{c,LJD}^* = 0.699$, $\rho_{c,LJD}^* = 0.644$ for the system. The three-dimensional L-J-D theory¹¹ predicts a critical temperature of 1.30 for argon, which is surprisingly close to the observed value. The predicted critical density of 0.5656 is, however, about 80% larger than that observed experimentally.

E. Possible Phase Transition

In Table I, pairs of values are given for the temperature, pressure, and potential energy of state number 10. This is reflected in Fig. 2 as a pair of points connected by a dashed line. During an extended dynamics calculation for this "state", the thermodynamic functions exhibited a long-period, large amplitude oscillation superimposed upon the usual higher-frequency statistical fluctuations. The values given in the table are the approximate mean values of the maxima and minima of the long-period oscillation. While such behavior on the part of the thermodynamic functions is similar to that observed by Alder and Wainwright¹ during calculations in the phase transition region for hard spheres, it is probable that the oscillations observed here are more closely related to critical phenomena. (e)

IV. MICRO-STRUCTURE AND LOCAL ORDERING

A. Graphical Displays

Much of the existing quantitative information regarding the microscopic characteristics of dense fluids takes the form of correlation functions obtained by mathematical transformation of scattering intensity data for electromagnetic radiation or thermal neutrons.^{12, 13} Unfortunately, these correlation functions are primarily of a macroscopic nature, and the statistical averaging implicit in the scattering data may mask important details of the microscopic properties of the system under investigation. The scalar pair correlation function $g(r)$, for example, provides no indication of the nature of the local micro-structures thought to be responsible for the peculiarities observed in the absorption spectra of mercury dissolved in various simple liquids (vide infra). In contrast, graphical displays of computer-generated dynamics data permit the detailed examination of the microscopic structures and kinetics characteristic of the model fluids.

Three types of graphical displays have been investigated: static plots or "snapshots" of the system configuration at some instant of time, dynamic plots in the form of motion pictures created from sequences of snapshots for successive times, and plots of the trajectories of particle centers over selected time intervals. Figures 3-5 are snapshots of the system in states $[T^* = 0.927, \rho_R = 0.6781]$, $[T^* = 1.436, \rho_R = 0.6781]$, and

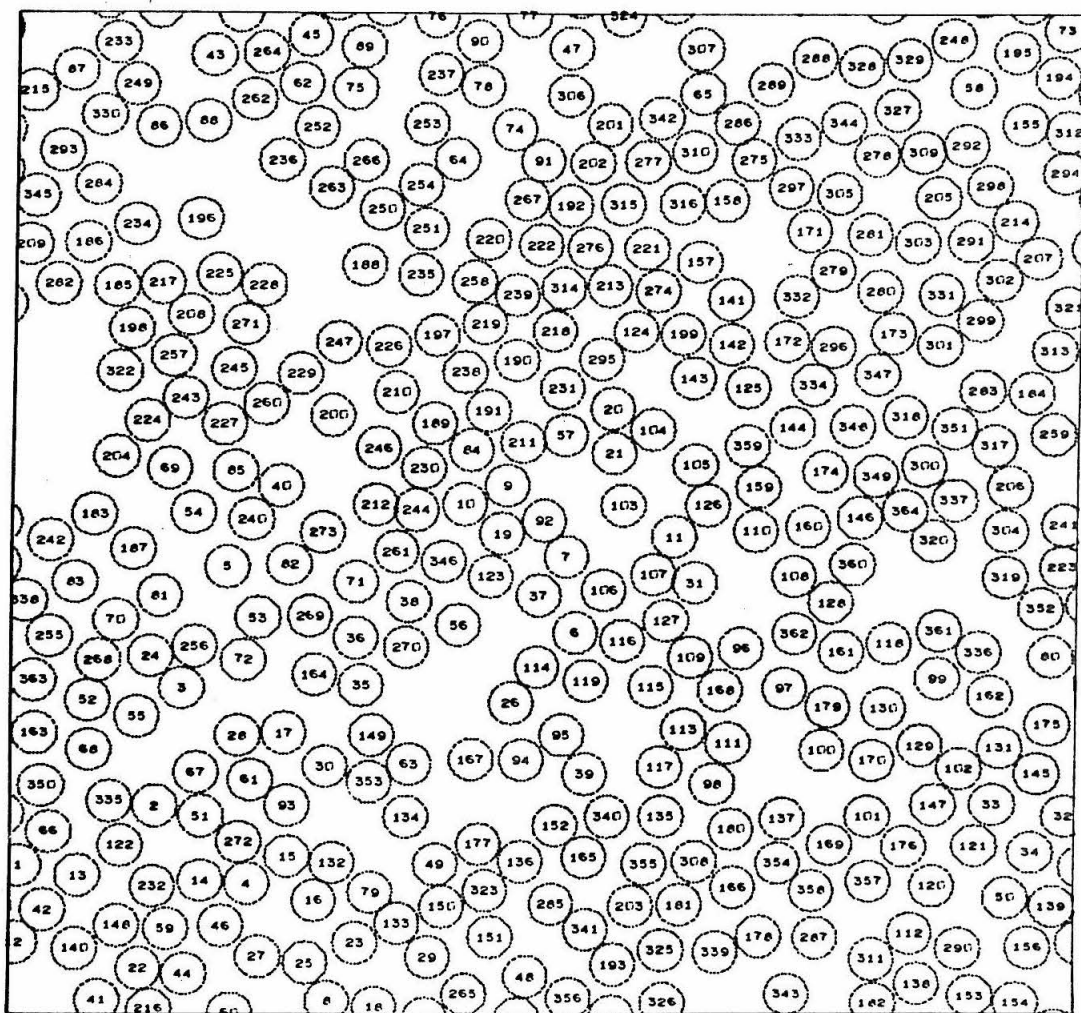


FIG. 3. Snapshot of instantaneous system configuration in state
 $T^* = 0.927$, $\rho_R = 0.6781$.

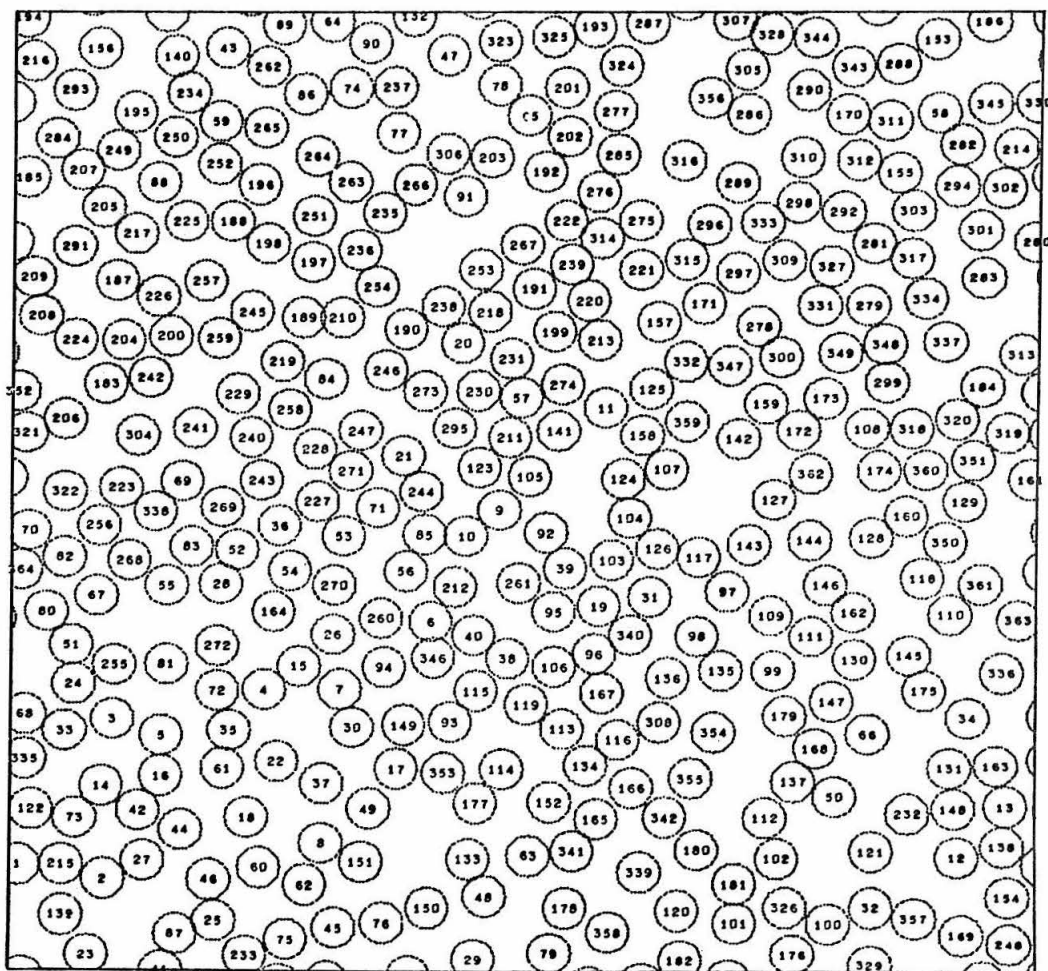


FIG. 4. Snapshot of instantaneous system configuration in state $T^* = 1.436$, $\rho_R = 0.6781$.

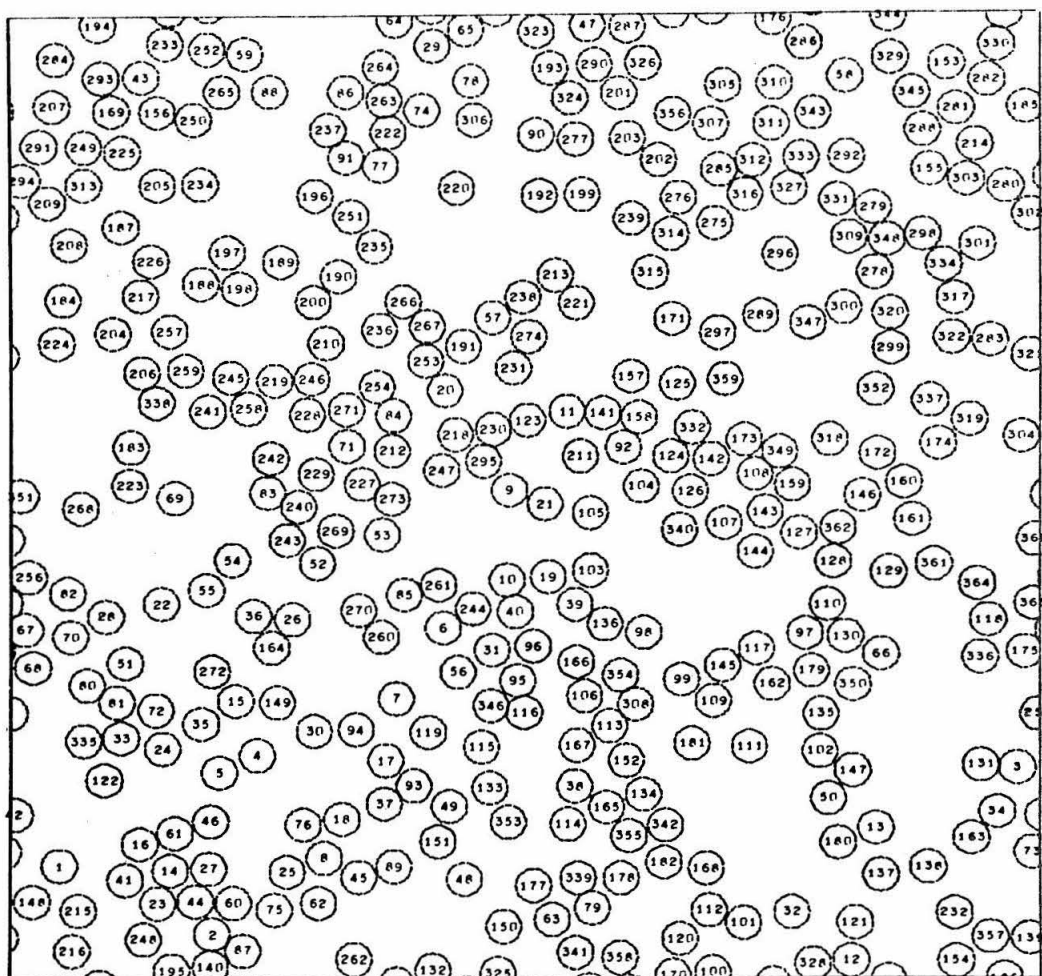


FIG. 5. Snapshot of instantaneous system configuration in
state $T^* = 1.145$, $\rho_R = 0.4645$.

[$T^* = 1.145$, $\rho_R = 0.4645$], respectively (states 3, 1, and 16 of Table I, respectively). The circles representing the disk-particles are drawn with relative diameter σ , and the superimposed numbers serve to identify the particles for purposes of comparison between snapshots for different times during the same calculation.

B. Holes or Vacancies

The presence of "holes" or "vacancies" in the particle distributions, even at the temperatures and densities shown in Figs. 3-4, is perhaps the most striking feature of the system micro-structures. Comparison of the $g(r)$ functions from liquid argon at several densities between the triple and critical point has indicated¹⁴ that thermal expansion of the real simple liquids must be accompanied by the formation of vacancies. But the phenomenon we observe here differs somewhat from that envisioned by the "fluidized vacancy" model for the liquid state. The vacancies appearing in the figures are quite irregular, and many encompass areas of several σ^2 . Furthermore, comparison of snapshots at various times during the same calculations has shown that many vacancies persist in the same region for times in excess of 3×10^{-12} sec.

Examination of plots of particle trajectories and dynamic plots of the system micro-kinetics has indicated that two factors are associated with the persistence of the vacancies: the attractive inter-particle potential and geometric effects. Attractions

between particles near the edge of a vacancy create, in essence, a "microscopic surface tension" that effectively prevents individual edge particles from moving out into the unoccupied area. Furthermore, single particles migrating into a vacancy several σ in diameter encounter a potential surface with a steep positive gradient toward the center of the vacancy; their subsequent motion is then largely restricted to migration along the edges. The disappearance of a larger vacancy is therefore usually associated with the concerted movement of a number of adjacent particles. At liquid-like densities, however, geometric effects--i.e. "jamming"--hinder the relative motion of local groups of particles and consequently motions of the type involved in the collapse of a vacancy.

The degree and stability of local ordering in the system is qualitatively a much stronger function of density than of temperature. More precisely, the disordering effect of thermal motion is diminished by increasing density. At low densities, the available void area permits the rearrangement of local micro-structures to proceed relatively unimpeded--whereas at higher, liquid-like densities geometric effects play a predominant role in the system micro-kinetics. This is further illustrated in Figs. 6-8 to be discussed in the next section.

C. Vacancies and Spectral Lineshapes

Vacancies of the sort observed here have also been postulated in conjunction with an explanation of the spectral features of mercury atoms dissolved in nonpolar fluids. The appearance of a maximum in the absorption spectrum of Hg in high density fluid argon¹⁵ very near the position of the Hg absorption line in crystalline argon was thought¹⁶ indicative of the presence of local solid-like regions or clusters in the fluid. A second component, resolved from the first and shifted to lower energy, was thought to arise from Hg atoms at cluster interfaces or near vacancies. The relative intensities of the two components change in a qualitatively expected way, the lower energy component becoming relatively more intense and the higher energy "solid-like" component gradually fading away with decreasing fluid density. At very low argon densities, neither component is present.

The two-dimensional snapshots obtained from the molecular dynamics data are consistent with this explanation for the mercury spectrum. The actual presence of solid-like regions and the large and persistent vacancies, the increased prevalence of vacancies vs solid-like regions with decreasing density (compare Figs. 3 and 5), and the lack of success in finding alternative explanations¹⁷ for the spectra all point to the plausibility of the original explanation. A quantitative description of the line shape is, however, still lacking.

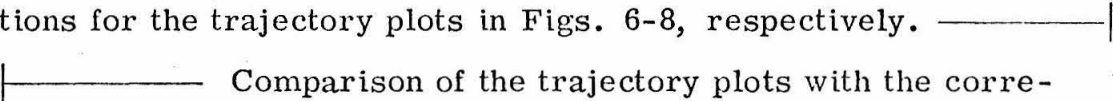
D. Clustering and Equilibration Processes

In Sec. II a clustering phenomenon was mentioned with respect to the time required for re-equilibration of the system after an "instantaneous expansion". Dynamic plots of the data from calculations for several different density states show that immediately after an expansion the particles in the system collect into numerous small clusters. If the final density is not too low, these clusters remain in contact through the pair potential and re-equilibration of the system occurs rapidly. At very low densities, however, the clusters may first equilibrate within themselves to produce a pseudo-equilibrium that may persist for times on the order of 2×10^{-12} sec before collisions between clusters permit the redistribution of energy over a significant fraction of the total system. Even in an equilibrium low-density state the contact between groups of particles may remain tenuous, resulting in occasional transient large-amplitude fluctuations in the instantaneous temperature and pressure of the system occurring when clusters collide.

V. SOME COMMENTS ON DIFFUSION PROCESSES^(f)

A. Trajectory Plots

Figures 6-8 show plots of particle trajectories for periods of 2×10^{-12} sec. The small circles mark the initial positions of the particle centers, and the irregular lines extending from the circles represent the paths of the centers during the remainder of the 2×10^{-12} sec interval. The dashed lines enclose regions to be noted specifically below.

The snapshots in Figs. 3-5 show the initial system configurations for the trajectory plots in Figs. 6-8, respectively.  Comparison of the trajectory plots with the corresponding snapshots provides some indication of correlations between local particle distributions and characteristic thermal motion.

B. Microdiffusive Motions

The particle motions exhibited in Figs. 6-8 may be qualitatively grouped into two modes: crystalline-like vibration and diffusive migration. The diffusive motion might further be divided into single-particle migration and cooperative "chain" or "cluster" diffusion. Comparison of Figs. 6-8 with the corresponding snapshots shows that vibration-like motions occur primarily in regions of high local density, while the more extensive diffusive motions are generally associated with vacancies or regions of low local density. Regions 3 in Fig. 6 and 1 in Fig. 8 show examples of cluster-diffusion into vacancies, while the indicated region in Fig. 7 shows

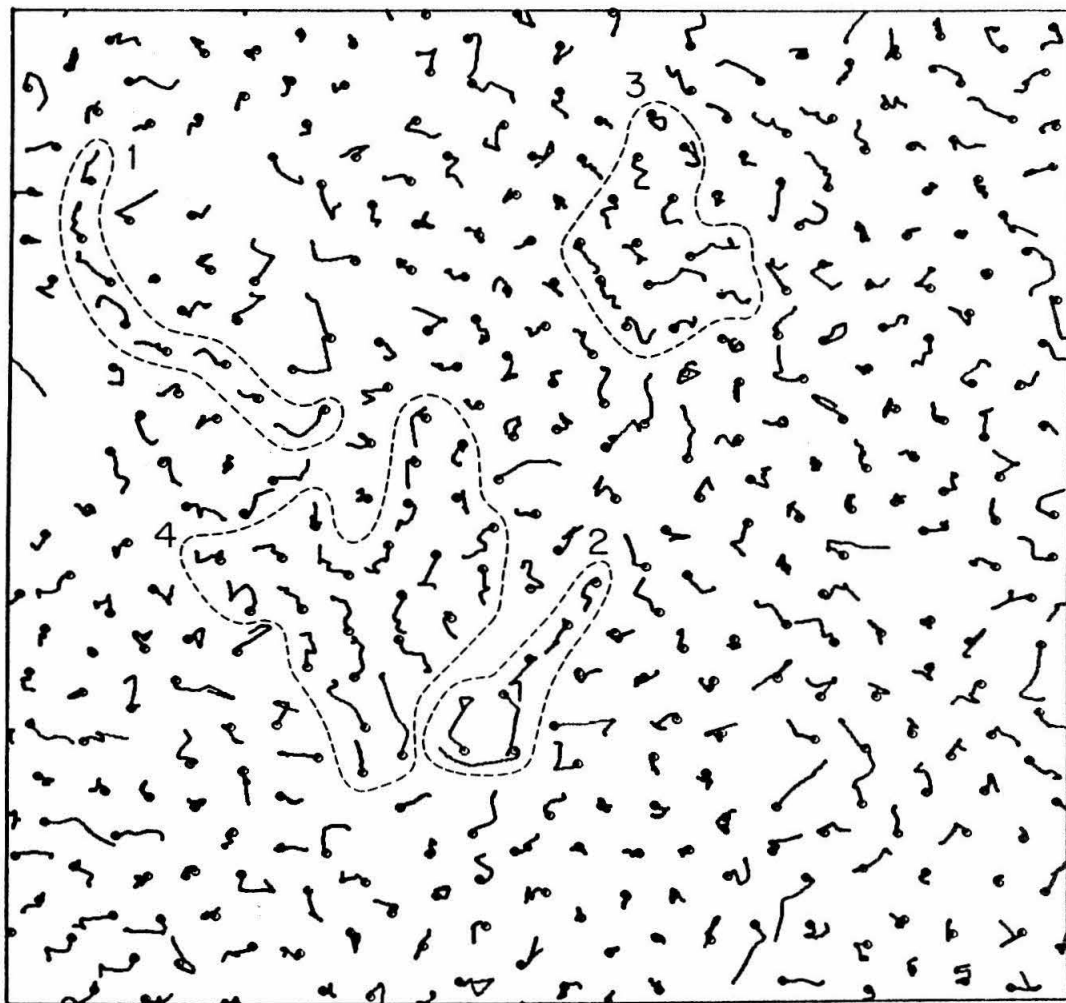


FIG. 6. Particle trajectories over a 2×10^{-12} sec interval in the system in state $T^* = 0.927$, $\rho_R = 0.6781$.

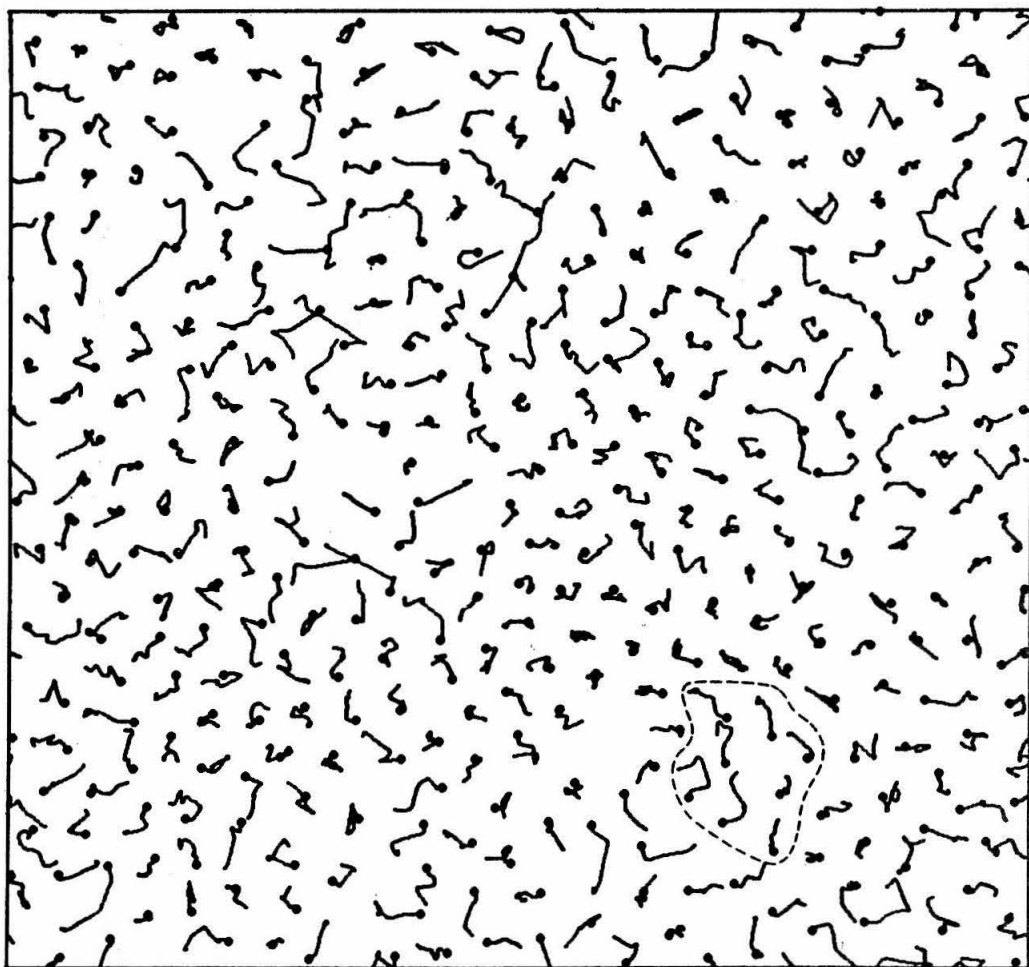


FIG. 7. Particle trajectories over a 2×10^{-12} sec interval in the system in state $T^* = 1.436$, $\rho_R = 0.6781$.

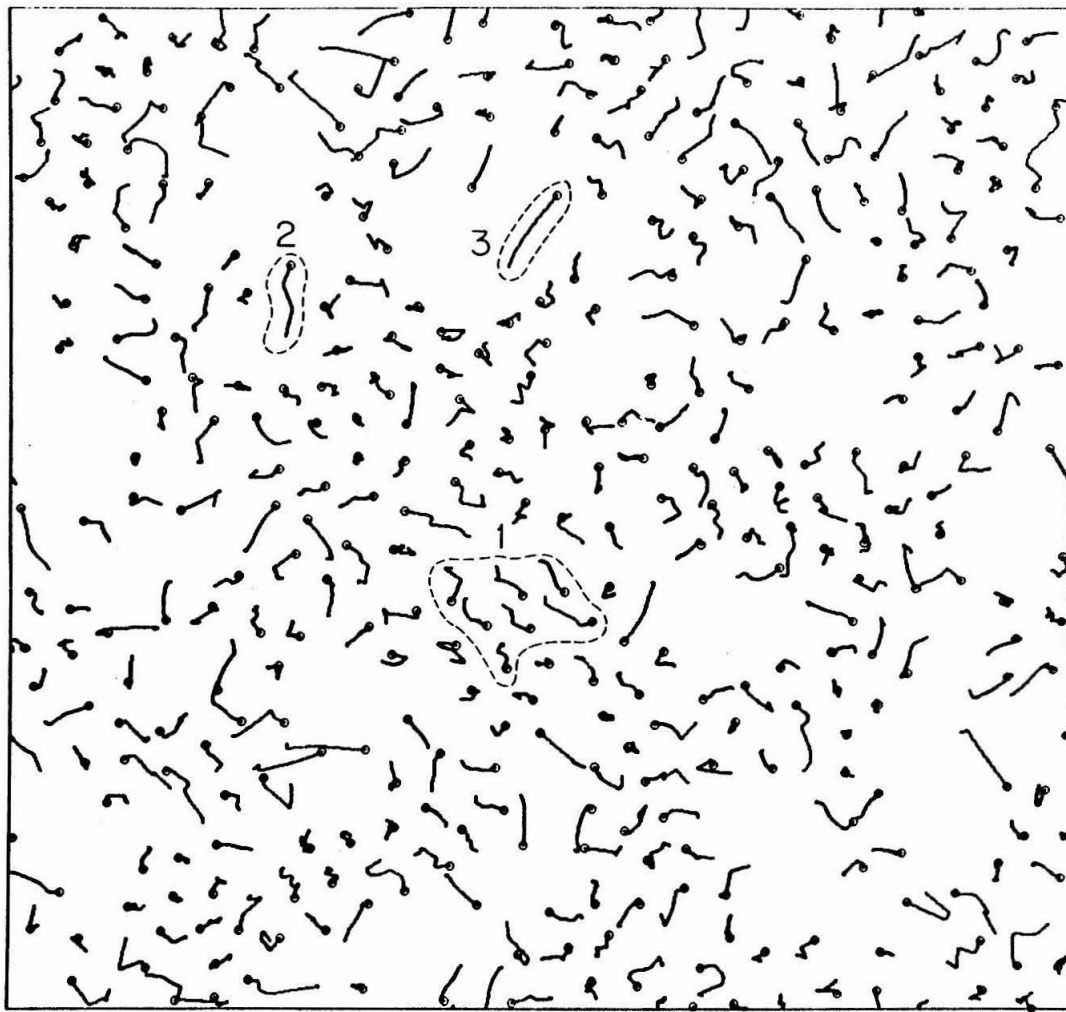


FIG. 8. Particle trajectories over a 2×10^{-12} sec interval in the system in state $T^* = 1.145$, $\rho_R = 0.4645$.

cluster-diffusion resulting in vacancy formation. Chain-diffusion is evident in regions 1 and 2 in Fig. 6; in region 2, the migration is along the edge of a vacancy. Region 4 in Fig. 6 shows a complex mixture of chain and cluster-diffusion in a region of low local density. Single-particle, uncorrelated migration of the sort executed by the particles in regions 2 and 3 in Fig. 8 is not conspicuous in the plots from the higher density states. Indeed, such uncorrelated motion is common only in the highest temperature, lowest density states examined.

C. Relation to Diffusion Theories

The micro-kinetics exhibited in the trajectory plots differ in various respects from those envisioned by existing theoretical models for diffusion in dense fluids. The cooperative nature of the motion--even at high temperature--is particularly striking, and could not be adequately described by a random-walk or Brownian-motion mechanism. While vacancies and regions of low local density appear to be intimately associated with diffusion processes, the motions exhibited in the trajectory plots would seem to be poorly described by a "jump-diffusion" model. Specifically, jump-diffusion implies a mechanism in which diffusion proceeds by the independent step-migration of single particles. Dynamic plots of the data from which the trajectory plots were created show, however, that the local groups of long trajectories in Figs. 6-8 arise from the concerted migration of the participating particles, rather than by successive jumps or knock-on collisions. We believe the system accomplishes this type of diffusive motion through the attractive inter-particle potential--groups of particles pulling each

other along--combined with the constraints imposed by the repulsive interactions in a crowded environment.

D. Micro-structure and Diffusion

Rahman⁶ has recently shown that the direction of displacement of a particle over short times is correlated with instantaneous distortions in the symmetry of its local environment; that is, an asymmetry in the spatial distribution of neighbors about a particle imposes a preferred direction on its subsequent thermal motion. Correlations of this sort would be expected to decay rapidly after times of the order of the characteristic relaxation time for the system, due to both thermal rearrangement of the local environment and motion of the particle itself. This idea is substantiated by a comparison of the 0.5×10^{-12} sec value given by Rahman for the "time of maximum correlation" with the velocity autocorrelation function presented in the same paper.

At first glance, the almost continuous diffusive migration indicated by some of the 2×10^{-12} sec particle trajectories shown in Figs. 6-8 would appear to be inconsistent with the short-time mechanism for micro-diffusion described by Rahman. Similarly, the rapid decay of the velocity autocorrelation function⁶ indicates that, on the average, the instantaneous direction of motion of a particle will change significantly several times during a 2×10^{-12} sec interval. Examination of the trajectory plots shows, however, that: (1) over any short-time interval, only a small fraction of the particles in a high-density system attain any appreciable diffusive displacement, and (2) migrating particles are generally associated with a group, all members of which

are diffusing in roughly the same direction. In a cooperative mechanism, then, the thermal motions of the neighbors about a diffusing particle are such as to maintain a continuous, or nearly continuous, environmental distortion in the same general direction as that in which the particle is migrating. That is, the particle executes micro-diffusive displacements in accordance with the short-time mechanism described by Rahman, but in a local environment which is itself involved in diffusive migration.

E. Cooperative Diffusion and Chemical Kinetics^(g)

The cooperative nature of diffusive motion in dense fluids is particularly important from the standpoint of chemical reaction kinetics since, within the framework of such a mechanism, a particle may undergo a relatively large diffusive displacement while encountering few, if any, "new" particles. A theoretical treatment of reaction kinetics based on a random walk model for diffusion and employing bulk diffusion coefficients for the reactants might then be expected to predict reaction rates (or more precisely, reactant encounter frequencies) in excess of those observed experimentally. Noyes¹⁸ has discussed this aspect of theoretical rate calculations in conjunction with a detailed analysis of kinetic data for iodine atom recombination in CCl_4 , drawing the conclusion that the microscopic anisotropy of the solvent may play an important role in the overall mechanism of even simple "diffusion-controlled" reactions. In particular, such would be the case when the reactant

and solvent molecules are of comparable size and mass since, under those conditions, the mechanism for reactant encounter would differ most markedly from that suggested by the random-walk model for reactant diffusion. A detailed analysis of particle encounter mechanisms in the molecular dynamics model will be the topic of a following paper.

VI. DISCUSSION

Several aspects of the microscopic properties of dense fluids have been discussed. Of these, the observations that: (1) the system micro-structure includes relatively large and persistent vacancies, and (2) cooperative mechanisms appear to be the dominant mode in diffusion processes, are perhaps most important. In evaluating the evidence presented for these qualitative observations, several factors must be considered. In particular, the densities and temperatures of the states examined thus far, and the dimensionality of the model deserve special comment.

While the relative densities of the states listed in Table I are all essentially liquid-like, they are somewhat lower than those of solvents generally employed in chemical reaction systems at STP conditions. From a "chemical" viewpoint, then, the amount of void area evident in Figs. 3 and 4 may be somewhat overemphasized. The apparent concentration of much of this void area into persistent vacancies--as opposed to a more random distribution of particles throughout the available space--is nonetheless

striking, especially when it is realized that the temperatures of all the states studied are very likely super-critical. The clustering in the high temperature, low density state shown in Figs. 5 and 8 is also rather surprising, and is indicative of the importance of the attractive inter-particle potential in determining the micro-structure of the fluid state.

The densities of the states examined are particularly important with respect to the discussion of diffusion mechanisms. Considering the high temperatures, one would expect the low density states to exhibit a high degree of structural disorder accompanied by a large amount of uncorrelated "free" particle motion, while at very high densities, one might conclude that there would be insufficient void area available to permit the concerted transit of clusters of more than a very few particles. Preliminary analysis of data from calculations for a 404-particle system in several states with $\rho^* = 0.7014$ indicates, however, that cooperative mechanisms remain the dominant mode for diffusion even at this higher density, —————| although chain-diffusion becomes considerably more prevalent than cluster-diffusion as the available void area is decreased. (h) It is conceivable that single-particle (jump-diffusion) mechanisms might become more important at very high densities and lower temperatures. However, our observation that the correlations in the particle motions appear to be strongly associated with the attractive inter-particle potential would indicate that uncorrelated migration should become less rather than more important with decreasing temperature.

Futrelle¹⁹ has suggested certain simple relationships between thermodynamic quantities in two and three dimensions. For microscopic processes, the absence of a third degree of freedom could have a significant effect. In particular, "geometric effects" should be relatively more important in two dimensions than in three. With respect to the formation and persistence of vacancies, however, the "microscopic surface tension" due to the attractive inter-particle potential appears to be much more important than any geometric factor--and the potential energy contributing to this effect would be enhanced in three dimensions.

ACKNOWLEDGEMENTS

The author wishes to thank Dr. R. P. Futrelle for many hours of helpful discussion and consultation, and Professor G.W. Robinson for his support and aid in the preparation of this paper.

APPENDIX

Calculations based on a two-dimensional Lennard-Jones-Devonshire theory have been performed to obtain some purely theoretical thermodynamic data for comparison with the molecular dynamics results. In this Appendix, we briefly describe the manner in which these calculations were performed. The —————|

comparison of the L-J-D results with the molecular dynamics data is presented in Table II in the main body of this paper.

The canonical partition function Z_N for a two-dimensional system of N disk-particles of mass \underline{m} confined to area A is related to the configurational partition function Q_N by:

$$Z_N(A, T) = \left(\frac{2\pi m}{h^2 \beta} \right)^N Q_N(A, T), \quad (A1)$$

where h is Planck's constant and $\beta = (1/k_B T)$. Within the framework of the Lennard-Jones-Devonshire cell theory, Q_N has the form:

$$Q_N(A, T) = \exp(-\beta \Phi_0) a_f^N, \quad (A2)$$

where Φ_0 is the lattice energy when all particles lie at the centers of their respective cells, and the free area a_f is given by:

$$a_f = \int_{\text{cell}} \exp \{ -\beta [\psi(\underline{r}) - \psi(o)] \} d\underline{r}. \quad (A3)$$

In Eq. (A3), $\psi(\underline{r})$ is the energy of a particle at \underline{r} relative to the center of its cell, and the integration is over the interior of the cell.

In computing Φ_0 and a_f , it is convenient to group together the energy contributions of successive "shells" of neighboring particles (nearest, second-nearest, etc., ... neighbors). The formulations are also simplified by transformation to reduced units, as described in Sec. III. The reduced lattice energy is then given by:

$$\Phi_0^* = \frac{\Phi_0}{N\epsilon} = 2 \sum_n m_n \{ \alpha_n^{-12} - \alpha_n^{-6} \}, \quad (\text{A4})$$

where m_n is the number of particles in the n^{th} neighbor shell, α_n the distance between n^{th} -nearest neighbors in units of σ , and where, for the truncated pair potential, the summation is over only those shells for which $\alpha_n \leq 2.5$. In this calculation, we assume the centers of the cells to lie at the vertices of a regular two-dimensional hexagonal lattice.

The free area integral a_f is calculated using a "smeared field" approximation²⁰ to obtain an angle-independent average cell potential. In this two-dimensional theory, the "smeared" cell potential $\langle \psi(\rho) - \psi(o) \rangle^*$ may be calculated from the formula

$$\langle \psi(\rho) - \psi(o) \rangle^* = \sum_n m_n \left(\frac{1}{\pi} \right) \int \{ \varphi^*([\alpha_n + \rho^2 - 2\alpha_n \rho \cos \theta]^{\frac{1}{2}}) - \varphi^*(\alpha_n) \} d\theta, \quad (\text{A5})$$

where $\langle \psi(\rho) - \psi(o) \rangle^*$, in units of ϵ , is now a function only of displacement ρ in units of σ , and φ^* is the truncated reduced pair potential.

Integration of Eq. (A5) yields

$$\langle \psi(\rho) - \psi(o) \rangle^* = 4 \sum_n m_n \{ (\alpha_n - \rho)^{-6} P_5(x) - (\alpha_n - \rho)^{-3} P_2(x) \} - 4 \sum_n m_n \{ \alpha_n^{-12} - \alpha_n^{-6} \}, \quad (\text{A6})$$

where the P_i are Legendre polynomials, and x is given by:

$$x = (\alpha_n^2 + \rho^2) / (\alpha_n^2 - \rho^2).$$

The cell potential is plotted as a function of ρ for several reduced areas A^* in Fig. A-1. As in the case of the three-dimensional L-J-D theory,²¹ the minimum of the cell potential does not lie at the center of the cell for densities lower than about 0.7. This problem is not so serious in the two-dimensional theory, since the central "hump" in the cell potential is relatively lower in two dimensions than in three. In particular, the total cell energy at the two-dimensional critical point (vide infra) is positive, which is not the case in three dimensions.

With the cell field formulated as in Eq. (A6), the reduced free area integral becomes

$$a_f^* = \int_0^{\rho_{\max}} \exp \{ -\beta \epsilon \langle \psi(\rho) - \psi(o) \rangle^* \} \sigma^2 2\pi \rho \, d\rho, \quad (\text{A7})$$

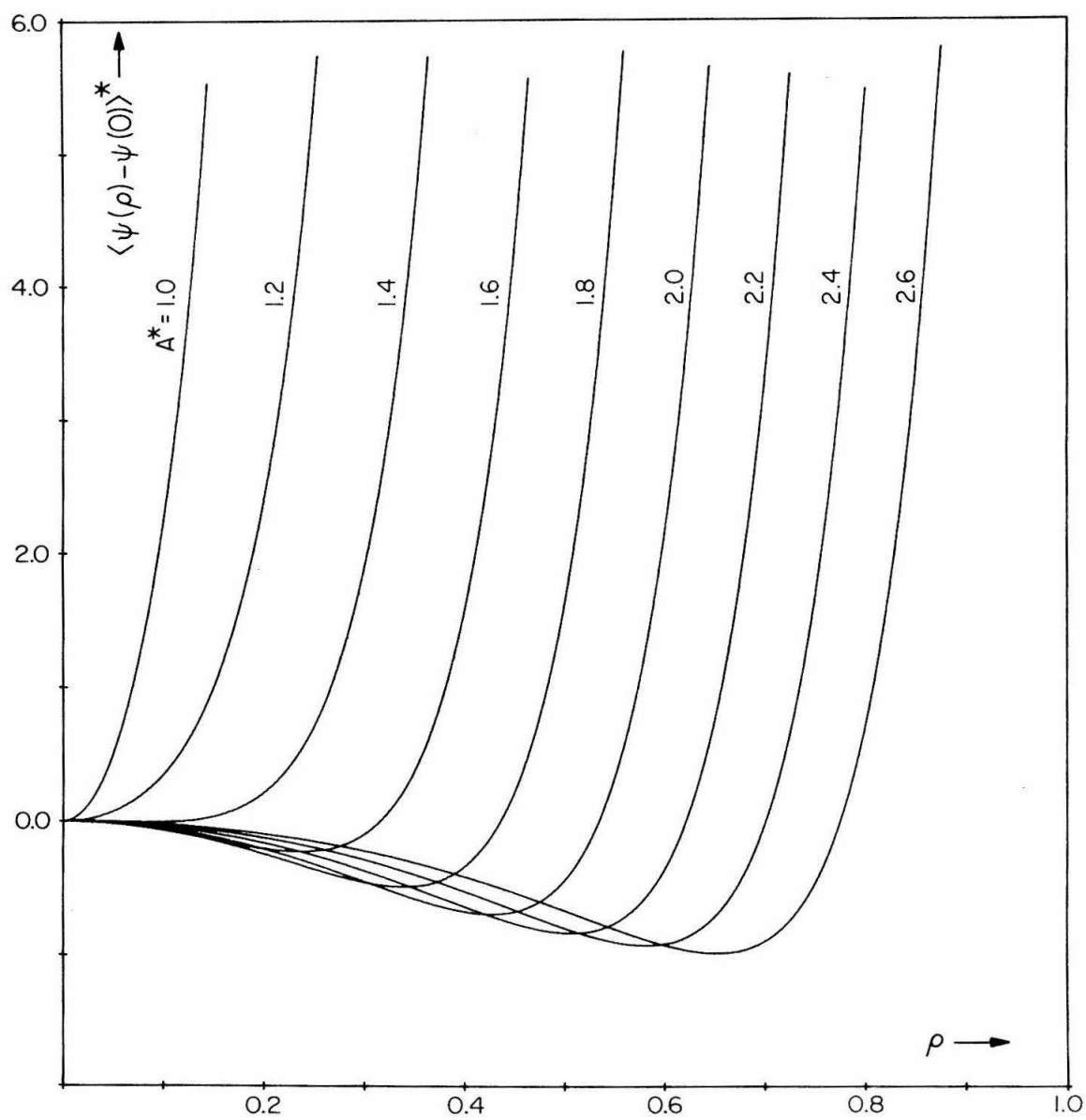


FIG. A-1. Plots of the "smeared" cell potential for several reduced lattice areas.

where ρ_{\max} may be chosen so that $\pi\rho_{\max}^2 = A^*$. In practice, the integral in Eq. (A7) is computed numerically, and in all cases discussed here the integrand was found to approach zero rapidly for values of ρ somewhat less than ρ_{\max} .

The canonical partition function Z_N is related to the Helmholtz free energy F by the well-known equation:

$$F = -kT \ln Z_N .$$

In reduced units,

$$F^* = \frac{F}{N\epsilon} = -T^* \ln \left(\frac{2\pi m}{h^2 \beta} \right) + \Phi_0^* - T^* \ln a_f^* . \quad (A8)$$

In Fig. A-2, F^* is plotted as a function of A^* for several temperatures. The pressure isotherms in Fig. A-3 are obtained from the F^* isotherms by numerical differentiation. While the pressure isotherms for lower temperatures exhibit the familiar sigmoid shape, the negative slope of the isotherms at large values of A^* is insufficient to permit the determination of an approximate coexistence region. A "critical point" may, however, be determined from the conditions

$$\left(\frac{\partial P^*}{\partial A^*} \right)_{T^*} = \left(\frac{\partial^2 P^*}{\partial A^{*2}} \right)_{T^*} = 0 ,$$

which are found numerically to hold for the state

$$T_c^* = 0.699 \quad A_c^* = 1.552$$

$$P_c^* = 0.474 \quad (\rho_c^* = 0.644)$$

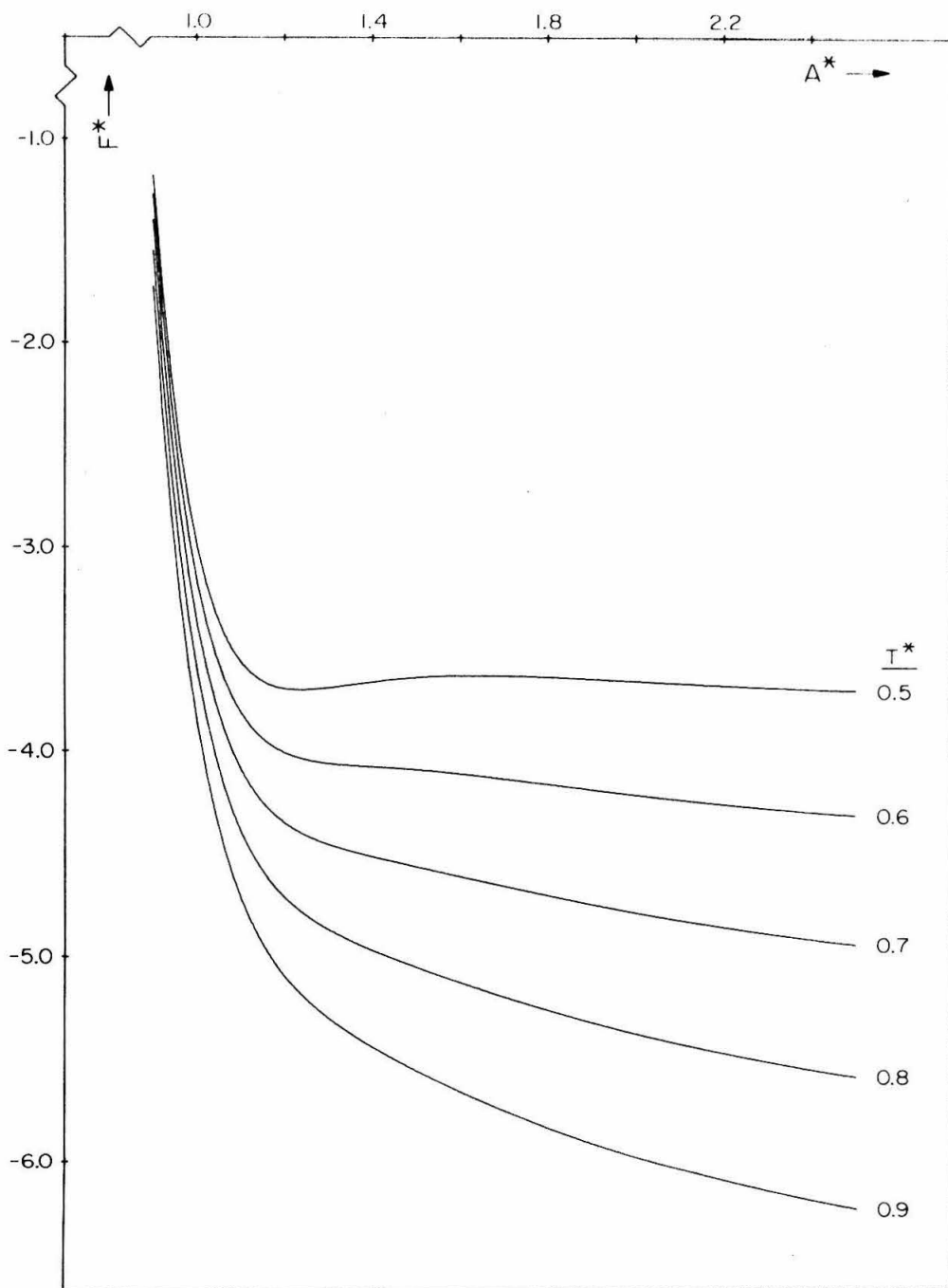


FIG. A-2. Plots of reduced free energy isotherms for several temperatures.

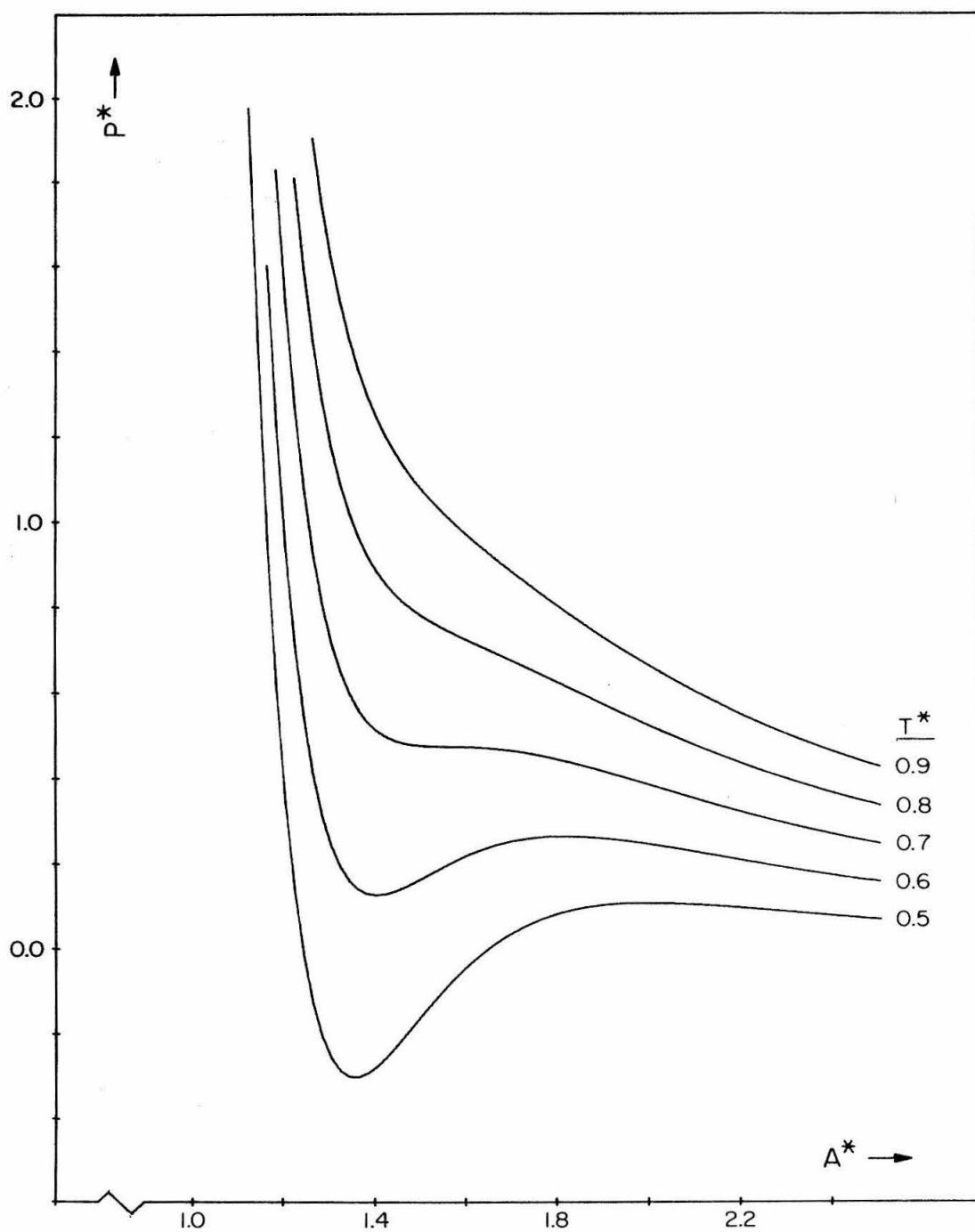


FIG. A-3. Plots of reduced pressure isotherms for several temperatures.

REFERENCES FOR PAPER NO. 1

1. B. J. Alder and T. E. Wainwright, J. Chem. Phys. 31, 459 (1959); ibid. 33, 1439 (1960).
2. B. J. Alder and T. E. Wainwright, Phys. Rev. 127, 359 (1962).
3. B. J. Alder, Phys. Rev. Letters 12, 317 (1964).
4. B. J. Alder and T. Einwohner, J. Chem. Phys. 43, 3399 (1965).
5. A. Rahman, Phys. Rev. 136, A405 (1964).
6. A. Rahman, J. Chem. Phys. 45, 2585 (1966).
7. L. Verlet, Phys. Rev. 159, 98 (1967); ibid. 165, 201 (1968).
8. J. L. Lebowitz, J. K. Perkus, and L. Verlet, Phys. Rev. 153, 250 (1967).
9. These values obtained by numerical conversion of experimental data provided in G. A. Cook, Ed., Argon, Helium and the Rare Gases (Interscience Publishers, Inc., New York, 1961), Vol. I.
10. C. F. Prenzlow and G. D. Halsey, Jr., J. Phys. Chem. 61, 1158 (1957).
11. J. A. Barker, Lattice Theories of the Liquid State, E. A. Guggenheim, J. E. Mayer, and F. C. Tompkins, Eds. (Pergamon Press, Ltd., Oxford, England, 1963), p. 61.
12. P. A. Egelstaff, Brit. J. Appl. Phys. 16, 1219 (1965).
13. H. H. Paalman and C. J. Pings, Rev. Mod. Phys. 35, 389 (1963).
14. H. Eyring and R. P. Marchi, J. Chem. Educ. 40, 562 (1963).
15. J. Robin, R. Bergeon, L. Galatry, and B. Vodar, Discussions Faraday Soc. 9, 30 (1956).
16. G. W. Robinson, Mol. Phys. 3, 301 (1960).

17. S. N. Vinogradov and H. E. Gunning, J. Phys. Chem. 68, 1962 (1964).
18. R. M. Noyes, J. Am. Chem. Soc. 86, 4529 (1964).
19. R. P. Futrelle, private communication.
20. See, for example, J. A. Barker, op. cit., p. 50.
21. See, for example, the discussion in J. M. H. Levelt and E. G. D. Cohen, Studies in Statistical Mechanics, J. De Boer and G. E. Uhlenbeck, Eds. (North-Holland Publishing Co., Amsterdam, 1964), Vol. II, p. 143 ff.

C. Notes and Addenda to Paper No. 1

- a. Papers dealing with purely theoretical treatments of the liquid state have in recent years begun to show an increasing consciousness of the results obtained through computer calculations of the sort described here. To date, comparisons between computer and theoretical results have largely been limited to such quantities as the equation-of-state or radial distribution function. But as information regarding the computer simulation techniques becomes more widely disseminated, it is expected that theoreticians will also begin to look to the computer results for guidance in the development of new theoretical models.
- b. Further analysis indicates that, at least for the present, simulation studies of a monatomic solute-solvent system are not practical. That is not to say that the basic simulation calculations could not be performed using existing computer hardware. Rather, the information one might hope to acquire from such an investigation would not seem to justify the necessary expenditures of programming effort and computer time.
- c. The periodic boundary conditions can indeed interfere with the calculation of transport-related time-correlation functions from the simulation data. In particular, the analysis programming must be provided with a facility to check for the migration of particles across adjacent edges of the space-box.

- d. The "reduced" thermodynamic quantities defined here are the two-dimensional analogues of the reduced quantities described by J. M. H. Levelt and E. G. I. Cohen in Studies in Statistical Mechanics, J. De Boer and G. E. Uhlenbeck, Eds. (North-Holland Publishing Co., Amsterdam, 1964), Vol. II, p. 144 ff, and are compatible with the so-called "theory of corresponding states."
- e. At first sight, this possible phase transition might seem to offer an interesting opportunity for further study. The experience reported by Alder and Wainwright indicates however that the molecular dynamics technique is not well suited to an investigation of the phase transition region for a model fluid. It is difficult to achieve a genuine separation of phases in a system of (relatively) so few particles; instead, the system as a whole oscillates between the two alternative phases as the dynamics calculation proceeds. The systems of "hard" particles studied by Alder and Wainwright were found to transit from phase to phase in the space of a single thermal oscillation, thus yielding well-defined intervals during which the system was in one phase or the other. But there is reason to believe that a system of particles interacting with a "softer", attractive potential would shift from phase to phase much more slowly, making it difficult to determine even equilibrium thermodynamic properties for either of the phases.
- f. A more detailed analysis of diffusion in the model fluid is presented in Paper No. 3, the manuscript for which is reproduced in subsection IV. B, page 129.

- g. A quantitative analysis of the effect of a cooperative diffusion mechanism upon the kinetics of a "diffusion-controlled" reaction in solution is provided in Paper No. 4, the manuscript for which is reproduced in subsection IV.C, page 179.
- h. A graphic display of diffusion in the high density model fluid is provided by the trajectory plot reproduced as Fig. 2 in Paper No. 3, page 133.

D. Paper No. 2

"Anomalies" in the Radial Distribution Functions
for Simple Liquids*

Paul L. Fehder

Arthur Amos Noyes Laboratory of Chemical Physics,[†]
California Institute of Technology, Pasadena, California 91109

Abstract. Subsidiary features appearing in the radial distribution functions obtained by x-ray or neutron diffraction measurements on a number of simple liquids have long been the object of speculation and some controversy. Distribution functions calculated from the configuration data for a computer-simulated model of a dense fluid of Lennard-Jones disks show similar additional structure. In the case of the model system, this additional structure may reflect an alternative configuration for local ordering within the fluid.

*This work was supported in part by a grant from the National Science Foundation, No. GP-7258.

[†]Contribution No. 3928.

I. INTRODUCTION

Since publication of the early results by Eisenstein and Gingrich,¹ small subsidiary features appearing in the experimentally measured radial distribution functions $g(r)$ for a number of simple liquids have been the object of speculation and some controversy. These subsidiary features usually take the form of sub-peaks or shoulders superimposed upon the otherwise smooth undulations of the "principal" structure of the distribution function, and most frequently appear in the region of the first principal minimum.

The controversy surrounding these "anomalous" features in $g(r)$ encompasses a number of different factors. From a theoretical standpoint, the existence of such sub-structure in the radial distribution functions for the simplest of liquids (e.g., the liquified noble gases) could have serious implications with respect to the statistical mechanics of dense fluids. The additional structure might for example be considered indicative of the importance of many-body potentials at liquid-like densities. Or alternatively, the subsidiary structure might be attributed to correlations in the spatial distributions of particles in a liquid spanning greater distances and many more particles than is presently suspected.

Unfortunately, the issue is clouded by the complexity of the analytical procedures that must be employed to obtain $g(r)$ from experimental diffraction data.² Several authors have, on the basis of the folding theorem,³ attributed the subsidiary features appearing in their published radial distribution functions to finite truncation of the Fourier inversion integral. In a recent study of the data from liquid krypton, Khan⁴ however has concluded that the principal source of these irregularities lies in the experimental data themselves rather than in the truncation error. This view is also supported by Mikolaj and Pings,⁵ although they suggest that the irregularities are probably due to errors in the experimental measurements while Khan is of the opinion that the features appearing in the krypton data reflect actual structure in the liquid. The effect on the resultant $g(r)$ of systematic errors in the experimental intensity measurements has been examined by Finbak.⁶

Another factor contributing to the controversy is that
 |————— some measurements have shown subsidiary structure while others have not. Subsidiary features appeared in the functions obtained by x-ray measurements on neon,⁷ argon,¹ and xenon,⁸ and by neutron measurements on krypton,⁹ but were absent in the data from neutron measurements on neon¹⁰ and argon,¹¹ and from two more recent x-ray measurements on argon.^{5, 12} Some new measurements by Smelser,¹³ extending the work of Mikolaj and Pings to higher densities, indicate that these features may appear in the distribution functions for only a relatively narrow

range of thermodynamic states having densities somewhat higher than the critical density but lower than that of the triple point. Thus the scarcity of data for "intermediate" densities may provide a partial explanation for the apparent inconsistency of the experimental results reported thus far.

In a recent paper ¹⁴ this author reported some preliminary results from a series of computer calculations simulating the microscopic dynamics of a two-dimensional dense fluid of Lennard-Jones disks. The radial distribution functions computed directly from the time-dependent particle positions exhibit subsidiary features similar to those appearing in some of the experimentally determined functions reported in the literature. Since the system parameters are well defined in the simulation calculations and the microscopic structure of the model fluid can be examined in great detail, it is felt that our findings may shed new light on the nature and authenticity of the features in real liquids.

II. METHOD OF CALCULATION

The computational algorithm and techniques used in performing the simulation calculations have been described in detail in our previous paper¹⁴ and the earlier paper by Rahman.¹⁵ In essence, the computer programs perform a simultaneous step-wise numerical time-integration of the equations of motion of the several hundred particles comprising the model fluid. Reduced variables¹⁶ are employed, and the positions and velocities of the particles are recorded on magnetic tape after each step in the integration for subsequent analysis.

Since preparation of the manuscript for Ref. 14, calculations simulating five additional temperature-density states of the model fluid have been completed. Thermodynamic data for these five states are presented in Table I.

For two dimensions the radial distribution function is given by:

$$g(r) = \left(\frac{A}{N}\right) \left[\frac{n(r)}{2\pi r \Delta r} \right] ,$$

where A and N are the area and number of particles in the system, respectively, and n(r) is the time-average number of particles situated at a distance $r \pm (\Delta r/2)$ from a given particle. In practice, n(r) is averaged over the distribution of neighbors around each of the N particles in the system, and then over the configurations of the system for a large number of successive times. The functions were computed to a radius $r = 3.5$ with an incremental Δr value of 0.025,

TABLE I. Thermodynamic state data from additional molecular dynamics calculations.^a

N	ρ_R	ρ^*	$T^* = K^*$	P^*	V^*	U^*
404	0.7527	0.7014	0.982	1.736	-1.898	-0.917
404	0.7527	0.7014	0.766	1.004	-1.999	-1.233
404	0.7527	0.7014	0.676	0.834	-2.008	-1.332
444	0.8272	0.7708	1.341	4.386	-1.888	-0.546
444	0.8272	0.7708	0.904	2.635	-2.093	-1.189

^aThis table is an addendum to Table I in Ref. 14. The entries in the table are: N is the number of particles in the system. ρ_R and ρ^* are the relative and reduced densities of the thermodynamic state. T^* is the temperature, K^* the kinetic energy, P^* the pressure, V^* the potential (internal) energy, and U^* the total energy of the thermodynamic state, all expressed in reduced units.¹⁶

and averaged over times that varied between 0.5 and 1.4×10^{-12} sec with calculations at intervals of either 3.0 or 5.0×10^{-14} sec.

III. STRUCTURE OF THE RADIAL DISTRIBUTION FUNCTIONS

Figure 1 is a diagram of the temperature-density states of the model fluid for which radial distribution functions have been computed. Specific states will be referred to according to the numbering in Table II. Examples of the calculated functions are shown in Figs. 2-5. For syntactic simplicity, the radial distribution functions obtained by experimental measurements on real fluids will hereafter be referred to as "experimental functions," and those calculated from the simulation data as "model functions."

The principal structure of the model functions appears in all respects quite similar to that of the experimental functions reported in the literature. In general, the overall structure of the radial distribution function for the model fluid is a much stronger function of density than of temperature in the temperature and density ranges examined. More precisely, the sensitivity to temperature is amplified by decreasing density. This effect is illustrated, for example, by the average number of neighbors and peak-height data presented in Table II.

The model functions for the five states with densities above 0.7 exhibit three well-defined maxima (see, e.g., Fig. 2), indicating that additional maxima would probably have been observed had the functions been computed to larger radius. At lower densities the third

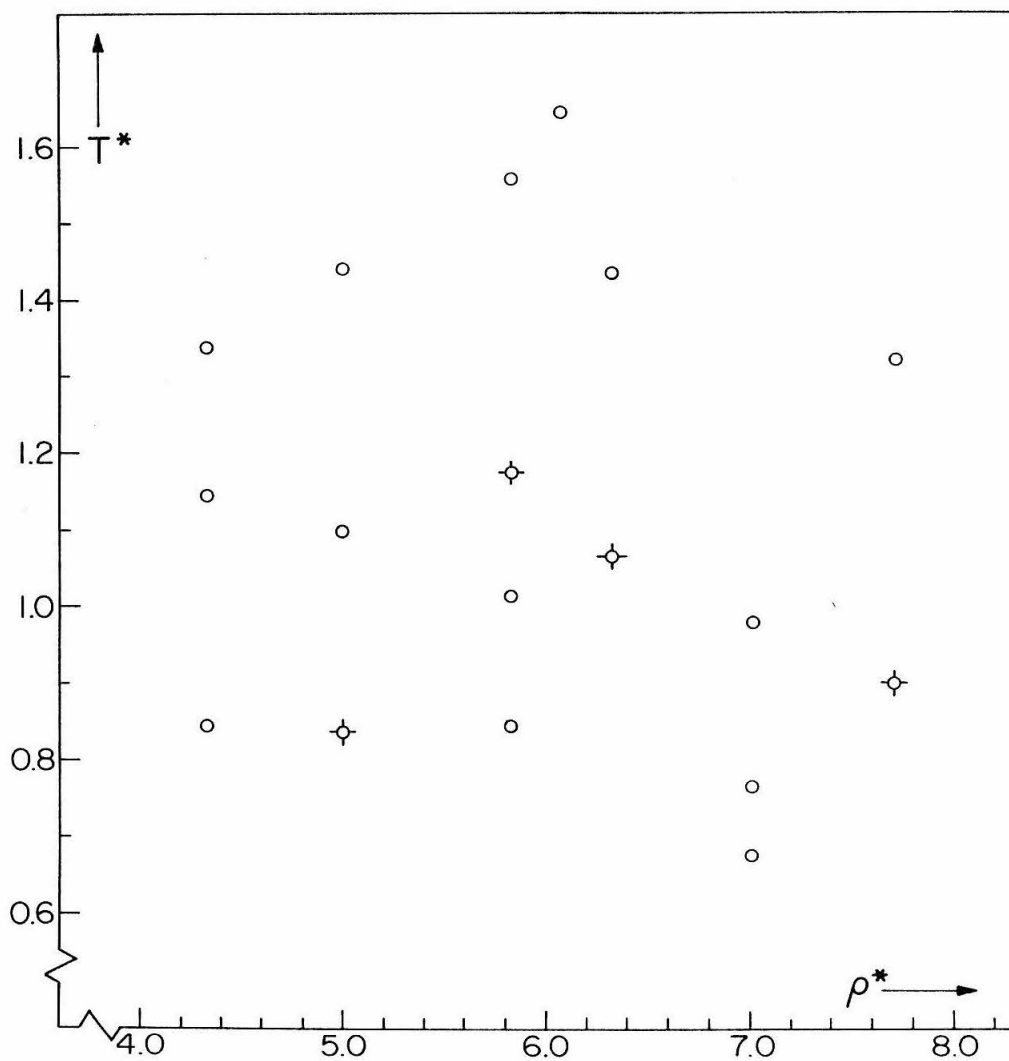


FIG. 1. Temperature-density states of the model system for which radial distribution functions were computed. Accents indicate states for which functions are shown in accompanying figures.

TABLE II. $g(r)$ Function Data Summary.^a

ρ^*	T^*	g_{\max}	r_1	r_2	\bar{n}_1	\bar{n}_2
0.7708	1.324	2.96	1.07	2.13	5.71	10.62
0.7708	0.904	3.22	1.09	2.15	5.73	10.78
0.7014	0.982	2.82	1.09	2.20	5.46	10.72
0.7014	0.766	3.06	1.10	2.20	5.37	10.38
0.7014	0.676	3.11	1.12	2.20	5.36	10.12
0.6319	1.436	2.29	1.12	2.23	4.90	9.96
0.6319	1.067	2.55	1.12	2.20	4.93	9.80
0.6064	1.645	2.23	1.12	2.23	4.75	9.42
0.5824	1.558	2.25	1.12	2.25	4.54	8.67
0.5824	1.175	2.46	1.12	2.23	4.62	8.78
0.5824	1.015	2.54	1.12	2.23	4.67	8.11
0.5824	0.845	2.55	1.12	2.22	4.70	8.94
0.4993	1.441	2.13	1.12	----	4.12	----
0.4993	1.099	2.31	1.12	----	4.13	----
0.4993	0.838	2.59	1.12	2.21	4.14	7.31
0.4328	1.339	2.14	1.12	2.28	3.40	----
0.4328	1.145	2.41	1.12	----	3.53	----
0.4328	0.844	2.60	1.12	2.23	3.60	5.94

^aThe entries in this table are: ρ^* , T^* are the reduced density and temperature of the thermodynamic state, respectively. g_{\max} is the value of the distribution function at the first principal maximum. r_1 , r_2 are the positions of the first and second principal maxima. \bar{n}_1 , \bar{n}_2 are the average numbers of first- and second-nearest neighbors, obtained by integrating under the first and second principal maxima, respectively. The integrations were performed from minimum to minimum. Blank spaces in the table indicate that the second maximum was insufficiently well-defined to permit evaluation of the indicated quantity.

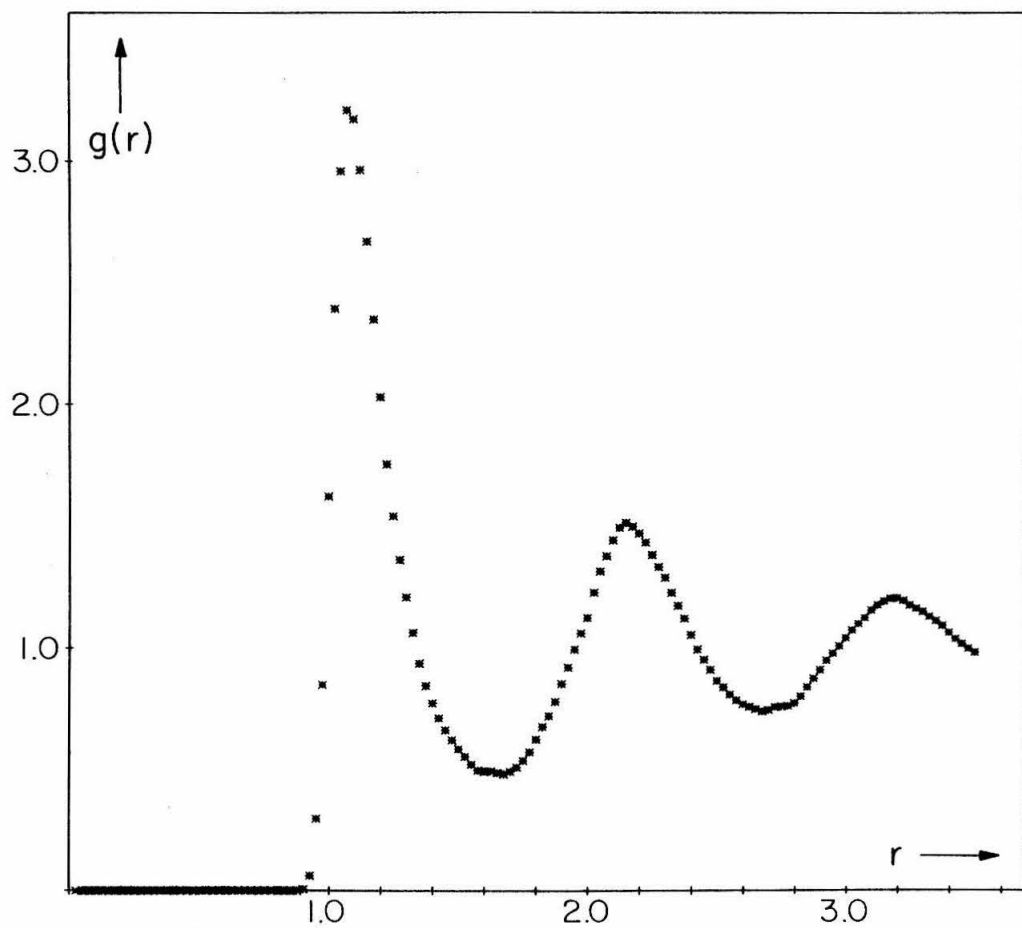


FIG. 2. Radial distribution function for the state $T^* = 0.904$,
 $\rho^* = 0.7708$.

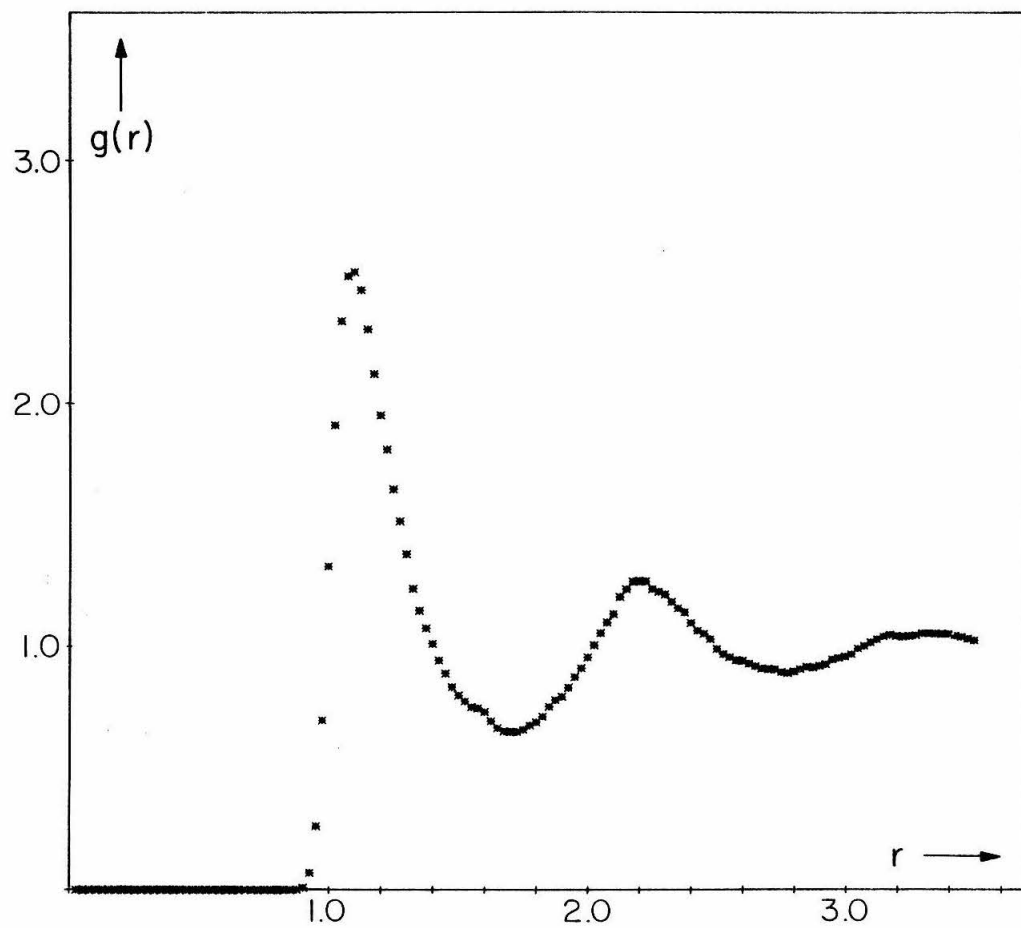


FIG. 3. Radial distribution function for the state $T^* = 1.067$,
 $\rho^* = 0.6319$.

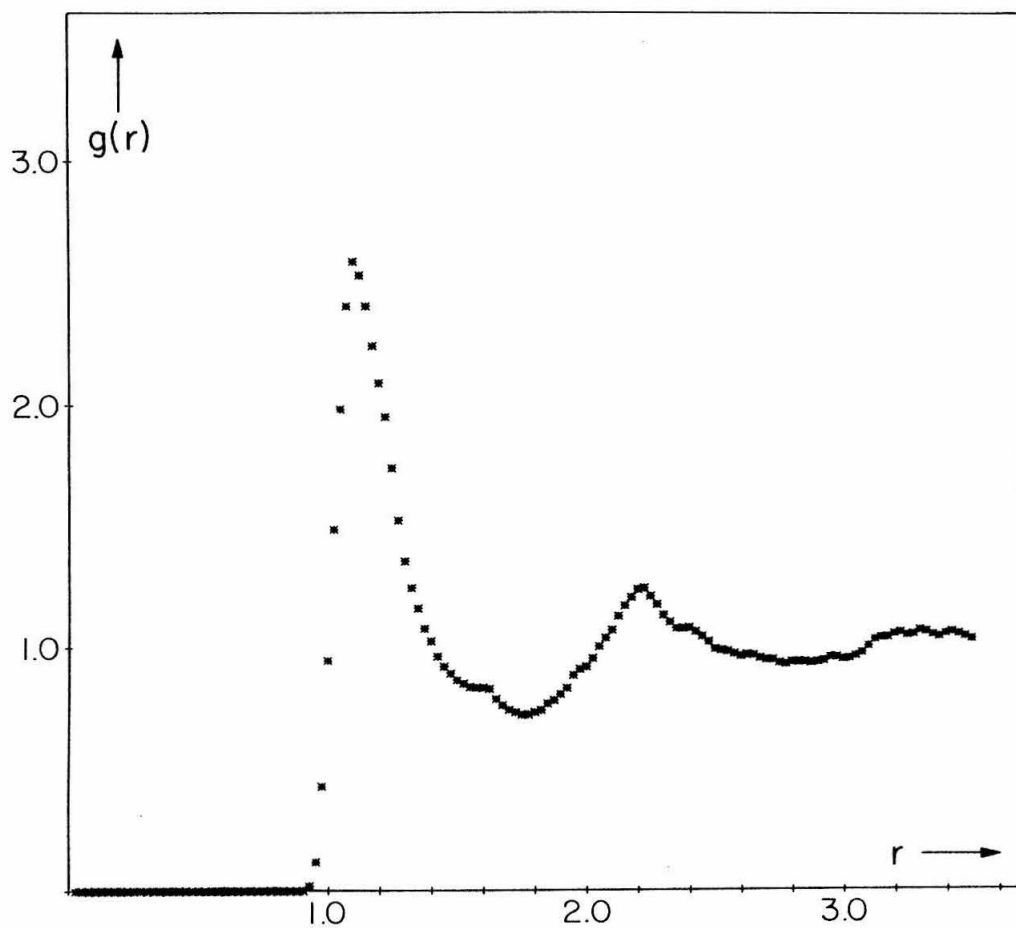


FIG. 4. Radial distribution function for the state $T^* = 0.838$,
 $\rho^* = 0.4993$.

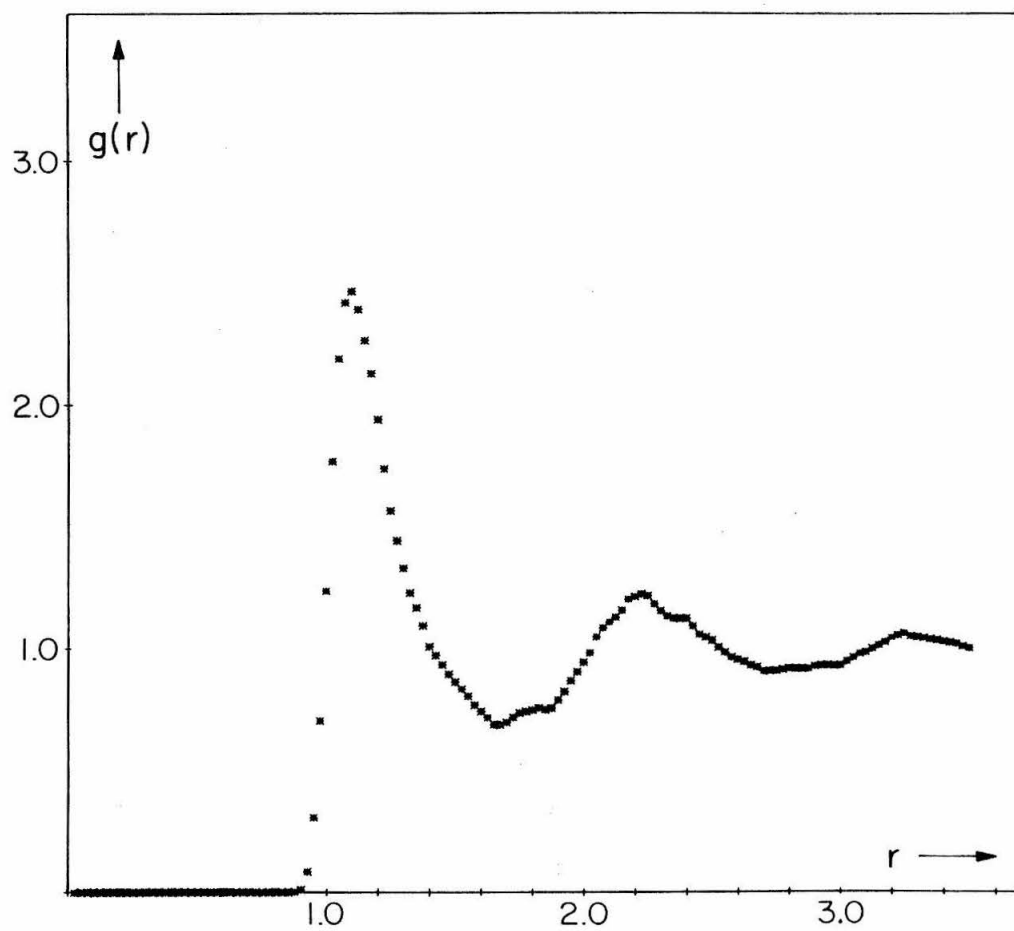


FIG. 5. Radial distribution function for the state $T^* = 1.175$,
 $\rho^* = 0.5824$.

maximum disappears with increasing temperature; for the two densities below 0.5, weak third maxima are discernable only in the functions for the lowest temperature states (states 15 and 18).

In the functions for the five high-density ($\rho^* > 0.7$) states the first principal maximum exhibits a slight shift to smaller radius with increasing temperature. For densities below 0.7, the position of the first maximum remains constant at $r = 1.12$,¹⁷ irrespective of temperature or density. This latter behavior is in accord with that observed by Mikolaj and Pings⁵ in their measurements on liquid argon. The shape of the small-radius edge of the first maximum in the model functions also appears to be relatively insensitive to changes in thermodynamic state; the large-radius side of the peak does however show noticeable temperature broadening at lower densities.

For densities below 0.65, the second principal maximum shows appreciable broadening and a shift to larger radius with increasing temperature; the magnitude of both effects is enhanced by decreasing density. In the functions for the three states with density 0.7014 the position of the second maximum is constant at 2.20, while in the two states with density 0.7708 this maximum shows a slight shift to smaller radius with increasing temperature. The positions of the first and second maxima in the distribution functions are listed in Table II.

In summary, at lower densities the position of the first principal maximum is insensitive to both temperature and density while

the second maximum exhibits a density-dependent shift to larger radius with increasing temperature. At high densities, both maxima shift to smaller radius with increasing temperature.

In addition to the principal structure, three persistent subsidiary features also appear in the radial distribution functions for the model fluid. These are described separately below:

Feature I: This feature appears as a small shoulder at the base of the first principal maximum and occurs at a radius of 1.55-1.60.

A slight shift to smaller radius is noted with decreasing temperature. The feature appears only very weakly in the functions for densities above 0.70 (Fig. 2), and at low densities is frequently obscured by broadening of the first maximum. It is most prominent in Figs. 3 and 4.

Feature II: This feature appears as a small shoulder at the base of the second principal maximum. It is generally centered at a radius of about 1.85, although a shift to larger radius is observed with decreasing temperature. The feature is not seen for densities above 0.70, and at lower densities is absorbed into the second maximum at low temperatures. The feature is most evident in Fig. 5; there is a slight indication of its presence in Figs. 3 and 4.

Feature III: This feature appears as a shoulder or small sub-peak on the large-radius side of the second principal maximum. It is most apparent at a radius of 2.4, but shifts to larger radius with decreasing temperature. The feature is not seen at high densities and may disappear with temperature broadening of the

second maximum at low densities. It is most prominent in Figs. 4 and 5.

The distribution functions shown in Figs. 2-5 have been selected to illustrate the positions and forms taken by the three features discussed above. In general, none of the features, except perhaps III, is particularly striking when viewed against the background of the principal structure of the distribution functions. The recurrent appearance of the features in the model functions, and the regularity of their behavior with changes in temperature and density suggests however that they are indeed indicative of real structure in the model fluid.

IV. DISCUSSION

A. General Comments

The Lennard-Jones pair potential was used exclusively in the simulation calculations, thus precluding the possibility that complex, many-body potentials could be responsible for the subsidiary features appearing in the radial distribution functions for the model fluid. Furthermore, the complications introduced by the Fourier transformation required in experimental measurements of $g(r)$ are absent, since the model functions were computed directly from the time-dependent particle positions provided by the simulation data.

B. Behavior of the Principal Structure

At low densities (e. g. , $\rho^* < 0.5$), the microscopic structure of the model fluid might best be characterized as a loosely-connected "net" of small, irregular clusters.¹⁸ Most particles are in close contact with only two or three neighbors and, with the large amount of unoccupied area available in the system at these low densities, thermal motion can easily introduce disorder. Since the equilibrium hexagonal closest-packed configuration is both the lowest energy and the densest mode of packing in two dimensions, this disordering is equivalent to an "expansion" of the clusters and is reflected in the broadening on the large-radius side of the first principal maximum and the outward shift of the second maximum with increasing temperature. A comparable broadening on the small-radius side of the first maximum is prevented by the repulsive "core" of the pair potential. The extensive broadening of the second and succeeding maxima is also indicative of the high degree of disorder that is possible in the presence of so much unoccupied space.

As the density of the fluid is increased, the disordering effect of thermal motion is progressively attenuated by geometric or "excluded volume (area)" phenomena; that is, the motion of a given particle may be severely restricted by the repulsive potentials of other particles surrounding it. At densities such as that shown in

Fig. 6, for example, geometric phenomena may be responsible for correlations in the spatial distribution of the particles within regions of perhaps $20\text{--}50\sigma^2$ in area. Although the mechanism is not entirely clear, we believe the temperature-dependent shift of the first maximum at high densities can be attributed to these geometrically-induced correlations. As the temperature of the fluid is increased, the corresponding increase in the average per-particle kinetic energy permits neighboring particles to approach each other somewhat more closely during the crystalline-like vibrations characteristic of higher density regions of the fluid.¹⁹ However, since no comparable shift in the maximum is observed for densities below 0.7, this "penetration" effect is not in itself sufficient to explain the observed shift.^(a)

C. The Subsidiary Structure

Graphical displays of the simulation data have led us to conclude that at least two of the subsidiary features appearing in the model functions may be attributed to the presence of alternative configurations for local ordering within the model fluid. The two-dimensional hexagonal closest-packed configuration, shown in Fig. 7a for a group of four particles, is the most prevalent mode of ordering observed in the microstructure of the model. But at densities below 0.65, small local groups of particles are also frequently observed in a square closest-packed configuration such as that shown in Fig. 7b. If we assume that the nearest-neighbor distance in both configurations

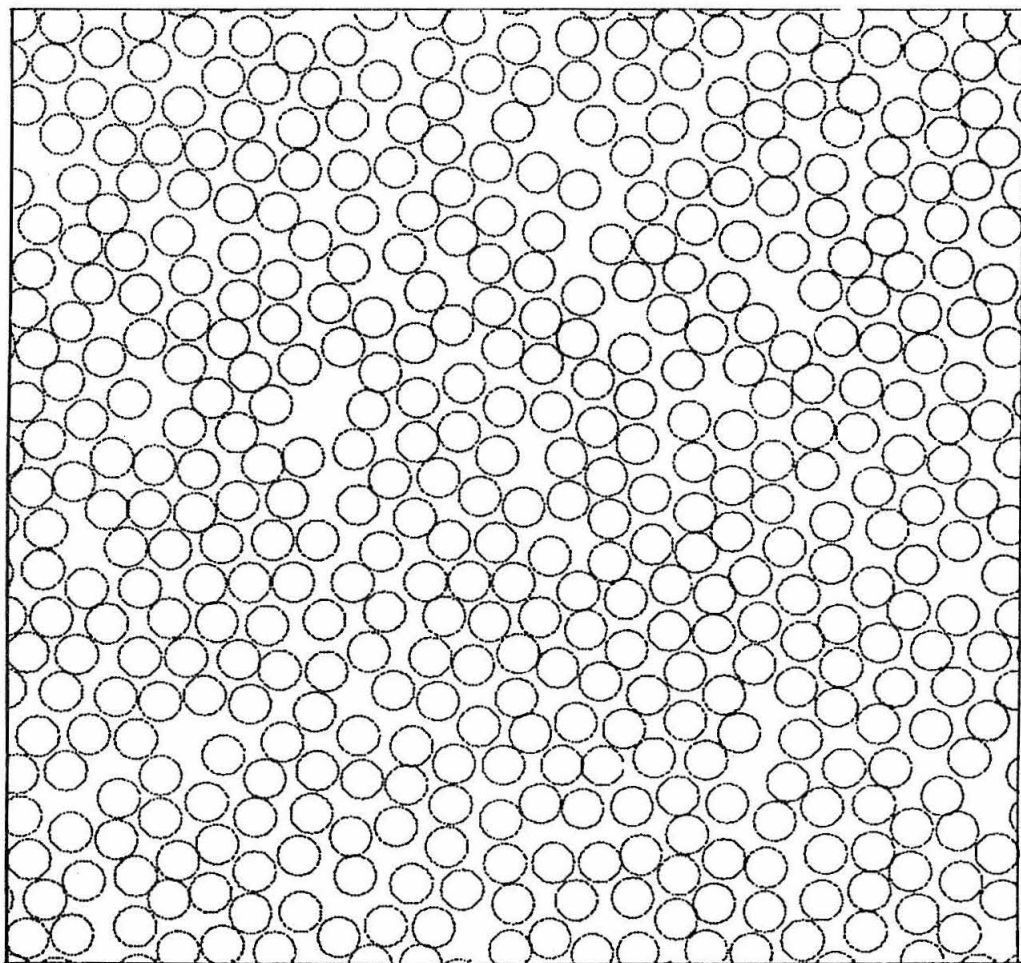


FIG 6. "Snapshot" of instantaneous system configuration in state $T^* = 0.904$, $\rho^* = 0.7708$ (state 2, Table II).

Particles are plotted with diameter σ . The radial distribution function for this state is shown in Fig. 2.

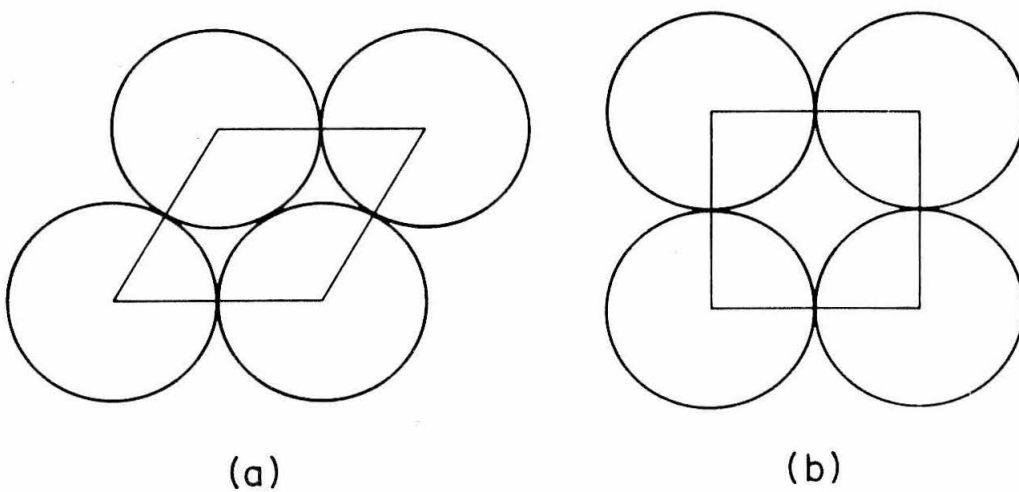


FIG. 7. Hexagonal (a) and square (b) packing configurations for small local groups of particles.

is roughly 1.12, the distance at which the Lennard-Jones pair potential is at a minimum, then both configurations contribute to the principal maxima in $g(r)$. The second-nearest neighbor distances in the square and hexagonal configurations would then be 1.59 and 1.94, respectively. These distances correspond closely to the radii at which Features I and II appear in the radial distribution functions.^(b)

The disappearance of Feature I at high densities can be explained in terms of the difference in the packing densities for the ideal hexagonal and square configurations, but the similar disappearance of Feature II remains something of a puzzle. As indicated in Fig. 8, the "second-neighbor shell" in the two-dimensional hexagonal closest-packed configuration is actually comprised of two groups of six particles each, one group at a distance of 1.94, the other at 2.25 (given a nearest-neighbor distance of 1.12). If, as we have suggested, geometric constraints produce a high degree of order in the fluid at high densities, then one would expect the second principal maximum to show a progressively stronger splitting with increasing density. Indeed, since $g(r) \propto n(r) \cdot r^{-1}$, the "ideal" maximum at 1.94 should be more prominent than the one at 2.25.

A possible explanation for the behavior of Feature II lies in consideration of the form of the "average" potential field presented to a particle in the fluid as a function of the bulk density of the system. At low densities, the average particle is found to be located in a potential formed by the attractive and repulsive components

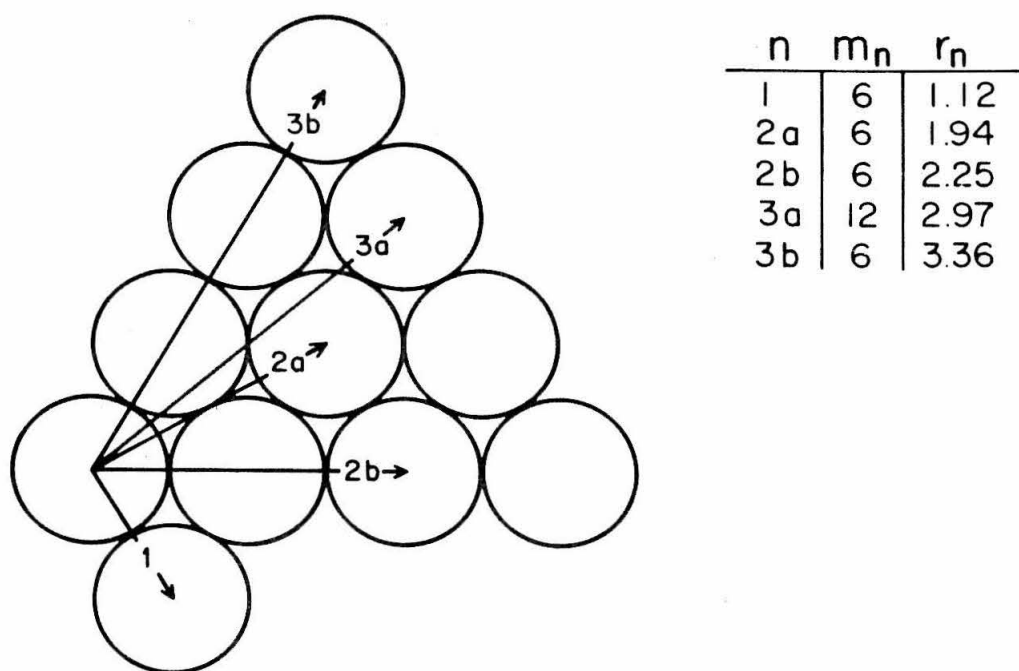


FIG. 8. Ideal two-dimensional hexagonal close-packing.

Figure shows section of ideal lattice and indicates first three neighbor "shells." Table at right gives distance (r_n) and number of particles (m_n) in each "shell" n .

of its interaction with two or three close neighbors, while at very high densities a particle is largely restricted to the steep-sided potential "well" formed by the repulsive cores of its closely-packed neighbors. But over a narrow range of moderately high densities, the potentials of the neighbors surrounding a particle may sum together so as to produce a steep-sided well having a bottom that is essentially "flat" over a radius of perhaps 0.2σ . As an example of this phenomenon we may cite the behavior of the "smeared" cell potential that arises in the Lennard-Jones-Devonshire theory of the liquid state.²⁰ For reduced densities above about 0.8, the cell potential increases rapidly with displacement away from the center of the cell, while for densities below about 0.65 the minimum in the potential moves away from the center of the cell, leaving a small local maximum in that position. But for densities around 0.7, the gradient of the potential is essentially zero out to a distance of about 0.15σ from the center of the cell, then increases rapidly with further displacement. This kind of effective potential could lead to lesser degree of local order than that present at either higher or lower densities. It is interesting to note that Feature II disappears from the radial distribution function at some density between 0.63 and 0.70.

In summary then we suggest that, as the density of a simple fluid is increased, the factors contributing to ordering within the microstructure of the fluid may go through three distinct phases. At low densities the attractive component of the interparticle

potential is the principal ordering agent, while at very high densities geometric effects arising from the repulsive component of the potential become dominant. For a narrow range of moderately high densities however neither component may be effective over at least short distances and hence, in this narrow range of densities, the fluid may show a lesser degree of short-range order than for either higher or lower densities.

D. Conclusions

While the preceding interpretation of the two-dimensional radial distribution functions appears to be consistent with the presently available data, it must nevertheless be considered "tentative" until methods are devised to obtain a more quantitative description of some of the microscopic effects suggested by our arguments. It should for example be possible to obtain from the simulation data an approximate measure of the time-average relative "concentrations" of hexagonal and square packing in the model fluid for different temperatures and densities.^(c) The calculations will also be extended to three-dimensional model systems, provided sufficient computer time is made available for this investigation.^(d) But on the basis of the two-dimensional data presented here, we are led to conclude that the subsidiary features appearing in some experimental radial distribution functions reflect actual structure in simple liquids, and that this structure may arise from the existence of alternative configurations for local ordering.

ACKNOWLEDGMENTS

The author wishes to thank Drs. S. C. Smelser and C. J. Pings for several helpful discussions regarding the experimental measurement of radial distribution functions, and Dr. G. W. Robinson for his help in the preparation and analysis of the data presented here.

REFERENCES FOR PAPER NO. 2

1. A. Eisenstein and N. S. Gingrich, Phys. Rev. 58, 307 (1940);
ibid. 62, 261 (1942).
2. See, for example, J. R. Randall, The Diffraction of X-Rays and
Electrons by Amorphous Solids and Gases (John Wiley and Sons,
Inc., New York, 1934), p. 107; B. E. Warren and N. S. Gingrich,
Phys. Rev. 46, 368 (1934); V. N. Filipovich, Sov. Phys. --Tech.
Phys. 1, 391, 409 (1956); H. H. Paalman and C. J. Pings, Rev.
Mod. Phys. 35, 389 (1963).
3. J. Waser and V. Schomaker, Rev. Mod. Phys. 25, 671 (1953).
4. A. A. Khan, Phys. Rev. 136, A1260 (1964).
5. P. G. Mikolaj and C. J. Pings, J. Chem. Phys. 46, 1401 (1967).
6. C. Finbak, Acta Chem. Scand. 3, 1279, 1293 (1949).
7. D. Stirpe and C. W. Tompson, J. Chem. Phys. 36, 392 (1962).
8. J. A. Campbell and J. H. Hildebrand, J. Chem. Phys. 11,
334 (1943).
9. G. T. Clayton and L. Heaton, Phys. Rev. 121, 649 (1961).
10. D. G. Henshaw, Phys. Rev. 111, 1470 (1958).
11. D. G. Henshaw, Phys. Rev. 105, 976 (1957).
12. N. S. Gingrich and C. W. Tompson, J. Chem. Phys. 36, 2398
(1962).
13. S. Smelser, Ph. D. Thesis, California Institute of Technology,
1969. To be made available through University Microfilms.
14. P. L. Fehder, J. Chem. Phys. 50 2617 (1969).
15. A. Rahman, Phys. Rev. 136, A405 (1964).

16. See Refs. 14 and 15 regarding the use of "reduced" dynamical variables. For additional information, see the discussion of J. M. H. Levelt and E. G. D. Cohen, Studies in Statistical Mechanics, J. DeBoer and G. E. Uhlenbeck, Eds. (North-Holland Publishing Co., Amsterdam, 1964), Vol. II, p. 114 ff.
17. This corresponds closely to the distance at which the Lennard-Jones pair potential is at a minimum; $r_{\min} = 2^{1/6} \sigma \cong 1.1225 \sigma$.
18. See, for example, Fig. 5 in Ref. 14.
19. See, for example, the plots of particle trajectories in the model fluid shown in Figs. 6 and 7 in Ref. 14.
20. The Lennard-Jones-Devonshire theory for the two-dimensional model fluid is developed in the Appendix of Ref. 14. Figure 9 in that reference is a plot of the "smeared" cell potential for several reduced densities.

E. Notes and Addenda to Paper No. 2

- a. If the "penetration effect" is to play an important role in causing the temperature-dependent shift of the first principal maximum, the form of the "effective" interaction between adjacent particles--when the average interactions with surrounding particles in the fluid are taken into account--must begin to change rather rapidly with increasing reduced density above 0.63. In particular, the repulsive r^{-12} core of the Lennard-Jones pair potential may be "softened" by attractive interactions with nearby particles, while the repulsive cores of the close-packed neighbors would tend to "stiffen" the attractive r^{-6} component of the pair potential.
- b. To date, no similar structural explanation for Feature III has been found. Neither the hexagonal nor square configurations, nor any reasonable spatial combination of the two would seem to yield a "preferred" neighbor distance of approximately 2.4σ .
- c. It may in practice be rather difficult to calculate the "concentrations" of square and hexagonal packing in the model fluid. In particular, there exist at present no well-defined mathematical criteria for determining, for example, just how "square" or how "hexagonal" is the spatial distribution of points in a local region of a "partially-ordered" lattice. For further discussion of this point, see Section V.

- d. Verlet has reported the radial distribution functions for some twenty-five temperature-density states of a three-dimensional model fluid of 864 Lennard-Jones particles [Phys. Rev. 165, 201 (1968)]. The data span a range of reduced densities from 0.450 to 0.880, and the functions plotted from the tabularized values reported in the paper are smooth and show no subsidiary structure. But the very lack of statistical scatter in the reported function values suggests that the distribution functions computed directly from the simulation data may have been numerically smoothed as an aid to the computation of the other correlation functions and transforms dealt with in the paper. Were Verlet unaware of the possible presence of subsidiary structure in his raw distribution functions data, small features of the sort appearing in our two-dimensional functions or in the experimental functions measured by Smelser could have been removed by the numerical smoothing procedure.

SECTION IV

DIFFUSION, RELATIVE DIFFUSION, AND CHEMICAL
REACTION KINETICS IN DENSE FLUIDS

A. Introductory Comments

The two papers reproduced in this section deal with the results of a rather novel analysis of the simulation data. The qualitative observation that diffusion in the dense model fluid is a cooperative process was reported in Paper No. 1 (section III. B). In Paper No. 3, this observation is placed on a quantitative basis.

Analysis of the simulation data shows that the cooperative mechanism for diffusion in the model fluid conforms to the statistical predictions of existing theories of singlet or self-diffusion in simple liquids. The singlet mean square displacement and velocity autocorrelation functions computed from the simulation data behave in the theoretically predicted manner; indeed, the calculated distributions of individual particle displacements over a range of different time intervals all fit quite closely the functional form predicted by the simple two-dimensional random-walk model. But further analysis also shows that short-range dynamic correlations associated with the cooperative diffusion mechanism retard the relative diffusion of proximate particles in the model fluid--a fact of some significance with respect to chemical reaction kinetics in solution. A new theoretical treatment of relative diffusion in dense fluids, devised by Dr. C. A. Emeis, is found to reproduce the phenomena observed in the model fluid with surprising accuracy.

The first step in any bimolecular chemical reaction must obviously be the encounter between the two reactant molecules. But if short-range "cooperative" correlations retard the relative diffusion of solute molecules as they approach each other in solution, the rate at which new reactant-pairs are formed would be reduced. In Paper No. 4 the Emeis treatment for relative diffusion is applied to the Smoluchowski theory of "diffusion-controlled" reaction kinetics in solution. It is found that this more accurate treatment of reactant encounter dynamics may effect a significant reduction in the predicted rate of reaction.

B. Paper No. 3

The Microscopic Mechanism for Self-Diffusion and
Relative Diffusion in Simple Liquids*

P. L. Fehder, C. A. Emeis,[†] and R. P. Futrelle[‡]

Arthur A. Noyes Laboratory of Chemical Physics,
California Institute of Technology, Pasadena, California 91109

Abstract. Graphical displays of computer-generated data simulating the microscopic dynamics of a two-dimensional dense fluid of Lennard-Jones disks indicate that the microscopic mechanism for diffusion in simple liquids may be largely cooperative in nature. Although it is unlikely that this cooperative mechanism would have a macroscopically discernable effect upon singlet or self-diffusion in real liquids, short-range correlations associated with the cooperative processes can affect the chemically important relative diffusion of solute molecules separated by short distances in a liquid solvent. The statistical time-correlation functions describing self-diffusion in the model fluid are found to behave in a manner

* This work was supported in part by a grant from the National Science Foundation, No. GP-7258.

[†] Present address: Koninklijke/Shell Laboratorium, Amsterdam, Holland.

[‡] Present address: North American/Rockwell Science Center, Thousand Oaks, California 91360.

consistent with existing theoretical treatments of diffusion in simple liquids. The relative diffusion of particles separated by distances of 1-3 diameters is however found to proceed more slowly than predicted by theories that neglect correlations in the motions of neighboring particles at liquid-like densities. A theoretical formalism that permits an accurate description of relative diffusion in the model fluid is developed.

I. INTRODUCTION

In a recent paper,¹ one of us (PLF) discussed the initial results obtained from a series of computer calculations simulating the microscopic dynamics of a two-dimensional dense fluid of Lennard-Jones disks. Preliminary analyses of the simulation data led to several interesting observations. "Snapshots" of the instantaneous configuration of the model fluid show for example that, even at temperatures well above critical, the microscopic structure of the fluid contains relatively large and surprisingly persistent "holes" (see, e.g., Fig. 1). Although a number of theories of the liquid state² have previously postulated the existence of holes or "vacancies" in the structure of real simple liquids, the phenomenon we observe differs both qualitatively and quantitatively from that seemingly suggested by the theoretical models. In particular, the holes appearing in the model fluid bear no obvious relationship to the size and shape of a single fluid particle. And furthermore, individual holes are observed to persist in the same region of the

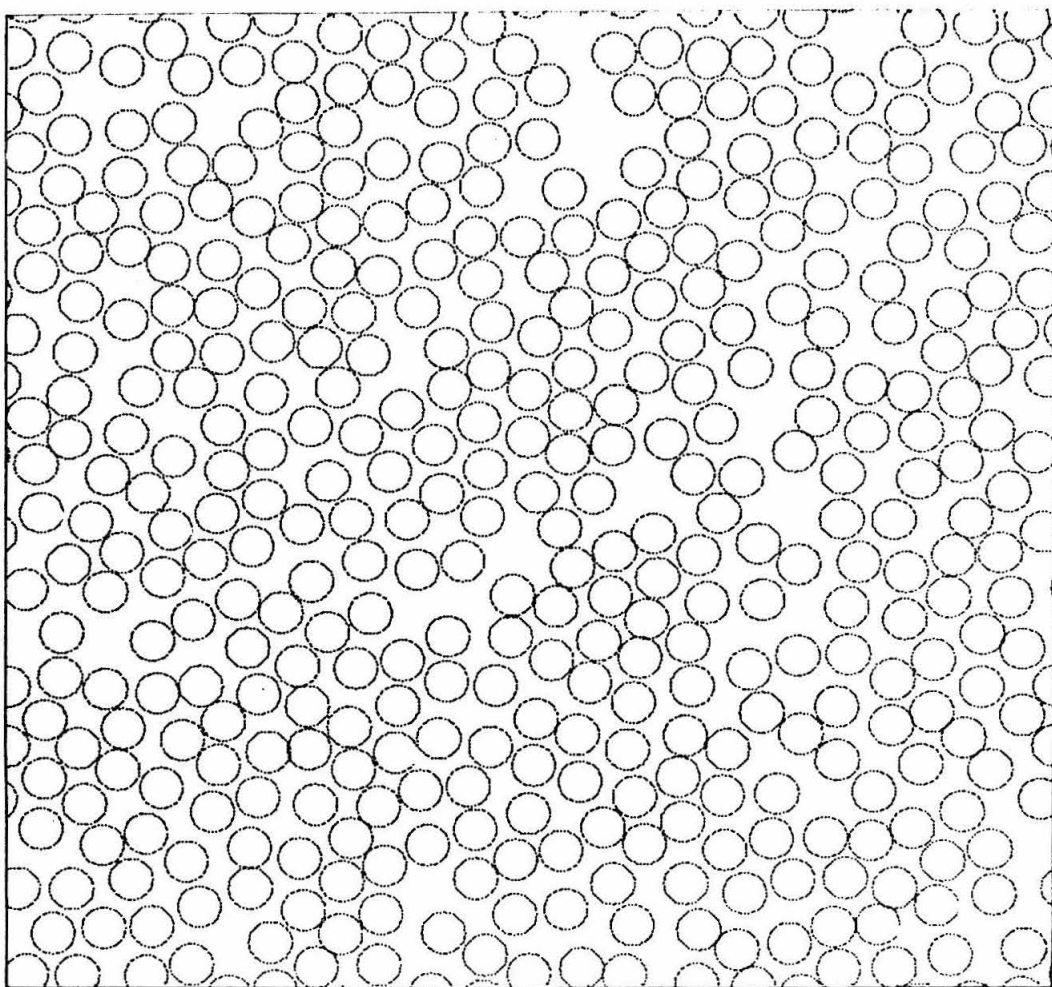


FIG. 1. "Snapshot" of an instantaneous configuration of the model fluid in state No. 3 (Table I). The particles are drawn with diameter σ , the distance parameter in the Lennard-Jones pair potential.

fluid for times well in excess of the characteristic kinetic relaxation time for the system. One quantitative measure of the structural ordering within the fluid, the radial distribution function, is discussed in a second paper.³

Graphical display techniques were also used to examine the microscopic mechanism for diffusion within the fluid. Plots of the particle trajectories such as that shown in Fig. 2 indicate that, even over intervals of 6.0×10^{-12} sec and longer, extensive diffusive migration is largely restricted to small, local groups or "chains" of particles situated in the vicinity of a hole. Furthermore, dynamic displays (motion pictures) of the simulation data show that the migration of these local groups of particles occurs in a concerted manner. That is, at liquid-like densities cooperative effects play an important role in the mechanism for diffusion in the model fluid.

Until recently, self-diffusion in simple liquids has been treated in terms of theoretical models based upon some modification of either the Brownian-motion mechanism or the jump-diffusion mechanism characteristic of solids. In the next section we examine several theoretical formulations describing diffusion in dense fluids and compare the behavior of the functions computed from the simulation data with that predicted by various theories. Although the microscopic mechanism for diffusion in the model fluid appears to differ markedly from that envisioned by the existing theories, the statistically-averaged distribution and correlation functions

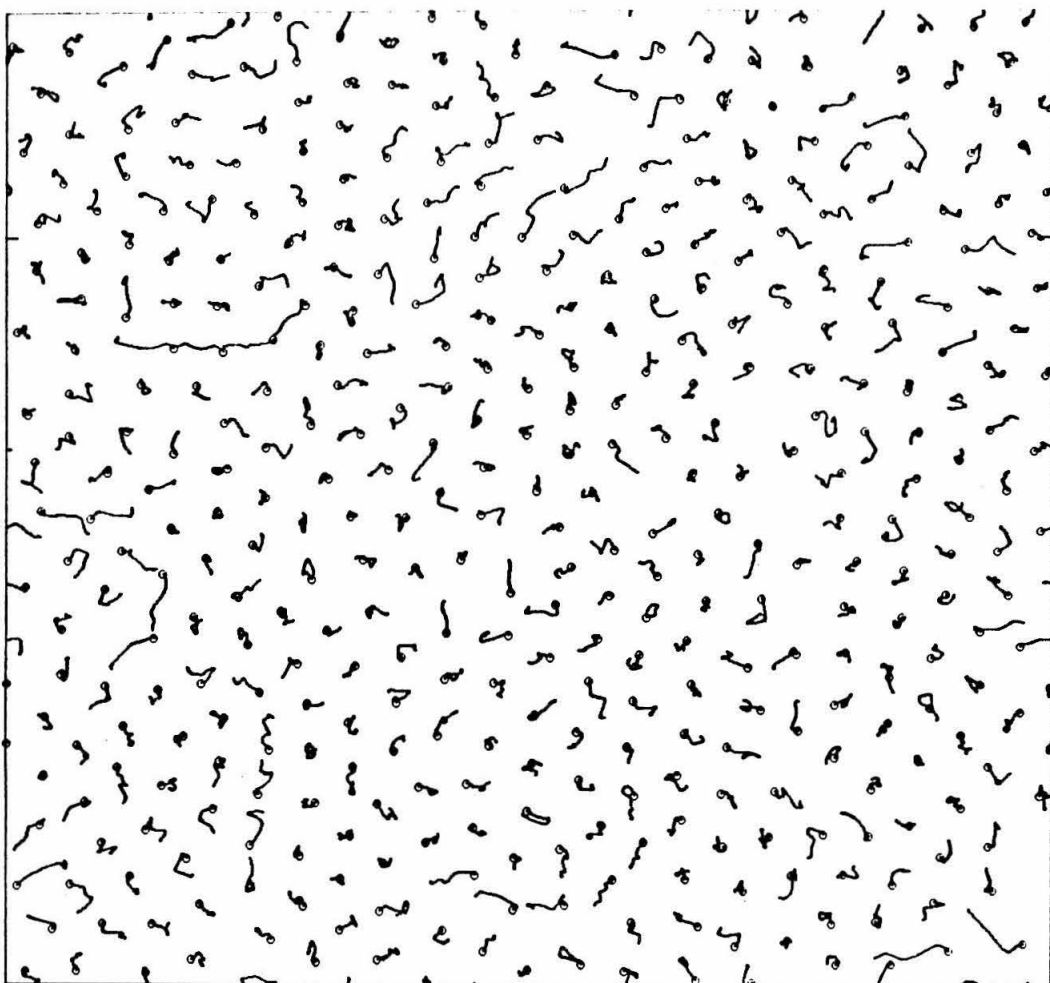


FIG. 2. Trajectories of the particles in the model fluid in state No. 3 (Table I). The small circles mark the initial positions of the particles and the irregular lines extending therefrom the paths of the centers during the remainder of a 2×10^{-12} sec interval. The initial configuration also corresponds to that shown in Fig. 1.

computed from the simulation data are found to behave in a manner consistent with theoretical predictions.

The importance of cooperative phenomena in the mechanism for diffusion becomes much more apparent when the relative diffusion of pairs of particles is investigated. Relative diffusion within the model fluid is examined in some detail in Sec. III, and it is found that the coefficients describing the relative diffusion of particles separated by distances of 1-3 diameters have values significantly lower than would be predicted by theories that fail to take account of correlations in the motion of neighboring particles in a liquid. This result has important implications with respect to, for example, the chemical kinetics of very fast--"diffusion-controlled"--reactions in solution; indeed, a phenomenon similar to that which we observe in the model fluid has previously been postulated to explain the difference between the theoretical and experimental rates for iodine atom recombination in solution.⁴⁻⁷

There are a large number of processes in which the relative motion of two particles is important. Many dielectric and electromagnetic phenomena require knowledge of the correlation of some function of the relative positions of a pair of particles at time 0 and the relative position at a later time t . Conversely, certain light scattering experiments can be interpreted to yield information of relative motion. In order to understand such motion theoretically we must start with its simplest aspects rather than the entire time-dependent two-particle distribution itself. The second moment or

mean square relative displacement is probably the most fundamental parameter describing the relative diffusion process which is why we study it in this paper (Sec. IV.). Another important process, diffusion-controlled reaction rates, is treated in a forthcoming paper.

II. SINGLET DIFFUSION

A. Mathematical Formulation

Singlet⁸ diffusion in fluids is characterized, at the molecular level, by the time-dependent mean square displacement of the fluid particles

$$\sum(t) = \langle [\underline{r}_{\underline{k}}(t) - \underline{r}_{\underline{k}}(0)]^2 \rangle \quad , \quad (1)$$

where $\underline{r}_{\underline{k}}$ is the position vector to particle \underline{k} , measured in the laboratory coordinate system, and the time \underline{t} is measured from an arbitrarily selected zero. The function is symmetric and in simple liquids becomes linear with increasing $|\underline{t}|$ after an "induction" time τ_ℓ of the order of 10^{-12} sec.

The time-dependent behavior of $\sum(t)$ can be interpreted in terms of the familiar velocity autocorrelation function

$$A_v(t) = \langle \underline{v}_{\underline{k}}(0) \cdot \underline{v}_{\underline{k}}(t) \rangle \quad , \quad (2)$$

where $\underline{v}_{\underline{k}}(s)$ is the velocity of particle \underline{k} at time \underline{s} . The velocity autocorrelation function, like $\sum(t)$, is symmetric and invariant with uniform time translation. Since

$$\underline{r}_{\underline{k}}(t) - \underline{r}_{\underline{k}}(0) = \int_0^t \underline{v}_{\underline{k}}(s) ds,$$

we have

$$\sum(t) = \langle [\underline{r}(t) - \underline{r}(0)]^2 \rangle = \langle \int_0^t \underline{v}(s) ds \cdot \int_0^t \underline{v}(u) du \rangle \quad , \quad (3)$$

where the subscript \underline{k} has been dropped for notational simplicity. The average $\langle \underline{v}(s) \cdot \underline{v}(u) \rangle$ is unaffected by uniform time translation

$$\langle \underline{v}(s) \cdot \underline{v}(u) \rangle = \langle \underline{v}(s+s') \cdot \underline{v}(u+s') \rangle .$$

Letting $s' = -u$ and $s - u = a$, we have

$$\sum(t) = \int_0^t \int_0^t \langle \underline{v}(a) \cdot \underline{v}(0) \rangle ds du, \quad (4)$$

and using variables \underline{s} and \underline{a} (Jacobian unity) leads to the result

$$\begin{aligned} \sum(t) &= 2t \int_0^t \left(1 - \frac{a}{t}\right) \langle \underline{v}(a) \cdot \underline{v}(0) \rangle da \\ &= 2t \int_0^t A_V(a) da - 2 \int_0^t A_V(a) a da . \end{aligned} \quad (5)$$

In liquids, the ensemble-averaged velocity autocorrelation decays rapidly with increasing $|t|$ and essentially vanishes after times of the order of 10^{-12} sec. Either the interval τ_e during which the function decays to e^{-1} of its $t = 0$ value, or the time τ_0 required for the correlation to essentially vanish is generally equated with the kinetic relaxation time for the system. This relaxation time is also frequently associated with the average time required for the fluid particles to execute one "free path" displacement.

Equation (5) can then be rewritten

$$\sum(t) = 2tI_1^0 - 2I_2^0, \quad (6)$$

where $I_1^0 = \int_0^{\tau_0} A_V(a) da$ and $I_2^0 = \int_0^{\tau_0} A_V(a) a da$ are both constants.

It can then be seen that the "induction" time τ_l for $\sum(t)$ may be equated with τ_0 , and that the slope of the linear portion of

$\sum(t > \tau_0)$ is given by $2I_1^0$.

B. Singlet Diffusion Data for the Model Fluid

In two dimensions, the slope of the linear portion of the mean square displacement function is related to the coefficient for singlet diffusion D_s by the Einstein formulation

$$\dot{\Sigma}(t) = 4D_s \quad (\text{two dimensions; } t > \tau_0) \quad , \quad (7)$$

where it is assumed that $\Sigma(\tau_0)$ is small compared to molecular dimensions. Comparison with Eq. (6) then yields the additional relation

$$D_s = \frac{1}{2} I_1^0 = \frac{1}{2} \int_0^{\tau_0} A_v(a) da \quad . \quad (8)$$

A similar formulation is obtained by Zwanzig⁹ to describe the diffusion of a Brownian particle, although an additional limiting function is inserted in the autocorrelation integral in place of the assumption that $\Sigma(\tau_0)$ is small.

In calculations of the two diffusion functions from the simulation data, additional statistical averaging is obtained by taking advantage of the mathematical properties of the functions. If for example the equilibrium simulation data span an interval of 1.5×10^{-11} sec, functions can be computed to a maximum time of $t = 1.0 \times 10^{-11}$ sec from several zero times and then averaged together. The symmetry can also be exploited by calculating the functions for $t < 0$ from zero times near the end of the interval spanned by the simulation data; the functions for both $t < 0$ and $t > 0$ can then be averaged on the basis of absolute t .

As described in Ref. 1, dynamical variables entering into the simulation calculations are "reduced" in units involving \underline{m} the particle mass, and σ and ϵ , the distance and energy parameters in the Lennard-Jones pair potential

$$\varphi_{\text{LJ}}(r) = 4 \epsilon \left\{ (\sigma/r)^{12} - (\sigma/r)^6 \right\}.$$

In particular, distances are expressed in units of σ , so that values of $\sum(t)$ and D_s are obtained in units of σ^2 and $\sigma^2 \cdot \text{sec}^{-1}$, respectively. Reduced units consistent with those described in Refs. 1 and 10 will be used throughout the remainder of this paper.

Mean square displacement and velocity autocorrelation functions were computed to times of 1.1×10^{-11} and 6.0×10^{-12} sec, respectively, from the simulation data for five equilibrium temperature-density states of the model fluid. A comparison of the singlet (self-) diffusion coefficients obtained by least-squares fitting the linear portion of the $\sum(t)$ function and by Simpson's Rule numerical integration of the $A_v(t)$ function for each state is contained in Table I. Values for τ_e , τ_0 , and $\sum(\tau_0)$ are also listed in the Table, and the mean square displacement function for the liquid-like state $\rho^* = 0.7014$, $T^* = 0.676$ (state No. 3 in Table I) is plotted in Fig. 5.

The poor agreement between the two D_s values calculated for each state may be attributed to the relatively large thermal fluctuations that can occur in a system of only 400 or so particles. The normalized velocity autocorrelation functions

TABLE I. Singlet diffusion data from mean square displacement and velocity autocorrelation

functions.								
State	N	ρ^*	T^*	from velocity autocorrelation function		from mean square displacement		
				$D_s(\sigma^2 \cdot \text{sec}^{-1})$	$\frac{\tau_e}{(\times 10^{12} \text{ sec})}$	$D_s(\sigma^2 \cdot \text{sec}^{-1})$	$\sum(\tau_0)(\sigma^2)$	
					τ_0			
1	404	0.7014	0.982	5.34×10^{10}	0.242	2.52	$5.52 \pm 0.04 \times 10^{10}$	0.481
2	404	0.7014	0.766	4.92×10^{10}	0.272	3.00	$4.95 \pm 0.03 \times 10^{10}$	0.493
3	404	0.7014	0.676	4.20×10^{10}	0.260	4.00	$4.39 \pm 0.05 \times 10^{10}$	0.560
4	444	0.7708	1.341	4.81×10^{10}	0.187	1.50	$4.89 \pm 0.04 \times 10^{10}$	0.282
5	444	0.7708	0.904	3.08×10^{10}	0.203	2.88	$3.36 \pm 0.09 \times 10^{10}$	0.362

$$A_v^*(t) = \langle \underline{v}_k(t) \cdot \underline{v}_k(0) \rangle / \langle \underline{v}_k(0)^2 \rangle$$

for each of the five states were found to decay rapidly (as indicated by the τ_e values) to a value of about 0.05, but to approach zero much more slowly thereafter with oscillations of a magnitude as great as ± 0.05 . Thus while the values for τ_e could be determined quite accurately, the values for τ_0 listed in the table are somewhat subjective and are truly indicative only of the upper limits applied to the integration specified in Eq. (8).

C. Time-Dependent Distribution of Particle Displacements

Although the mean square displacement and velocity autocorrelation functions provide a convenient statistical description of diffusion, the averaging implicit in the calculation of these functions may obscure important details of the diffusion mechanism. To obtain a more precise measure of singlet diffusion within the model fluid, distributions $W(\underline{r}, t)\Delta r$ of the absolute displacements \underline{r} of the particles over intervals of $t = 1.0, 1.0, 3.0, \dots 6.0 \times 10^{-12}$ sec were computed from the simulation data for state No. 3 (Table I).

In two dimensions, a random-walk mechanism for diffusion leads to a distribution of displacements of the form

$$W(\underline{r}, t)\Delta r = [(\underline{r} \cdot \Delta \underline{r})/2\delta] \exp(-r^2/4\delta), \quad (9)$$

where $W(\underline{r}, t)\Delta r$ is the fraction of the particles displaced a distance $r \pm (\Delta r/2)$ from their initial positions after time interval t , and the

quantity $\delta = \delta(t)$ is related to the singlet diffusion coefficient by $\delta = D_s t$. The six distribution functions computed from the simulation data were found to fit the functional form in Eq. (9) quite closely, although $\delta(t)$ must be adjusted to account for the non-zero "induction" time in the model fluid. To obtain a random-walk diffusion coefficient, the function in Eq. (9) was least-squares fitted to the six distribution functions. The resulting $\delta(t)$ values are listed in Table II, and a comparison of the computed and fitted distributions for $t = 6.0 \times 10^{-12}$ sec is shown in Fig. 3. The four $\delta(t)$ values for $t \geq 3.0 \times 10^{-12}$ sec show a linear dependence on t . A least-squares fit through the four values yields a random-walk coefficient of $D_s = \delta(t) = 3.74 \times 10^{10} \sigma^2 \cdot \text{sec}^{-1}$, which may be compared to the values 4.39 and $4.20 \times 10^{10} \sigma^2 \cdot \text{sec}^{-1}$ obtained from the $\Sigma(t)$ and $A_v(t)$ functions for state No. 3.

D. Comparison with Theoretical Models

As we have described in the Introduction and in Ref. 1, the microscopic mechanism for diffusion in the high-density model fluid differs qualitatively from that suggested by existing theoretical treatments of diffusion in simple liquids. Although the "holes" appearing in the microstructure of the fluid play a role rather similar to that supposed by a jump-diffusion mechanism, jump-like motion is not observed in dynamic displays (motion pictures) of the simulation data. Rather, the migration of local groups of particles--see, e.g., Fig. 2--proceeds more or less continuously

TABLE II. Random-walk diffusion coefficient factors.

$t \times 10^{12} \text{ sec}$	$\delta(t)$	standard deviation of fit
1.0	0.0268	0.0018
2.0	0.0593	0.0020
3.0	0.0940	0.0019
4.0	0.1321	0.0018
5.0	0.1695	0.0018
6.0	0.2063	0.0016

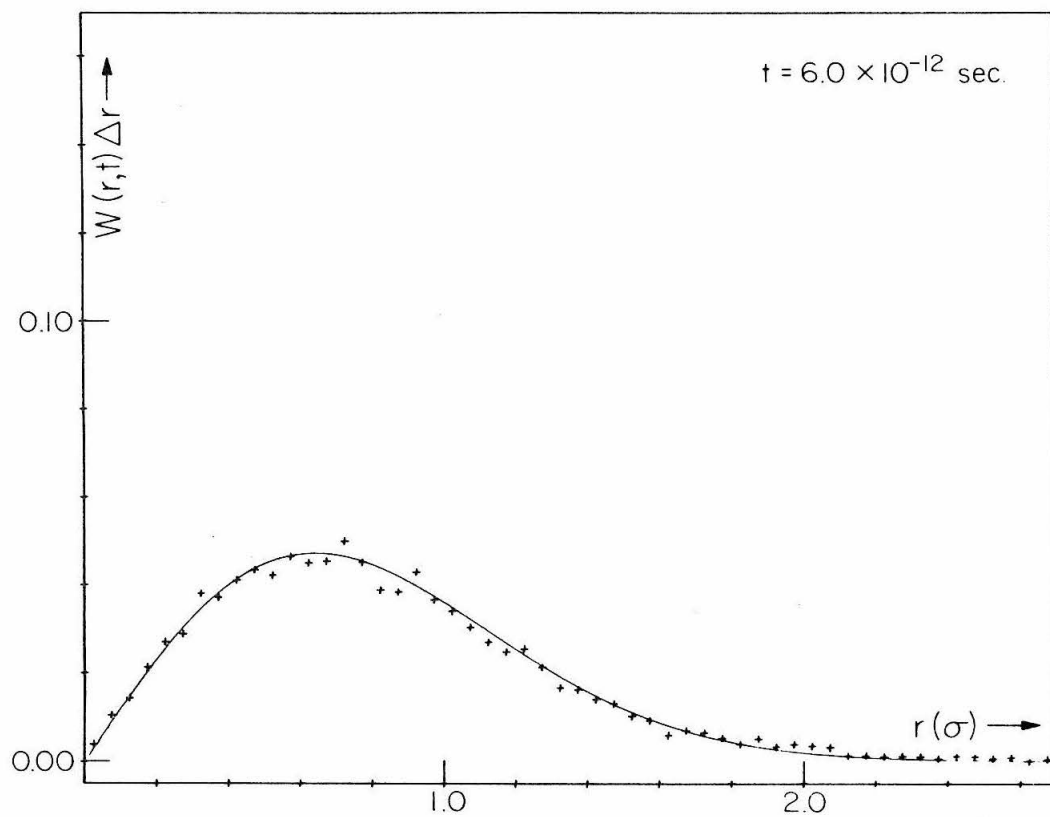


FIG. 3. Comparison of the distribution of particle displacements $W(r, t)\Delta r$ in the model fluid after 6×10^{-12} sec and the functional form predicted by two-dimensional "random-walk" theory. The distribution from the model fluid was calculated from the simulation data for state No. 3 (Table I).

except for small, short-range oscillations ("jiggling") consonant with the rapid decay of the velocity autocorrelation function. The smooth $W(r, t)$ distributions discussed above are also inconsistent with a jump-diffusion interpretation.

The close agreement between the calculated displacement distributions and the functional form for $W(r, t)$ predicted by random-walk theory is rather surprising in view of the cooperative phenomena exhibited in graphic displays of the simulation data. Diffusive motion in the model fluid could hardly be termed "random", since the migration of each particle is obviously closely coupled to the motions of the particles immediately surrounding it. Neither would a Brownian-motion mechanism of the sort treated by Kirkwood¹¹ seem to provide an adequate description of the microscopic processes observed in the graphical displays. In particular, it is difficult to conceive of a physical interpretation for the "friction constant" employed in Brownian-motion treatments if cooperative phenomena play an important role in the diffusion mechanism.

In light of our observations of the model fluid, we suggest that the mechanism for singlet diffusion in simple liquids is more accurately described in terms of microscopic processes occurring on three different time scales:

1. For very short times (e.g., of the order of 10^{-13} sec), the motion of a particle is strongly correlated with the instantaneous positions and velocities of the particles immediately surrounding it. Although not accessible to direct experimental

measurement in real liquids, this phenomenon has been examined in detail by Rahman¹² using computer-simulation data for a dense, three-dimensional fluid of Lennard-Jones particles. The correlation is found to vanish rapidly after times of the order of the characteristic relaxation time for the fluid, and is thus in accord with the assumed relationship between τ_0 (or τ_e) and the time required for the average fluid particle to traverse one "free path".

2. Over longer, albeit still microscopic times ($2.0-5.0 \times 10^{-12}$ sec in the dense model fluid) cooperative phenomena dominate the diffusion process and the migration of an individual particle is closely correlated with the displacements of its immediate neighbors. The apparent physical relationship between these cooperative phenomena and the "holes" in the microstructure of the model fluid suggests that the average time during which cooperative motion continues within a local region of a liquid be intuitively associated with the "relaxation time" for the redistribution of unoccupied volume ("excess volume") within the liquid.
3. After times of the order of $10^{-10} - 10^{-9}$ sec, the residual effects of the cooperative phenomena vanish and diffusion takes on the appearance of a more nearly "random" process.

There is an alternate view, an analogy that can be drawn, which eases the discrepancy between the cooperative motion and the simple diffusion models. In equilibrium statistical mechanics one may define one, two, ... , n-body distribution functions in a liquid. The one-particle distribution function is completely trivial, it is a constant $=V^{-1}$, where V is the volume of the liquid. The two-body distribution function is quite non-trivial. Its correlation function $g(r)$ depends on r , the interparticle separation, vanishes at $r=0$, oscillates strongly for a few molecular diameters, and then decays to unity for large r . Thus the one-body function contains no hint of the complex structure of $g(r)$. In a quite similar way the one-particle diffusion which behaves rather simply contains little or no hint of the cooperative motion in the liquid when two or more molecules are viewed simultaneously.

III. RELATIVE DIFFUSION AND COOPERATIVE PHENOMENA

A. Mathematical Formulation

Within the framework of classical statistical mechanics, relative diffusion in dense fluids is conveniently described by the time-dependent mean square displacement function

$$\Delta_v(t) = \langle [\underline{r}_{ij}(t) - \underline{r}_{ij}(0)]^2 \rangle, \quad (10)$$

where \underline{r}_{ij} is the vector between the centers of two particles \underline{i} and \underline{j} , and the time \underline{t} is measured from an arbitrarily selected zero.

Manipulation of the RHS of Eq. (10) yields the result

$$\Delta_v(t) = \langle \Delta \underline{r}_i(t)^2 \rangle + \langle \Delta \underline{r}_j(t)^2 \rangle - 2\langle \Delta \underline{r}_i(t) \cdot \Delta \underline{r}_j(t) \rangle, \quad (11)$$

where $\Delta \underline{r}_i(t) = \underline{r}_i(t) - \underline{r}_i(0)$ is the vector displacement of particle \underline{i} after time \underline{t} , measured in the laboratory coordinate system, and $\Delta \underline{r}_j(t)$ is similarly defined.

Substituting from Eq. (1) yields

$$\Delta_v(t) = \sum_i(t) + \sum_j(t) - 2\langle \Delta \underline{r}_i(t) \cdot \Delta \underline{r}_j(t) \rangle \quad (12a)$$

$$= 2\sum(t) - 2C(t), \quad (12b)$$

where (b) is the result for a single-component fluid and $C(t)$ represents the cross-correlation factor $\langle \Delta \underline{r}_i(t) \cdot \Delta \underline{r}_j(t) \rangle$.

Theoretical treatments of chemical reaction kinetics in solution frequently invoke a model in which the diffusion of molecules of one reactant is examined in a reference frame such that the

molecules of the second reactant are held stationary.¹³ If for example the reaction under consideration is represented by $A + B \rightarrow AB$, the theory might attempt to calculate the flux of diffusing B molecules upon a stationary molecule of reactant A. In such a model, it would then be standard practice to describe the diffusion of the B molecules by an "effective" diffusion coefficient

$$D'_B = D_A + D_B , \quad (13)$$

where D_A and D_B are the bulk diffusion coefficients of species A and B, respectively.

A simple analysis shows that the function $\Delta_v(t)$ is equivalent to the "effective" singlet diffusion function $\sum'_{i,j}(t)$ for one particle of an $[i,j]$ pair in a coordinate system fixed to the center of the other particle. Comparison of Eqs. (7) and (12a) then shows that the formulation in Eq. (13) is equivalent to an assumption that the cross-correlation factor $C(t)$ is uniformly zero; that is, that the relative motion of a pair of reactant molecules is uncorrelated at all distances.

A quantitative measure of the short-range correlations associated with the cooperative phenomena observed in the model fluid can be obtained by calculating $\Delta_v(t)$ and $C(t)$ functions for different sets of pairs of particles, where the pairs $[i,j]$ comprising each set are selected on the basis of the scalar distance $r_{ij}(0)$ between the centers of the two particles at the chosen zero time. This procedure can be represented mathematically by appending a "selection"

function $h[r_{ij}(0)]$ to the formulations given above:

$$\Delta_v(t;h_n) = \langle [\underline{r}_{ij}(t) - \underline{r}_{ij}(0)]^2 h_n[r_{ij}(0)] \rangle \quad (14a)$$

$$C(t;h_n) = \langle [\Delta \underline{r}_i(t) \cdot \Delta \underline{r}_j(t)] h_n[r_{ij}(0)] \rangle , \quad (14b)$$

where the value of $h[r_{ij}(0)]$ is unity if $r_{ij}(0)$ is within the desired range of initial distances, and zero otherwise. The subscript \underline{n} on \underline{h} will be used to specify the range of $r_{ij}(0)$ values "selected" by that function.

Since "selection" of the pairs should not affect the ensemble-averaged singlet diffusion of the particles comprising each pair, Eq. (12b) can be rewritten

$$\Delta_v(t;h_n) = 2\sum(t) - 2C(t;h_n) . \quad (15)$$

Correlations in the motions of the selected pairs are therefore evidenced by non-zero values for the cross-correlation factor $C(t;h_n)$ or alternatively, deviations of the pair displacement function from twice the slope of the singlet function $\sum(t)$ computed from the same simulation data.

B. Relative Diffusion in the Model Fluid

The simulation data for state No. 3 was analyzed to obtain $\Delta_v(t;h_n)$ and $C(t;h_n)$ functions for sets of pairs with $r_{ij}(0)$ distances corresponding to the average first and second nearest-neighbor distances in the fluid at that temperature and density. In Fig. 4 the two $r_{ij}(0)$ "selection" ranges are shown in relation to the radial

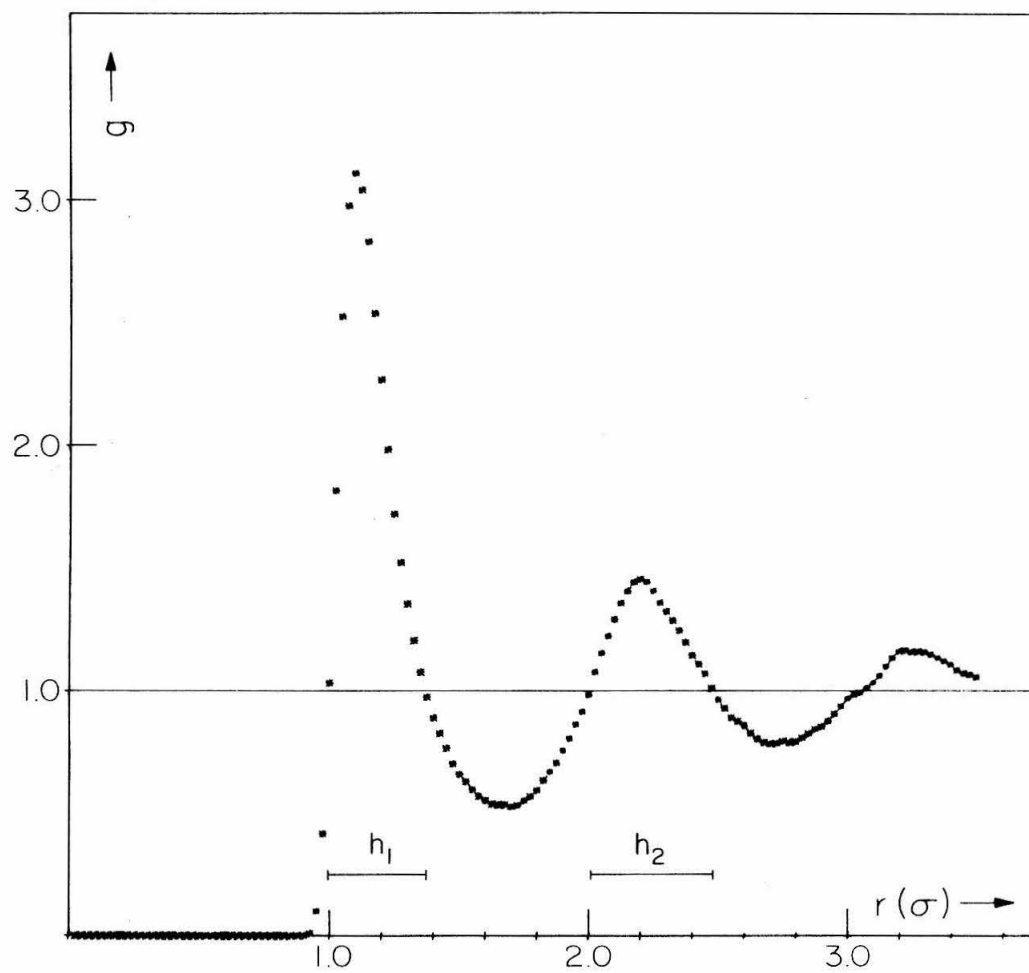


FIG. 4. The radial distribution function $g(r)$ for the model fluid in state No. 3. The h_1 and h_2 pair selection intervals are also indicated.

distribution function for state No. 3; the two ranges will hereafter be referred to as " h_1 " and " h_2 ", as indicated in the figure.

In Fig. 5 the relative diffusion functions are shown in comparison to the singlet function $\sum(t)$ for state No. 3. The greater degree of correlation exhibited by the h_1 pairs is in intuitive accord with our description of the distance dependence of the cooperative processes occurring in the model fluid. More interesting however is the fact that the slopes of the cross-correlation functions for both sets of pairs remain positive over the entire 1.1×10^{-11} sec interval spanned by the calculations. The correlations associated with the cooperative processes must therefore persist for much longer times than suggested even by the graphical displays of the particle trajectories.

Comparison of the $\Delta_v(t;h_n)$ and $\sum(t)$ functions plotted in Fig. 5 shows that the coefficient for relative diffusion must decrease significantly for particles approaching within two, and perhaps even three or four diameters of each other. The motions of particles separated by large distances in the fluid are totally uncorrelated [$C(t;h_\infty) = 0$]; then Eqs. (7) and (12b) indicate that the "effective" coefficient describing the diffusion of one particle i relative to another particle j must for large r_{ij} be equal to twice the coefficient for singlet (self-) diffusion. But as two particles approach each other more closely, cooperative processes slow their average relative motion until, as shown by comparing the slopes of the $\sum(t)$ and $\Delta_v(t;h_1)$ functions plotted in Fig. 5, the coefficient describing

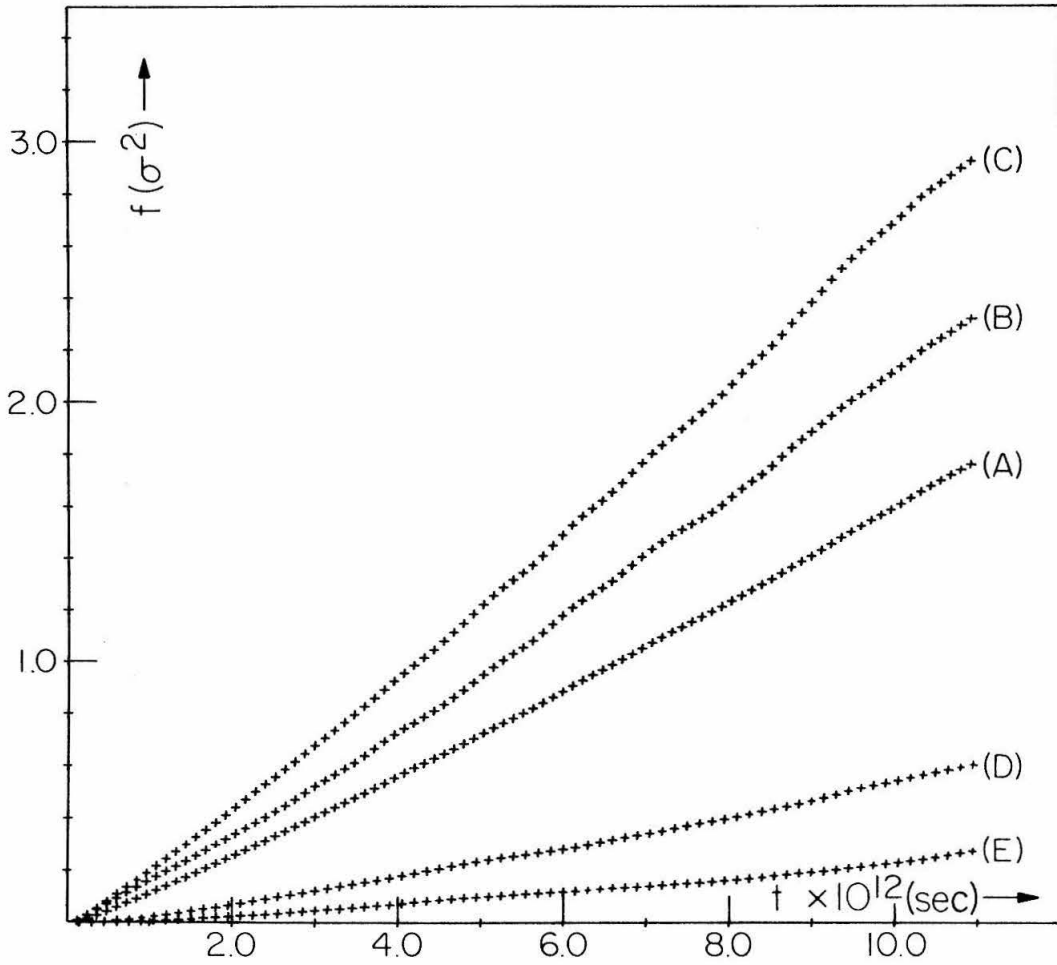


FIG. 5. Comparison of singlet and relative mean square displacement functions computed from the simulation data for state No. 3 of the model fluid. A: $\Sigma(t)$; B: $\Delta_V(t; h_1)$; C: $\Delta_V(t; h_2)$; D: $C(t; h_1)$; E: $C(t; h_2)$.

their relative diffusion may fall to only approximately 65% of the larger- r_{ij} value.

The singlet diffusion of the particles "selected" for relative diffusion calculations cannot differ from the singlet diffusion of the system as a whole except through statistical fluctuations due to the finite sample size. Rearrangement of Eq. (15) yields

$$\sum(t) = \frac{1}{2} \Delta_v(t; h_n) + C(t; h_n).$$

The relative diffusion functions computed directly from the simulation data combine as indicated to reproduce the $\sum(t)$ function for state No. 3 within 1-2%.

C. A Simple Physical Model

In theoretical treatments of various liquid state phenomena, it is frequently convenient to define an "effective" pair potential or "potential of mean force" $\psi(r)$ that describes the average interaction between a pair of molecules when interactions with the other, neighboring molecules are taken into account. To a first approximation, this "effective" potential can be obtained from the familiar radial distribution function $g(r)$ ¹⁴:

$$\psi(r) = -k_B T \ln g(r), \quad (16)$$

where k_B is the Boltzmann constant and T the temperature of the liquid. In Fig. 6 the mean potential function for state No. 3 is shown

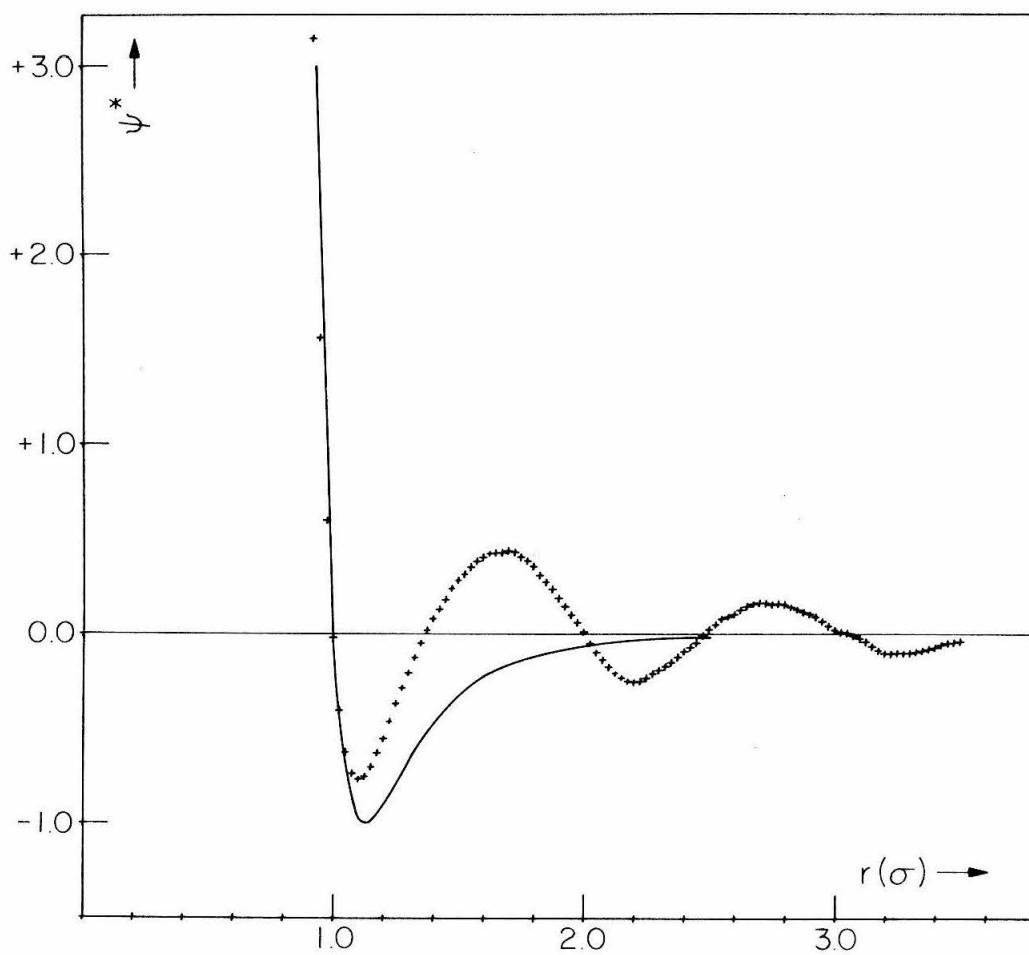


FIG. 6. Comparison of the mean potential $\psi(r)$ for state No. 3 of the model fluid and the Lennard-Jones pair potential used in the simulation calculations.

in comparison with the Lennard-Jones pair potential used in the simulation calculations.

Although further analysis shows (vide infra) that the mean potential defined by Eq. (16) is not in itself sufficient to treat the relative diffusion functions computed from the simulation data, $\psi(r)$ can serve as a convenient intuitive device for interpreting the microscopic diffusion processes observed in the model fluid. Unlike the simple Lennard-Jones pair potential, $\psi(r)$ exhibits several successive maxima and minima corresponding to the first, second, third, ..., etc., "shells" of neighbors around a particle in the fluid. A particle diffusing toward another particle must therefore cross several successively higher potential "barriers" before the two particles can come into direct contact. And conversely, a particle diffusing away from another particle in the fluid may become "trapped" momentarily in each of the successive minima in $\psi(r)$.

As in the case of singlet diffusion, a more detailed picture of the microscopic processes occurring in the model fluid is provided by distributions of various quantities related to the relative diffusion mechanism. Figures 7 and 8 show for example the distributions $w(r, t; h_n)$ for the h_1 and h_2 pairs "selected" in the analysis of the simulation data for state No. 3, where $w(r, t; h_n)\Delta r$ is the fraction of the pairs of particles $[i, j]$ selected by h_n which at time t are separated by a distance $r_{ij}(t) = r \pm (\Delta r/2)$. An increment $\Delta r = 0.05\sigma$ was used in the calculations.

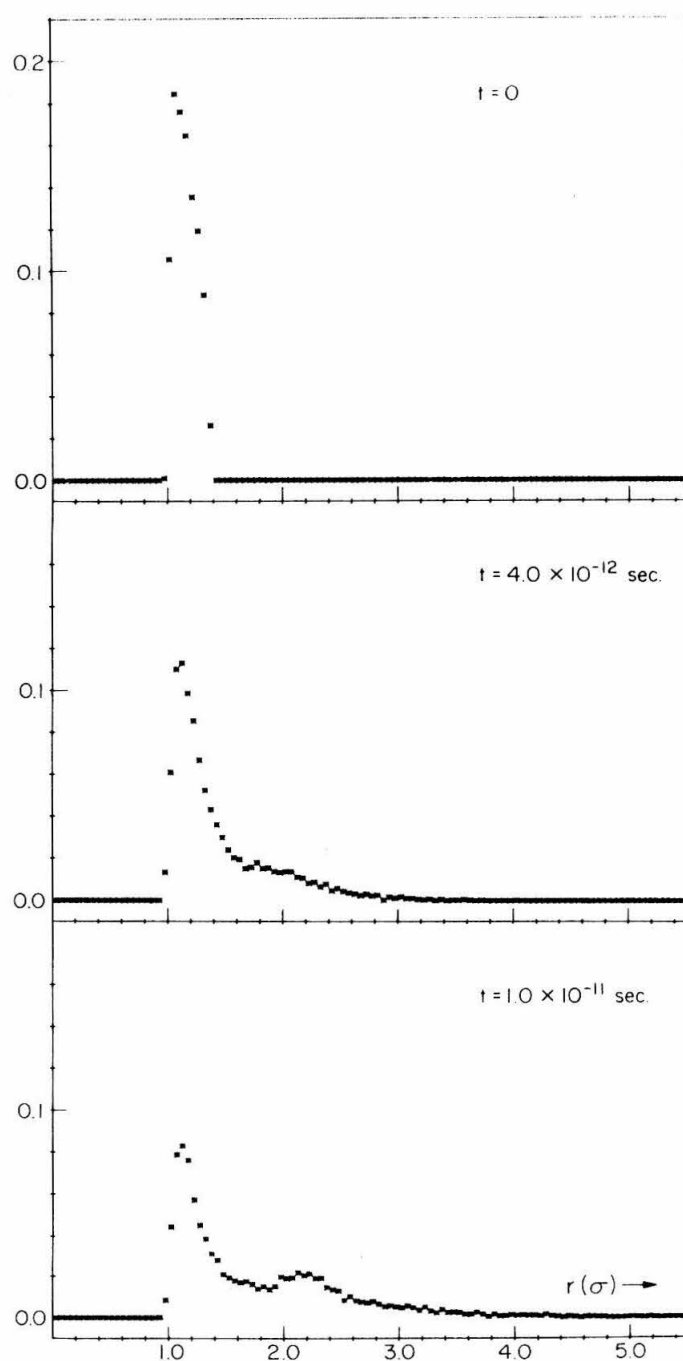


FIG. 7. Time-dependent distribution of pair separations $w(r, t; h_1)\Delta r$ for the h_1 pairs in the simulation data for state No. 3 of the model fluid.

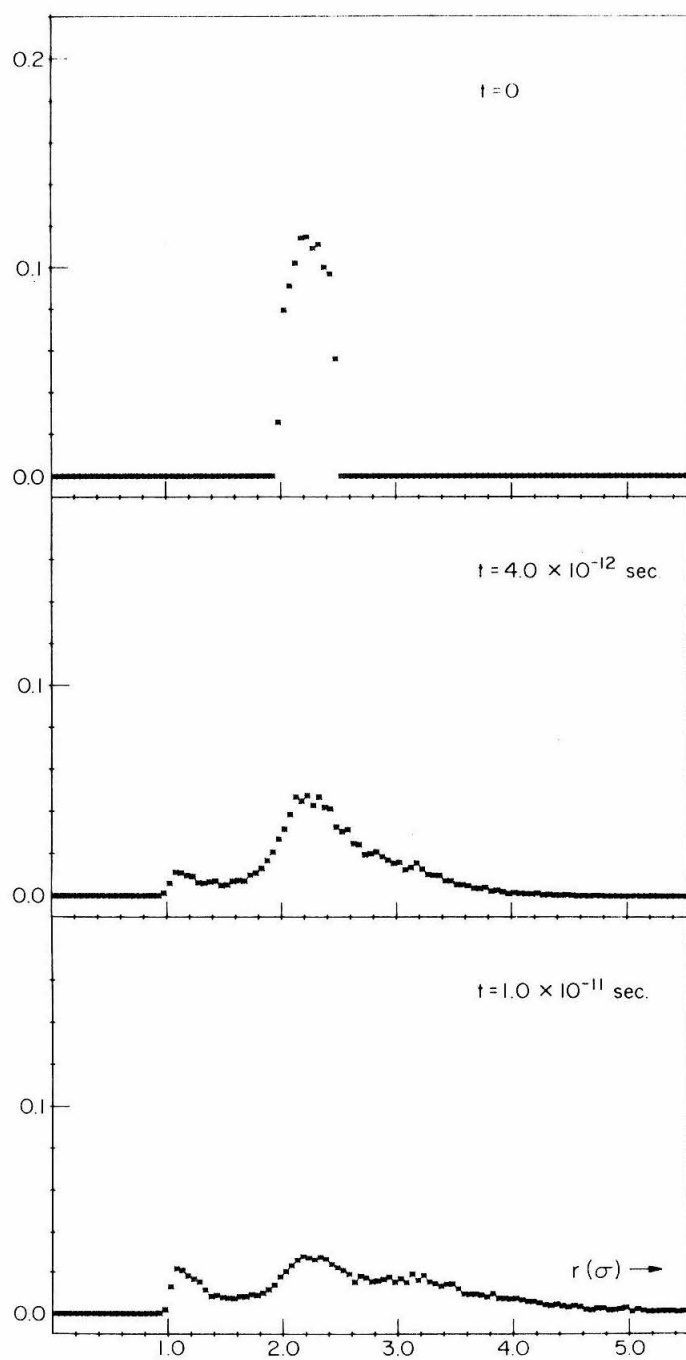


FIG. 8. Time-dependent distributions of pair separations $w(r, t; h_2)$ for the h_2 pairs in the simulation data for state No. 3 of the model fluid.

The intuitive value of $\psi(r)$ is evidenced by the $t = 1.0 \times 10^{-11}$ sec distributions shown in the Figures. Comparison of Figs. 4 and 6 shows that the particles comprising the h_1 and h_2 pairs were just those particles separated by distances $r_{ij}(0)$ corresponding to the positions of the first and second minima in $\psi(r)$, respectively. Figure 7 then shows that, during an interval of 10^{-11} sec, a significant fraction of the h_1 pairs surmounted the first local maximum in $\psi(r)$ and became trapped in the second minimum; Fig. 8 shows that the h_2 pairs become distributed between the first, second, and third minima during an equal time interval.

If the motions of the two particles comprising each pair were uncorrelated, the contributions $\langle \Delta \tilde{r}_i(t) \cdot \Delta \tilde{r}_j(t) \rangle$ to the cross-correlation function $C(t; h_n)$ from the pairs in either set would be distributed symmetrically about zero. In Fig. 9 the distributions of contributions to $C(t; h_1)$ for $t = 4.0 \times 10^{-12}$ and 1.0×10^{-11} sec are shown; the asymmetry of the distributions is obvious.

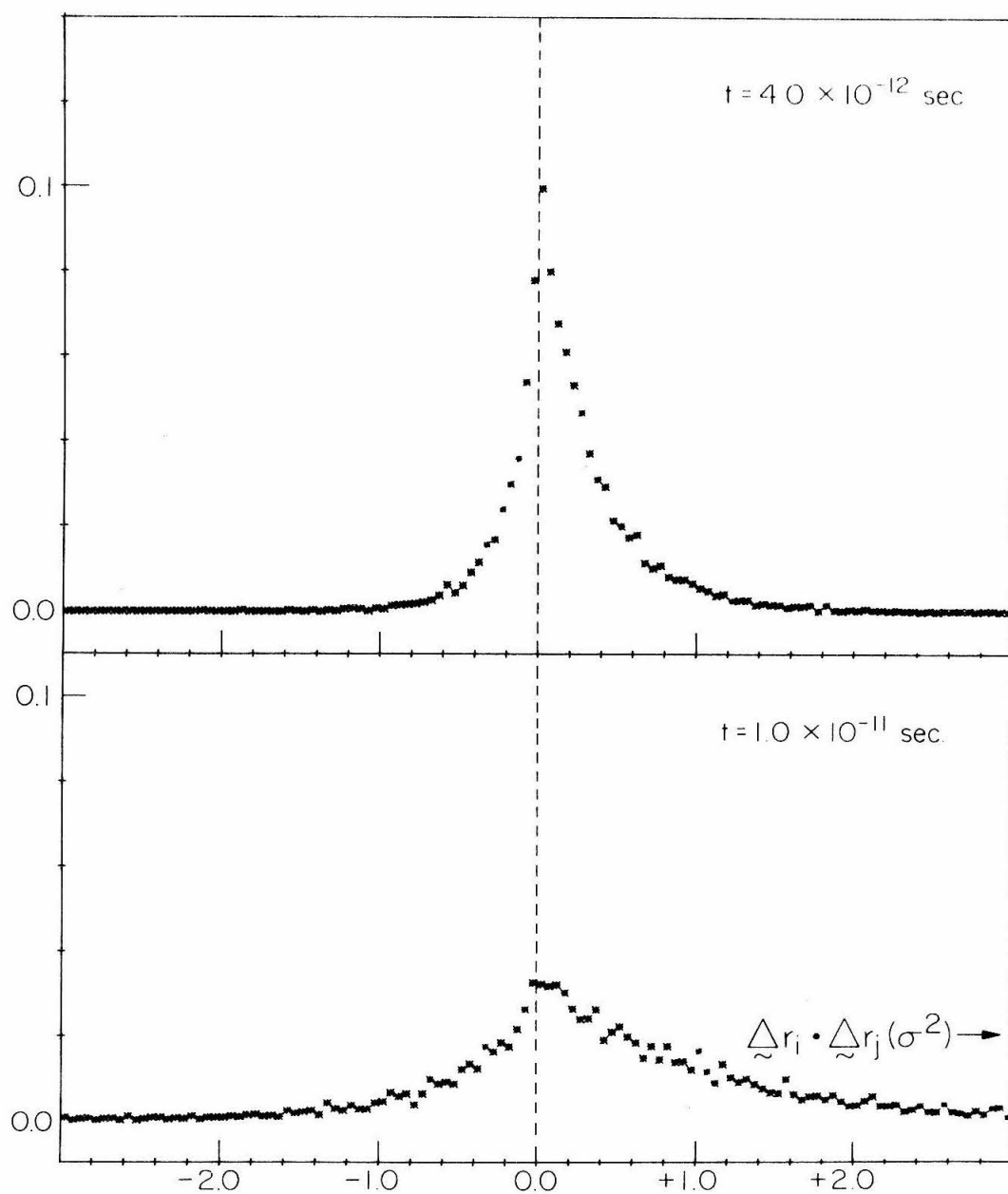


FIG. 9. Distributions of the contributions to the cross-correlation function $C(t; h_1)$ for the h_1 pairs in the simulation data for state No. 3 of the model fluid.

IV. THEORETICAL TREATMENT OF RELATIVE DIFFUSION

A. Mathematical Formalism

The relative diffusion of two particles in two dimensions is conveniently described in terms of the motion of one particle in a coordinate system (r, θ) fixed to the center of the other particle.

The relative diffusion tensor $\underline{\underline{D}}_R$ then has the form

$$\underline{\underline{D}}_R = \begin{pmatrix} D_{rr} & 0 \\ 0 & D_{\theta\theta} \end{pmatrix},$$

where D_{rr} and $D_{\theta\theta}$ are the coefficients for radial and tangential diffusion, respectively, and the off-diagonal elements vanish by symmetry. The angle θ may be measured from some fixed axis in the laboratory coordinate system.

Were the diffusive motions of proximate particles in the fluid totally uncorrelated, the relative diffusion coefficients would both be constant and equal to twice the coefficient for singlet (self-) diffusion. The data presented in the preceding section show however that cooperative processes retard the relative diffusion of particles separated by short distances. Furthermore, solutions to the two-dimensional diffusion equation including only the potential of mean force $\psi(r)$ defined by Eq. (16) do not reproduce the relative diffusion phenomena observed in the model fluid (vide infra). We therefore develop a formalism that incorporates both $\psi(r)$ and r -dependent coefficients $D_{rr}(r)$ and $D_{\theta\theta}(r)$.

It is not immediately evident that this approach can be rigorously justified. But as we shall show below, the resulting formalism permits an accurate quantitative reproduction of the relative diffusion functions computed from the simulation data. Moreover, this formalism has the particular advantage that, once $D_{rr}(r)$ and $D_{\theta\theta}(r)$ have been determined, the influence of cooperative phenomena upon the kinetics of very fast chemical processes in solution can be readily evaluated. This aspect of relative diffusion in liquids will be treated in a forthcoming paper.

Consider a concentration distribution $c(r, \theta, t)$ of particles around a given particle in the fluid. The time-dependent behavior of this distribution is then given by

$$\begin{aligned} \frac{\partial c(r, \theta, t)}{\partial t} = & \frac{1}{r} \frac{\partial}{\partial r} \left\{ r D_{rr}(r) \left[\frac{\partial c(r, \theta, t)}{\partial r} + \frac{c(r, \theta, t)}{k_B T} \frac{dv(r)}{dr} \right] \right\} \\ & + \frac{1}{r^2} D_{\theta\theta}(r) \frac{\partial^2 c(r, \theta, t)}{\partial \theta^2}, \end{aligned} \quad (17)$$

where $v(r)$ is the average potential interaction between two particles separated by distance r in the fluid,¹⁵ and we have assumed the Einstein expression for the friction constant. It is difficult to obtain a direct quantitative measure of tangential relative diffusion in the model fluid. The scalar analogue of $\Delta_v(t; h_n)$,

$$\Delta_s(t; h_n) = \langle [r_{ij}(t) - r_{ij}(0)]^2 h_n[r_{ij}(0)] \rangle, \quad (18)$$

does however provide a convenient measure of radial relative diffusion and can be readily computed from the simulation data.

Let $c_r(r, t)$ be the average concentration of particles at a distance r from a given particle. Then

$$c_r(r, t) = \frac{1}{2\pi} \int_0^{2\pi} c(r, \theta, t) d\theta, \quad (19)$$

and integration of Eq. (17) yields

$$\frac{\partial c_r}{\partial t} = \frac{1}{r} \frac{\partial}{\partial r} \left\{ r D_{rr}(r) \left[\frac{\partial c_r}{\partial r} + \frac{c_r}{k_B T} \frac{dv(r)}{dr} \right] \right\}. \quad (20)$$

Consider an instance where $c_r(r, 0)$ is zero except for a narrow band of neighbors at $r = r_0$. The scalar mean square displacement of these particles at later times is given by

$$\Delta_s(t; h_0) = \frac{\int_0^\infty c_r(r, t) (r - r_0)^2 r dr}{\int_0^\infty c_r(r, t) r dr}. \quad (21)$$

Application of iterative numerical techniques permits solution of Eq. (20) and then Eq. (21) for finite concentration distributions $c_r(r, 0)$ corresponding to the sets of pairs used in calculating the relative diffusion functions discussed in Sec. III. Various formulations for $D_{rr}(r)$ can therefore be tested until the $\Delta_s(t; h_n)$ functions computed directly from the simulation data are reproduced. The resulting concentration distributions $c_r(r, t)$ can also be converted and compared to $w(r, t; h_n)$ distributions of the sort shown in Figs. 7 and 8, providing an additional test of the theoretical formalism

An approximate measure of $D_{\theta\theta}(r)$ within an interval $r_1 \leq r \leq r_2$ is provided by the difference between the scalar and vector

functions $\Delta_s(t; h_n)$ and $\Delta_v(t; h_n)$ for pairs $[i, j]$ with initial separations $r_1 \leq r_{ij}(0) \leq r_2$. Let $c_\theta(\theta, t)$ be the average concentration of particles lying in an angular wedge $\theta \rightarrow \theta + d\theta$ centered on a given particle in the fluid. Then

$$c_\theta(\theta, t) = \int_0^\infty c(r, \theta, t) r \, dr. \quad (22)$$

In the instances we will be treating here, $c(r, \theta, t)$ and $\partial c(r, \theta, t)/\partial t$ both vanish strongly at $r = 0$ and $r = \infty$. Multiplication of Eq. (17) by \underline{r} and integration then yields

$$\frac{\partial c_\theta}{\partial t} = \int_0^\infty \frac{1}{r^2} D_{\theta\theta}(r) \frac{\partial^2 c(r, \theta, t)}{\partial \theta^2} r \, dr. \quad (23)$$

Consider a concentration distribution $c(r, \theta, 0)$ that is non-zero for $r = r_0$. For times sufficiently short that displacements in the radial direction can be neglected, the term $D_{\theta\theta}(r)/r^2$ can be approximated by $D_{\theta\theta}(r_0)/r_0^2$, and Eq. (23) reduces to

$$\frac{\partial c_\theta(\theta, t)}{\partial t} = \frac{1}{r_0^2} D_{\theta\theta}(r_0) \frac{\partial^2 c_\theta(\theta, t)}{\partial \theta^2}. \quad (24)$$

If the tangential displacements are also small, the boundary values of θ required to normalize a solution of Eq. (24) can be taken as $-\infty$ and $+\infty$, rather than 0 and 2π . We then obtain the result

$$\overline{[\theta(t) - \theta(0)]^2} = \frac{2}{r_0^2} D_{\theta\theta}(r_0) t. \quad (25)$$

Subtracting Eq. (18) from Eq. (14a) and simplifying yields the identity

$$\Delta_v(t;h_n) - \Delta_s(t;h_n) = 2\langle r_{ij}(t)r_{ij}(0)[1 - \cos\{\theta(t) - \theta(0)\}]h_n \rangle. \quad (26)$$

For short times we may set $r_{ij}(t) \cong r_{ij}(0) = r_0$ and approximate the cosine by the first two terms of the series expansion. The identity in Eq. (26) then reduces to

$$\Delta_v(t;h_n) - \Delta_s(t;h_n) \cong r_0^2 \langle [\theta(t) - \theta(0)]^2 h_n \rangle,$$

and substitution from Eq. (25) yields the final expression

$$\Delta_v(t;h_n) - \Delta_s(t;h_n) \cong 2D_{\theta}(r_0)t. \quad (27)$$

B. Relative Diffusion Coefficients for the Model Fluid

The formalism developed above was applied to further analysis of the simulation data for state No. 3 (Table I). For syntactic simplicity, functions or distributions computed from the simulation data will hereafter be referred to as "model" functions or distributions, while those calculated on the basis of the theoretical formalism will be referred to as "theoretical" functions, etc.

A final empirical formula for $D_{rr}(r)$,

$$\begin{aligned} D_{rr}(r) &= 2D_s \{1 - (0.4/r^{0.25})\} & \text{for } r \leq 3\sigma \\ &= 2D_s \{1 - [0.4/r^{(0.5r - 1.25)}]\} & r > 3\sigma \end{aligned} \quad (28)$$

was obtained by repeated calculations, based on Eqs. (20) and (21) with $v(r)$ set equal to $\psi(r)$, until the scalar functions $\Delta_s(t;h_n)$

computed directly from the simulation data were reproduced. The final theoretical and model Δ_s functions computed for the h_1 and h_2 pairs are shown in Figs. 10 and 11, respectively. Theoretical functions were also computed for $D_{rr} = 2D_s$ (uncorrelated motion assumption) with $v(r)$ set equal to $\psi(r)$, to the "soft sphere" potential

$$\begin{aligned}\varphi_{ss}(r) &= 4\epsilon(\sigma/r)^{12} && \text{for } r \leq \sigma \\ &= 0 && r > \sigma,\end{aligned}$$

and (for the h_1 pairs only) to the Lennard-Jones pair potential $\varphi_{LJ}(r)$. These additional theoretical functions are also plotted in the two figures.

The theoretical functions obtained with $v(r) = \psi(r)$ and $D_{rr} = 2D_s$ (curves C in both Figs. 10 and 11) show that, at least within the theoretical framework established above, the mean potential defined by Eq. (16) does not provide an adequate measure of the microscopic processes hindering relative diffusion in the dense model fluid. The extent to which $\psi(r)$ does retard the relative diffusion of first nearest-neighbors--represented here by the h_1 pairs--is illustrated by curves C and D in Fig. 10, obtained with $v(r) = \psi(r)$ and $v(r) = \varphi_{ss}(r)$, respectively. It is interesting to note however that $\psi(r)$ does not similarly depress the rate of radial relative diffusion for the h_2 pairs (comparing curves B and C in Fig. 11), probably due to the relative shallowness of the second minimum in the mean potential. Although the Lennard-Jones

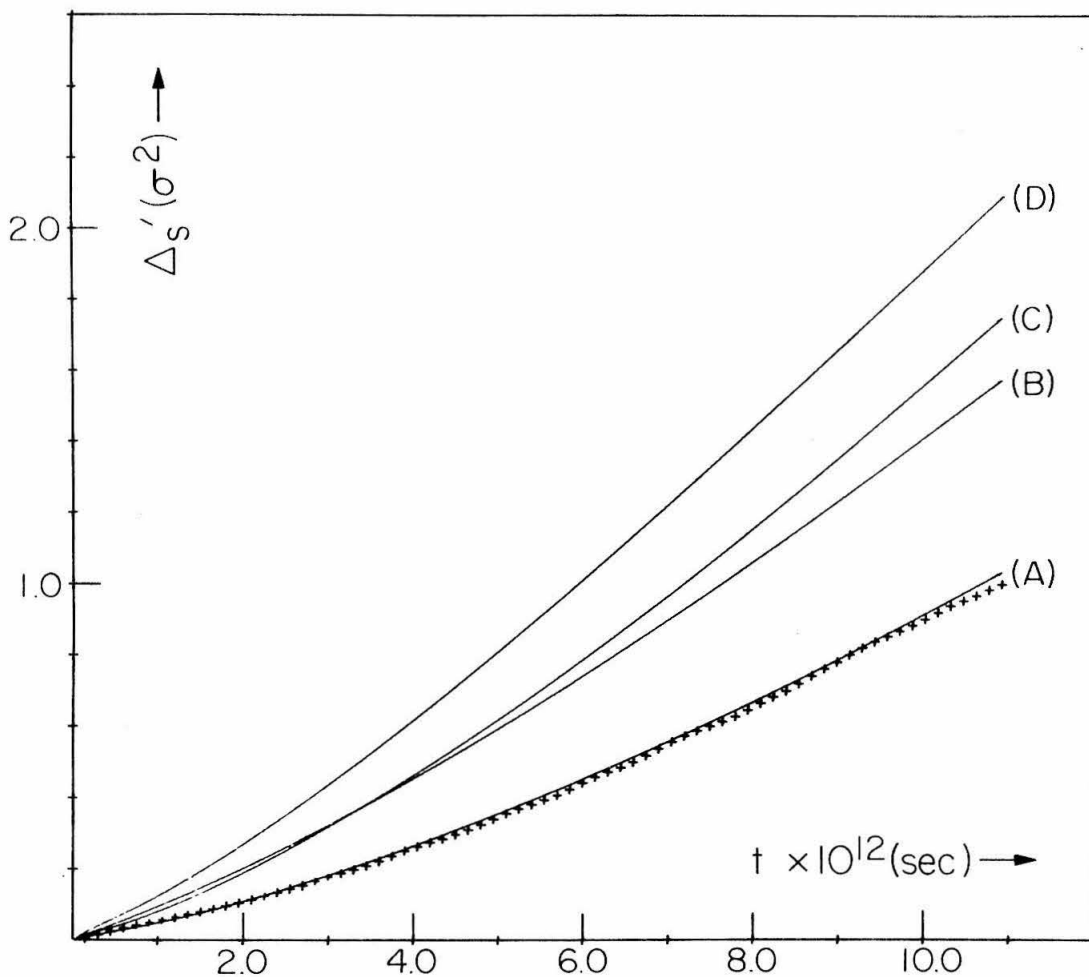


FIG. 10. Comparison of the scalar relative diffusion function $\Delta_S(t;h_1)$ computed from the simulation data for state No. 3 of the model fluid (+++++) and theoretical functions (—) computed with various combinations of $v(r)$ and $D_{rr}(r)$.
 A: $v(r) = \psi(r)$ and $D_{rr}(r)$ as given in Eq. (28); B: $v(r) = \varphi_{LJ}(r)$ and $D_{rr} = 2D_S$; C: $v(r) = \psi(r)$ and $D_{rr} = 2D_S$; D: $v(r) = \varphi_{SS}$ and $D_{rr} = 2D_S$.

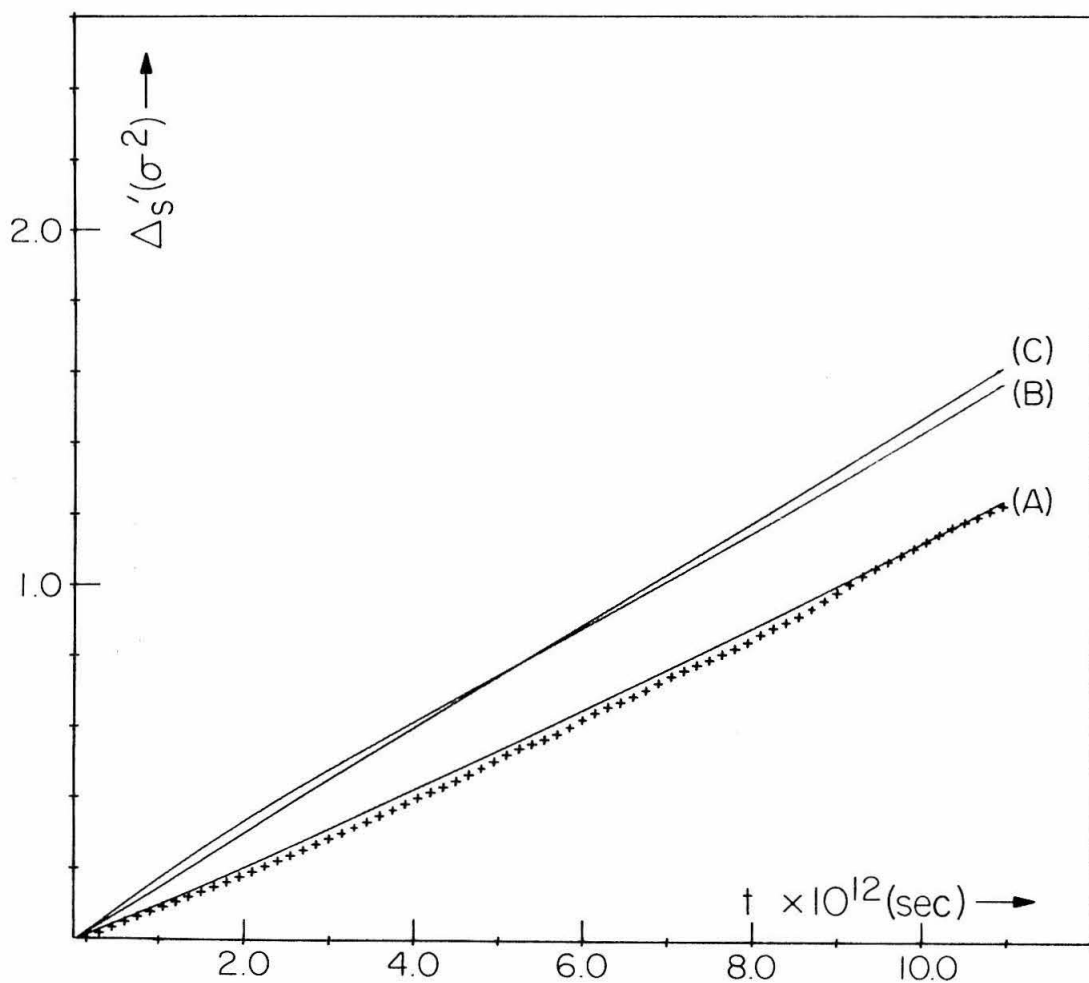


FIG. 11. Comparison of the scalar relative diffusion function $\Delta_S(t;h_2)$ computed from the simulation data for state No. 3 of the model fluid (+++++) and theoretical functions (—) computed with various combinations of $v(r)$ and $D_{rr}(r)$.
 A: $v(r) = \psi(r)$ and $D_{rr}(r)$ as given in Eq. (28); B: $v(r) = \varphi_{ss}$ and $D_{rr} = 2D_S$; C: $v(r) = \psi(r)$ and $D_{rr} = 2D_S$.

potential yields even a slower rate for the relative diffusion of the h_1 pairs (curve B in Fig. 10) when it is assumed that $D_{rr} = 2D_s$, the predicted distributions $w(r, t; h_1)$ obtained with $v(r) = \varphi_{LJ}(r)$ are in qualitative disagreement with those calculated directly from the simulation data (vide infra).

Approximate values for $D_{\theta\theta}(r)$ were computed, according to Eq. (27), from the Δ_v and Δ_s functions for the h_1 and h_2 pairs and the set of pairs--the " $h_{1\frac{1}{2}}$ " pairs--with $r_{ij}(0)$ lying between the h_1 and h_2 selection ranges. The value of the coefficient for each range was obtained from the slope of the least-squares line fitted through the difference function $\{\Delta_v(t; h_n) - \Delta_s(t; h_n)\}$ computed at intervals of 3×10^{-14} sec from $t = 0.25 \times 10^{-12}$ to 1.75×10^{-12} sec. In all three cases the rms deviation from the linear fit was less than $1.5 \times 10^{-3} \sigma^2$, while the maximum ($t = 1.75 \times 10^{-12}$ sec) value for each of the difference functions was approximately $0.2 \sigma^2$. The resulting approximate coefficient was

$$\begin{aligned} D_{\theta\theta}(r) &\cong 1.38 D_s && \text{for } 0.999 \sigma \leq r < 1.368 \sigma \text{ ("}h_1\text{"}) \\ &\cong 1.57 D_s && 1.368 \sigma \leq r < 1.979 \sigma \text{ ("}h_{1\frac{1}{2}}\text{"}) \\ &\cong 1.54 D_s && 1.979 \sigma \leq r < 2.481 \sigma \text{ ("}h_2\text{"}), \end{aligned}$$

where $D_s = 4.39 \times 10^{10} \sigma^2 \cdot \text{sec}$ is the coefficient for self-diffusion for state No. 3.

It was initially supposed that relative diffusion in the dense model fluid might be anisotropic; a pair of neighboring particles might for example rotate more easily than diffusing toward or away from each other. The results presented here indicate however

that--at least for the state of the model fluid we have examined--cooperative processes depress the rates of radial and tangential relative diffusion about equally.

It is interesting to note that the value of $D_{\theta\theta}(r)$ obtained for the $h_{1\frac{1}{2}}$ "selection" interval is somewhat higher than the values obtained for either the h_1 or h_2 intervals. Figure 4 shows that the particles comprising the $h_{1\frac{1}{2}}$ pairs were initially separated by $r_{ij}(0)$ distances lying between the average first and second nearest-neighbor distances in the model fluid. The higher value of $D_{\theta\theta}$ obtained for this intermediate range of separations could therefore indicate that a particle migrating between the first and second neighbor "shells" of another particle must move tangentially until it can find or force its way into an empty "slot" in one of the "shells".

C. Theoretical Concentration Distributions

Although the theoretical formalism developed in Sec.IV.A above permits us to reproduce quite accurately the scalar functions $\Delta_s(t;h_n)$ computed from the simulation data, the empirical method whereby the functional form for $D_{rr}(r)$ is determined may cast some doubt upon the validity of the overall theoretical treatment. The concentration distributions $c_r(r,t)$ obtained by numerical integration of Eq.(20) can however easily be converted into the corresponding $w(r,t;h_n)$ distributions, and thus provide a severe test of the accuracy with which the theoretical treatment describes radial relative diffusion in the model fluid.

In Fig. 12 the theoretical $w(r, t; h_n)$ distributions obtained with $v(r) = \psi(r)$ and the empirical coefficient $D_{rr}(r)$ given by Eq. (28) are compared to the corresponding model distributions for $t = 1.0 \times 10^{-11}$ sec. The quantitative agreement between the theoretical and model distributions for both the h_1 and h_2 pairs is quite good.

The theoretical distributions shown in Fig. 12 are also reproduced in Fig. 13 for comparison with the distributions obtained with $D_{rr} = 2D_s$ and $v(r) = \psi(r)$, $v(r) = \varphi_{ss}$, and (for the h_1 pairs only) $v(r) = \varphi_{LJ}(r)$. The "soft-sphere" and Lennard-Jones potentials yield distributions differing qualitatively from those computed from the simulation data. And while the distributions obtained with $v(r) = \psi(r)$ but with $D_{rr} = 2D_s$ or $D_{rr}(r)$ as given in Eq. (28) appear rather similar, the "no correlation" assumption ($D_{rr} = 2D_s$) is seen to permit the initial $w(r, 0; h_n)$ distribution for either set of pairs to "decay" more rapidly than actually observed in the model fluid.

V. DISCUSSION

The motion of single particles and pairs of particles is fundamental to the kinetics of liquids. A proper understanding of this kinetics is necessary to more fully explain a large number of phenomena including transport coefficients (the viscosity and thermal conductivity), diffusion controlled chemical reactions, electromagnetic scattering, dielectric relaxation, etc. Using molecular dynamics we have studied

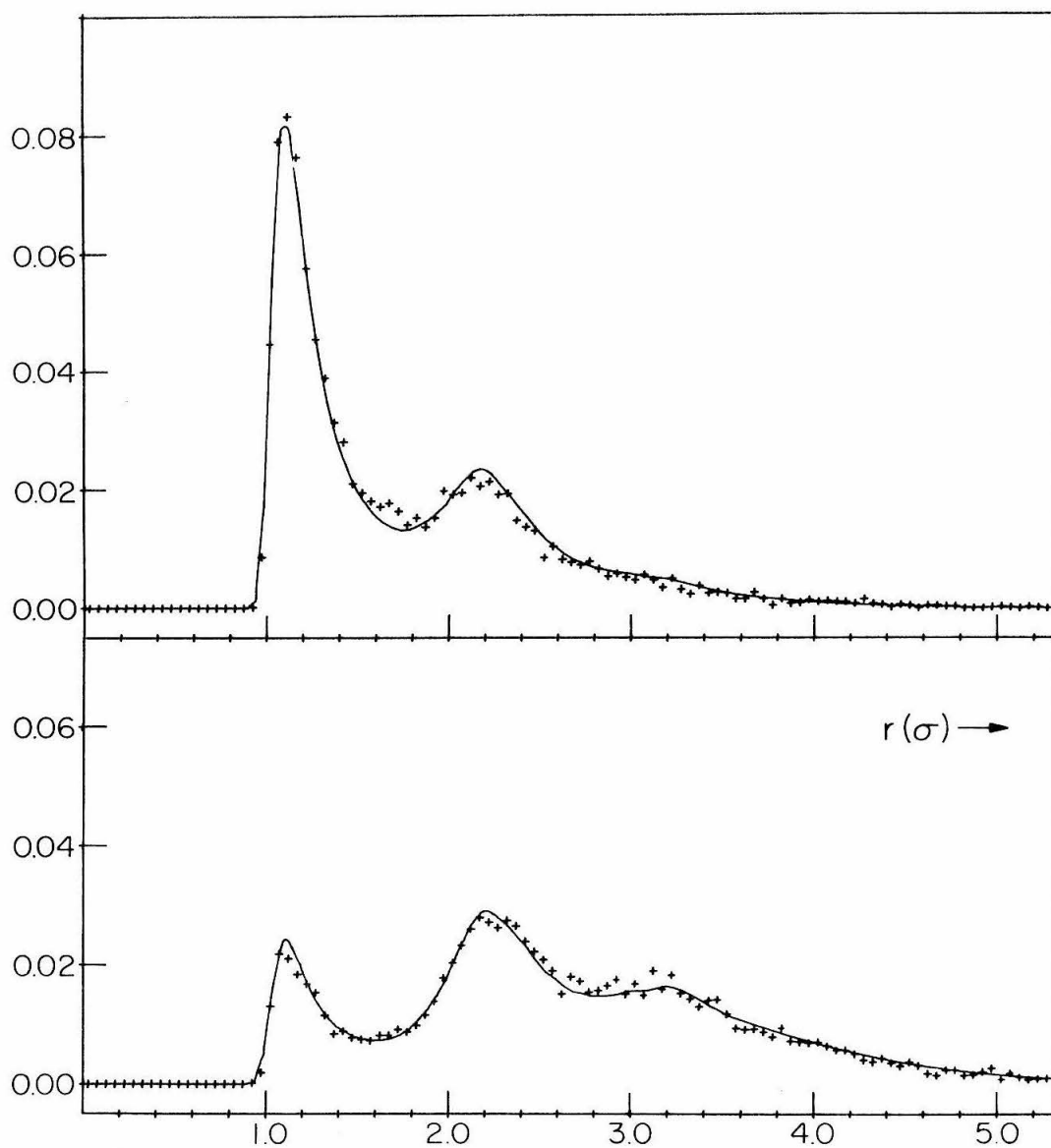


FIG. 12. Comparison of the time-dependent distributions of pair separations $w(r, t; h_n)$ for $t = 10^{-11}$ sec computed from the simulation data for state No. 3 of the model fluid (+++++) and the theoretical formalism with $v(r) = \psi(r)$ and $D_{rr}(r)$ as given in Eq. (28).

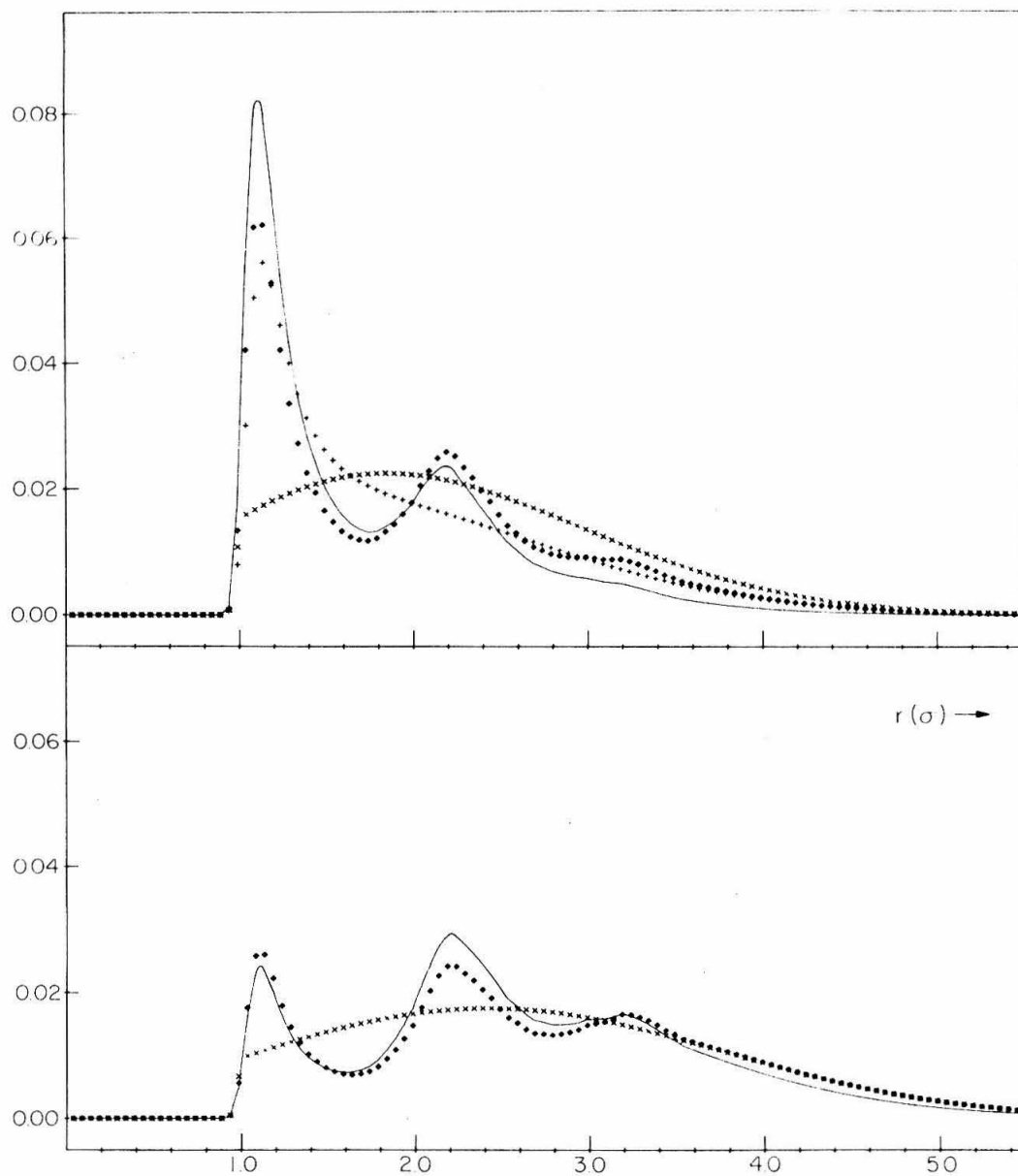


FIG. 13. Comparison of the theoretical distributions of pair separations $w(r, t; h_n)$ obtained with different combinations of $v(r)$ and $D_{rr}(r)$. —: $v(r) = \psi(r)$ and $D_{rr}(r)$ as given in Eq. (28); \blacklozenge : $v(r) = \psi(r)$ and $D_{rr} = 2D_S$; +++++: $v(r) = \varphi_{LJ}(r)$ and $D_{rr} = 2D_S$; xxxxx: $v(r) = \varphi_{SS}$ and $D_{rr} = 2D_S$.

these kinetic properties directly from a number of points of view.

We conclude from our study of the graphical displays that particle motion at liquid densities is highly cooperative; the particles tend to move in chains. Much the same "chain motion" has been observed in molecular dynamics studies of melting in two-dimensional liquids. The other important structural feature which we have exhibited are the "holes" which appear to be different from the vacancy-like holes postulated in certain liquid structure theories.

Our more exacting study of relative motion starts with the relative diffusion of mean square relative displacement. This mean square displacement term decomposes simply into a singlet mean square displacement term and a correlation term. In addition, the relative diffusion depends on the set of initial ($t=0$) relative displacement values chosen. To gain insight into the details of the process we chose certain ranges for the initial relative displacement which lay in the first few nearest neighbor shells where we expected the correlation term to be important. The correlation term was found to be significant in these regions.

To study the nature of this significant correlation in a more explicit manner we then introduced two basic physical effects into a mathematical model for the relative diffusion process. We employed the Fokker-Planck equation with various potentials and various dependences for the diffusion coefficient as a function of r . The long time behavior of the distribution function for the density of the system as a function of the relative coordinate is rather simple: For small r ,

of the order of a few molecular diameters, the distribution must approach the equilibrium radial distribution function. This determined our choice of the potential as the potential of the mean force. At large distances the mean square displacements of the two particles are uncorrelated so that all that is required in this region is that the mean force vanish (which it does) and that the relative diffusion coefficient become twice the singlet value. With these features of our Fokker-Planck analysis established, the only indeterminant feature remaining was the dependence of the radial diffusion coefficient $D_{rr}(r)$ on r . When $D_{rr}(r)$ was appropriately chosen, we showed that not only could we produce essential agreement with the mean square relative displacement calculated for the various regions, but also we could reproduce the molecular dynamics results for the time-dependent distribution function itself.

We conclude that--since the other aspects of the Fokker-Planck analysis are essentially predetermined--we can fully explain the details of relative diffusion by a single scalar function, the radial component of the relative diffusion tensor $D_{rr}(r)$. This function $D_{rr}(r)$, determined in an empirical manner to match the molecular dynamics results, is less than $2D_S$, the value for uncorrelated motion, so that relative diffusion is inhibited for particle separations of a few molecular diameters. Referring to Eq. (28) we see that in the important region of the first few neighbor shells, $D_{rr}(r)$ is of the order of $0.6 \times 2D_S$, an approximate 40% reduction in

diffusion in this region. Our study of angular diffusion showed that the diffusion tensor was essentially isotropic; no additional new phenomena were discovered by our study of $D_{\theta\theta}(r)$.

Now that the basic details of the relative diffusion process have been elucidated, the major emphasis should shift to the application of these results to the many phenomena we have described which depend on the relative motion of two atoms or molecules in a liquid. These studies will in turn suggest further research into the fundamental properties of two particle motion in liquids.

REFERENCES FOR PAPER NO. 3

- ¹P. L. Fehder, J. Chem. Phys. 50, 2617 (1969).
- ²See, for example, H. Eyring and R. P. Marchi, J. Chem. Educ. 562 (1963), and the discussion in J.M.H. Levelt and E.G.D. Cohen in Studies in Statistical Mechanics, Vol. 2, J. deBoer and G. E. Uhlenbeck, Eds., North-Holland Publishing Co., Amsterdam, Holland, 1964, p. 178 ff.
- ³P. L. Fehder, "'Anomalies' in the Radial Distribution Functions of Simple Liquids," manuscript in preparation.
- ⁴R. M. Noyes, J. Amer. Chem. Soc. 78, 5486 (1956).
- ⁵H. Rosman and R. M. Noyes, J. Amer. Chem. Soc. 80, 2410 (1957).
- ⁶R. M. Noyes, Z. Elektrochem. 64, 153 (1960).
- ⁷R. M. Noyes, J. Amer. Chem. Soc. 86, 4529 (1964).
- ⁸We use the term "singlet" here to distinguish between the diffusion of individual molecules in a fluid and the time-dependent relative displacements of pairs of molecules (relative diffusion).
- ⁹R. Zwanzig, Annu. Rev. Phys. Chem. 16, 67, Annual Reviews, Palo Alto (1965).
- ¹⁰J.M.H. Levelt and E.G.D. Cohen, op. cit.
- ¹¹J. G. Kirkwood, J. Chem. Phys. 14, 180 (1946).
- ¹²A. Rahman, J. Chem. Phys. 45, 2585 (1966).
- ¹³See, for example, R. M. Noyes in Progress in Reaction Kinetics, Vol. 1, G. Porter, Ed., Pergamon Press, New York, 1961, p. 128.

¹⁴P. A. Egelstaff, An Introduction to the Liquid State, Academic Press, New York, 1967, p. 16.

¹⁵We use $v(r)$ rather than $\psi(r)$ here for the sake of generality. In later calculations based on these theoretical formulations we may wish to try several different expressions for the mean potential.

C. Paper No. 4

The Microscopic Mechanism for Diffusion, and
the Rates of Diffusion-Controlled Reactions in
Simple Liquid Solvents¹

C. A. Emeis² and P. L. Fehder

Contribution No. 3945 from the Arthur Amos Noyes

Laboratory of Chemical Physics, California

Institute of Technology, Pasadena, California 91109

Abstract. Standard theoretical treatments of chemical reaction kinetics generally neglect any mean interaction potentials or "excluded volume" effects that might interfere with the relative diffusion of a pair of reactant molecules in solution. Analyses of the computer-generated simulation data for a model dense fluid of Lennard-Jones disks have shown that the microscopic mechanism for diffusion in simple liquids is largely "cooperative" in nature, and that short-range correlations associated with this cooperative mechanism tend to slow the relative diffusion of pairs of molecules approaching to within 3-4 diameters of each other. In this paper we examine the impact of these results upon the theoretical prediction of diffusion-controlled reaction rates and the physical interpretation of several other very fast chemical processes in solution.

The use of diffusion models to treat the kinetics of fast reactions in solution was first proposed by Smoluchowski³ and has more recently been reviewed by Noyes.⁴ Although this approach is widely used and frequently provides satisfactory order-of-magnitude predictions of rate constants, several fundamental difficulties remain. These difficulties appear to stem primarily from a lack of detailed information regarding the microscopic mechanism for diffusion in liquids. In particular, the manner in which this mechanism might affect the relative motions of molecules in a liquid is not well understood.

In Smoluchowski-type treatments of chemical reaction kinetics, it is frequently assumed that the relative diffusion of molecules of two reactant species is described by a coefficient that is just the sum of the bulk diffusion coefficients for the two species in solution. This assumption is equivalent to a supposition that no ————|
|————correlation exists between the time-dependent relative displacements of two solute molecules and their relative positions and motions at previous times. It is not altogether clear that this supposition is valid for molecules that are separated by only short distances, and indeed a deviating behavior--the so-called "solvent cage effect"--was long ago suggested by Rabinowitch.⁵ The results obtained by Noyes and co-workers from their investigations of iodine atom recombination rates^{6,7} and the wavelength dependence of the quantum yield for iodine photodissociation⁸⁻¹⁰ in solution also suggest that these short-range correlations may have a measurable effect upon the kinetics of certain very fast chemical processes.

In order to obtain additional information regarding the microscopic structure and kinetics characteristic of simple liquids, one of us (PLF) has recently completed a series of computer calculations simulating the microscopic dynamics of a two-dimensional dense fluid of Lennard-Jones disks. In two previous papers we have presented the results from some preliminary analyses of the simulation data¹¹ and a detailed investigation of the mechanism for diffusion and relative diffusion in the model fluid.¹² The purpose of this paper is to examine the impact of our previous findings upon the treatment of diffusion-controlled reaction kinetics in solution. Related topics, such as the "solvent cage effect" and the wavelength dependence of quantum yields for photodissociation in solution will also be discussed briefly.

Diffusion in Simple Liquids

Examination of graphical displays of the simulation data has led to several intuitively important observations regarding the microscopic character of simple liquids. For example, "snapshots"¹³ of the instantaneous configuration of the model system (see, e.g., Figure 1) provide evidence that the "excess" volume acquired by a liquid through thermal expansion is localized into relatively large, irregular "holes". Although a number of theories of the liquid state¹⁴ have postulated the existence of holes in the microstructure of real liquids, the phenomenon we observe differs from that suggested by the theoretical models in two significant ways:

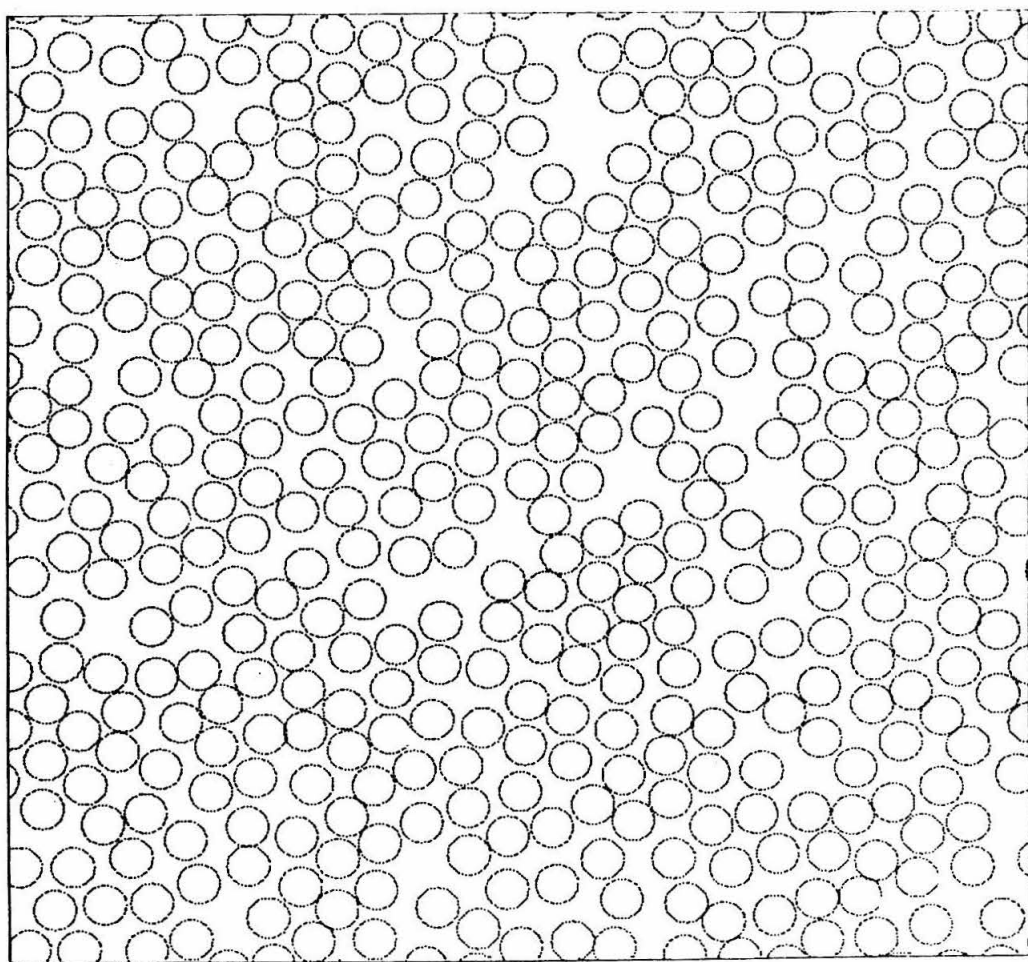


FIG. 1. "Snapshot of an instantaneous configuration of the model fluid in a liquid-like state. The particles are plotted with a diameter σ , the distance parameter in the Lennard-Jones pair potential.

(i) the holes appearing in the model fluid bear no relationship to the size and shape of an individual fluid particle; that is, the holes do not appear as "vacancies" in an otherwise quasi-crystalline structure, and (ii) comparison of snapshots for successive times shows that a given hole may persist in the same region of the fluid for times of the order of 5×10^{-12} sec--well in excess of the characteristic kinetic relaxation time (ca. 2.5×10^{-13} sec) for the system. A more detailed analysis of the microscopic structure of the model fluid, and the relationship between this structure and the structure of real simple liquids is presented elsewhere.¹⁵

Plots such as those shown in Figure 2 of the trajectories of the particles in the model fluid provide some insight into the microscopic mechanism for diffusion in simple liquids. As can be seen in the figure, extensive diffusive migration is--over a surprisingly long time interval--largely restricted to local groups of particles in the region of a hole. Furthermore, motion pictures created from the simulation data show that the local groups of long trajectories arise from a concerted migration of the particles involved, rather than from successive "jumps" or knock-on collisions. Diffusion in the model fluid therefore proceeds by a mechanism that is largely cooperative in nature, and it is reasonable to assume that similar cooperative phenomena occur in real liquids.

Although it is unlikely that cooperative phenomena of the sort we observe in the model fluid would have a macroscopically discernable effect upon singlet¹⁶ diffusion in real liquids, the short-range

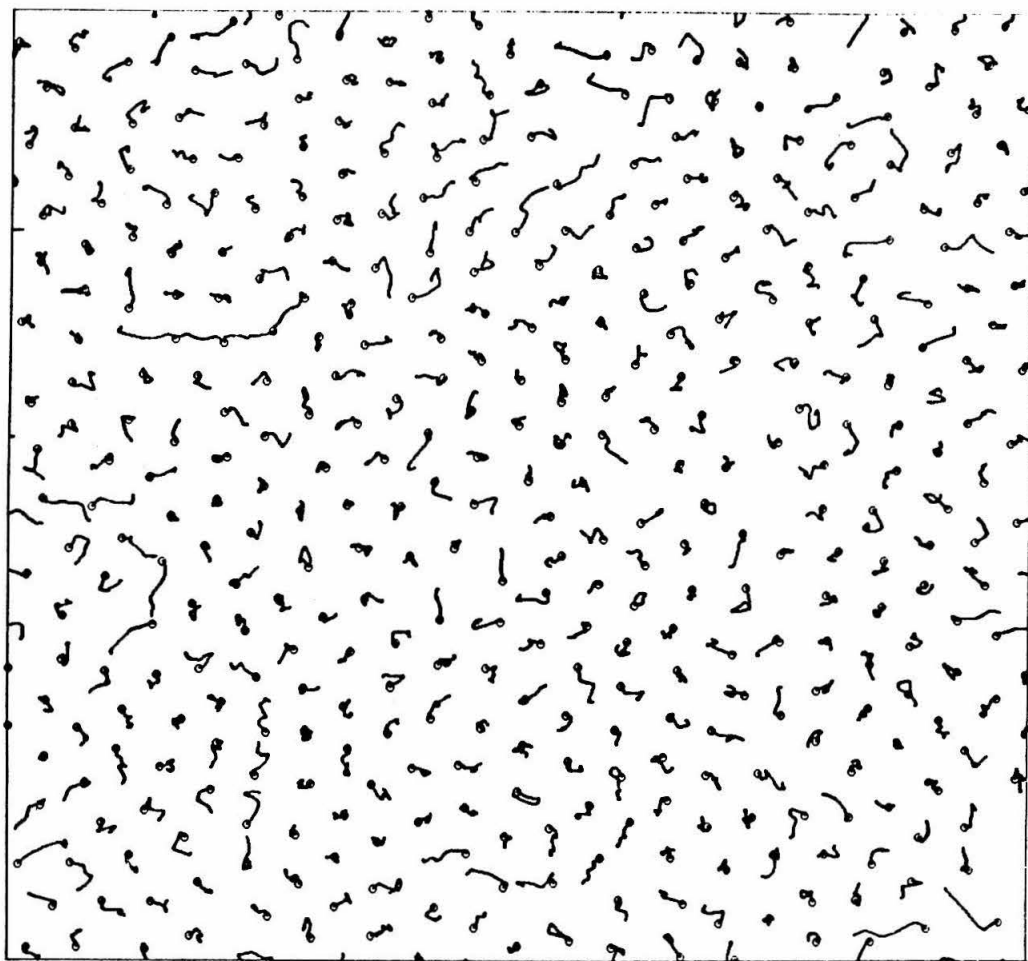


FIG. 2. Trajectories of the particles in a liquid-like state of the model fluid. The small circles mark the initial positions of the particles and the irregular lines extending therefrom the paths of the centers during the remainder of a 2×10^{-12} sec interval. The initial configuration also corresponds to that shown in Fig. 1.

correlations associated with these phenomena become more important when the relative diffusion of molecules in solution is examined. It is convenient to describe relative diffusion in terms of the motion of one molecule in a coordinate system fixed to the center of the other; in two dimensions, the relative diffusion tensor \underline{D}_R then has the form:

$$\underline{D}_R = \begin{pmatrix} D_{rr} & 0 \\ 0 & D_{\theta\theta} \end{pmatrix},$$

where D_{rr} and $D_{\theta\theta}$ are the coefficients for radial and tangential diffusion, respectively, and the off-diagonal elements of the tensor vanish by symmetry.

Consider a solution of two solute species, X and Y, in a solvent S. It is easily shown¹² that, if the diffusive motions of the X and Y molecules are completely uncorrelated, the coefficients describing the diffusion of X molecules relative to Y molecules (or vice versa) are just equal to the sum of the bulk diffusion coefficients for X and Y in S. In statistical terms,¹⁷ this means that the average square of the time-dependent displacements of an X molecule relative to a Y molecule (or vice versa) is just the sum of the time-dependent mean square displacements of the X and Y molecules taken separately. And by analogy, if no correlations exist between the motions of molecules in a one-component (X = Y = S) fluid, the coefficients D_{rr} and $D_{\theta\theta}$ describing the relative diffusion of pairs of the molecules would both be equal to just twice the coefficient D_s for self-diffusion.

Molecules separated by large distances in the model fluid diffuse independently. But analysis of the simulation data has also shown¹² that short-range "cooperative" correlations slow the relative motions of molecules approaching to within about 3-4 diameters of each other. In terms of chemical reaction kinetics in solution, this result implies that the standard Smoluchowski-type treatments may _____ | overestimate the frequency of reactant-pair encounters--and thus, overestimate the rates of so-called "diffusion-controlled" reactions. Conversely, the computer results also indicate that encounter pairs will remain in close proximity longer than predicted by an "independent" diffusion model. In the case of reactions having a non-negligible activation energy or those requiring a specific steric configuration of the reactant molecules, the depressed rate of reactant encounter may therefore be offset by an increased probability of reaction upon encounter.

To a good approximation, relative diffusion in solution may be treated in terms of the average force $F(r)$ acting between two molecules when interactions with the surrounding solvent molecules are taken into account. A convenient form for the mean force in a one-component liquid is obtained from the familiar radial distribution function $g(r)$:¹⁸

$$F(r) = - \frac{d\psi(r)}{dr} = k_B T \frac{\partial}{\partial r} [\ln g(r)] , \quad (1)$$

where $\psi(r)$ is the potential of the mean force, k_B is the Boltzmann constant, and T the temperature of the liquid. In Figure 3, the mean potential obtained for a liquid-like state of the model fluid is shown in comparison with the Lennard-Jones pair potential used in the simulation calculations. Unlike the simple pair potential, $\psi(r)$ exhibits a number of subsidiary maxima and minima corresponding to the first, second, ..., etc., "shells" of neighbors surrounding a molecule in a liquid. Thus, in the mean force model for relative diffusion, a molecule diffusing toward another molecule in solution must cross several successively higher potential "barriers" before the two molecules come into direct contact.

Numerical solutions of the two-dimensional diffusion equation including $\psi(r)$ have shown¹² however that the mean force is not in itself sufficient to account for the relative diffusion phenomena observed in the model fluid; to obtain agreement with the simulation data it was also necessary to lower the value of D_{rr} for pairs of particles separated by short distances. Although the precise physical meaning of this empirical variation in the relative diffusion coefficient is not entirely clear, we believe that it reflects the inability of a time-averaged function like $\psi(r)$ to account completely for the role played by transient geometric or "excluded volume" effects in the microscopic mechanism for diffusion at liquid-like densities. The two-dimensional diffusion equation including both $\psi(r)$ and a relative diffusion coefficient of the form,

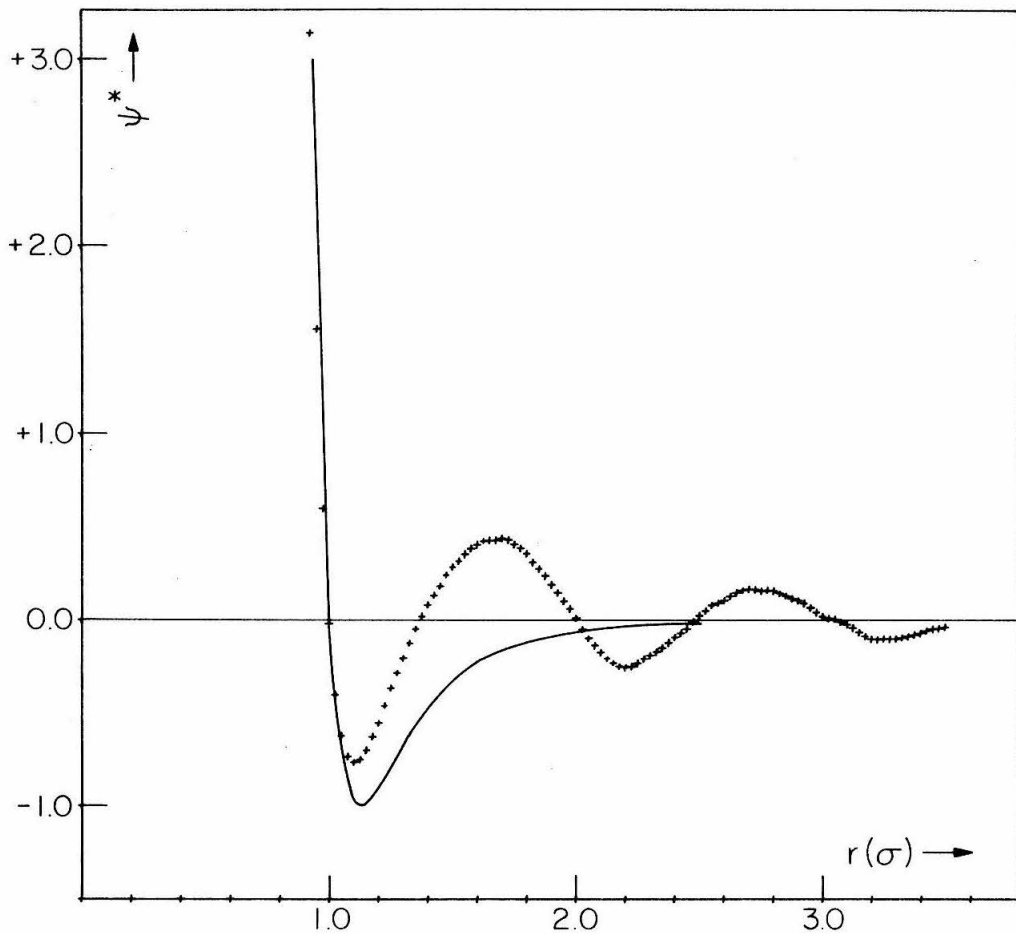


FIG. 3. Comparison of the potential of the mean force $\psi(r)$ calculated for the liquid-like state of the model fluid shown in Figs. 1 and 2 and the Lennard-Jones pair potential used in the simulation calculations.

$$\begin{aligned}
 D_{rr}(r) &= 2D_s(1 - 0.4/r^{0.25}) && \text{for } r < 3\sigma \\
 &= 2D_s[1 - 0.4/r^{(0.5r - 1.25)}] && \text{for } r > 3\sigma,
 \end{aligned} \tag{2}$$

where σ is the distance parameter in the Lennard-Jones pair potential

$$\varphi_{LJ}(r) = 4\epsilon \{ (\sigma/r)^{12} - (\sigma/r)^6 \} ,$$

was found to reproduce quite accurately the relative diffusion functions computed directly from the simulation data.

Reaction Kinetics in Solution

In this section we obtain expressions describing the rates of so-called "diffusion-controlled" reactions in two- and three-dimensional solutions. The derivation follows closely that presented by Noyes,⁴ but is extended to take into account both the mean force and the functional $D_{rr}(r)$ discussed above. The physical reasoning in support of this treatment has been discussed in detail elsewhere^{7, 19-21} and will not be reproduced here.

Three-dimensional Solution. Consider again the solution of two solute species, X and Y, in solvent S. Let us assume that the X and Y molecules exert no long-range forces on each other, and that initially the molecules of each species are distributed randomly throughout S in the way they would be if the other species were not present. Furthermore, let us assume that at some zero time we can "turn on" a diffusion-controlled reaction $X + Y \rightarrow \text{products}$ in the solution. We wish then to calculate the rate of the reaction at subsequent times.

Very soon after the reaction is initiated, most of the X molecules that were near Y molecules at $t = 0$ will have reacted so that the concentration of Y molecules near a still unreacted X will, on the average, be somewhat lower than the remaining bulk concentration of Y in the solution. This situation is then analogous to the existence of a concentration gradient in Y around the remaining X molecules. In most systems of chemical interest, a steady-state condition is quickly achieved such that the next flux Φ of Y molecules

toward X molecules along this gradient is the same at all distances away from the centers of the X molecules and is just sufficient to provide for the rate at which the X molecules react. If $c(r)$ is the average concentration of Y at a distance r from the center of an X molecule, the flux of Y molecules through a sphere of radius r about an X is given by

$$\Phi = 4\pi r^2 D_{rr}(r) \left\{ \frac{\partial c(r)}{\partial r} + \frac{c(r)}{k_B T} \frac{dU(r)}{dr} \right\}, \quad (3)$$

where $D_{rr}(r)$ is the radial coefficient for the relative diffusion of X and Y molecules, and $U(r)$ is the potential of the mean force acting on X-Y pairs in the solution. But in steady state, this net flux must be balanced by the rate at which Y molecules are depleted from solution by reaction:

$$\Phi = k c(\rho) \exp [U(\rho)/k_B T], \quad (4)$$

where ρ is the X-Y distance at which reaction can occur, and k is the rate constant that would be observed were an equilibrium distribution of solute molecules maintained in the system.

Combining eqs(3) and (4) and solving for the steady-state concentration yields

$$c(r) = \exp[-U(r)/k_B T] \left\{ c(\infty) - \frac{kc(\rho)}{4\pi(rD)^*} \exp[U(\rho)/k_B T] \right\}, \quad (5)$$

where the quantity $(rD)^*$ is given by:

$$(rD)^* = \left\{ \int_r^\infty \exp[U(s)/k_B T] \frac{ds}{D_{rr}(s)s^2} \right\}^{-1}. \quad (6)$$

The microscopic distribution $c(r)$ is not accessible to direct experimental measurement. Instead, kinetics data are used to determine the macroscopic second-order rate constant k' based on the bulk concentration $[Y]$ of Y :

$$\Phi = k'[Y] . \quad (7)$$

To a good approximation, $[Y]$ in eq (7) may be equated with $c(\infty)$. Comparison of eqs (4) and (7) then shows that

$$c(\infty) = \frac{k}{k'} c(\rho) \exp[U(\rho)/k_B T] . \quad (8)$$

Substituting this result into eq (5) with $r = \rho$ and rearranging, we obtain the final expression

$$k' = \frac{k}{1 + [k/4\pi(\rho D)^*]} , \quad (9)$$

which differs from the expression obtained by Noyes⁴ in that the quantity $(\rho D)^*$, defined in eq (6) at $r = \rho$, is calculated with reference to the mean potential $U(r)$ and an r -dependent coefficient $D_{rr}(r)$.

For reactions of the type: $X + X \rightarrow \text{products}$, the right-hand sides of eqs (4) and (7) must be multiplied by a factor of 2, leading to:

$$k' = \frac{k}{1 + [k/2\pi(\rho D)^*]} . \quad (10)$$

Two-dimensional solution. If we attempt to carry out a similar derivation for the rate of reaction in a two-dimensional solution, we quickly come upon a striking difference between the situations in two and three dimensions. For the sake of simplicity, let us first assume that D_{rr} is independent of r , and that any interaction $U(r)$ between X and Y molecules can be ignored. Then in two dimensions the steady-state condition is represented by:

$$kc(\rho) = 2\pi r D_{rr} \frac{\partial c(r)}{\partial r}, \quad (r > \rho). \quad (11)$$

Equation (11) is identical to the expression obtained for three dimensions by equating the right-hand sides of eqs (3) and (4), except that the factor $2\pi r$ for the circumference of a circle appears in place of $4\pi r^2$, the surface area of a sphere.

Integration of eq (11) yields the result

$$c(r) = c(\rho) \left\{ 1 + (k/2\pi D_{rr}) \ln(r/\rho) \right\}, \quad (12)$$

which indicates that $c(\infty)$ must be infinite if a steady-state condition is to be maintained. We conclude that diffusion in two dimensions does not provide a sufficient supply of inflowing Y molecules to sustain a steady-state concentration gradient.* The concentration

* The same conclusion obtains if the mean potential $U(r)$ and variations in $D_{rr}(r)$ can be neglected for X-Y distances greater than some value R . Equations (11) and (12) are then valid for $r > R$, requiring that $c(\infty)$ be infinite for a steady-state condition to be achieved.

$c(\rho)$ --and hence the observed rate of reaction k' --must therefore decrease monotonically with increasing time until reaction is complete.

In contrast to eq (8), the time-dependent macroscopic rate factor $k'(t)$ for a diffusion-controlled reaction in two dimensions is given by

$$k'(t) = k \frac{c(\rho, t)}{c(\infty)} \exp[U(\rho)/k_B T] \quad (13)$$

for times t sufficiently short that the bulk concentration of Y [here approximated by $c(\infty)$] does not change appreciably. Solutions to eq (13) can then be obtained by numerical integration of the system of equations

$$\frac{\partial c(r, t)}{\partial t} = \frac{1}{r} \frac{\partial}{\partial r} \{ r D_{rr}(r) [\frac{\partial c(r, t)}{\partial r} + \frac{c(r, t)}{k_B T} \frac{dU(r)}{dr}] \} \quad (14a)$$

$$\frac{\partial c(\rho, t)}{\partial t} = -k c(\rho, t) \exp[U(\rho)/k_B T] \quad (14b)$$

from the initial condition

$$c(r, 0) = c(\infty) \exp[-U(r)/k_B T] \quad , \quad (15)$$

where (14a) is the diffusion equation in two dimensions and (14b) accounts for the depletion of Y molecules due to reaction.

Results

Rate factors k' for a diffusion-controlled reaction $X + Y \rightarrow$ products in two- and three-dimensional solutions were computed for a variety of combinations of $D_{rr}(r)$ and $U(r)$. It was assumed that the species X and Y distinguish themselves from the solvent only in their ability to react with each other; otherwise, the potential $U(r)$ and the relative diffusion coefficient D_{rr} for an X - Y pair were assumed to be the same as for a pair of solvent molecules. The "equilibrium" rate constants k were calculated from two- and three-dimensional kinetic gas theory with the assumption that every collision would result in reaction. The distance ρ at which reaction can occur was taken equal to the σ parameter in the Lennard-Jones pair potential.

Two-dimensional Solution. The rate calculations for two dimensions were based on the liquid-like state of the model fluid shown in Figures 1 and 2 and examined in detail in ref 12. The value of the self-diffusion coefficient for this state is $D_s = 4.39 \times 10^{10} \sigma^2 \text{sec}^{-1}$; the potential of the mean force $\psi(r)$ is shown in Figure 3.

The time-dependent behavior of $k'(t)$ for four different $D_{rr}(r)$ - $U(r)$ combinations is shown in Figure 4. In order to determine the effect of the interaction $U(r)$ on the rate of reaction, $k'(t)$ was calculated with a fixed value of $D_{rr} = 8.78 \times 10^{10} \sigma^2 \text{sec} = 2D_s$ for $U(r > \rho) = 0$ (curve D), $U(r) = \psi(r)$ (curve B), and for $U(r)$ equal to the Lennard-Jones pair potential $\phi_{LJ}(r)$ (curve A). Curve C was obtained with

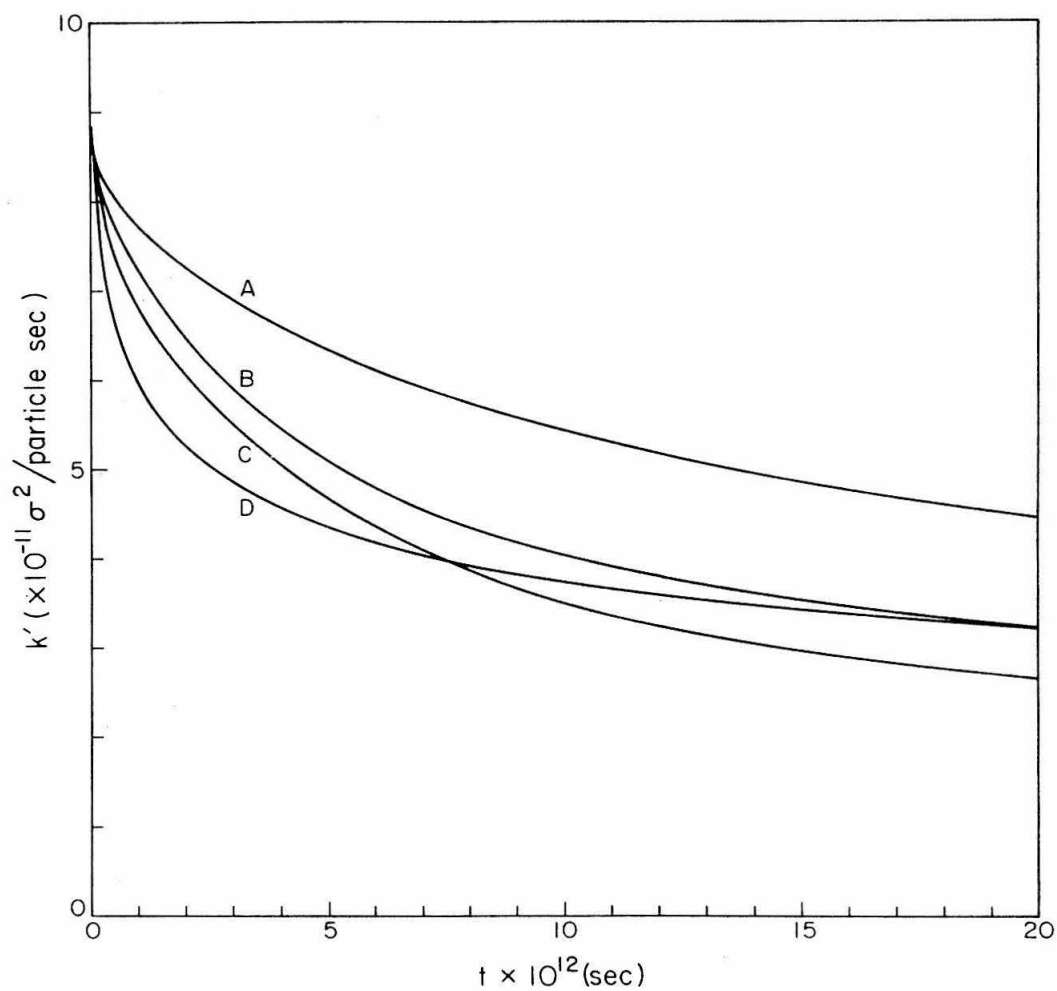


FIG. 4. Plot of the time-dependent macroscopic rate constants for a diffusion-controlled reaction in two dimensions. The mathematical assumptions leading to each of the four curves are identified in the text.

$U(r) = \psi(r)$ and $D_{rr}(r)$ as given in eq (2). Curve C therefore represents the most accurate evaluation of $k'(t)$ for a diffusion-controlled reaction in the model fluid.

During the first stage of the reaction, the rate is primarily determined by the equilibrium ($t < 0$) concentration of closely associated X-Y pairs provided by $U(r)$ according to eq (15). But after a brief induction time these initial pairs are depleted from solution by reaction, and the rate thereafter is determined by the rate at which new encounter-pairs are formed through diffusion. The Lennard-Jones potential, which provides both the highest initial concentration of X-Y pairs and the least resistance to relative diffusion, yields the highest reaction rate (curve A) over the entire 2×10^{11} sec interval spanned by Figure 4. Comparison of curves A and B shows the effect upon the reaction rate of the "barriers" to relative diffusion provided by the mean potential $\psi(r)$, while curve C indicates the additional lowering of the reaction rate that is obtained when the "adjusted" coefficient $D_{rr}(r)$ is included in the calculations.

Three-dimensional Solution. Liquid argon at a temperature 108.18°K and density 1.261 g/cm^{-3} was used as a model for the reaction system in the three-dimensional rate calculations. The radial distribution function $g(r)$ for this state has been measured by Smelser,²² and a tabulation of the function was kindly provided by that author. The Lennard-Jones potential parameters for argon are $\sigma = 3.405 \text{ \AA}$, $\epsilon/k_B = 119.80^\circ\text{K}$,²³ and the self-diffusion coefficient for argon in this state is $D_s = 4.37 \times 10^{-5} \text{ cm}^2 \text{ sec}^{-1}$.²⁴ From

Table I. Calculated Steady-State Rate Constants
for a Diffusion-Controlled Reaction in Liquid Argon

$U(r)$	$D_{rr}(r)$	$(\rho D)^*$ $\text{cm}^3 \cdot \text{sec}^{-1}$	k' $\ell \cdot \text{mol}^{-1} \cdot \text{sec}^{-1}$
0	$2D_s$	2.12×10^{-12}	1.00×10^{10}
$\psi(r)$	$2D_s$	2.23×10^{-12}	1.03×10^{10}
Lennard-Jones	$2D_s$	2.67×10^{-12}	1.14×10^{10}
0	$\left\{ \begin{array}{l} \text{as given} \\ \text{in eq (2)} \end{array} \right\}$	1.50×10^{-12}	0.79×10^{10}
$\psi(r)$		1.60×10^{-12}	0.83×10^{10}
Lennard-Jones		1.96×10^{-12}	0.95×10^{10}

these parameters a value $k = 3.70 \times 10^{10} \text{ l./mol}^{-1} \text{ sec}^{-1}$ is obtained for the "equilibrium" constant.

The predicted values for k' obtained from eqs (6) and (9) for several combinations of $U(r)$ and $D_{rr}(r)$ are listed in Table I. Standard theoretical treatments of chemical reaction kinetics in solution generally neglect any mean pair potentials or "excluded volume" effects that might interfere with the relative diffusion of the reactant molecules. To determine the effect of including a reactant-pair potential in the calculations, k' was computed for $U(r > \rho) = 0$, $U(r) = \psi(r)$, and $U(r)$ equal to the Lennard-Jones potential with D_{rr} constant and equal to $2D_s$ for all X-Y distances. Comparison of the values obtained for $U(r) = 0$ and $U(r) = \psi(r)$ shows that the predicted rate of reaction in three dimensions is not changed appreciably when a quasi-realistic interaction like $\psi(r)$ is incorporated into the theory.

Although the magnitude of short-range "cooperative" correlations in the relative diffusion of molecules in real liquids is not known and is not presently accessible to direct experimental measurement, some estimate of the effect of these correlations would have upon the kinetics of diffusion-controlled reactions is obtained by calculating k' under the assumption that $D_{rr}(r)$ for the three-dimensional solution varies as the ratio $D_{rr}(r)/2D_s$ observed in the two-dimensional model fluid. The final three entries in Table I show the effect of $U(r)$ when the rate constant is calculated with a coefficient $D_{rr}(r)$ that decreases for small reactant-pair separations as indicated by eq (2). For each of the three assumed forms for $U(r)$, the predicted value for k' is lowered about 20% when the r -dependent coefficient is included in the calculations.

The small change in k' that is obtained when $\psi(r)$ is included in the calculations probably reflects the partial cancellation of two opposing effects: As in two dimensions, the "barriers" to relative diffusion presented by an oscillatory potential like $\psi(r)$ would tend to decrease the rate of reaction. Yet any potential having an attractive component extending beyond $r = \rho$ would tend to increase the minimum ^{distance} ~~distance~~ within which a pair of molecules would have to approach each other before reaction becomes probable, and hence would tend to increase the reaction rate. This latter effect is illustrated by the relatively large increase in k' that is obtained when $U(r)$ is set equal to the Lennard-Jones pair potential and either form of $D_{rr}(r)$ is assumed. A similar effect is also observed in two dimensions, as may be seen by comparing curves A and D in Figure 4.

The substantial decrease in the predicted value for k' that is obtained when an r -dependent relative diffusion coefficient is incorporated into the calculations may--within the framework of the Smoluchowski model for diffusion-controlled reactions in solution--be attributed to the fact that a functional form for $D_{rr}(r)$ like that given in eq (2) tends to slow the relative diffusion of a pair of reactant molecules just in the region where the gradient in $c(r)$ is greatest. A more thorough analysis of this phenomenon would require an investigation of the steady-state concentration distributions that are established when various combinations of $U(r)$ and $D_{rr}(r)$ are assumed.

Discussion

In light of the results presented here and in two previous papers,^{11, 12} we may draw several conclusions regarding the mechanical influence of the solvent upon the microscopic kinetics of simple chemical reactions in solution. Data obtained from the computer simulation of a model dense fluid of Lennard-Jones disks ~~has~~ ^{have} shown that diffusion in simple liquids may proceed by a mechanism that is, at the molecular level, largely "cooperative" in nature; and further, that this cooperative mechanism tends to retard the relative diffusion of molecules separated by short distances in the liquid.

For solutions in which the solute and solvent molecules are physically similar, the average force acting between a pair of solute molecules may be approximated by the mean potential $\psi(r)$ obtained from the experimentally accessible²⁵ radial distribution function $g(r)$ for the solvent. Our calculations have shown however that this time-averaged mean potential does not provide a complete description of the transient "excluded volume" effects that apparently play an important role in relative diffusion phenomena at liquid-like densities. A more accurate description of relative diffusion in the two-dimensional model fluid was obtained from a theoretical treatment that included both $\psi(r)$ and r -dependent relative diffusion coefficients. Unfortunately it is difficult to estimate, on the basis of the two-dimensional simulation data alone, the relative importance of short-range "cooperative" correlations in the mechanism

for diffusion in real, three-dimensional liquids. The presence of an additional degree of freedom would be expected to decrease the dynamic importance of excluded volume effects; yet the relative diffusion of two molecules in a three-dimensional liquid must involve interactions with a much larger number of neighboring solvent molecules. Although direct experimental observation of relative diffusion phenomena in real liquids is not at present possible, analyses similar to those described in ref 12 of existing simulation data for three-dimensional model fluid^{26, 27} should yield some insight into the problem.

The results presented in this paper indicate that the decrease in the coefficient describing the relative diffusion of reactant-pairs separated by short distances is an important factor in determining the steady-state rate for a diffusion-controlled reaction in real systems. The mean potential $\psi(r)$ can nonetheless serve as a convenient intuitive device for interpreting a number of chemically important processes occurring in solution. In our investigation of diffusion in the simulated fluid,¹² we observed that pairs of particles diffusing away from each other tended to become "trapped" momentarily in first, second, and third nearest-neighbor positions. This phenomenon is reminiscent of the so-called "solvent cage effect", and can to a first approximation be ascribed to the successive potential "barriers" to relative diffusion presented by $\psi(r)$.

Photodissociation of a molecular solute is another process that "samples" the microscopic structure and dynamics of the

solvent in local regions of a solution. Noyes and co-workers⁹ have investigated the wavelength dependence of the quantum yield for photodissociation of molecular iodine in a number of nonreactive solvents and determined¹⁰ that the experimental results are not reproduced by a theoretical model that neglects the microscopic structure of the solvent surrounding the reaction site. For longer wavelengths--such that the excess energy over that required to break the iodine-iodine bond is small--the simple "solvent continuum" theory is found to predict quantum yields larger than those observed experimentally; yet for progressively shorter wavelengths the observed quantum yield is found to increase more rapidly than predicted by the theory.

On the basis of the model for relative diffusion phenomena presented in this paper, the experimental quantum yield data can be interpreted in terms of transient processes dependent upon the iodine-solvent interaction described by $\psi(r)$ and longer-lived processes dependent upon $D_{rr}(r)$. Immediately after dissociation, the separating iodine atoms encounter the "barrier" in $\psi(r)$ between first and second nearest-neighbor positions. If the excess energy provided by the exciting photon is small, the atoms are reflected from the barrier and recombine quickly; but if the excess energy is sufficient to permit the separating atoms to reach second nearest-neighbor positions, the barrier will tend to keep them apart and thus prevent recombination. Furthermore, if $D_{rr}(r)$ increases with increasing r , pairs of atoms that initially achieve a large

separation will diffuse away from each other more quickly, and thus be even less likely to recombine. In reality of course, the successive maxima in $\psi(r)$ and the r -dependence of $D_{rr}(r)$ are the result of interactions between the solute iodine atoms and surrounding solvent molecules, and are truly descriptive only of an equilibrium situation. Monchick²⁸ has however presented a theoretical treatment of photodissociation processes that includes an "effective" potential much like $\psi(r)$, although no theory incorporating both $\psi(r)$ and an r -dependent relative diffusion coefficient has previously been treated.

Acknowledgements

We wish to thank Professor G. Wilse Robinson for his helpful discussions and his critical reading of this paper. One of the authors (CAE) gratefully acknowledges the support of The Netherlands Organization for the Advancement of Pure Research (Z.W.O.).

REFERENCES FOR PAPER NO. 4

- (1) This work was supported in part by a grant from the National Science Foundation, No. GP-7258.
- (2) Present address: Koninklijke/Shell Laboratorium, Amsterdam, Holland.
- (3) M. von Smoluchowski, Z. Phys. Chem., 92, 129 (1917).
- (4) R.M. Noyes in "Progress in Reaction Kinetics," Vol. 1, G. Porter, Ed., Pergamon Press, New York, 1961, p 128.
- (5) E. Rabinowitch, Trans. Faraday Soc., 33, 1225 (1937); and W.C. Wood, Trans. Faraday Soc., 32, 1381 (1936).
- (6) H. Rosman and R.M. Noyes, J. Amer. Chem. Soc., 80, 2410 (1957).
- (7) R.M. Noyes, ibid., 86, 4529 (1964).
- (8) R.M. Noyes, ibid., 77, 2042 (1955).
- (9) L.F. Meadows and R.M. Noyes, ibid., 82, 1872 (1960).
- (10) R.M. Noyes, Z. Elektrochem., 64, 153 (1960).
- (11) P.L. Fehder, J. Chem. Phys., 50, 2617 (1969).
- (12) P.L. Fehder, C.A. Emeis, and R.P. Futrelle, "The Microscopic Mechanism for Self-Diffusion and Relative Diffusion in Simple Liquids," manuscript in preparation.
- (13) A detailed description of the graphical display techniques employed in analysis of the simulation data is provided in ref 11.
- (14) See, for example, H. Eyring and R.P. Marchi, J. Chem. Educ., 40, 562 (1963), and the discussion in J.M.H. Levelt and E.G.D. Cohen in "Studies in Statistical Mechanics," Vol. 2,

J. deBoer and G.E. Uhlenbeck, Eds., North-Holland Publishing Co., Amsterdam, Holland, 1964, p 178 ff.

(15) P.L. Fehder, " 'Anomalies' in the Radial Distribution Functions of Simple Liquids, " manuscript in preparation.

(16) We use the word "singlet" here to distinguish between the migration of individual molecules in solution and the relative diffusion of pairs of molecules.

(17) See, for example, R. Zwanzig, Annu. Rev. Phys. Chem., 16, 67 (1965).

(18) P.A. Egelstaff, "An Introduction to the Liquid State, " Academic Press, New York, N.Y., 1967, p 16.

(19) P. Debye, Trans. Electrochem. Soc., 82, 265 (1942).

(20) F.C. Collins and G.E. Kimball, J. Colloid Sci., 4, 425 (1949).

(21) F.C. Collins, ibid., 5, 499 (1950).

(22) S. Smelser, Ph.D. Thesis, California Institute of Technology, Pasadena, California, 1969. To be made available through University Microfilms.

(23) J.O. Hirschfelder, C.F. Curtiss, and R.B. Bird, "Molecular Theory of Gases and Liquids, " John Wiley & Sons, Inc., New York, N.Y., 1954, p 165.

(24) J. Naghizadeh and S.A. Rice, J. Chem. Phys., 36, 2710 (1962).

(25) See, for example, ref 18 or H.H. Paalman and C.J. Pings, Rev. Mod. Phys., 35, 389 (1963).

- (26) A. Rahman, Phys. Rev., 136, A405 (1964); J. Chem. Phys., 45, 2585 (1966).
- (27) L. Verlet, Phys. Rev., 159, 98 (1967).
- (28) L. Monchick, J. Chem. Phys., 24, 381 (1956).

SECTION V

FORMAL LANGUAGE FOR THE DESCRIPTION
OF LIQUID STRUCTURES--A PROPOSAL

A. Explanatory Comments

In this section we discuss a proposal that a formal language for the description of partially-ordered structures be developed. It is felt that such a language would prove particularly useful as a means of describing and discussing the microscopic structures characteristic of dense fluids, and thus might provide the basis for new and more facile theoretical treatments of the liquid state. Much of the material presented here is reproduced from a proposal prepared in early 1967, and is specifically directed toward analysis of the two-dimensional simulation data discussed elsewhere in this dissertation. The extension of many of the concepts to the treatment of real, three-dimensional dense fluids--or the three-dimensional simulation data accumulated by Rahman, Verlet, and others--is however obvious.

B. Statement of the Problem

During the last several decades a great deal of effort has been directed toward the development of an adequate theoretical treatment for the liquid state. Only limited success has however been achieved in this area of endeavor, in the sense that none of the existing theories yield formulations for the various measurable thermodynamic and statistical quantities that are valid over the entire range of liquid-like densities and temperatures. Furthermore, many of these theoretical

treatments furnish only limited insight into the microscopic processes underlying the macroscopic observables; even in instances where a given treatment does accurately predict the values of these observables, one may doubt the validity of the model for the liquid state that is assumed as a basis for the theoretical formulations.

This state of affairs is indeed rather unfortunate. Most chemistry is observed in liquid-phase systems, and in many cases certain assumptions must be made regarding the role of, say, a liquid solvent in the mechanism of a given class of reactions. For example, the proposed mechanisms for many molecular rearrangements assume that the solvent forms a "cage" around the reacting molecule. While such assumptions may be considered "reliable" in the sense that they have found wide applicability in explicating the mechanisms of numerous reactions, there still exists little definitive evidence regarding the microscopic kinetics of liquid systems.

The solution to many of these problems would appear to rest with a better understanding of the microscopic structure of liquids. Information of the type necessary for the development of such an understanding cannot be obtained by "normal" experimental methods. Computer calculations of the sort described elsewhere in this dissertation can, however, yield information of just this nature. If the models employed in these calculations do indeed reflect the microscopic behavior of real, simple liquids (and there is good evidence to indicate that they do), then we have information available regarding not only instantaneous structure, but also the manner in which this structure evolves with time.

If an intuitive understanding of the sort envisioned here is to result from an examination of the structural data generated by these calculations, it will be necessary to develop some convenient means of describing the observed structures. While a list of the Cartesian coordinates of all the particles in a system constitutes a detailed and exact description of the system structure, this description provides little immediately useful information. Some means must therefore be found for describing these structures in a more abstract manner. It is proposed here that the possibility of developing a well-defined formal language of structure be examined. This language would have, as its "universe of discourse," the structures of partially-ordered arrays of particles. A general discussion of some of the properties of this language and a few of the difficulties that one might expect to encounter in its development is provided below.

C. A Formal Language of Partially-Ordered Structures

In many respects, the problem we propose to investigate is similar to the problems treated in the field of automatic pattern recognition. The structures that we will wish to describe in the language are, in reality, patterns--but these "patterns" are of a sort that has not as yet been adequately investigated. Most of the research in automatic pattern recognition has involved the recognition of a certain well-defined set or "lexicon" of patterns in a signal containing varying amounts or types of noise. In some instances, as in the case of recognition of handwritten characters, this "noise" takes the form of

differences in the representation (in the signal) of the same pattern. In such instances it is, however, the recognition of the pattern represented by the signal--and not the analysis of the accompanying noise--that is important. Hence, research in this area has centered about the development of techniques for the elimination of such noise from the signal, or the selection (discovery) of recognition criteria that are unaffected by the type of noise encountered in the particular problem under investigation.

The "patterns" that will comprise the universe of discourse of the language we propose to develop are not so well defined. It might be possible to define, for a given class of systems (partially-ordered arrays), a lexicon consisting of a small set of "idealized" local structures. For example, one element of a lexicon for the language describing two-dimensional systems of the type described elsewhere in this dissertation might be related to the "hexagonal closest-packing" structure. Such a lexicon would probably have little utility in itself, however, since instances of these "idealized" structures might encompass only a small fraction of the total number of points in any given system. Furthermore, it is quite likely that the deviations from these idealized local structures are more important than the structures themselves. We therefore require that the semantics of our formal language be such that these deviations may be described in an exact and mathematically meaningful manner.

Our language of structure must also embody a facility for describing precisely and accurately a second characteristic property of

partially-ordered structures: the "decay" of the local order about some point in the system with displacement from that point. It is generally the case in partially-ordered systems that the particles adjacent to any given particle are distributed in an almost perfectly ordered manner. At larger distances from the selected particle this ordering becomes less and less regular, until no suggestion of the original local structure persists. Furthermore, the local structures about two points some distance from each other are often "inconsistent" in the sense that neither structure would be compatible with a regular extension of the other. We must therefore be able to describe, within the language, the extent to which any particular system exhibits this property. Although several methods might be considered, the mode of description must be mathematically meaningful, and would probably take the form of a "decay function."

The properties of formal languages in general have been investigated in the field of mathematical linguistics. In particular, application of the techniques developed in this field of inquiry should allow us to determine the mathematical limitations of the formal language we construct and the constraints that must be placed upon the language to make it meaningful. We must, however, place an additional constraint on the language: that descriptions (of structures) rendered in the language be related in some precise manner to the general concepts of classical statistical mechanics. In practice, this constraint would probably take the form of a requirement that statements in the language be directly related to the classical configuration integral.

D. The Radial Distribution Function $g(r)$

The radial distribution function $g(r)$ is an empirical measure of the order present in a partially-ordered array of particles (points). In two dimensions, the function is given by the formula

$$g(r) = \left(\frac{A}{N} \right) \left[\frac{n(r)}{2\pi r \Delta r} \right]$$

where N is the number of particles in the system and A the area to which the system is confined, and $n(r)$ is the time-average number of particles situated at a distance $r \pm (\Delta r/2)$ from a given particle in the system. The function therefore indicates the time-average relative density of the system around some given particle as a function of distance from that particle.

The radial distribution function for a perfectly ordered lattice of particles consists of a series of "spikes" corresponding to the various coordination "shells" of neighbors around each particle in the lattice. For a partially-ordered array, such as the particles in a dense fluid undergoing thermal agitation, the spikes are broadened into overlapping peaks as is shown by the functions reproduced in section III. D. The first maximum is generally rather large, with succeeding maxima decreasing in height and increasing in breadth; the function approaches unity for large values of r .

For a given value of (Δr) , the height of the maxima and the distance to which the oscillations extend are a strong function of overall system density. The widths of the peaks are generally a function of both system and temperature. Several facts should be noted here:

1. The radial distribution function can be integrated. Thus, the area under the first peak of the function is a measure of the average coordination number of a particle in the system. Because the successive peaks in the function overlap, some well-defined method must be used to distinguish between the contributions from the two peaks on either side of a local minimum [see, for example, P. G. Mikolaj and C. J. Pings, Phys. Chem. Liquids, 1, 93 (1968)].
2. The radial distribution function provides information regarding only the average spatial distributions of particles. Even rather gross "defects" in the structure (such as the presence of large "holes" or vacancies in an otherwise tightly-packed array of particles) may be concealed by the averaging implicit in the computation of the $n(r)$ values.
3. It follows from (2) above that, in general, a $g(r)$ function contains very little information regarding the structure of the array from which it is derived. While integration of a portion of the function can provide a value for the average number of particles situated in a circular band (in two dimensions) at some distance from a given particle, one can obtain no information from the function regarding the relative positions of these particles.
4. There exists some evidence to indicate that oscillations in the radial distribution function may bear only a trivial relationship to partial ordering in a dense fluid. Functions computed from the spatial distributions of randomly packed steel spheres exhibit

oscillations rather similar to those shown in the figures in section III. D. Thus it is possible that these oscillations may only reflect the fact that the individual particles in a packed array occupy space.

E. Geometrical Neighbors

Let A be a set of m points α_i , $i = 1, 2, \dots, m$, randomly distributed in a (planar) two-dimensional space. For the moment, assume that m is sufficiently large that irregularities at the edges of the array of points can be ignored. Alternatively, consider the space in which the points are distributed to be periodic (as described in section III. B), and assume that the density of points in this space is not so low that complications arise in the procedures discussed below.

The geometrical neighbors of a point $\alpha_k \in A$ are determined (defined) in the following manner:

If one draws vectors from α_k to all the other points $\alpha_j \neq k$ in the array, and the perpendicular bisectors to these vectors, the set γ_k^1 of points that are geometrical neighbors of α_k has as elements those points that are associated with the perpendicular bisectors forming the smallest closed polygon about α_k . (Note that α_k must be enclosed by this polygon.)

Let π_k^1 denote the polygon, and β_k^1 the set of perpendicular bisectors forming the sides of π_k^1 . Several lemmas follow:

Lemma 1. π_k^1 must be convex (i. e., no interior angle of π_k^1 may be greater than 180°).

Lemma 2. γ_k^1 must include the point closest to α_k in the array. Let η_k denote this point in the following.

Lemma 3. γ_k^1 must contain at least three members.

Several theorems may now be stated:

Thm. 1. The vector between α_k and some $\alpha_j \in \gamma_k^1$ need not intersect its perpendicular bisector at a point on the perimeter of π_k^1 .

Thm. 2. The polygon π_k^1 encloses that region of the space that is nearer to α_k than to any other $\alpha_j \in A$.

Consider now the set of polygons \mathcal{P}^1 , where:

$$\mathcal{P}^1 = \{\pi_i^1 \mid \pi_i^1 \text{ is the geometrical neighbor-determining polygon for point } \alpha_i \in A\}$$

and the set of sets of geometrical neighbors, \mathcal{G}^1 :

$$\mathcal{G}^1 = \{\gamma_i^1 \mid \gamma_i^1 \text{ is the set of geometrical neighbors to point } \alpha_i \in A\}$$

Obviously $\pi_k^1 \in \mathcal{P}^1$ and $\gamma_k^1 \in \mathcal{G}^1$, where π_k^1 and γ_k^1 are as defined previously. The following theorems can then be stated:

Thm. 3. Any point α_k must be a geometrical neighbor of all the points that are its geometrical neighbors;

$$\text{i. e. , } \alpha_j \in \gamma_k^1 \Rightarrow \alpha_k \in \gamma_j^1$$

Thm. 4. No two elements in \mathcal{P}^1 may enclose the same region in space (i. e. , no two polygons in \mathcal{P}^1 may overlap).

Thm. 5. Taken together, the elements of \mathcal{P}^1 completely fill the space occupied by the array.

Thm. 6. If $\alpha_j \in \gamma_k^1$ (which implies $\alpha_k \in \gamma_j^1$ from (3) above), the polygons π_j^1 and π_k^1 share a common side; that is, one side of π_j^1 is identically a side of π_k^1 .

The fundamental defining concept of geometrical neighbors can be extended in the following manner:

Consider again the logical "diagram" employed in our initial definition of the geometrical neighbors of point α_k . Circumscribing polygon π_k^1 there are numerous other polygons. Let us denote the smallest of these that completely encloses (does not intersect with) π_k^1 by π_k^2 . In a similar manner, we may define π_k^3 , π_k^4 , etc. Again, we repeat that each succeeding polygon must completely enclose those polygons internal to it (i. e. , no π_k^n may intersect any π_k^m for $m < n$ --which implies that none of the polygons may intersect).

Associated with each polygon π_k^n , there will be a set of points which may be denoted by γ_k^n . Similarly, we may define the sets \mathcal{P}^n and \mathcal{G}^n .

Let Γ_k denote the set which has as elements the set of "extended" geometrical neighbors of point α_k ;

i. e., $\Gamma_k = \{\gamma_k^n | \gamma_k^n \text{ is the set of particles associated with the } n\text{th polygon, } \pi_k^n, \text{ about point } \alpha_k\}$

From the definition above, it is clear that for $\gamma_k^n, \gamma_k^m \in \Gamma_k$, where $n \neq m$, we have $\gamma_k^n \cap \gamma_k^m = \emptyset$. We may now state a theorem:

Thm. 7. All $\alpha_{j \neq k} \in A$ (all the other points in the array) are geometrically related, in the sense of our discussion here, to the point α_k ;

$$\text{i. e., } \bigcup_i \gamma_k^i = A$$

Stated another way: Every point in the array is a member of some $\gamma_k^i \in \Gamma_k$.

The concept of geometrical neighbors, in its initial and "extended" forms, therefore provides several new methods for describing the structure of a randomly-distributed array of points. It can probably be shown that the spatial configuration of such an array is completely specified by \mathcal{G}^1 and the positions of some point α_k and its nearest neighbor η_k . It is also probable that an array can be reconstructed on the basis of a knowledge of some Γ_k and the positions of the points α_k and η_k in the array. Numerous other theorems and relationships remain to be discovered.

F. Discussion

Elsewhere in this dissertation we have described some computer calculations that simulate a two-dimensional dense fluid. The data

generated by these calculations should serve as an excellent basis for initial efforts to develop a formal language of partially-ordered structures. The ultimate goal of such an investigation should of course be to develop a language applicable to real, three-dimensional structures. But in view of the ^{scarcity}~~lack~~ of really useful background information in this area of inquiry, it would appear prudent to confine any initial efforts to less complex structures. One-dimensional structures, on the other hand, are rather too simple since they present no opportunity to treat disorder in terms of angular distributions.

Two-dimensional structures offer a second advantage: they may be represented in pictorial form, and thus should be more easily conceptualized. This ease of conceptualization might play an important role in determining the success or failure of any attempt to develop a language of structure. Once the basic techniques have been discovered it should however be a simple matter to extrapolate to systems having a third degree of freedom.

In subsections D and E we discussed two schemes for characterizing the structure of a partially-ordered system. The significance of the radial distribution function is certainly easily grasped, and the function does bear a direct theoretical relationship to the statistical mechanical configuration integral. But it has been pointed out, this function provides little definitive information about structure because of the "averaging" implicit in its measurement (from a given structure). In particular, one cannot obtain from the function (except in a few very special cases) detailed information regarding the extent to which the represented structure exhibits local ordering, or the "rate" at which

this ordering decays with displacement. While detailed information of this sort is of only marginal importance from a thermodynamic point of view, it does find significance in the interpretation of spectroscopic and kinetics data from high-density systems, and thus should be treated adequately by any formal language of structure.

The concepts of geometrical neighbor relationships, on the other hand, are perhaps rather too complex. While information regarding the neighbor relationships that exist in a given structure characterizes the structure in a detailed manner, such information is certainly not directly related to the general notions of local order and disorder. Furthermore, it would seem that such information is perhaps even more difficult to "understand" than is simple particle position data.

Information regarding the polygons associated with geometrical neighbor relationships might however be more closely related to concepts of local and long-range ordering. For example, if we consider systems of the sort simulated by our computer calculations, information regarding the average shape of the polygons π_k^1 might be closely related to the extent of local ordering. A statement to the effect that most of the polygons π_k^1 in a given system are nearly perfect hexagons would indicate that the system exhibits a high degree of local ordering. The existence of a number of highly distorted polygons in the set \mathcal{P}^1 would indicate that the structure contains vacancies or "holes." Similarly, information regarding the average shapes of the higher-order polygons, π_k^n ($n > 1$), might be related to the concept of "decay" of local order at larger displacements.

We should note however that a decision to employ such a mode of description in a formal language of structure merely serves to defer many of the difficulties that are involved in the treatment of partially-ordered structures. That is, if this mode of description is to be employed, one must develop some method for describing the "amount of regularity" a given polygon exhibits. Nonetheless, it would seem that such an approach offers some basis for optimism, if only because of the large amount of information available regarding the mathematical properties of plane geometric figures.

SECTION VI

PROPOSITIONS

PROPOSITION 1: Elucidation of the Role of SO₂ in
Atmospheric Aerosol Formation

Abstract

The results of an experiment involving the irradiation of artificial "polluted" atmospheres would seem to indicate that SO₂ must necessarily be present in the urban atmosphere if the aerosol associated with photochemical smog is to be formed. Certain aspects of the experiment suggest, however, that these results may have been only an artifact of the physically unrealistic or "unnatural" conditions prevailing in the experimental apparatus. Since these results have in recent years been used as supporting evidence for legal action against industries burning high sulfur content fuels it is proposed that the experiments be repeated, with special care being taken to reproduce the physical conditions actually existing in the daytime urban atmosphere.

PROPOSITION 1

ELUDICATION OF THE ROLE OF SO_2 IN
ATMOSPHERIC AEROSOL FORMATIONIntroduction

Although the problems of urban air pollution have been studied intensively for at least a decade, few really definitive or comprehensive theories regarding the chemical basis for the observed phenomena have yet been advanced. The principal stumbling block to those who would devise such theories is the complexity of the chemical "system" in which the phenomena occur. Hydrocarbons of nearly every type (aliphatic, olefinic, aromatic, etc.) have been identified in mass spectra taken of urban atmospheric samples, and the presence of nitrogen oxides, sulfur oxides, and ozone is generally accepted.¹ Large numbers of experiments have shown that such mixtures are photochemically active, and a number of partial mechanisms have been suggested (see, for example, Ref. 1). Although it has not been conclusively shown that free radicals are present in the urban atmosphere, their presence is implied by a number of the proposed mechanisms. It should also be noted that, since a number of the proposed reactions are known to have rate constants within two or three orders of magnitude of each other, the "primary" reaction sequence in such a complex system may depend upon the relative concentrations of the various types of reactants. It is certainly beyond the scope of this proposal to present a comprehensive summary of the work in this area reported in the

literature. Considering the complexity of the problem though, it is generally conceded that a considerable amount of additional experimental data must be gathered before even a partial understanding of the overall photochemical mechanism may be established.

One of the primary "symptoms" of air pollution is the reduction of visibility by atmospheric particulates. Even when release of the more common types of particulates (smoke, dust, etc.) is rigidly controlled, light-scattering aerosols are formed under the conditions under which the other prominent "symptoms" of photochemical smog (eye irritation, odor, and plant damage) are found to occur. Although a great deal of data has been amassed regarding the formation of synthetic aerosols under laboratory conditions, the mechanisms by which the atmospheric aerosols are formed are not clearly understood. In particular, the role of sulfur dioxide in aerosol formation remains undetermined.

Background

Knowledge of the composition of smog-like aerosols is largely derived from the work of Mader and co-workers.² In these experiments, aerosol was collected from the Los Angeles atmosphere by passing large volumes of polluted air through filters consisting of two sheets of Whatman No. 43 filter paper. Ether extracts of the filters were subjected to elemental analysis, a number of chemical tests for specific organic functional groups, and infrared spectroscopic examination.

The data obtained from samples collected on different days, and

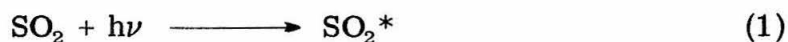
different smog conditions were found to be in good agreement. It should be noted, however, that Goetz and co-workers³ have found organic aerosols to be unstable with respect to both evaporation and oxidation. It is therefore possible that the data reported by Mader, et al. may not accurately reflect the total composition of the particulates present in the polluted Los Angeles atmosphere. Average values for the elemental composition of the samples analyzed and reported in Ref. 2 are given below:

<u>element</u>	<u>% (by wt.)</u>	<u>atom ratios</u>
carbon	67.9	1.00
hydrogen	9.2	1.63
nitrogen	1.2	0.015
oxygen	20.7	0.229
sulfur	0.62	0.0034
halogen	0.49	---

The infrared absorption spectra of the ether extract solutions and the residues obtained by evaporation of the solvent exhibited a strong absorption in the 5.8μ (1724 cm^{-1}) region, indicating the presence of organic carbonyls. Prominent bands were also observed at 2.9, 3.4, 6.15, 6.9, 7.3, 7.9, and 11.4 microns. Although only a qualitative assignment of these bands is possible, the observed spectra would be consistent with the presence of aliphatic, aromatic, and olefinic compounds containing carbonyl and nitrate ester functional groups. The possible presence of epoxides, peroxides, hydroperoxides, and compounds containing the covalent sulfate and amino or amido groups is also indicated. These assignments are, in part, confirmed by the

chemical tests, specific tests for the presence of aldehydes, ketones (and methyl ketones), and organic acids all being positive. The presence of peroxidic materials in the residue was indicated by the liberation of iodine from buffered potassium iodide solutions.

If the preceding data can be considered a standard, it must be said that little success has been achieved in attempts to produce "realistic" aerosols under laboratory conditions--except in cases where the reactants were obtained from automobile exhaust. It is known that the irradiation of SO_2 in air containing traces of water results in the formation of an aerosol. The kinetics and mechanism of the photo-oxidation of SO_2 have been studied by Hall⁴ and Gerhard and Johnstone.⁵ The final product of these reactions is, however, sulfuric acid. It might also be noted that the first step in the proposed mechanism is:



This assumption is justified by the high dissociation energy of sulfur dioxide--far in excess of the energies that might be absorbed from solar radiation.

Although the role of nitrogen oxides (principally NO and NO_2) in photochemical smog-producing reactions is thought to be at least partially understood, the connection between the reactions involving these oxides and possible reactions involving SO_2 is unclear. A comprehensive survey of the available data regarding nitrogen oxide-induced photochemical reactions is presented in Ref. 1. The pertinent results from experimentation in this area may however be briefly stated.

The important reaction involving nitrogen oxides is thought to be:



The atomic oxygen produced by this reaction may react with molecular oxygen to produce ozone, or organic compounds--principally olefins and aromatics--to produce biradicals. These products may then react further, with other atmospheric contaminants, to produce a complex mixture of products and secondary reactive species.

Since NO is the principal nitrogen-containing compound found in auto exhaust, some mechanism must exist for its conversion to NO₂ if reaction (2) is to be of any importance. Although reaction schemes involving the nitrogen oxides and molecular oxygen have been studied, these have been found to produce only small steady-state concentrations of NO₂--indicating that organics must also provide important pathways for this conversion. Indeed, a large amount of experimental data has been collected showing the effect of organic impurities on irradiated NO-air and NO₂-air systems, and this data would tend to support the hypothesis that organics play a prominent role in the initial conversion of NO to NO₂.

That NO₂ is the primary reactant in reaction schemes leading to the more noxious substances found in smog is indicated by a large mass of experimental data regarding yields of these substances vs. time of irradiation. In particular it is noted that, when NO is the principal nitrogen-containing reactant in laboratory systems simulating polluted

air, induction periods of up to one-half hour are observed before measurable concentrations of ozone and PAN (peroxyacyl nitrate compounds--thought to be the chief cause of eye irritation and plant damage) are formed. At the same time, it is found that this induction period corresponds to the time required for the almost total conversion of NO to NO₂ in the system. Similar experiments involving aerosol formation in NO-hydrocarbon-SO₂ systems have exhibited comparable induction times.⁶

Although a number of research groups have reported data regarding aerosol formation by photochemical reaction in gas phase systems, it would appear that the "definitive" experimental data--as indicated by the number of references to this work found in other papers--is considered to be that reported by Prager and co-workers.⁶ Summarizing briefly, Prager, et al. sought to study the formation of aerosols in static and dynamic gas-phase systems containing measured concentrations of nitrogen oxides, single hydrocarbons, and SO₂. Oxygen containing 100 ppm water vapor was used as the diluent, and a General Electric AH-6 mercury lamp as the source of radiation. The results obtained in these experiments indicate that:

- (i) No aerosol is formed when aliphatic hydrocarbons constitute the organic reactant.
- (ii) Simple straight-chain monoolefins with fewer than six carbon atoms do not yield aerosol when irradiated with NO₂ alone. If SO₂ is added in small quantities, large amounts of aerosol are formed.

- (iii) Higher molecular weight monoolefins, particularly those having highly-branched or cyclic structures, produce aerosol when irradiated in the presence of NO_2 . Addition of small quantities of SO_2 does not measurably increase the yield or rate of formation of aerosol.
- (iv) In systems requiring the presence of SO_2 for aerosol formation, the yield of aerosol is found to vary inversely with the length of time that the system is irradiated before SO_2 addition.
- (v) Irradiation of systems containing NO_2 and diolefins produces some aerosol, but the reaction is quite slow. Addition of SO_2 to the initial reactants increases both the yield and rate of reaction.

In "dynamic" experiments, a filter was placed in the outlet stream from the reactor. Aqueous extracts of the filters were found to be very acidic, and to form precipitates when added to solutions containing Ba(II) .

Analysis

Consideration of the above information would lead one to conclude that:

- (i) SO_2 must play an important role in atmospheric aerosol formation, since a major fraction of the organic material present in automobile exhaust consists of compounds containing five or fewer carbon atoms.⁷
- (ii) Reactive intermediates formed in the nitrogen oxides-initiated photolysis mechanisms must also play a part in the reaction sequences involving SO_2 .

- (iii) The main constituent of the aerosol present in polluted urban atmospheres must be sulfuric acid.

Conclusion (iii) is obviously incorrect, in light of the information reported by Mader and co-workers. The author would also contend that, although the data obtained by Prager and co-workers would tend to support conclusions (i) and (ii), certain features of their experimental technique might have created these effects as artifacts. Three such features are felt to be of particular importance:

The use of pure oxygen as a diluent is somewhat questionable, particularly in light of previous statement regarding the dependence of the true reaction sequence on relative reactant concentrations. Specifically, the presence of oxygen in such large concentrations would tend to alter rather radically the relative importance of mechanisms involving atomic oxygen and ozone.

It is quite likely that the effects involving SO_2 observed by Prader, et al. resulted from the use of a mercury arc as a source of radiant energy. Although these experimenters report using a borosilicate glass (Pyrex) filter to remove radiation with wavelengths shorter than 3000 \AA , the available transmission vs. wavelength data for Pyrex⁸ indicates that nearly all of the intensity in the strong Hg doublet centered at 3128 \AA , and a large fraction of the intensity in the doublet centered at 3022 \AA passes such a filter. A sketch of the relevant portion of the spectral intensity distribution for solar radiation is provided in a recent paper by Searle and Hirt.⁹ Examination of this distribution shows that solar radiation

contains very little intensity in the 3022 Å region, and not a great deal in the 3128 Å region--indicating that a mercury arc lamp provides a rather unrealistic source of illumination for such experiments. In experiments involving SO₂, this inaccuracy may be of particular importance because of the presence of a major absorption band for the molecule in the 2600 - 3200 Å region.¹⁰ Thus, one might suspect that the photooxidation reactions studied by Hall, and Gerhard and Johnstone are responsible for the aerosol formation reported by Prager et al. This suspicion is further supported by the properties reported for the aqueous filter extracts.

There exists some experimental evidence¹¹ indicating that, while the lower molecular weight monoolefins do not produce aerosol when irradiated with NO₂, addition of low concentrations of these compounds to systems containing higher molecular weight compounds--which do exhibit aerosol formation when irradiated--increases the yield of particulate. This information suggests that the lower m. w. olefins may be important in the formation of aerosols even in the absence of sulfur dioxide.

Proposal

Examination of the above information and that presented in Ref. 1 indicates that additional experimental data must be obtained before the true role of SO₂ in aerosol formation can be established with any degree of certainty. In the collection of these data, the author feels that careful attention should be paid to:

- (i) The composition of the diluent gas, with respect to both oxygen and water vapor content.
- (ii). The intensity vs. wavelength distribution in the output of the illuminating lamp.

Specifically, it is proposed that a series of experiments similar to those reported by Prager and co-workers be run. In these experiments however, purified laboratory air containing controlled concentrations of water vapor would be used as a diluent, and a lamp such as a Sylvania "Sun Gun" (essentially a blackbody at 3400° K, with 365w power dissipation) as the illumination source. A water filter could be employed to absorb a large portion of the infrared energy output by this source, and neutral density filters might be inserted between the source and the reaction chamber to decrease the intensity of the radiation to levels comparable to solar radiation.

Initial experiments should certainly include a re-examination of the systems studied by Prager et al. If it is found that SO_2 does indeed induce aerosol formation in NO_2 -low m. w. olefin systems, a thorough analysis of the composition of the aerosol should be obtained using chemical and spectroscopic techniques. These analyses should also be compared with those reported by Mader and co-workers,² and analyses of the aerosols formed in systems with and without SO_2 should be compared in an attempt to find correlations. Experiments of the type reported by Stevenson,¹¹ involving mixtures of low and high molecular weight olefins might also be run, and the products obtained from such reaction mixtures studied to discover whether or not the presence of

higher molecular weight compounds is important in determining the role played by lower molecular weight olefins in aerosol formation.

REFERENCES FOR PROPOSITION 1

1. A. P. Altshuller and J. J. Bufalini, Photochem and Photobio. 4, 97 (1965).
2. P. P. Mader, R. D. MacPhee, R. T. Lofbery, and G. P. Larson, Ind. Eng. Chem. 44, 1352 (1952).
3. A. Goetz and T. Kallai, "Formation and Decay of Photochemical Aerosols", Div. of Water and Waste Chemistry, 142nd National Meeting of the ACS. Atlantic City, N.J., Sept. 9-14, 1962.
4. T. C. Hall, Jr. and F. E. Blacet, J. Chem. Phys. 20, 1745 (1952).
5. E. R. Gerhard and H. F. Johnstone, Ind. Eng. Chem. 47, 972 (1955).
6. M. J. Prager, E. R. Stephens, and W. E. Scott, Ind. Eng. Chem. 52, 521 (1960).
7. A. J. Haagen-Smit, private communication; see also Proc. Am. Petrol. Inst. 37, 171 (1957).
8. Glass Color Filters, Corning Glass Works, Corning, N. Y. (1963).
9. N. Z. Searle and R. C. Hirt, J. Opt. Soc. Am. 55, 1413 (1965).
10. R. W. B. Pearse and A. G. Gaydon, The Identification of Molecular Spectra (Chapman and Hall, London, 1963), p. 268.
11. H. J. R. Stevenson, Thesis, Kettering Laboratory, University of Cincinnati, 1969.

PROPOSITION 2: A Spectroscopic Search for an HgCO Complex

Abstract

The addition of moderate amounts of carbon monoxide to low pressure mixtures of mercury vapor and ethylene in a helium carrier has been found to increase the rate of the photoproduction of acetylene by a factor of 2.5. A careful analysis of the system suggests that a $\text{Hg}(^3\text{P}_1)\text{-CO}$ complex may be responsible for the observed rate increase. Because of the synthetic importance of mercury-sensitized photochemical reactions, experiments seeking spectroscopic evidence for the excited Hg-CO complex are proposed.

PROPOSITION 2

A SPECTROSCOPIC SEARCH FOR AN HgCO COMPLEX

Introduction

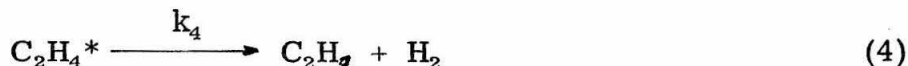
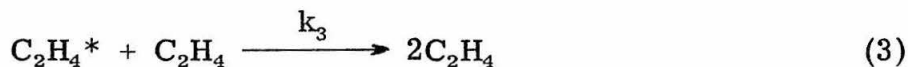
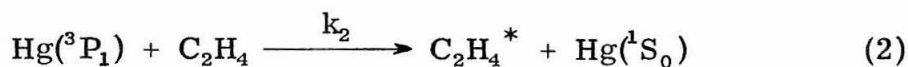
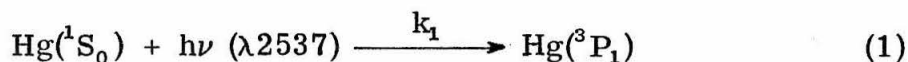
The ability of mercury vapor to act as a sensitizing agent in photochemical reactions of organic substrates has long been recognized. Because of the synthetic importance of such reactions, a great deal of experimental data has been collected in this area and published in the literature. Although it is beyond the scope of this proposal to provide even a brief review of the available literature, the book by Cvetanovic¹ is said to contain a comprehensive summary of the available cross-section and mechanistic data.

In a recently-published article, Homer and Lossing² report having found that addition of moderate amounts of carbon monoxide to low pressure mixtures of mercury vapor and certain organic compounds in helium increases the rate of the photolytic decomposition of the organic species by as much as a factor of 2.5. Reactions run under both dynamic and static conditions exhibited comparable behavior, and mass spectrometric analysis of the reaction mixture after photolysis showed no anomalous products (e. g. , Hg or CO addition compounds) to be present. After an extensive experimental study of the effect, using ethylene as the organic reagent, it was concluded that the observed results could only be explained in terms of a mechanism involving the formation of an excited HgCO complex having a lifetime of about 3.10^{-5} sec.

Background

The apparatus used in the experiments reported by HL is described in detail in Ref. 2. In essence, the dynamic reactor (used in most of the experiments) consists of a fused silica tube around which a water-jacketed low pressure mercury lamp is wrapped. The gaseous reaction mixture is passed through the tube, and a small sample removed directly into the ionization chamber of a mass spectrometer at a point a few millimeters below the end of the irradiated zone. The length of the irradiated zone may be varied with a metal shutter which is slipped over the tube, and which may be moved between the tube and the lamp.

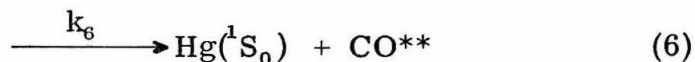
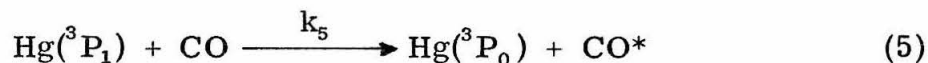
Nearly all the experimental data was collected on reaction mixtures containing ethylene as the organic species. LeRoy and Steacie³ have shown the mercury-sensitized photodecomposition of this compound to proceed by the mechanism:



HL measured an effective lifetime for a quantum of $\lambda 2537 \text{ \AA}$ radiation to be $4.65 \cdot 10^{-6}$ sec. in their system, which may be compared with the known lifetime of the $\text{Hg}({}^3\text{P}_1)$ state: $1.0 \cdot 10^{-7}$ sec. No products other than acetylene and hydrogen could be found in the irradiated reaction

mixture, and with moderate pressures of ethylene (~ 0.02 Torr) and varying pressures of CO ($P_{\text{max}} = 0.2$ Torr), the additional decrease in ethylene caused by the addition of the CO was found to be equal to the increase in acetylene formed ($\pm 2\%$).

The mechanism represented by reactions (1)-(4) shows that, under the conditions described above, linear relationships should exist between ΔP and $[C_2H_4]$, and ΔP and $I(\Delta t)$, where ΔP is the amount of ethylene decomposed, $[C_2H_4]$ the ethylene concentration in the reaction mixture prior to irradiation, I the intensity of the radiation, and (Δt) the time of irradiation, when the amount of decomposition is small. These relationships were indeed found to be linear in systems containing no CO, and to retain their linearity upon the addition of the gas. At higher pressures of CO, the "special effect" of the gas was found to disappear due to quenching of the $Hg(^3P_1)$ state.⁴ The quenching takes place by the mechanisms:



Comparing the efficiencies of CO and N_2 as quenching agents,⁴ and assuming that k_6 is negligible small,⁵ the rate constants for the above reactions are found to be:

$$k_5 = 0.37 \times 10^{10} \text{ l} \cdot \text{mole}^{-1} \cdot \text{sec}^{-1}$$

$$k_6 = 5.47 \times 10^{10}$$

Metastable $\text{Hg}(^3\text{P}_0)$ atoms are known to decompose ethylene, but kinetic arguments show that reaction (5) cannot be responsible for the observed rate increase when CO is added.

Although substantial rate increases were obtained when CO was added to systems containing anisole or acetone as the organic reactants, no similar effect was observed in systems containing n-butane, propane, or cyclopropane. Thus it would appear that the new active species formed upon addition of CO has a preference for attack on π -bonds. Additions of CO_2 and H_2O to systems containing ethylene were found to produce minor effects. Because of the diminutive character of these effects compared to those observed with CO addition, they were not investigated in detail.

Analysis

Examination of the paper by Homer and Lossing² leaves one with the impression that their investigation of the problem has been both complete and accurate. Although inaccuracies may have been present in some of the kinetic data employed in their computations, it would appear that the probability that an excited mercury-CO complex exists is sufficiently high to warrant an attempt to observe it spectroscopically.

One might hope to observe such a complex in either the ultra-violet or infrared regions. Oldenberg⁶ and others have shown that the $\lambda 2537 \text{ \AA}$ line of mercury is rather sensitive to the environment of the emitting atom. Kwok⁷ has used this sensitivity to obtain information on the environment of $\text{Hg}(^3\text{P}_1)$ atoms in liquid argon and other simple

liquids. Thus, one might expect to observe "parasite" bands associated with the $\lambda 2537$ line if HgCO complexes do indeed exist. This technique is not without pitfalls; the most serious of these involves the diffuse bands appearing in the 2537 Å region that are attributed to Hg₂ and other van der Waals molecules. These bands have however been studied extensively,⁸ and it should be possible to distinguish between them and any emission due to HgCO. It is also quite possible that, at the low pressures which must necessarily be employed to avoid excessive quenching of the Hg(³P₁) state, these diffuse bands would not be seen at all.

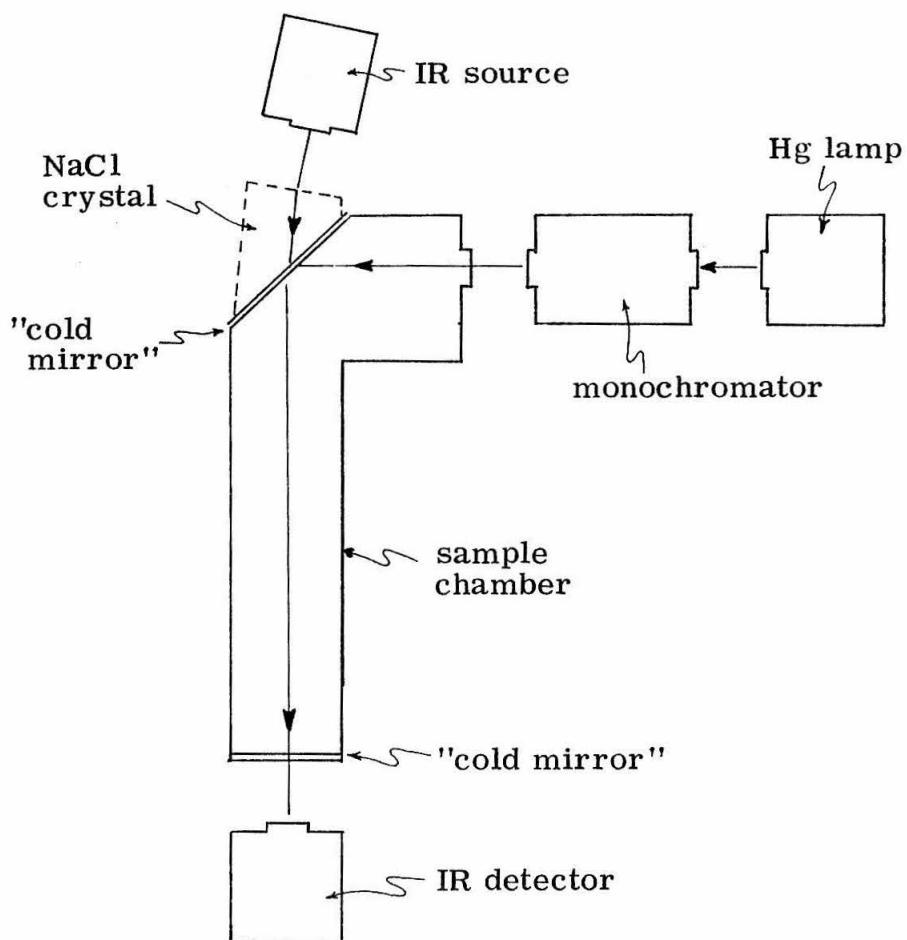
Several effects might be observed in the infrared region. Karl and Polanyi⁹ have shown that CO atoms are excited vibrationally by collision with Hg(³P₁) atoms; indeed, this information was obtained by observing CO emission in the infrared. Since complexing would certainly affect the force constant of the C-O bond--probably by weakening it--one might hope to observe anomalous emission bands due to vibrational transitions of the complexed CO molecules. Emission from uncomplexed CO might, however, obscure the much weaker emission from the complexed CO. Observation of anomalous CO absorption can probably be discarded for the same reason.

Perhaps most promising would be the possibility of observing either absorption or emission by the complex itself. Because of the masses of the atom/molecule involved and the probable weakness of the interaction, one would expect the Hg-CO stretching vibration to appear at very low wavenumbers, thus placing it in a region of the spectrum uncluttered by other extraneous emission or absorption.

Proposal

It is proposed that an attempt be made to obtain spectroscopic evidence for the excited HgCO complex predicted by Sheer and Fine¹⁰ and subsequently by Homer and Lossing.² A simple apparatus for this experiment might consist of nothing more than a pyrex cell fitted with a quartz window to admit the exciting radiation, and a LiF window to allow observation of the resultant emission in both the ultraviolet and infrared regions. A low pressure mercury lamp could be used as the source of exciting radiation, and a monochromator inserted between the lamp and the cell to isolate the 2537 Å line. When using such an apparatus to observe emission in the ultraviolet region, a filter containing mercury vapor and NO might be positioned between the cell and the spectrograph to absorb most of the 2537 Å emission. If such a filter were employed, care would have to be taken to ascertain that any anomalous emission observed did not arise in the filter.

For infrared absorption experiments, an apparatus of the type shown in the diagram on the next page might be used. In this apparatus, the ultraviolet exciting radiation and the infrared radiation are brought into co-incidence by reflecting the ultraviolet radiation off a surface that passes infrared (e. g., a "cold mirror"¹¹) using a specially shaped crystal of LiF or NaCl. A similar "cold mirror" could be employed to prevent the ultraviolet radiation from entering the infrared detector by reflecting it back along the cell.



Hg-CO Infrared Absorption Apparatus

REFERENCES FOR PROPOSITION 2

1. R. J. Cvetanovic, Progress in Reaction Kinetics (Pergamon Press, London, 1964), Vol. II, p. 41.
2. J. B. Homer and F. P. Lossing, Can. J. Chem. 44, 143 (1966).
3. D. J. LeRoy and E. W. R. Steacie, J. Chem. Phys. 10, 676 (1942).
4. M. W. Zemansky, Phys. Rev. 36, 919 (1930).
5. A. B. Callear and R. G. W. Norrish, Proc. Roy Soc. (London) A266, 299 (1962).
6. O. Oldenberg, Phys. Rev. 46, 210 (1934).
7. J. Kwok, Ph.D. Thesis, Department of Chemistry and Chemical Engineering, California Institute of Technology, Pasadena, California, 1965.
8. G. Herzberg, Molecular Spectra and Molecular Structure; I. Spectra of Diatomic Molecules (van Norstrand, Princeton, N. J., 1950), p. 394.
9. G. Karl and J. C. Polyani, J. Chem. Phys. 38, 271 (1963).
10. D. Scheer and G. R. Fine, J. Chem. Phys. 36, 1264 (1962).
11. For a description of special filters and wavelength-selective mirrors, see Pamphlet U-73 from Special Product Sales, Kodak Apparatus Division, Eastman Kodak Co., Rochester, New York.

PROPOSITION 3: Improvements on the Photochemical Space
Intermittency Method for Measuring the
Diffusion Coefficients of Free Halogen
Atoms in Solution

Abstract

The photochemical space intermittency (PSI) effect provides the basis for one of the few practical methods of obtaining an experimental measure of the diffusion coefficients for free halogen atoms in solution. Instrumental deficiencies have severely limited the accuracy of previous PSI measurements, but more recent advances in spectrophotometer design and in illumination sources (principally, the c. w. laser) may alleviate most of these instrumental difficulties. Since the chemical kinetics of free halogen atoms in solution may provide a key to our understanding of the microscopic dynamic processes occurring in liquids, it is suggested that the PSI measurements on I_2 in CCl_4 be repeated using apparatus of modern and more sophisticated design.

PROPOSITION 3

IMPROVEMENTS ON THE PHOTOCHEMICAL SPACE
INTERMITTENCY METHOD FOR MEASURING THE
DIFFUSION COEFFICIENTS OF FREE HALOGEN
ATOMS IN SOLUTIONIntroduction

The chemical kinetics of reactive free radicals in solution provide one of the few conveniently accessible experimental "probes" for the microscopic dynamic processes occurring in real liquids. The free halogen atoms formed by photodissociation of the parent diatomic molecules are especially useful in this context because of their spherical symmetry. Dynamic interactions between the molecules of a solute and a liquid solvent are more easily envisioned--intuitively--when at least the solute molecules are spherically shaped. Furthermore, the recombination reaction for free halogen atoms in solution is, for all practical purposes, strictly diffusion-controlled; the reaction requires only a negligible (if any) energy of activation and no specific steric configuration for the re-combining atoms.

Consider a solution of molecular halogen X_2 in some inert solvent S. If this solution is illuminated with light of frequency ν , where $h\nu$ is in excess of the dissociation energy for X_2 , two processes take place:



Actually, three different sequences of events may follow the absorption of a photon by an X_2 molecule. The two dissociating X atoms may either:

- (i) rebound from the surrounding solvent molecules and recombine immediately, or
- (ii) penetrate the surrounding solvent a short distance, come to thermal equilibrium, and then diffuse back together and recombine (geminate recombination), or
- (iii) penetrate the surrounding solvent and diffuse away from each other to combine with atoms formed at other reaction sites.

In most liquid solvents, under conditions easily attainable in the laboratory, sequences (i) and (ii) occur too rapidly to be observed experimentally. By process (P1) then, we refer only to those dissociation events such that the two X atoms diffuse away from each other to a point at which geminate recombination or their recombination with atoms produced at other sites become equally probable.

With this defined limitation, the rates for processes (P1) and (P2) are given by

$$\frac{d[X]}{dt} = 2\phi q \quad \text{and} \quad -\frac{d[X]}{dt} = 2k[X]^2$$

respectively, where q is the rate of light absorption in einsteins/l. sec, ϕ the quantum yield for the photodissociation process, and k the rate constant, in l./mole sec, for the recombination reaction in S under the prevailing conditions of temperature, density, etc. If thermal dissociation is negligible, a steady-state condition such that:

$$\phi q = k[X]^2 \quad (1)$$

is established in the illuminated solution after a macroscopically modest "induction" period. If τ is the average lifetime of X atoms that re-combine with atoms from other reaction sites, then:

$$\tau = \frac{[X]}{2\phi q} = \frac{1}{2k[X]} \quad , \quad (2)$$

and by re-arrangement with Eq. (1) we also have:

$$k/\phi = q/[X]^2 \quad (3)$$

$$\text{and} \quad k\phi = 1/4q\tau^2 \quad . \quad (4)$$

The quantities ϕ , k , and τ all provide some insight into the nature of solute-solvent interactions, and a variety of experimental techniques have been used to obtain independent measurements of each of these quantities for iodine in a number of different solvents.

Rabinowich and Wood¹ measured $[I]$ --and hence, k/ϕ --in hexane and CCl_4 by measuring the decrease in I_2 absorption when the solutions were illuminated by an intense beam of monochromatic light perpendicular to the monitoring beam. Spectrophotometric monitoring of $[I_2]$ was also used, in combination with flash photolysis, by Marshall and Davidson² and later by Willard and co-workers^{3, 4} to measure k directly in CCl_4 , hexane, and heptane at room temperature.

Zimmerman and Noyes⁵ measured τ --and hence, $k\phi$ --in hexane at 25° by using a rotating sector technique to determine the effect of "chopping" the illuminating light at different frequencies on the rate

of the exchange reaction between isotopically labeled iodine and trans-diiodoethylene.

Of the three quantities ϕ , k , and τ , the quantum yield ϕ , as defined, is perhaps most closely related to the "chemically important" processes occurring in solution. Taken together, the post-dissociation sequences (i) and (ii) described above are an instance of the so-called "solvent cage effect"; thus ϕ provides--by exclusion-- a measure of the ability of the solvent to encage the dissociating atoms and prevent them from escaping the reaction site. Lampe and Noyes⁶ used a scavenger technique with allyl iodide and oxygen to measure directly the quantum yield for $\lambda 4358$ light in hexane, CCl_4 , and hexachloro-1,3-butadiene at three different temperatures. The same scavenger technique was used by Booth and Noyes⁷ to measure ϕ in six solvents whose relative viscosities at 25° covered a range of 10^3 , while Meadows and Noyes⁸ used the exchange reaction between diiodoethylene and isotopically labeled I_2 to measure the quantum yields for seven different wavelengths between 4047 \AA and 7350 \AA in hexane and hexachloro-1,3-butadiene at 25° .

It is generally assumed that the excess energy (over that required to dissociate the halogen atom) provided by the exciting photon is converted into kinetic energy for the separating free atoms. Thus the wavelength dependence of the quantum yield provides some indication of the average rigidity of the solvent structure surrounding an unexcited solute molecule. In some instances where the quantum yield has been measured at several different temperatures in the same solvent,⁶ Arrhenius plots of $\log \phi$ vs $(1/T)$ have been used to determine

an activation energy for the post-dissociation sequence (iii). The energy values obtained in this manner are of the order of those required for diffusion processes--but the entire procedure must be considered somewhat naive when it is remembered that the microscopic structure of the solvent must itself change with temperature.

Background

The bulk diffusion coefficients D for reactive solute species provide another chemically important measure of solute-solvent dynamics. But because of their very high reactivity (and hence, short lifetimes), the diffusion coefficients for free halogen atoms in solution cannot be determined using standard experimental methods. In 1959 Noyes⁹ suggested the "photochemical space intermittency" effect as a means of measuring D for short-lived species produced and destroyed in pairs, and in cooperation with Salmon¹⁰ showed the effect to exist for iodine in hexane. A more extensive investigation by Levison and Noyes¹¹ has provided diffusion data for iodine atoms in CCl_4 at 25° and 38° .

In essence, the photochemical space-intermittency technique is the space-analogue of the rotating sector (time-intermittency) method⁵ for measuring τ . It can be shown by intuitive argument⁹ (supported now by experimental results) that the space-average steady-state concentration of X atoms in a solution of X_2 illuminated by a sharply-defined pattern of light and dark areas is dependent not only on the total incident illumination, but on the size and spacing of the light areas as well. The local distribution of X atoms in the illuminated solution is

governed by Fick's second law of diffusion;

in the light areas:

$$\frac{\partial [X]}{\partial t} = D\nabla^2 [X] + 2\phi q - 2k[X]^2 = 0 \quad (5)$$

and in the dark areas:

$$\frac{\partial [X]}{\partial t} = D\nabla^2 [X] - 2k[X]^2 = 0 \quad (6)$$

where it is assumed that $[X]$ is so low that D is constant throughout the system, and the quantities ϕ , q , and k are as defined previously. For a given pattern of illumination, Eqs. (5) and (6) become a pair of simultaneous, geometrically coupled second-order differential equations; in general, these equations do not have an analytical solution in terms of known mathematical functions. Noyes⁹ has, however, obtained numerical solutions (probably by using an iterative technique similar to that employed by Emeis to solve the theoretical diffusion model discussed in Paper No. 3, section IV. B) for two regular patterns: the "zebra" pattern of parallel light and dark strips, and the "leopard" pattern of circular light spots arranged on a two-dimensional hexagonal grid. We describe only the solutions for the "leopard" pattern here, since that pattern shows the greater space-intermittency effect and was the pattern used by Levison and Noyes.¹¹

If the origin is taken as the center of a light spot and polar coordinates are used, Eqs. (5) and (6) for the "leopard" pattern become:

$$\frac{1}{r} \frac{d}{dr} \left(r \frac{d[X]}{dr} \right) + \frac{1}{r^2} \frac{d^2[X]}{d\theta^2} = \frac{2k[X]^2 - 2\phi q}{D} \quad (\text{in light}) \quad (7)$$

$$= 2k[X]^2/D \quad (\text{in dark}). \quad (8)$$

It is convenient to introduce "reduced" variables similar to those used with the time-intermittency method;¹² then:

$$\frac{1}{\rho} \frac{d}{d\rho} \left(\rho \frac{d\gamma}{d\rho} \right) + \frac{1}{\rho^2} \frac{d^2\gamma}{d\theta^2} = \gamma^2 - 1 \quad (\text{in light}) \quad (9)$$

$$= \gamma^2 \quad (\text{in dark}), \quad (10)$$

where:

$$\gamma = (k/\phi q)^{\frac{1}{2}} [X] \quad (11)$$

is a normalized concentration that would attain a value of unity for homogeneous illumination of the solution with light of the same intensity as that in the individual spots, and:

$$\rho = (4\phi q k/D^2)^{\frac{1}{4}} r \quad (12)$$

Experimentally, one measures $\bar{\gamma}/\bar{\gamma}_\infty$ where $\bar{\gamma}$ is the ratio of the space-average concentration of X atoms in the pattern-illuminated solution to the concentration that would be observed were the solution homogeneously illuminated by light of the same intensity, and $\bar{\gamma}_\infty$ is the limiting value of $\bar{\gamma}$ for a very coarse pattern having the same fraction of the solution illuminated. Noyes calculated $\bar{\gamma}/\bar{\gamma}_\infty$ as a function of ρ_L , the reduced radius of the light spots, and f , the ratio of the separation of the centers of adjacent spots to the diameter of a

single spot, for a range of ρ_L values between 0.1 and 100 with $f = 2, 3$, and 5; the ratio of light to dark areas in the "leopard" pattern is uniquely defined by f regardless of the size of the individual light spots. Thus if one measures $\bar{\gamma}/\gamma_\infty$ in a solution for a number of patterns with differing r -values but the same f -value (the concentration $[X_2]$ and the intensity of the incident illumination are generally also held constant from pattern to pattern), the experimental data can be fitted to the calculated curves to obtain the factor $(4\phi qk/D^2)^{\frac{1}{4}}$ relating ρ to r . Then if q is measured also, and ϕ and k are known independently, the value of D is determined.

Analysis

Levison and Noyes¹¹ (LN) used the apparatus shown schematically in the figure¹³ below to measure D for iodine atoms in CCl_4 at 25° and 38° . The exchange reaction⁸ between isotopically labeled I_2 and trans-

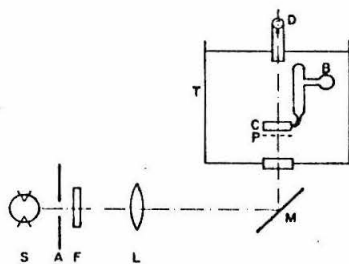


Fig. 1.—Schematic representation of apparatus.

diiodoethylene was employed to measure $[\text{I}]$ and hence $\bar{\gamma}/\gamma_\infty$ in the illuminated solution. A CCl_4 solution 1.41×10^{-4} M in I_2 and 0.107 M in diiodoethylene was degassed by repeated freezing and melting under vacuum in

bulb B, and then transferred to the circular cell C for illumination. The cell was 1.8 cm in diameter and 0.5 cm thick. Temperature control was maintained by immersing the cell in constant-temperature bath T.

Illumination was provided by a medium pressure (CH5) mercury

arc S surrounded by a water jacket. The light was passed through circular aperture A, rendered parallel by lens L, and reflected vertically through pattern P and thence the cell by mirror M. Interference filter F was used to isolate the 4358 Å Hg emission line, and the intensity of the incident beam monitored by photometric detector D; the detector was calibrated using the ferrioxalate actinometer reaction of Parker and Hatchard.¹⁴

Measurements were made for twelve different patterns with spot sizes ranging from a minimum diameter of 0.00796 cm to a maximum diameter of 0.1002 cm. The patterns were made by photographic reduction of a mechanically drawn master pattern of 10,000 spots with ratio $f = 3$. Examination of the patterns with a microdensitometer showed the background areas between spots to be completely opaque, and the photographic density of individual light spots to be essentially homogeneous across a given pattern.

The theoretical calculations completed by Noyes⁹ were predicated on certain assumptions that cannot be met in actual laboratory practice. Several of the more important assumptions are:

- (i) that diffusion is the only process whereby I atoms are transported from light areas to dark areas,
- (ii) that the concentration of labeled molecular iodine is uniform throughout the solution during illumination,
- (iii) that there is an absolute discontinuity in the intensity of the illuminating light between the light and dark areas, at the edge of a beam, and

- (iv) that the beam of light arising from each spot in the pattern is uniform in intensity and perfectly collimated.

By a straightforward quantitative analysis, LN show that the conditions obtaining in their apparatus are such that assumptions (i) and (ii) were met within the limits of other experimental uncertainties. The optical properties of the apparatus were, however, found to be somewhat less creditable.

The sharpness of the optical pattern emerging from the solution was tested by exposing films placed flush against the top of the illuminated cell. Examination of these films with a microdensitometer showed that: (1) the transition from complete illumination to total darkness at the edge of each beam took place over a distance of the order of 0.001 cm, and (2) the emerging beams were elliptical, with major and minor axes 0.0170 and 0.0032 cm, respectively, larger than the diameters of the circular openings forming them; both of these effects were independent of the actual size of the spots in the pattern P.

The diffuse "transition region" at the edge of each beam is attributed to dispersion within the bulk of the solution, and probably would not be eliminated by refinements in the apparatus. Since the 0.001 cm width of this region was less than 20% of the r. m. s. diffusive displacement attained by a free iodine atom in the CCl_4 solution, LN assumed that it was not necessary to apply corrections to their data for this effect. Boundary sharpness might however become a significant parameter in measurements involving more viscous solvents.

The poor collimation of the illuminating light is somewhat more critical, as is evidenced by the fact that the deflection along the major

axis of each beam (0.0170 cm) was more than twice the diameter of the spots (0.00796 cm) in the finest pattern. The ellipticity of the emerging beams was undoubtedly due to the linear nature of the mercury arc source and the finite size of the aperture A; by further experimentation with the apparatus after the fact (after the $\overline{\gamma}/\overline{\gamma}_{\infty}$ measurements had been completed) it was determined that the sizes of the beams emerging from the top of the cell were affected only slightly by the position of the lens L, but were strongly dependent upon the size of the aperture. Although LN applied a correction to their experimental data to account for the effect of poor beam collimation, this correction was only approximate in nature and least serviceable for the smaller beam diameters. And since the photochemical space intermittency effect is largest for very fine patterns of light and dark areas, the $\overline{\gamma}/\overline{\gamma}_{\infty}$ measurements made with these patterns are of prime importance in determining the "fit" between the experimental data and the calculated $(\overline{\gamma}/\overline{\gamma}_{\infty})$ vs ρ_L curves.

Proposal

Because of the potential importance¹⁵ of the data obtained thereby, we propose that the photochemical space intermittency measurements reported by Levison and Noyes¹¹ be repeated and extended using apparatus of an improved and more sophisticated design. The following modifications to the apparatus employed by LN are suggested:

- (i) The mercury arc source should be replaced by an argon ion c. w. laser.

- (ii) The optical system should be re-arranged such that the illuminating light passes vertically, from top to bottom, through the cell.
- (iii) The cell and the surrounding temperature bath should be modified to permit spectrophotometric monitoring of the concentration of molecular iodine--and hence by exclusion, of free iodine atoms--in the illuminated solution.

The argon ion laser emits highly monochromatic light at the following wavelengths: 4579 Å, 4658 Å, 4765 Å, 4880 Å, 4965 Å, 5017 Å, and 5145 Å, with approximately 80% of the total output power being equally divided between the 4880 and 5145 Angström lines. All seven of these lines fall well within the range of wavelengths employed in the quantum yield measurements by Meadows and Noyes,⁸ and thus should be suitable for space intermittency measurements on iodine.

The superior optical properties of laser light are well known¹⁶ and need not be discussed in detail here. With respect to photochemical space intermittency measurements, the high degree of collimation exhibited by laser sources is of particular importance. For example, the output beam of a Ratheon Model LG-12 argon ion laser measures 2.2 mm in diameter at the exit aperture and exhibits a divergence of less than 40 seconds of an arc;¹⁷ this may be contrasted with the 36' (major axis) and 7' (minor axis) divergences of the elliptically uncollimated illuminating beam employed by LN.

If the cell containing the illuminated solution is isolated from mechanical disturbances (vibration, buffeting by the flow of fluid in

the temperature bath, etc.), convection currents arising from thermal inhomogeneities created by absorption of energy from the illuminating light then become the chief mode for non-diffusive transport of iodine atoms. By a straightforward quantitative argument, LN have shown convection to be of negligible importance in their own experimental measurements; but with the increased usable intensities offered by laser sources, thermal effects from illumination may become more significant. Since the illuminating light is attenuated slightly by passage through the solution, modification of the optical system so that the light is brought into the cell from the top would create a slight positive thermal gradient along each beam and thus, to a limited extent, retard convection.

The diiodoethylene exchange technique used by LN is perhaps unnecessarily complicated in terms of the number and type of mechanical manipulations that must be performed external to the actual space intermittency apparatus. The technique also introduces additional empirical quantities--such as the rate constant for the exchange reaction itself--and their attendant uncertainties into the overall determination of D . Spectrophotometric monitoring of I_2 absorption has been employed previously¹⁻⁴ to measure iodine atom concentrations in solution, but has the disadvantage that $[I]$ is determined as a fractionally small change (frequently of the order of a few percent) in I_2 absorption intensity.

Recent advances in split-beam spectrophotometer design¹⁸ and low-noise photometric detector electronics now permit changes in optical density of the order of 1 in 10^3 to 1 in 10^4 to be measured; thus

by using spectrophotometric equipment of optimum design, it should be possible to increase the accuracy of the $\overline{\gamma}/\overline{\gamma}_{\infty}$ measurements by a factor of 10 over that estimated⁸ for the diiodoethylene exchange technique. The size of the monitoring beam would have to be large in comparison to the spacing of the light areas in the intermittency pattern if a true space-average measure of the iodine atom concentration is to be obtained, but this would seem to present no problem in view of the beam sizes employed in commercial spectrophotometers (e.g., Beckman model DU, Cary model 14, Beckman IR-12, etc.). If an argon ion laser is used for illumination, a band rejection filter can be used to exclude scattered illuminating light from the spectrophotometer detector; highly efficient band rejection filters are now commercially available for most laser wavelengths.

REFERENCES FOR PROPOSITION 3

1. E. Rabinowitch and W. C. Wood, Trans. Faraday Soc. 32, 547, (1936).
2. R. Marshall and N. Davidson, J. Chem. Phys. 21, 2086 (1953).
3. R. L. Strong and J. E. Willard, J. Am. Chem. Soc. 79 2098 (1957).
4. S. Aditya and J. E. Willard, J. Am. Chem. Soc. 79, 2680 (1957).
5. J. Zimmerman and R. M. Noyes, J. Chem. Phys. 18, 658 (1950).
6. F. W. Lampe and R. M. Noyes, J. Am. Chem. Soc. 76, 2140 (1954).
7. D. Booth and R. M. Noyes, J. Am. Chem. Soc. 82, 1868 (1960).
8. L. F. Meadows and R. M. Noyes, J. Am. Chem. Soc. 82, 1872 (1960).
9. R. M. Noyes, J. Am. Chem. Soc. 81, 566 (1959).
10. G. A. Salmon and R. M. Noyes, J. Am. Chem. Soc. 84, 672 (1962).
11. S. A. Levison and R. M. Noyes, J. Am. Chem. Soc. 86, 4525 (1964).
12. R. M. Noyes, J. Am. Chem. Soc. 73, 3039 (1951).
13. This figure is reproduced directly from Ref. 11.
14. C. A. Parker and C. G. Hatchard, Proc. Roy. Soc. (London) A235, 518 (1956).
15. See, for example, R. M. Noyes, J. Am. Chem. Soc. 86, 4529 (1964).

16. P. M. Rentzepis, Photochem. and Photobio. 8, 579 (1968).
17. Argon Ion Laser Model LG-12, Ratheon Company Laser Advanced Development Center, Waltham, Massachusetts (1965).
18. R. Rikmenspoel, Rev. Sci. Instr. 36, 497 (1965).

PROPOSITION 4: A Molecular Dynamics Study of Cavity
Formation Works in a Simple Liquid

Abstract

In the years since 1936, experimental evidence has collected in support of Eyring's original speculation regarding the presence of "holes" or "voids" in the microscopic structure of simple liquids. Several theoretical treatments of liquid state phenomena have been based on assumptions regarding the amount of thermodynamic work that must be extended to form cavities of various sizes and shapes in real liquids, but a direct experimental test of these assumptions is not at present possible. As an alternative, it is suggested that the possibility of using the molecular dynamics technique to obtain estimates of cavitation works in realistic model fluids be investigated.

PROPOSITION 4

A MOLECULAR DYNAMICS INVESTIGATION OF CAVITY
FORMATION WORKS IN A SIMPLE LIQUIDIntroduction

In 1936 Eyring¹ suggested that the "excess" volume acquired by a simple liquid through thermal expansion might be collected into individual "holes" or "voids", rather than being distributed randomly and homogeneously throughout the fluid structure. This suggestion was at the time entirely intuitive in nature, but has since found some support in the results obtained by x-ray thermal neutron scattering measurements on simple liquids.² For example, the average coordination number of an atom of liquid argon decreases with thermal expansion of the liquid from between 10 and 11 at the melting point to approximately 4 at about five degrees below the critical temperature.³ Yet during this expansion, the average distance between nearest neighbors remains constant at about 3.8 Å--indicating that the atoms must cluster together, leaving the "excess" volume of expansion to void regions distributed throughout a more or less tightly packed lattice structure.

The results achieved through the application of Eyring's suggestion to the then existing "cell" theories⁴ of the liquid state--the so-called "hole" theory⁵--were uniformly rather disappointing.⁶ But in recent years the more sophisticated "significant structure" theory⁷ has devolved from Eyring's initial insight, and this latter theory has

met with surprising success in treating the physical properties of a wide variety of liquids.⁸

Aside from the theoretical implications, information regarding the size, shape, and other physical properties of the holes occurring in simple liquids may provide a key to our understanding of the dynamic processes characteristic of liquids at the molecular level. The "significant structure" theory, for example, envisions holes or "vacancies" the size of a single molecule, and thus suggests a "jump" mechanism for diffusion in liquids.⁹ On the other hand, the results of some recent computer calculations simulating a dense fluid of Lennard-Jones disks¹⁰ indicate that the holes occurring in real liquids may be relatively larger and quite irregular--a notion consistent with a diffusion mechanism that is "cooperative" in nature.¹¹ It would seem therefore that a detailed investigation of the energies or works associated with the formation of cavities of various sizes and shapes in a physically realistic model dense fluid might serve to shed some light on both the equilibrium and non-equilibrium (dynamic) properties of the liquid state.

Background

In an early development of the so-called "scaled-particle" theory, Reiss, Frisch, and Lebowitz¹² (RFL) were able to obtain an approximate analytical expression for the equation-of-state of a hard-sphere fluid. This formulation was found to reproduce the results of previous machine simulation calculations¹³ quite accurately, to the extent that the first five virial coefficients derived from the

theoretical expression were in good agreement with those obtained computationally. The agreement for the first three coefficients was in fact exact.

The central idea of the "scaled-particle" theory is that it is possible to obtain a very good a priori estimate of the reversible work $W(r)$ that must be extended to create a spherical cavity of radius r in a fluid. The incremental work necessary to expand the radius of the cavity from r to $(r+dr)$ is given as a sum of volume and surface contributions:

$$dW(r) = p \cdot 4\pi r^2 dr + \sigma(r) \cdot 8\pi r dr \quad , \quad (1)$$

where p is the internal pressure of the fluid, and $\sigma(r)$ is a quantity like a surface tension.

If r is sufficiently large, $\sigma(r)$ becomes a true surface tension σ_0 so that

$$W(r) \cong \left(\frac{4}{3} \pi r^3 \right) p + (4\pi r^2) \sigma_0 \quad , \quad (2)$$

but for smaller r an additional term must be added to account for the curvature dependence of the surface work:

$$W(r) = \left(\frac{4}{3} \pi r^3 \right) p + (4\pi r^2) \sigma_0 [1 - (2\delta/r)] \quad , \quad (3)$$

where δ is a distance corresponding to the thickness of the inhomogeneous layer at the surface of the cavity. The first term on the RHS of Eqs. (2) and (3) may be thought of as the PV work necessary to introduce a hollow rigid sphere of radius r into the fluid; σ_0 then

becomes the interfacial tension between the fluid and a perfectly rigid wall, and is not the surface tension at a liquid-vapor interface.

RFL were able to obtain an exact expression for $W(r < a/2)$ in a fluid of hard spheres of diameter a by making use of the fact that a cavity of such small dimensions can contain at most the center of only one particle. The work is given by:

$$W(r) = -k_B T \ln \left\{ 1 - \frac{4}{3} \pi r^3 \rho \right\}, \quad \left(r \leq \frac{a}{2} \right) \quad (4)$$

where k_B is the Boltzmann constant, and T and ρ are the temperature and number density of the fluid, respectively. By matching Eqs. (3) and (4) at $r = a/2$, Reiss, Frisch, Helfand, and Lebowitz¹⁴ (RFHL) also obtained an extrapolation formula for $W(r)$ valid to beyond $r = a$. This formula is of the form:

$$W(r) = K_0 + K_1 r + K_2 r^2 + K_3 r^3 \quad (5)$$

where the K 's are given by lengthy expressions involving temperature, pressure, and density.

Using the extrapolation formula, it is possible to treat a dilute solution of a hard-sphere solute in a hard-sphere solvent. If the solvent and solute molecules have diameters a and b , respectively, then introduction of a solute molecule into the solution is equivalent to the introduction of a cavity of radius $r_s = (a+b)/2$. The chemical potential μ_h of the solute is therefore given by:

$$\mu_h = k_B T \ln \{ \rho_2 \Lambda_2^3 \} + W(r_s) \quad (6)$$

where:

$$\Lambda_2 = (h^2/2\pi m_2 k_B T)^{\frac{1}{2}} \quad (7)$$

and m_2 and ρ_2 are the molecular mass and density of the solute, respectively, and h is Planck's constant. The first term on the RHS of (6) is the free energy of mixing of the solute with the solvent.

Equation (6) is valid only for solutions so dilute that the solute molecules remain independent of one another, and is limited in accuracy by the accuracy of the extrapolation formula (5). RFHL have however expanded upon Eqs. (5) and (6) to obtain expressions for the partial pressure p_2 of the solute (assuming the vapor above the solution to be ideal) and the Henry's law constant $k_H = p_2/\rho_2$.

RFHL have also extended the theory to fluids of particles interacting with physically more realistic potentials by using a simple modification of the coupling parameter technique.¹⁵ The method is predicated on the assumption that the total interparticle potential can be factored into two components: a "hard" potential

$$\begin{aligned} \varphi_h(r) &= \infty & \text{for } r \leq a ; \\ &= 0 & \text{for } r > a , \end{aligned} \quad (8)$$

and an unspecified "soft" potential $\varphi_s(r)$. The total potential is then written as:

$$\varphi(r; \xi_h, \xi_s) = \varphi_h(r; \xi_h) + \xi_s \varphi_s(r) \quad (9)$$

where ξ_h and ξ_s are coupling parameters such that the hard "core" of

the potential is fully coupled to the remainder of the fluid when $\xi_h = a$, and the "soft" potential is fully coupled when $\xi_s = 1$.

The chemical potential of the fluid is calculated by introducing an additional particle in two stages: in the first stage, ξ_h is "charged" from 0 to a (The hard "core" of the particle is expanded to its full size) with $\xi_s = 0$; in the second stage, the "soft" potential is introduced by charging ξ_s from 0 to 1. If the full chemical potential is represented by $\mu(\xi_h, \xi_s)$, then the portion of the chemical potential calculated in the first stage, $\mu_h = \mu(a, 0)$, is approximated by equation (6)--assuming $b = a$, or that the solute and solvent molecules are identical. Calculation of the remainder of the chemical potential, $\mu_s = \mu(a, 1) - \mu(a, 0)$ is however much more difficult, and for this reason applications of the "extended" theory to real liquids¹⁶ have been somewhat limited.

In the course of developing a rigorous basis for the old Frenkel-Band equilibrium cluster theory of association,¹⁷ Stillinger¹⁸ has also obtained expressions relating the equation-of-state of a dense fluid to quantities corresponding to cavity formation works. In essence, the theoretical development involves a factorization of the grand partition function for a fluid into terms associated with the partition functions for clusters of different numbers of particles--a procedure somewhat similar to the well-known Mayer expansion technique¹⁹ for the grand ensemble, except that the interaction between each cluster and the remainder of the fluid is expressed in terms of the reversible isothermal work necessary to form the cavity in which the cluster resides. That is, the contribution of a cluster of s

particles to the grand partition function is divided into two parts: a contribution due to interactions between the s particles internal to the cluster, and a contribution due to the work $W_s(\underline{r}_1 \dots \underline{r}_s)$ necessary to form a cavity in the fluid into which the cluster can be placed.

The cavities envisioned by the Frenkel-Band theory differ physically from those dealt with in the "scaled-particle" theory. The Frenkel-Band concept of clustering is based upon the idea of particle "overlap"; two particles are said to overlap when their centers lie within some fixed distance \underline{b} of each other (Stillinger¹⁸ discussed the criteria pertinent to the choice of an optimum value for \underline{b} for a specific application of the theory). The theory then defines a "cluster" as a group of geometrically related particles such that each pair of particles in the group either overlap themselves or are indirectly connected by an unbroken sequence (or chain) of overlapping particles. Since by definition no particle in a cluster may overlap other particles in the fluid external to the cluster, the cavity in which a cluster of s particles resides must be such that none of the other fluid particles lie within a distance \underline{b} of the positions $\underline{r}_1 \dots \underline{r}_s$ occupied by the cluster particles. The works $W_s(\underline{r}_1 \dots \underline{r}_s)$ entering into the Frenkel-Band theory therefore apply to the formation of possibly very irregular and convoluted cavities--in contrast to the smooth spherical cavities envisioned by the "scaled-particle" theory.

The full mathematical development of the Frenkel-Band theory is quite lengthy, and to this author's knowledge, the theory has not actually been applied to the treatment of real fluids. The main

stumbling block to application of the theory would however seem to be the calculation of approximate values for the cavitation works; in the next section we describe a method whereby cavitation works in realistic dense fluids can be estimated.

Analysis

The so-called "molecular dynamics" technique for simulating the microscopic dynamics of a dense fluid has been discussed at length elsewhere in this dissertation. Of specific interest here is the fact that it is possible to apply a well-defined perturbation to the fluid during the course of the dynamics integration; in particular, it should be possible to introduce a cavity into the fluid in a nearly reversible manner, and to calculate the work extended in the process.

In theory, any number of different methods might be used to introduce the cavity into the fluid. For example:

- (i) A repulsive potential "barrier" the size and shape of the desired cavity could be pushed slowly into position in the fluid from the outside.
- (ii) A repulsive potential could be expanded slowly around a point in the fluid, in a manner analogous to that envisioned in the development of the "scaled-particle" theory.
- (iii) A repulsive potential may be slowly "charged" throughout the region in the fluid to be occupied by the cavity, thus permitting the particles initially occupying that region to drain away.

In practice, the first method does not seem to be well suited for use in

conjunction with the molecular dynamics technique. This is especially so because of the periodic boundary conditions most often employed in the dynamics calculations; with these boundary conditions, the space to which the simulated fluid is confined is closed upon itself so that, effectively, no "outside" to the system exists.

The second method might be used to best advantage for calculations involving the formation of a spherical cavity having strictly repulsive boundaries (the classic "scaled-particle" model), while the third method could be used for the introduction of an irregular cavity (of the Frenkel-Band type) or a cavity surrounded by an extended attractive potential. In terms of the computational effort (and hence, computer time) required, method (ii) would probably be more economical than method (iii); on the other hand, method (iii) might prove to yield a more nearly "reversible" type of expansion. At present it is difficult to see how, in practice, method (ii) might be used to introduce a cavity having both attractive and repulsive potential components.

The work extended in the formation of a cavity could conceivably be calculated as an integral of force over distance; that is, as a summation of the average forces acting upon the external shell of the cavity at each point in its incremental expansion. Noting however that isoenergetic models are most frequently used in conjunction with the molecular dynamics technique, it would seem that cavitation work might best be calculated as the overall change in the total energy of the system during introduction of the cavity.

Finally, we note that it is not actually necessary to introduce a cavity into the fluid to measure formation works for cavities representing

a single particle or a cluster of particles. Rather, a selected particle or group of particles already extant in the fluid can be removed by first fixing their positions and then slowly "discharging" their potential interactions with other particles external to the cavity [the inverse of method (iii)] .

Proposal

It is suggested that the feasibility of using the molecular dynamics technique to obtain estimates of cavitation works in realistic model dense fluids be investigated. The practical advantages and disadvantages of both methods (ii) and (iii) for introduction of a cavity should be examined, as should the practicability of the "particle discharging" method for obtaining negative cluster-cavitation works.

An approximate measure of the statistical variation that might be expected in the formation work values obtained for a given cavity should be determined by introducing identical cavities into several different regions of the fluid (starting with the same initial fluid configuration), and by introducing the same cavity into the fluid at different times (i. e., starting with different fluid configurations). The "reversibility" of a cavity introduction method can be tested by introducing a cavity and then removing it again; the total energy of the fluid should return to its initial value after the cavity is removed.

If the results of this investigation indicate that the "augmented" molecular dynamics technique does indeed provide a practical means of determining cavitation works, various aspects of the "scaled-particle" and Frenkel-Band theories might be examined. For example, the

validity of the "scaled-particle" treatment for realistic fluids could be tested by inserting calculated cavitation works into the theoretical equation-of-state formulations--and then comparing the predicted equation-of-state for the model fluid to that obtained computationally. By computing the formation works for the same cavity, first with only a hard "core" and then with both hard and soft potential components, the precision of the coupling parameter technique used to calculate μ_s in the "extended" version¹⁴ of the "scaled particle" theory could be determined.

REFERENCES FOR PROPOSITION 4

1. H. Eyring, J. Chem. Phys. 4, 283 (1936).
2. See, for example: P. A. Egelstaff, An Introduction to the Liquid State (Academic Press, New York, 1967).
3. A. Eisenstein and N. Gingrich, Phys. Rev. 62, 261 (1942).
4. J. E. Lennard-Jones and A. F. Devonshire, Proc. Roy. Soc. 163, 53 (1937); ibid., 165, 1 (1938).
5. F. Cernuschi and H. Eyring, J. Chem. Phys. 7, 547 (1939).
6. See, for example: J. M. H. Levelt and E. G. D. Cohen, Studies in Statistical Mechanics, J. de Boer and G. E. Uhlenbeck, eds., (North-Holland Publishing Co., Amsterdam, 1964), Vol. II, p. 178 ff.
7. H. Eyring, T. Ree, and N. Hirai, Proc. Nat. Acad. Sci. (U.S.) 44, 683 (1958); H. Eyring and T. Ree, ibid., 47, 526 (1961).
8. For a summary of the results achieved by the "significant structure" theory, see: H. Eyring and M. S. Jhon, Significant Liquid Structures (John Wiley & Sons, Inc., New York, 1969).
9. H. Eyring and M. S. Jhon, op. cit., p. 81 ff.
10. P. L. Fehder, J. Chem. Phys. 50, 2617 (1969).
11. See Paper No. 3, reproduced in section IV. B of this dissertation.
12. H. Reiss, H. L. Frisch, and J. L. Lebowitz, J. Chem. Phys. 31, 369 (1959).
13. M. N. Rosenbluth and A. W. Rosenbluth, J. Chem. Phys. 22, 881 (1954); W. W. Wood and J. D. Jacobsen, J. Chem. Phys. 27, 1207 (1957); T. E. Wainwright and B. J. Alder, AEC Report

Contract No. W-7405-eng-48, Radiation Laboratory at Livermore, University of California.

14. H. Reiss, H. L. Frisch, E. Helfand, and J. L. Lebowitz, J. Chem. Phys. 32, 119 (1960).
15. T. L. Hill, Statistical Mechanics, (McGraw-Hill Book Co., Inc., New York, 1956), p. 191 ff.
16. F. H. Stillinger, Jr., J. Chem. Phys. 35, 1581 (1961); H. Reiss and S. W. Mayer, ibid., 34, 2001 (1961); S. W. Mayer, ibid., 35, 1513 (1961); 38, 1803 (1963); S. J. Yosim and B. B. Owens, J. Chem. Phys. 39, 2222 (1963).
17. J. Frenkel, J. Chem. Phys. 7, 200, 538 (1939); W. Band, ibid. 7, 324, 927 (1939).
18. F. H. Stillinger, Jr., J. Chem. Phys. 38, 1486 (1963).
19. Reference 15, Chapter 5.

PROPOSITION 5

AN EXAMINATION OF SOLUTE DIFFUSION AS A FUNCTION
OF THE RELATIVE SIZES AND MASSES OF THE SOLUTE
AND SOLVENT MOLECULESAbstract

From a "chemical" point of view, the dynamic mechanism whereby material is transported from place to place in solution is one of the most important, yet least well understood processes occurring in nature. Unfortunately, the mathematical development of each of the manifold existing theories of transport in dense fluids would seem to adopt its own particular intuitive model for the diffusion mechanism, and then to make any necessary approximations in accord with some limiting form of that model. As a result, none of the existing theories is rigorously applicable to a vast majority of the solutions typically encountered in the laboratory. It is therefore suggested that the molecular dynamics technique be used to simulate a number of two-component dense fluid systems with different solute/solvent size and mass ratios, and that this simulation data then be examined in detail to determine the size- and mass-dependence of the solute diffusion mechanism.

PROPOSITION 5

AN EXAMINATION OF SOLUTE DIFFUSION AS A FUNCTION
OF THE RELATIVE SIZES AND MASSES OF THE SOLUTE
AND SOLVENT MOLECULESIntroduction

The existing theories of diffusion in dense fluids are so complex that a series of approximations have been necessary in order to obtain formulations that can be numerically evaluated for comparison with experiment. The proliferation of transport theories is in itself evidence of a fundamental lack of understanding regarding the dynamic processes characteristic of liquids at the molecular level. And as a consequence, the mathematical development of each theory would seem to adopt its own intuitive model for these microscopic processes, and thence to make the necessary approximations in accord with some limiting form of that model.

From a "chemical" point of view, the dynamic mechanism whereby material is transported from place to place in solution is one of the most important, yet least well understood processes occurring in nature. The first step in any bimolecular reaction is obviously the encounter between two reactant molecules, and thus the frequency with which a solvent brings reactive solute molecules into contact can, to a large extent, determine the overall rate of the ensuing reaction in that solvent. On the other hand, the suggested mechanisms for some complex organic chemical reactions are predicated on the assumption of a

"solvent cage effect"; that is, it is assumed that the surrounding solvent can encage the segments or fragments of a re-arranging molecule to prevent them from diffusing away from the vicinity of a reaction site.

Some of the existing theories of diffusion in liquids are, by extension,¹ applicable to chemical reaction kinetics in solution. The theoretical models for the "solvent cage effect"² have however largely been limited to a consideration of the processes that might occur within a small local region of a liquid, and are not readily extensible to full transport theories. Furthermore, the existing transport theories are generally each based on some limiting assumptions regarding the relative sizes and masses of the solute and solvent molecules, and therefore are not strictly applicable to the full range of possible solute-solvent systems.

An application of the so-called "molecular dynamics" technique to an investigation of diffusion in a two-dimensional dense fluid has been described elsewhere in this dissertation.³ The results obtained from this investigation were then applied to a simple modification of an existing, theoretical treatment of diffusion-controlled reaction kinetics in solution.⁴ Although the study detailed in Refs. 3 and 4, and nearly all of the molecular dynamics studies performed at other laboratories have been limited to single-component systems, the molecular dynamics technique should be readily extensible for simulation studies of two-, and even multi-component solutions.

Background

In accord with the time-correlation function approach to statistical mechanics,⁵ diffusion in solution may be described in terms of the mean square displacement and momentum and force autocorrelation functions

$$\Sigma(t) = \langle [\underline{r}_k(t) - \underline{r}_k(0)]^2 \rangle \quad (1a)$$

$$A_p(t) = \langle \underline{p}_k(t) \cdot \underline{p}_k(0) \rangle \quad (1b)$$

$$A_f(t) = \langle \underline{F}_k(t) \cdot \underline{F}_k(0) \rangle \quad (1c)$$

where $\underline{r}_k(s)$, $\underline{p}_k(s)$, and $\underline{F}_k(s)$ are the position, momentum, and force acting upon particle k at time s , respectively. The three functions are each invariant with uniform time translation [e.g., $\langle \underline{p}_k(t+s) \cdot \underline{p}_k(s) \rangle = \langle \underline{p}_k(t) \cdot \underline{p}_k(0) \rangle$]; the mean square displacement and momentum autocorrelation functions are symmetric; the force autocorrelation function is anti-symmetric.

It is generally assumed (although there is now some evidence to the contrary⁶) that the momentum autocorrelation function decays rapidly with increasing $|t|$ and vanishes after a macroscopically modest time interval t_0 . It can then be shown⁷ that the mean square displacement and momentum autocorrelation functions are related:

$$\Sigma'(t) = I_1^0 t - I_2^0, \quad (2a)$$

where
$$I_1^0 = \left(\frac{2}{m} \right) \int_0^{t_0} A_p(a) da, \quad (2b)$$

and
$$I_2^0 = \left(\frac{2}{m}\right) \int_0^{t_0} A_p(a) a da \quad . \quad (2c)$$

Thus $\Sigma(t)$ becomes linear with slope I_1^0 after an "induction" time t_0 .

Einstein⁸ showed that the diffusion coefficient D is given by

$$D = \frac{1}{6} \dot{\Sigma}(t > t_0) = I_1^0/6 \quad (3)$$

where it is assumed that $\Sigma(t_0)$ is small compared to molecular dimensions, and suggested that the coefficient for a solute might be represented as:

$$D = k_B T / \gamma \quad (4)$$

where k_B and T are the Boltzmann constant and the temperature, respectively, and γ is the "friction coefficient" acting upon an individual diffusing solute particle in the particular solvent. For a rigid spherical solute particle of radius r , Stokes⁹ found:

$$\gamma = 6\pi\eta r \quad , \quad (5)$$

and by combining equations (4) and (5), the familiar Stokes-Einstein equation

$$D = k_B T / 6\pi\eta r \quad (6)$$

is obtained, where $\eta = \eta(t)$ is the viscosity of the solvent.

Strictly speaking, the Stokes-Einstein equation is applicable only to particles that are much larger--and by implication, more massive--than the molecules of the solvent. For solutes of smaller spherical

particles, Bassett¹⁰ has found the expression:

$$\gamma = 6\pi\eta r \left(\frac{\beta r + 2\eta}{\beta r + 3\eta} \right) \quad , \quad (7)$$

where β is an empirical factor, ranging from 0 to ∞ , called the "coefficient of sliding friction." The physical interpretation of these "friction coefficients" is however somewhat questionable when the solute particles are the same size as, or smaller than the solvent molecules.

The Brownian Motion treatment for diffusion is predicated on the assumption that the autocorrelation function $A_f(t)$ of the forces acting upon a diffusing particle decays much more rapidly than the momentum autocorrelation function $A_p(t)$ for the particle, and thus is applicable in the limit of solute particles that are much more massive--and by implication, larger--than the molecules of the solvent. Stated another way, the Brownian Motion model for diffusion is one of a particle moving across a potential surface that varies rapidly with displacement compared to the size of the diffusing particle. This may be contrasted with the van der Waals model,¹¹ which assumes that a diffusing particle executes straight-line trajectories between hard "core" collisions with the solvent molecules. Alternatively, the van der Waals theory assumes that the force and momentum autocorrelation functions for a diffusing particle decay over similar time intervals, and thus is applicable in instances where the solute and solvent molecules are of approximately the same size and mass. Both theories predict a "random-walk" type of motion on the part of the diffusing

particle, but differ in the manner in which the step length and the stepping frequency for the "walk" are formulated.

Several transport theories are based on a "jump" model for diffusion. In this model, a diffusing particle is moved through a solvent by successive repetitions of a three step mechanism:

- (i) A void is opened in the solvent adjacent to the particle,
- (ii) the particle "jumps" from its initial position into the void,
and,
- (iii) the solvent molecules move into the void left behind by the particle after its "jump".

It is generally assumed that the diffusing particle must cross a potential "barrier" in moving from its initial position into the void.

The "activation theory"¹² of transport in dense fluids suggests that the diffusion coefficient of a solute be expressed as:

$$D = D_0 e^{-W/k_B T} \quad (8)$$

where D_0 is a constant and W is the sum of the energies necessary to form the void in step (i) and clear the potential barrier to step (ii). Then if D is known as a function of temperature, W and D_0 can be determined from the slope and intercept of an "Arrhenius" plot of $\ln D$ vs. $1/T$. This procedure must however be considered rather questionable, since the microscopic structure of the solvent--and hence, W --must itself be temperature-dependent.

The "significant structure"¹³ theory of transport is also based on a "jump" mechanism for diffusion, but differs from the "activation"

theory in that the "significant structure" model for the liquid state assumes that free-moving voids, or "fluidized vacancies", are naturally present in the micro-structure of simple liquids. The viscosity of a dense fluid is then formulated in terms of the resistance to a shear stress created by molecules jumping back and forth between adjacent "layers" in the fluid (essentially, the old Frenkel¹⁴ treatment), the number of vacancies in the fluid, and an absolute rate expression for the "jump" mechanism.

Analysis

Consider a solution of a solute A dissolved in a solvent S. Let r_A and r_S , and m_A and m_S be the radii and masses of the solute and solvent molecules, respectively, and let us assume that the ratios $(r_A/r_S) = R_r$ and $(m_A/m_S) = R_m$ can be varied at will. Then, referring to the diagram on the following page, we see that the Stokes-Einstein equation is strictly applicable only when $R_r \gg 1$ [region (a) in the diagram], while the Brownian Motion treatment is applicable when $R_m \gg 1$ [region (b)]. The van der Waals-Enskog treatment is valid in the region (c) where $R_r \cong R_m \cong 1$, and the "significant structure" transport theory--being a theory of self-diffusion--is applicable only for the situation where $R_r = R_m = 1$. The "activation" theory of solute diffusion is theoretically applicable to the entire range of R_r and R_m ratios, but is probably truly valid for none.

Most of the solutions typically dealt with in a chemistry laboratory would fall outside any of the indicated regions in the diagram. Unfortunately, a definitive experimental study of the size and mass

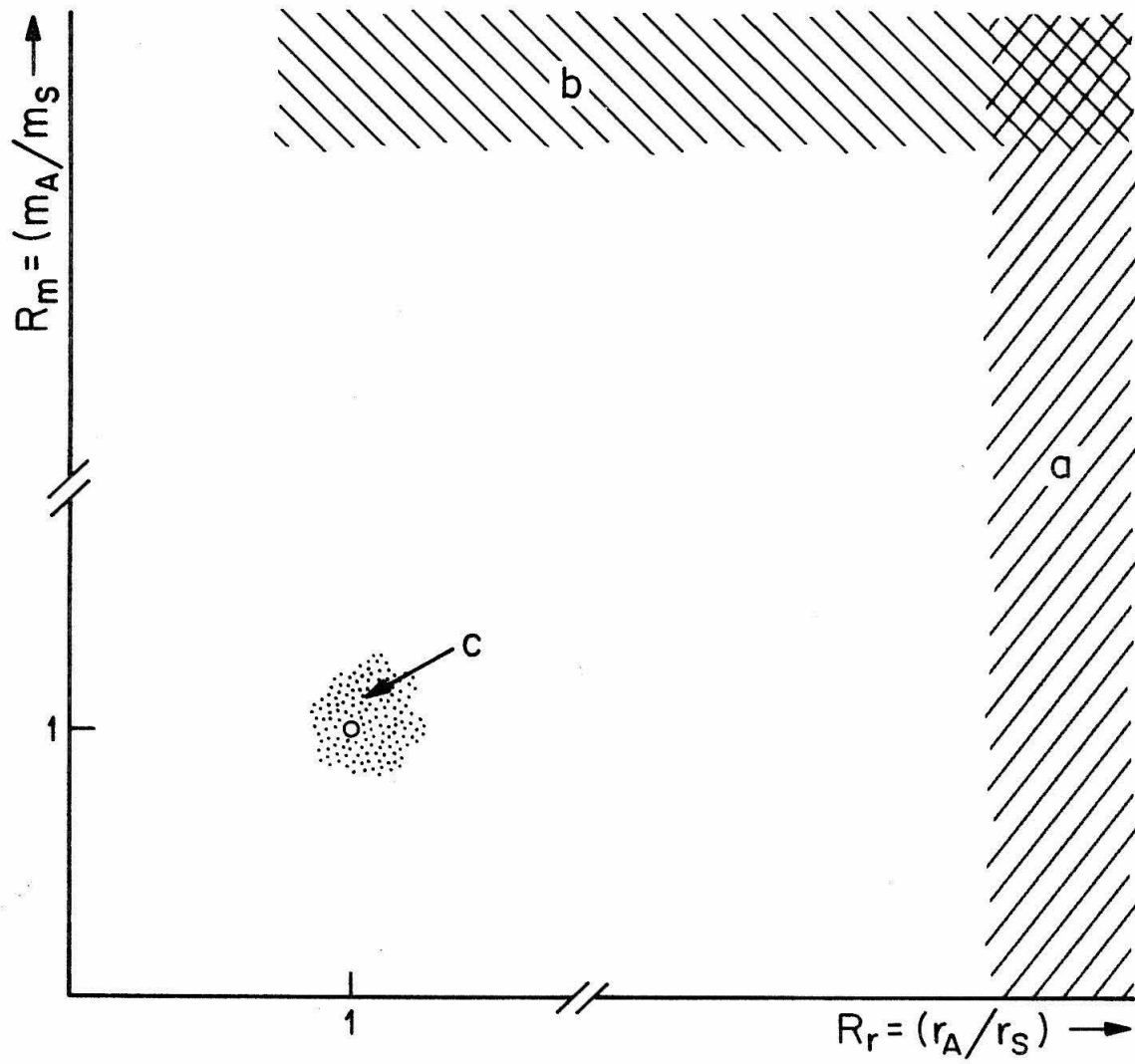


Diagram indicating regions of R_r - R_m space where various theories of solute diffusion are rigorously applicable.

dependence of solute diffusion in real liquids is not possible--primarily because groups of soluble substances having molecules of the same size but different masses (alternatively: molecules of the same mass but of different sizes) do not exist in nature. But by using the molecular dynamics technique, it should be possible to simulate, and then investigate in detail, the microscopic dynamic processes occurring in the two-component fluid systems having a wide range of solute/solvent size and mass ratios.

Proposal

The microscopic dynamic processes associated with transport in dense fluids are apparently so complex that it would seem injudicious to suggest that the mechanism for solute diffusion in real liquids could be completely elucidated by the results of a single experiment or group of experiments. The results of our previous analysis of self-diffusion in a dense fluid of Lennard-Jones disks³ indicate that, even at temperatures well in excess of the critical temperature, both the attractive and repulsive components of the pair interaction potential may play an important role in determining the diffusion mechanism. We therefore suggest that the initial studies of size and mass effects in solute diffusion be done with systems of hard spheres. If the results obtained in these studies appear promising, the investigation can then be extended to systems of particles interacting with a physically more realistic (e.g., the Lennard-Jones) pair potential.

Specifically, we suggest that the molecular dynamics technique be used to simulate a number of dense, two-component, hard-sphere

fluids with solute/solvent size and mass ratios falling on a uniform grid in $R_r - R_m$ space. A simple modification of the dynamics algorithm devised by Alder and Wainwright¹⁵ could be used for the simulation calculations, and many of the techniques described in Ref. 3 would probably be applicable to an analysis of solute diffusion in the model fluids. Even information regarding the functional dependence of the solute diffusion coefficient D_A or R_r and R_m could prove quite enlightening. And if this functional dependence is found to show some unexpected features, the actual mechanism for solute diffusion could be examined in graphical displays of the simulation data.

REFERENCES FOR PROPOSITION 5

1. R. M. Noyes, Progress in Reaction Kinetics, G. Porter, ed., (Pergamon Press, New York, 1961), Vol. 1, p. 129.
2. See, for example: R. M. Noyes, J. Chem. Phys. 18, 999 (1950).
3. Paper No. 3, page 129.
4. Paper No. 4, page 179.
5. R. Zwanzig, Annual Review of Physical Chemistry (Annual Reviews, Palo Alto, 1965), Vol 16, p. 67.
6. B. J. Alder and T. E. Wainwright, J. Phys. Soc. (Japan) 26, 267 (1969).
7. See Paper No. 3, p. 136 ff.
8. A. Einstein, Ann. der Phys. 17, 549 (1905).
9. G. G. Stokes, Camb. Trans. 9, 8, Papers III, 1 (1851).
10. Bassett, quoted by L. G. Lamb in Hydrodynamics (New York, 1945), p. 602.
11. J. H. Dymond and B. J. Alder, J. Chem. Phys. 45, 2061 (1966).
12. See, for example: P. A. Egelstaff An Introduction to the Liquid State (Academic Press, New York 1967), p. 151 ff.
13. H. Eyring and M. S. Jhon, Significant Liquid Structures (John Wiley & Sons, Inc., New York, 1969), p. 81 ff.
14. J. Frenkel, Kinetic Theory of Liquids (Dover Publications, Inc., New York, 1955).
15. B. J. Alder and T. E. Wainwright, J. Chem. Phys. 31, 459 (1959); ibid. 33, 1439 (1960).